ULB ECOLE POLYTECHNIQUE DE BRUXELLES

Detecting nonclassicality and estimating parameters in quantum phase space

Thèse présentée par Matthieu ARNHEM
en vue de l'obtention du grade académique de
Docteur en Sciences de l'Ingénieur et Technologie
Année académique 2021-2022

Sous la direction du Professeur Nicolas CERF,

promoteur

Centre for Quantum Information and Communication

Jury de thèse

Serge MASSAR (Université libre de Bruxelles, Président)
Ognyan ORESHKOV (Université libre de Bruxelles, Secrétaire)
Frédéric GROSSHANS (Sorbonne Université, France)
Radim FILIP (Palacký University, République Tchèque)
Nicolas J. CERF (Université libre de Bruxelles)

Matthieu Arnhem
Université libre de Bruxelles
École polytechnique de Bruxelles
50 av. F.D. Roosevelt - CP165/59
1050 Bruxelles
Belgique
Email: matthieu.arnhem@ulb.be

Thèse de doctorat présentée en séance publique le 1er juillet 2022 à l'Université libre de Bruxelles.

Jury: **Prof. Serge Massar**, Président du jury, ULB

Prof. Ognyan Oreshkov, Secrétaire, ULB

Dr. Frédéric Grosshans , Sorbonne Université, France

Prof. Radim Filip , Palacký University, Czech Republic

Prof. Nicolas J. Cerf, Promoteur, ULB

A papa, à maman,

à Cécile,

à ceux qui m'ont enseigné,

List of publications

The present thesis is based on the following publications

Published in peer-reviewed journals

- *Optimal Estimation of Parameters Encoded in Quantum Coherent State Quadratures*,
  Matthieu Arnhem, Evgueni Karpov, and Nicolas J. Cerf
  Appl. Sci. **2019**, *9*(20), 4264 (2019) : Special issue "Quantum Optics for Fundamental Quantum Mechanics", edited by M. Genovese and M. Gramegna [1]
  doi:10.3390/app9204264; arxiv:1907.04264v2
  The content of this article is covered in Chapter 4 of this thesis.

- *Realignment separability criterion assisted with filtration for detecting continuous-variable entanglement*,
  Anaelle Hertz, Matthieu Arnhem, Ali Asadian, and Nicolas J. Cerf
  Phys. Rev. A **104**, 022427 (2021) [2]
  doi:10.1103/PhysRevA.104.022427; arxiv:2104.07510v2
  The content of this article is covered in Chapter 6 of this thesis.

Submitted article

- *Multi-copy implementation of nonsclassicality criteria*,
  Matthieu Arnhem, Célia Griffet and Nicolas J. Cerf [3]
  arxiv:2205.12040
  doi:10.48550/arXiv.2205.1204
  The content of this article is covered in Chapter 8 of this thesis.

Acknowledgment

Une thèse est l'accomplissement d'un travail personnel de longue haleine. Elle se sera étendue sur six ans et dix mois dans mon cas. Néanmoins, il n'aurait pas été possible de l'accomplir sans l'aide et le soutien de nombreuses personnes que j'aimerais remercier dans les lignes qui suivent. La liste des personnes à citer est trop longue et je me contenterai dès lors de ne nommer que les personnes qui ont pris une part active à l'accomplissement de ma thèse et à mon parcours durant ces 7 dernières années et ce dans l'ordre chronologique de mes rencontres. Mes amis, connaissances, rencontres et membres de ma famille qui m'ont écoutées, soutenues, passé une soirée, une journée ou un week-end avec moi durant ma thèse ont formé un écosystème formidable et ont été tant de bulles d'air qui m'ont permis d'avancer. Je les remercie profondément et sincèrement même si je ne les nommes pas explicitement dans les paragraphes à venir.

Tout d'abord, j'aimerais remercier Evgueni Karpov qui a accepter d'encadrer mon mémoire. Tu as sans doute été la première personne à me faire confiance et ta gentillesse et ta disponibilité m'ont été précieuse dans les premières années de thèse. N'importe quand, je pouvais venir dans ton bureau et tu prenais le temps de m'introduire aux nouveaux concepts, de discuter de mes calculs et résultats, de m'accompagner lors de mes premières conférences et lors de nos réunions avec d'autres scientifiques.

Cela m'amène à Nicolas, qui également a accepté d'être le promoteur de mon mémoire et ensuite de ma thèse. Merci Nicolas de m'avoir fait confiance pour mener à bien ce projet de thèse. Après tant d'années à discuter et travailler ensemble, ta manière de penser et de faire la physique s'est peu à peu imprégnée dans ma manière de réfléchir et de faire de la recherche. Merci également de m'avoir accompagné en conférence, proposé des idées de projets et mis en contact avec de nombreuses personnes de notre domaine de recherche.

Je remercie ensuite Marc Haelterman et Philippe Emplit pour m'avoir fait confiance pour m'engager comme assistant temps plein pour leurs unités d'enseignement à la Solvay Brussels School. J'ai appris divers aspects sur la pédagogie académique et son vocabulaire ainsi que sur les défis de la gestion de grands auditoires.

Je remercie également Michel Allé et Nicolas Van Zeebroeck pour leur encadrement et leur professionalisme dans le gestion de leur équipe d'assistants pour les travaux de groupe que j'ai encadré. J'ai appris de nombreuses choses en encadrant ces travaux sur des sujets que je n'aurais sans doute jamais abordé sans avoir été assistant dans

votre unité d'enseignement.
J'aimerais également remercier Mathieu Brandeho, Anaëlle Hertz et Michaël Jabbour. Vous êtes les personnes qui, en tant que doctorants et doctorante à l'époque, m'ont introduit aux us et coutumes du QuIC, aux petits trucs et astuces et avec qui je pouvais parler aussi bien de recherche que d'autres sujets. Nous avons passé de belles soirées ensemble et même une coupe du monde (même si nous n'avons pas gagné la coupe inter-service de l'ULB). Plus particulièrement, j'ai une pensée pour Mathieu B. comme nous avons cohabité durant quelques années et partagé un quotidien. Nos discussions philosophiques du soir durant le souper ou du matin au petit déjeuner font encore échos dans ma mémoire. Anaëlle, j'ai particulièrement apprécié travailler avec toi. Le projet sur lequel nous avons travaillé ensemble m'a réellement permis d'approfondir la manière de faire la recherche dans ses aspects pratiques et techniques. Merci pour ton temps et tes conseils.
Tous les membres du QuIC que j'ai également cotoyé, doctorants, post-doc, membres du personnels académique et administratif que j'ai cotoyé et qui sont parties prenantes dans l'atmosphère de recherche détendue et ouverte du QuIC. En particulier je pense à Pascale, Christos, Zizhu, Jérémie, Ognyan, Raul, Atul, Krishna, Zoé, Stephan, Levon, Esteban, Chrysoula, Esteban, Uttam, Shantanav, Simon, Siddharta, Ravi, Julian, Lin-Qing, Hamed, Leo, Zacharie, Timothée, Enea, Antoine, Benoît. My experience at QuIC without all of you would not have been the same. Thank you all for the good atmosphere and discussions.
Je ne manquerai pas de citer Célia. Nous sommes entrés en contact vers la fin de ma thèse et au début de la tienne. Nous avons du collaborer dans ces moments difficiles de confinement. Cependant, cette collaboration fut très motivante pour moi, nous avons pu établir une communication efficace entre nous et nous nous sommes encouragés mutuellement. J'ai également appris pas mal de choses de ta manière de travailler et j'espère avoir pu t'apporter ce que j'ai pu apprendre durant ma thèse et que tu pourras en faire bon usage. Je te remercie donc d'avoir partagé et discuté de toutes les idées avec lesquelles je venais le matin après qu'elle m'aient réveillées durant la nuit.
Je remercie toutes ces personnes avec qui j'ai collaboré et partagé mes journées et avec lesquelles certaines collaborations sont devenues des amitiés.
Finalement, je tiens remercier tout spécialement ma famille proche, maman, papa et parrain. Vous avez tous les trois, à votre manière, contribué au succès de cette thèse. Depuis très jeune vous avez accompagné dans mon apprentissage et vous avez nourri ma curiosité pour m'intéresser aux phénomènes qui nous entourent. Je sais que vous êtes derrière moi et que je pourrai toujours compter sur vous. Finalement, j'aimerais remercier Laura, ma compagne. Sans toi et sans ton soutien quotidien et toujours renouvelé, je ne sais pas si je serai arrivé jusque-là. Tu m'as sans cesse encouragé et accompagné durant les moments les plus difficiles. Tu as en quelques sorte vécu cette thèse avec moi et je ne peux te remercier assez pour cela.

Abstract

Phase space is an essential mathematical tool for the study of dynamical systems in classical mechanics. This abstract space, whose coordinates are the dynamical variables of a system, can also be exploited for the characterization of systems in quantum physics, and more particularly in quantum optics. However, while the state of a moving particle in classical mechanics at a given time is represented by a point in phase space, the state of a photonic system in quantum optics is much more involved and must be represented by a quasi-probability distribution, such as the Wigner function. Compared to a pointlike distribution, this spreading accounts for the quantum nature of the system and originates from the Heisenberg uncertainty principle. Another specificity of quantum phase space that has no classical analogue lies in that a quasi-probability distribution may admit negative values or may not even be expressible as a regular function.

The representation of the state of the electromagnetic field in quantum optics is commonly based on quasi-probability distributions in quantum phase space. Here, the dynamical variables that are considered are the (x, p) quadratures of the electromagnetic field. Such a phase-space representation allows a visualization of the state and is an alternative to a description in terms of its density matrix. Importantly, there is generally no simple equivalence between the characteristics of the quasi-probability distribution and the properties of the corresponding quantum state. For example, the fact that the Wigner function admits negative values is a sufficient (but not necessary) condition for the non-classicality of the corresponding state (i.e., its incompatibility with a mixture of coherent states). Quantum phase space thus offers a wide playground for formulating interesting problems in quantum optics and quantum information.

In this thesis, we use the quantum phase space representation as the general context in order to investigate three distinct topics. First, we establish a protocol for estimating continuous parameters encoded in coherent states, focusing on the (x, p) quadratures of the field. Second, we define a new separability criterion that is suited to continuous-variable systems and propose an experimental implementation that relies on homodyne measurements. Finally, we put forward a new method in order to evaluate non-classicality criteria in phase space that is based on multicopy observables. We consider a few possible experimental implementations that make use of several identical copies of the quantum state under investigation.

In the first part of the thesis centered on quantum parameter estimation, we prove that our protocol for estimating quadrature pairs (x, p) encoded in coherent states is optimal, in the sense that it saturates the quantum Cramér-Rao bound based on the Fisher information for the estimation of each parameter. This then allows us to look into an effect observed by S. Iblisdir and N. J. Cerf in 2001 [4] namely that more information can be extracted about two variables encoded in two phase-conjugate coherent states rather than in two identical coherent states. We demonstrated the optimality of this phase-conjugate protocol and develop a general protocol for encoding and optimally estimating an arbitrary number of continuous parameters in the same number of coherent states.

In the second part of the thesis centered on entanglement, we start from the so-called realignment criterion for separability established by O. Rudolph in 2005 [5]. We define a variant, coined the weak realignment criterion, which is based on the same mathematics, namely the greatest cross norm, but offers the advantage that it admits a physical implementation allowing us to directly test the criterion without the need to access the whole density matrix of the state. In a next step, we improve the performance of this new criterion by supplementing it with a filtration stage through the optimized application of a so-called noiseless attenuator. This results in an improved weak realignment criterion, which may even surpass the original realignment criterion while keeping the implementation advantage.

In the third part of the thesis centered on non-classicality, we apply a multi-copy technique based on the assumption that we have several identical copies of the quantum state at our disposal. Following on a multicopy approach to uncertainty relations by A. Hertz *et al.* in 2019 [6], we turn to non-classicality criteria built on minors (i.e., determinants of sub-matrices) of some matrix of moments of the electromagnetic field in phase space. We first compare the performance of the criteria associated with different minors when considering known non-classical states and then develop the corresponding multicopy nonclassicality observables. Finally, we analyze the properties of these novel non-classicality criteria and propose experimental implementations for the most interesting ones.

Titre

Détection de la non-classicalité et estimation de paramètres dans l'espace des phases

Résumé

L'espace des phases est un outil mathématique essentiel pour l'étude des systèmes dynamiques en mécanique classique. Cet espace abstrait, dont les coordonnées sont les variables dynamiques d'un système, peut également être exploité pour la caractérisation des systèmes en physique quantique, et plus particulièrement en optique quantique. Cependant, alors que l'état d'une particule en mouvement en mécanique classique à un instant donné est représenté par un point dans l'espace des phases, l'état d'un système photonique en optique quantique est beaucoup plus complexe et doit être représenté par une distribution de quasi-probabilité, telle que la fonction de Wigner. Par rapport à une distribution ponctuelle, cette répartition rend compte de la nature quantique du système et trouve son origine dans le principe d'incertitude d'Heisenberg. Une autre spécificité de l'espace des phases quantique qui n'a pas d'analogue classique réside dans le fait qu'une distribution de quasi-probabilité peut admettre des valeurs négatives ou même ne pas être exprimable comme une fonction régulière.

La représentation de l'état du champ électromagnétique en optique quantique est généralement basée sur des distributions de quasi-probabilité dans l'espace des phases quantique. Ici, les variables dynamiques qui sont considérées sont les quadratures (x, p) du champ électromagnétique. Une telle représentation de l'espace des phases permet de visualiser l'état et constitue une alternative à une description en termes de matrice densité. Il est important de noter qu'il n'existe généralement pas d'équivalence simple entre les caractéristiques de la distribution de quasi-probabilité et les propriétés de l'état quantique correspondant. Par exemple, le fait que la fonction de Wigner admette des valeurs négatives est une condition suffisante (mais non nécessaire) pour la non-classicalité de l'état correspondant (c'est-à-dire son incompatibilité avec un mélange d'états cohérents). L'espace des phases quantique offre donc un vaste terrain de jeu pour formuler des problèmes intéressants en optique quantique et en information quantique.

Dans cette thèse, nous utilisons la représentation de l'espace des phases quantique comme contexte général afin d'étudier trois sujets distincts. Premièrement, nous établissons un protocole pour l'estimation de paramètres continus encodés dans des états cohérents, en nous concentrant sur les quadratures (x, p) du champ electro-

magnétique. Deuxièmement, nous définissons un nouveau critère de séparabilité adapté aux systèmes à variables continues et proposons une mise en œuvre expérimentale qui repose sur des mesures homodynes. Enfin, nous proposons une nouvelle méthode d'évaluation des critères de non-classicalité dans l'espace des phases, basée sur des observables multicopies. Nous considérons quelques implémentations expérimentales possibles qui utilisent plusieurs copies identiques de l'état quantique étudié.

Dans la première partie de la thèse centrée sur l'estimation des paramètres quantiques, nous prouvons que notre protocole d'estimation des paires de quadrature (x, p) codées dans des états cohérents est optimal, dans le sens où il sature la borne de Cramér-Rao quantique basée sur l'information de Fisher pour l'estimation de chaque paramètre. Ceci nous permet alors d'étudier un effet observé par S. Iblisdir et N. J. Cerf en 2001 [4], à savoir que l'on peut extraire plus d'informations sur deux variables encodées dans deux états cohérents de phase conjuguée plutôt que dans deux états cohérents identiques. Nous avons démontré l'optimalité de ce protocole à phase conjuguée et développé un protocole général pour encoder et estimer de manière optimale un nombre arbitraire de paramètres continus dans le même nombre d'états cohérents.

Dans la deuxième partie de la thèse centrée sur l'intrication, nous partons du critère dit de réalignement pour la séparabilité établi par O. Rudolph en 2005 [5]. Nous définissons une variante, appelée le critère de réalignement faible, qui est basée sur les mêmes outils mathématiques, à savoir la plus grande norme croisée, mais qui présente l'avantage d'admettre une implémentation physique nous permettant de tester directement le critère sans avoir besoin d'accéder à la matrice densité complète de l'état. Dans une seconde étape, nous améliorons les performances de ce nouveau critère en le complétant par une étape de filtration grâce à l'application optimisée d'un atténuateur sans bruit. Il en résulte un critère de réalignement faible amélioré, qui peut même surpasser le critère de réalignement original tout en conservant l'avantage de l'implémentation.

Dans la troisième partie de la thèse centrée sur la non-classicalité, nous appliquons une technique multicopie basée sur l'hypothèse que nous avons plusieurs copies identiques de l'état quantique à notre disposition. Suite à une approche multicopie des relations d'incertitude par A. Hertz *et al.* en 2019 [6], nous nous tournons vers des critères de non-classicalité construits sur des mineurs (c'est-à-dire des déterminants de sous-matrices) d'une certaine matrice de moments du champ électromagnétique dans l'espace des phases. Nous comparons d'abord les performances des critères associés à différents mineurs en considérant des états non-classiques connus, puis nous développons les observables de non-classicalité multicopies correspondantes. Enfin, nous analysons les propriétés de ces nouveaux critères de non-classicalité et proposons des implémentations expérimentales pour les plus intéressants.

Contents

List of Figures

List of Tables

1 Introduction

Concerning a historical point of view toward the advent of quantum mechanics. [1]

The 20^{th} century has seen the advent of two major revolution in physics : relativity on one side and quantum mechanics on the other side. Both of these theories had a deep impact on the way we understand fundamental notions such as space, time and events. However, these two theories are not independent since they arose from the same brains. Indeed, people like A. Einstein, W. Wien, H. Lorentz, H. Poincaré or M. Planck played a key role in the development of the theory of relativity. On the other side, the quantum theory was formalised by people like A. Einstein, E. Schrodinger, W. Heisenberg, N. Bohr, M. Born, G. Gamow, L. de Broglie, P. Dirac, E. Majorana, W. Pauli or M. Planck. Hence, these two circles of people are strongly overlapping.

However, if one goes back to the roots of quantum mechanics, one finds himself taken back to the 19^{th} century thermodynamics and the central notion of *entropy* S that avoids a physical system to be, in its future, in a state it has been in its past. Indeed, quantum mechanics might find its historical roots in the different conceptual status of this notion of entropy that was debated during the late 19^{th} century.

On one side, L. Boltzmann was defending the idea of atoms [2] and had a statistical interpretation of the entropy. His interpretation is summarized in the equation :

$$S = k_B \log(W), \tag{1.1}$$

where $k_B = 1.38\ 10^{-23} J/K$ is the so-called *Boltzmann constant* and W is the number of possible microstates of a system of a ideal gas constituted of identical particles. The number of microstates in agreement with the macrostate of the system involves combinatorial counting of the microstates. Hence, for L. Boltzmann, the entropy is an emerging notion from the statistics of the gas consituting particles.

On the other side, M. Planck in 1878, defended his PhD thesis entitled *Über den*

[1] in reference to [7].

[2] The existence of atoms has been accepted by the scientific community in 1906 after the work of J. Perrin.

zweiten Hauptsatz der mechanischen Wärmetheorie [3] where he defended that entropy is a fundamental concept. Hence, M. Planck and L. Boltzmann interpretation of entropy are rather distinct but M. Planck still needs to explain the mechanism of the irreversibility of events while L. Boltzmann's interpretation gives a statistical origin to irreversibility. M. Planck believes that the origin of irreversibility lies in the interaction between light and matter and hence, decide to consider the study of black body and black body radiation as a use-case. After weeks of work, M. Planck could successfully find an analytical expression for the black-body radiation (called Planck's law[8]) but at the expense of interpreting the vibrational energy of the oscillators [4] of the wall of the black body *not as a continuous, infinitely divisible quantity, but as a discrete quantity composed of an integral number of finite equal parts* where each such quantized energy writes :

$$\epsilon = h\nu, \tag{1.2}$$

where h is the *Planck's constant* and ν is the frequency of the oscillator. Hence, he had to admit that energy exchanges between matter and radiation in a black body were discrete and composed of quanta of value $\epsilon = h\nu$.

In 1905, A. Einstein put his hands on the black-body radiation and published a paper [7] where he introduced the photo-electric effect. In the introduction of the paper, he states that[5] *the energy of a light ray spreading out from a point source is not continuously distributed over an increasing space but consists of a finite number of energy quanta which are localized at points in space, which move without dividing, and which can only be produced and absorbed as complete units*. Hence, A. Einstein supported that not only matter and light exchange energy in quanta but light itself is constituted of quanta of energy. Finally, the spread of the Planck constant in physics reaches the fundamental concept of matter in 1913 when N. Bohr introduce his atom model, called *shell model* where electrons orbit around the nucleon on fixed and discretized orbits and can jump from an orbit to another by only emitting or absorbing a discrete number of energy quanta.

The quanta crisis is now total since the Planck constant is involved to describe matter and radiation. Hence, there was a need for the leading scientists of the beginning of the 20^{th} century to formalise what will become the theory of quantum mechanics. This has been possible since W. Nernst asked the Belgian industrialist and science enthousiast E. Solvay to organise and finance a conference in Brussels on the subject of *Radiation and the quanta*. E. Solvay accepted and found the first *Solvay Conference* that took place in the Metropole Hotel in Brussels with H. Lorentz as chairman. During this conference, major European physicists of that time such as W. Nernst, M. Brillouin, H. Lorentz, J. Perrin, W. Wien, M. Curie, H. Poincaré, M. Planck, A. Sommerfeld, M. de Broglie, J. H. Jeans, E. Rutherford, A. Eistein, P. Langevin and others could meet and exchange ideas about the quanta. This conference was later followed

[3] in english *On the second law of thermodynamics*
[4] or the atoms as we would say
[5] translated from German in [9]

by other Solvay conference in Brussels in 1913, 1921, 1924 and 1927 chaired by H. Lorentz. It was during the fifth Solvay conference in 1925 that A. Einstein said his now famous quote "*God does not play dice*" when expressing his scepticism about a probabilistic interpretation of quantum mechanics. During this fifth conference, representatives of the younger generation such as W. Heisenberg, N. Bohr, P. Dirac or W. Pauli where present. Hence, Brussels, as an international city in the heart of Europe in the early 20^{th} century, might arguably be considered as the birth place of quantum mechanics.

The first quantum revolution. In the middle of the 20^{th} century, quantum theory has been proven usefull for explaining many phenomena. Moreover, it has allowed to understand the structure of atoms as it provided a complete description of the orbitals of the hydrogen atom and light. Later, in 1963, R. J. Glauber established the foundation of the theory of quantum optics [10] that explains the coherence of a laser beam, a technology that was in development at that time. Today, lasers are at the center of all optical fiber communication systems and crucial for the internet's exchange of information between continents.

On the other side, in 1932, A. Wilson, after studying the application of quantum mechanics to conduction of electricity with W. Heisenberg, establish a theory explaining how energy bands for electrons allows a material to be conducting or an electrical insulator. Moreover, he witnessed another type of material called semi-conductor. This new type of material, that could be described as an insulator with a small energy gap, will lead J. Bardeen, W. Shockley and W. Brattain to discover the transistor, an electronic component at the earth of today's current information technology as computers are made of hundreds of billion of transistors.

Finally, it is possible to monitor the frequency of radiation of atoms in order to engineer atomic clocks. These atomic clocks allowed for a very accurate timekeeping capabilities and are essential for the navigation of satellites and the positioning technologies as the Global Positioning System (GPS).

The first quantum technological revolution allowed the creation and rise of essential technologies in our modern societies. However, they use the quantum description of matter and light but do not use directly the essential features and characteristics of quantum theory. Indeed, quantum exclusive properties such as entanglement was not used in the technological developments of the first quantum revolution.

The second quantum revolution. Since the early days of the *Age of information*, a significant effort has been made to build technological devices, such as computers, at smaller scales. Indeed, modern central processing units (CPU) contain tens of billions of transistor that have to fit in hundreds of mm^2. This device downsizing will

ultimately reach the boundary of the quantum physical world where a genuine quantum treatment is needed. Unexpectedly, using quantum physics in order to achieve informational objectives may even offer solutions with significantly improved performances compared to classical computers.

However, such quantum advantages come at the condition of a precise engineering of matter and light at the quantum scale. Hence, we may consider that the foundation of the *Quantum Technology era* started in the beginning of the 1980's with the first tests of Bell's theorem by J. Clauser [11] and A. Aspect [12]. It appeared that nonlocal, entangled and nonclassical correlation could be experimentally oberved in accordance with the predictions of A. Einstein, B. Podoslky and N. Rosen in their famous paper of 1935 [13] [6]. The second quantum revolution (or quantum information revolution) started later, in the 1990's, when multiple experiments and propositions where made showing how a proper use of quantum resources might have invaluable impacts on cryptography[14, 15], computational power[16, 17] and metrology [18]. These are now very active fields of research and have lead to a few first technological breakthrough such as quantum teleportation through satellites, gravitational field interferometers (such as LIGO) and secure quantum key distribution over 4600 km [19].

Numerous applications of quantum information technology require genuine quantum resources to be enabled, such as nonclassical states (e.g., Fock states or cat states) and entangled states (e.g., EPR states). Hence, there is a need for reliable criteria that can unambiguously certify the nonclassical or entangled nature of the states produced in the laboratory. Some work in this thesis is aimed at addressing this challenge.

Original contribution of the present thesis. The work presented in this thesis lies in the context of quantum optics. For this reason, the manuscript starts by reviewing some of the most important notions of quantum optics and phase-space representation. Also, we introduce the notations that will be used throughout the thesis for the quantum states and operation that we use. This in the content of Part I of the present thesis.

The following three parts (Part II, III, and IV) concern the three specific areas that we have contributed to in this thesis. We start each of these parts with an introduction where we review the tools and techniques that are specific to the associated fields and present the state of the art that is relevant to our original contribution. The details of our contributions are then developed in the subsequent section within each part. The order of Part II, III and IV simply follows the chronology of our contributions.

[6] Note that the first objective of this paper was to prove quantum mechanics was either an incomplete theory or non-local. Non-locality was not acceptable for Einstein, hence he concluded that the theory of quantum mechanics had to be completed by *hidden variables*.

Part II concerns the parameter estimation of continuous parameters encoded in coherent states. We demonstrate a conjecture stated by N. J. Cerf and S. Iblisdir in 2001 and we further generalize it with an optimal encoding and decoding strategy for encapsulating N continuous, real-valued parameters into N coherent states. This work uses the mathematical tools of quantum parameter estimation theory based on the quantum Cramér-Rao bound and Fisher information. Our original contribution is developed in more details in Chapter 4.

In Part III, we focus on a fundamental resource in quantum information theory, namely quantum entanglement. As it is generally difficult to assess if a quantum system is entangled or not (in which case it is called separable), an important endeavour consists in developing entanglement or separability criteria. We introduce a new separability criterion, called the weak realignment criterion, which enables a physical implementation in order to detect entanglement without the need for full state tomography. This new criterion is strengthened by a filtration procedure and benchmarked on Gaussian states. This original contribution is developed in more details in Chapter 6.

Finally, in Part IV, we focus on the notion of optical nonclassicality and on how to detect nonclassical quantum states, i.e., states that admit no classical counterpart (they cannot be expressed as convex mixtures of coherent states). We study the performance of nonclassicality criteria that can be derived from the matrix of moments of the electromagnetic field and design novel optical-nonclassicality observables that act on several replicas of a quantum state and whose expectation value coincides with the determinant of these matrices, hence providing witnesses of optical nonclassicality. These multicopy obervables are used to construct a family of physically implementable schemes using only linear optical operations and photon number detectors. This original contribution is developed in more details in Chapter 8.

Part I | Basics of quantum optics in phase space

2 | Quantum optics in phase space

2.1 Quantization of the electromagnetic field

The solution of the Maxwell's equations for the electric field $\mathbf{E}(\mathbf{r}, t)$ can be written as a decomposition in the different eigenfunctions, or mode functions, solving the Maxwell's equations as:

$$\mathbf{E}(\mathbf{r}, t) = \sum_{\mathbf{k},\lambda} E_{\mathbf{k}} \mathbf{e}_{\mathbf{k}}^{\lambda} \left[\alpha_{\mathbf{k},\lambda} \, e^{i(\mathbf{kr}-\omega_k t)} + \alpha_{\mathbf{k},\lambda}^{*} \, e^{-i(\mathbf{kr}-\omega_k t)} \right], \tag{2.1}$$

where k denotes the spatial mode number and λ the polarization.

The quantization of the electromagnetic field is done by replacing the complex dimensionless amplitudes α_k and α_k^* by the mutually adjoint operators $\hat{a}$ and $\hat{a}^\dagger$ respectively:

$$\begin{aligned} \alpha_k &\rightarrow \hat{a}_k, \\ \alpha_k^* &\rightarrow \hat{a}_k^\dagger, \end{aligned} \tag{2.2}$$

where k stands for both the spatial mode and polarization mode. The operators $\hat{a}_k$ and $\hat{a}_k^\dagger$ are called the *annihilation* and *creation operators* respectively (or *ladder operators*) because, as it will be detailed later, they will allow to annihilate and create particles associated with the electromagnetic field: photons. Hence, since photons are bosonic particles, the annihilation and creation operators $\hat{a}$ and $\hat{a}^\dagger$ do need to respect the bosonic commutation relations:

$$\begin{aligned} \left[\hat{a}_k, \hat{a}_{k'}\right] &= 0, \\ \left[\hat{a}_k^\dagger, \hat{a}_{k'}^\dagger\right] &= 0, \\ \left[\hat{a}_k, \hat{a}_{k'}^\dagger\right] &= \delta_{k,k'}, \end{aligned} \tag{2.3}$$

where $\delta_{k,k'}$ is the Kronecker symbol. These commutation relations can be written in a more compact form by defining the vectorial operator $\mathbf{a} := (\hat{a}_1, \hat{a}_1^\dagger, \hat{a}_2, \hat{a}_2^\dagger, ..., \hat{a}_n, \hat{a}_n^\dagger)^T$ composed of the creation and annihilation operators $\hat{a}_k$ and $\hat{a}_k^\dagger$ in each mode k and

the symplectic form matrix:

$$\Omega := \oplus_{k=1}^{n} \omega, \tag{2.4}$$

where:

$$\omega := \begin{pmatrix} 0 & 1 \\ -1 & 0 \end{pmatrix}, \tag{2.5}$$

is called the symplectic matrix. Hence, the bosonic commutation relations (2.3) become:

$$\left[\mathbf{a}_i, \mathbf{a}_j\right] = \Omega_{ij}, \tag{2.6}$$

where the labels i and j refer to the components of the vectorial operator $\mathbf{a}$ and not to the different modes.

Through the quantization of the electromagnetic field (2.2), the Hamiltonian of the electromagnetic field can be rewritten in terms of the ladder operators as [1]:

$$\hat{H} = \sum_k (\hat{a}_k^\dagger \hat{a}_k + \frac{1}{2}), \tag{2.7}$$

which is expressed in natural dimension where the reduced Planck constant $\hbar = 1$ and the mode frequency $\omega_k = 1$. Hence, the Hamiltonian is the sum of the photon number in each mode multiplied by the individual energy of a photon in that mode $\hbar\omega_k$ that is normalized to 1 in our convention.

The eigenstates of (2.7) are the so-called Fock states (see section 2.4.1 for more details) and are written in the Dirac bra-ket notation as $|n_k\rangle$. Hence, one can rewrite the Hamiltonian (2.7) as:

$$\hat{H} = \sum_k (\hat{n}_k + \frac{1}{2}), \tag{2.8}$$

where $\hat{n} = \hat{a}_k^\dagger \hat{a}_k$ is the *number operator* (or photon number operator). Consequently, the Fock states are the eigenvectors of the number operator of eigenvalue n_k as:

$$\hat{n}_k |n_k\rangle = n_k |n_k\rangle. \tag{2.9}$$

The eigenvalues n_k are natural numbers as the Fock state basis forms a complete discrete basis of the Hilbert space. Indeed, by applying the ladder operators one can travel, step by step, in the Fock states basis as:

$$\begin{aligned} \hat{a}|n\rangle &= \sqrt{n}\,|n-1\rangle, \\ \hat{a}^\dagger|n\rangle &= \sqrt{n+1}\,|n+1\rangle. \end{aligned} \tag{2.10}$$

with the constraint that:

$$\hat{a}|0\rangle = 0, \tag{2.11}$$

[1] As it will be pointed later, the Hamiltonian of the electromagnetic field is the same as for an harmonic oscillator. Hence, in what follows, a mode k will be understood as an harmonic oscillator.

where $|0\rangle$ is called the *vacuum state*. Hence, one can construct the Fock state $|n\rangle$ from the vacuum state $|0\rangle$ by applying the creation operator n times as follows:

$$|n\rangle = \frac{\hat{a}^{\dagger n}}{\sqrt{n!}}|0\rangle. \tag{2.12}$$

It is also possible to define, from the single mode annihilation and creation operators $\hat{a}$ and $\hat{a}^\dagger$, the *quadrature operators* of the electromagnetic field as:

$$\begin{aligned} \hat{x} &= \frac{\hat{a} + \hat{a}^\dagger}{\sqrt{2}}, \\ \hat{p} &= \frac{\hat{a} - \hat{a}^\dagger}{\sqrt{2}i}. \end{aligned} \tag{2.13}$$

These quadrature operators (2.13) do play an analogous role as, respectively, the position and the momentum operators of the harmonic oscillator. The commutation relations between the quadrature operators is:

$$[\hat{x}, \hat{p}] = i. \tag{2.14}$$

Hence, the uncertainty relation for quadratures writes:

$$\sigma_x^2 \, \sigma_p^2 \geq \frac{1}{4}, \tag{2.15}$$

where $\sigma_x^2 = \langle \hat{x}^2 \rangle - \langle \hat{x} \rangle^2$ is the variance in the quadrature x and $\sigma_x^2 = \langle \hat{p}^2 \rangle - \langle \hat{p} \rangle^2$ is the variance in the quadrature p. The eigenstates vectors of the quadrature operators are such that:

$$\begin{aligned} \hat{x}|x\rangle &= x|x\rangle, \\ \hat{p}|p\rangle &= p|p\rangle, \end{aligned} \tag{2.16}$$

where x, p are real numbers. Therefore, we remark that, in contrast to the number operator $\hat{n}$, the quadrature operators admit a continuous spectrum. Moreover, the continuous sets of vectors $\{|x\rangle\}$ and $\{|p\rangle\}$ form an orthogonal basis of the Hilbert space since:

$$\begin{aligned} \langle x|x'\rangle &= \delta_{xx'} = \delta(x - x'), \\ \langle p|p'\rangle &= \delta_{pp'} = \delta(p - p'), \end{aligned} \tag{2.17}$$

where δ is the Dirac delta distribution. These basis are also complete:

$$\begin{aligned} \int_{-\infty}^{\infty} dx \, |x\rangle\langle x| &= \mathbb{1}, \\ \int_{-\infty}^{\infty} dp \, |p\rangle\langle p| &= \mathbb{1}. \end{aligned} \tag{2.18}$$

The eigenbasis of the quadrature operators are related to each other through Fourier

transform:

$$\begin{aligned} |x\rangle &= \frac{1}{2\pi}\int_{-\infty}^{\infty} dp\, e^{-ixp}|p\rangle, \\ |p\rangle &= \frac{1}{2\pi}\int_{-\infty}^{\infty} dx\, e^{ixp}|x\rangle. \end{aligned} \tag{2.19}$$

Hence, the quadrature basis will be central in the study of the so-called *continuous variable* systems or CV-systems. These systems are a collection of n harmonic oscillators, each of them being described by an infinite-dimensional Hilbert space. In the case when they are described by operators with a continuous spectrum (such as the quadrature operators for the electromagnetic fields or the position and momentum operators), these systems are called continuous variable systems. Hence, a single harmonic oscillator can be described by infinite dimensional basis that is either the Fock-state discrete basis or the quadrature-state continuous basis and it will be possible to go from the discrete description to the continuous description.

2.2 Phase space representation

The phase space representation was introduced in classical mechanics in order to represent the dynamics of a system. Indeed, each degree of freedom of the system is an axis in the phase space representation. For an harmonic oscillator, the axis are the position and the momentum of the particle.

In quantum mechanics, the position and momentum of a particle are conjugate variables and the associated operators do not commute (2.14). Hence, the statistics of these variables have to satisfy uncertainty relations like the Heisenberg uncertainty relation and it has the effect that a quantum state cannot be represented on phase space as a single point like classical point masses. Therefore, they need to be represented by functions that share properties of probability distributions but not necessarily all of them. These functions are hence called *quasi-probability distributions*. In the following section, we present three of them : the Wigner function, the Glauber-Sudarshan P-function and the Husimi Q-function.

These quasi-probability functions are widely used in continuous variable quantum optics and information. They are related by convolution product with a Gaussian distribution. However, they differ from a classical probability density by different properties. For example, the Wigner function accept negative values. Therefore, these different properties lead to different criteria for detecting interesting quantum properties of the state represented by each of these functions.

2.2.1 Wigner function

Let us start with the Wigner function as it is the most common function used to represent a quantum state in phase space. Indeed, the Wigner function is not singular like the Glauber-Sudarshan P-function and admits negative values which is a good and visible witness of nonclassicality (the Husimi Q function is always positive).

The definition of the Wigner function of a state is based on the notion of *characteristic function*. Indeed, any state ρ can be represented by its characteristic function:

$$\chi(\gamma) = \mathrm{Tr}[\hat{D}(\gamma)\rho], \tag{2.20}$$

where $\hat{D}(\gamma)$ is the Weyl displacement operator (2.55) and $\gamma \in \mathbb{C}$. By taking the Fourier transform of the characteristic function, one finds the single mode Wigner function of the state ρ:

$$W(\alpha) = \frac{1}{\pi^2}\int_{-\infty}^{\infty} d\gamma\, e^{\gamma^*\alpha - \gamma\alpha^*}\chi(\gamma). \tag{2.21}$$

The multimode Wigner function is defined as

$$W(\mathbf{x},\mathbf{p}) = \frac{1}{(2\pi)^n}\int_{-\infty}^{\infty} d\mathbf{y}\, e^{-\mathbf{p}.\mathbf{y}}\langle \mathbf{x}+\frac{\mathbf{y}}{2}|\rho|\mathbf{x}-\frac{\mathbf{y}}{2}\rangle, \tag{2.22}$$

and $W(\mathbf{x},\mathbf{p}) = \tilde{W}(\mathbf{x},\mathbf{p})/(2\pi)^n$ where $\tilde{W}(\mathbf{x},\mathbf{p})$ is the Weyl transform of the multimode state ρ. The Weyl transform $\tilde{A}(\mathbf{x},\mathbf{p})$ of the operator $\hat{A}$ is defined as:

$$\tilde{A}(\mathbf{x},\mathbf{p}) = \int d\mathbf{y}\, e^{-\mathbf{p}.\mathbf{y}}\langle \mathbf{x}+\frac{\mathbf{y}}{2}|\hat{A}_S|\mathbf{x}-\frac{\mathbf{y}}{2}\rangle, \tag{2.23}$$

where $\hat{A}_S$ is the symmetric order form of $\hat{A}$ operator[2].

The Wigner function is normalized to one:

$$\int_{-\infty}^{\infty} d\mathbf{x}d\mathbf{p}\, W(\mathbf{x},\mathbf{p}) = 1, \tag{2.24}$$

which is a desired property for the Wigner function to represent a physical quantum state since $\mathrm{Tr}(\hat{\rho}) = 1$.

The marginals of the Wigner function are:

$$W(\mathbf{x}) = \int_{-\infty}^{\infty} d\mathbf{p}\, W(\mathbf{x},\mathbf{p}) = \langle \mathbf{x}|\rho|\mathbf{x}\rangle, \tag{2.25}$$

[2]For example, the symmetric order form of $\hat{x}\hat{p}$ is $\frac{\hat{x}\hat{p}+\hat{p}\hat{x}}{2}$

$$W(\mathbf{p}) = \int_{-\infty}^{\infty} d\mathbf{x}\, W(\mathbf{x}, \mathbf{p}) = \langle \mathbf{p}|\rho|\mathbf{p}\rangle. \tag{2.26}$$

At the origin of phase space, i.e. for $x = 0$ and $p = 0$, the value of the Wigner function writes:

$$W(0,0) = \frac{1}{\pi}\mathrm{Tr}[\rho\hat{\Pi}], \tag{2.27}$$

where $\Pi = (-1)^{\hat{a}^\dagger \hat{a}}$ is the parity operator.

One can use the Wigner function to evaluate the mean value of an operator $\hat{A}$ as:

$$\langle \hat{A} \rangle = \mathrm{Tr}[\rho \hat{A}] = \int_{-\infty}^{\infty} d\mathbf{x} d\mathbf{p} W(\mathbf{x}, \mathbf{p}) \tilde{A}(\mathbf{x}, \mathbf{p}), \tag{2.28}$$

2.2.2 Glauber-Sudarshan P-function

Any density operator $\hat{\rho}$ representing the quantum state of a single oscillator (bosonic) mode can be represented in a diagonal form in the coherent state basis $|\alpha\rangle$, namely

$$\hat{\rho} = \int P(\alpha)|\alpha\rangle\langle\alpha| d^2\alpha, \tag{2.29}$$

where $P(\alpha)$ is the Glauber-Sudarshan P-function. Note that $P(\alpha)$ completely defines state $\hat{\rho}$ and is normalized since $\mathrm{Tr}(\hat{\rho}) = 1$. A state $\hat{\rho}$ is said to be *classical* if its associated P-function behaves as a probability distribution $P(\alpha) = P_{cl}(\alpha)$, hence it is non-negative. Any convex mixture of coherent states $|\alpha\rangle$ is thus classical by definition. Conversely, a quantum state $\hat{\rho}$ is considered to be *nonclassical* if it cannot be written as a mixture of coherent states, i.e., if $P(\alpha) \neq P_{cl}(\alpha)$. Simple examples of nonclassical states include Fock states or squeezed states, whose P-functions are not regular (their expressions involve derivatives of Dirac δ-functions).

The expectation value of any normally-ordered operator function $:g(\hat{a}, \hat{a}^\dagger):$ of the annihilation $\hat{a}$ and creation $\hat{a}^\dagger$ operators can be expressed using the P-function as

$$\langle :g(\hat{a}, \hat{a}^\dagger): \rangle = \int d^2\alpha\, P(\alpha)\, g(\alpha, \alpha^*). \tag{2.30}$$

In this expression, the colon indicates normal ordering, which means that all creation operators must be placed on the left of annihilation operators. Hence, if the P-function $P(\alpha)$ admits negative values, then Eq. (7.2) can be negative for some well chosen function $g(\hat{a}, \hat{a}^\dagger)$, witnessing the nonclassicality of state $\hat{\rho}$. This suggests a close connection between the expectation values of normally-ordered functions and the nonclassical character of the P-function. Indeed, as observed in Ref. [20], any operator of the form $:\hat{f}^\dagger \hat{f}:$ is an Hermitian operator that yields a sufficient condition of nonclassicality (see Part IV).

2.2.3 Husimi Q-function

Finally, another function that is used to represent a quantum state ρ is the *Husimi Q-function* defined as the diagonal matrix elements of the density operator in a pure coherent state $|\alpha\rangle$:

$$Q(\alpha) = \frac{\langle\alpha|\rho|\alpha\rangle}{\pi} \geq 0. \tag{2.31}$$

The Husimi function is bounded:

$$Q(\alpha) \leq \frac{1}{\pi}. \tag{2.32}$$

The relation between the Husimi function $Q(\alpha)$ and the Glauber-Sudarshan function $P(\beta)$ is:

$$Q(\alpha) = \frac{\langle\alpha|\rho|\alpha\rangle}{\pi} = \frac{1}{\pi}\int P(\beta)\ |\langle\alpha|\beta\rangle|^2\ d^2\beta = \frac{1}{\pi}\int P(\beta)\ e^{-|\alpha-\beta|^2}\ d^2\beta. \tag{2.33}$$

Hence, the Husimi Q-Function is a Gaussian convolution of the Glauber-Sudarshan P-function. The Husimi Q-function is best suited for evaluating the anti-normally ordered operators[3] since:

$$\langle\hat{a}^n\hat{a}^{\dagger m}\rangle = \int \alpha^n\alpha^{*m}\ Q(\alpha,\alpha^*)\ d^2\alpha. \tag{2.34}$$

2.2.4 Unitary and symplectic transformations

The phase space representation of quantum systems is described by an associated algebra, called symplectic formalism, for expressing the unitary transformation of quantum states that we will review in this section.

Let us start by recalling how quantum states evolve under an unitary operator:

$$U = e^{iH}, \tag{2.35}$$

where H is the Hamiltonian describing the evolution of the state and needs to be hermitian $H = H^\dagger$. Hence, the operator U is obviously unitary $U^\dagger U = e^{-iH}e^{iH} = \mathbb{1}$. The state ρ evolves under unitary transformation as:

$$\rho \to U\rho U^\dagger. \tag{2.36}$$

An important class of unitary transformation are the *Gaussian transformations* which preserve the Gaussian character when applied to Gaussian states. These are the unitary operators which Hamiltonian is at most quadratic in the annihilation and cre-

[3] which means that all annihilation operators must be placed on the left of creation operators.

ation operators:

$$H_G = \hat{a}^\dagger \alpha + \hat{a}^\dagger F \hat{a} + \hat{a}^\dagger G \hat{a}^\dagger + h.c. \tag{2.37}$$

where α is a complex number and F and G are symmetric and complex $n \times n$ matrices (and *h.c.* stands for hermitian conjugate). These Gaussian unitaries do preserve the Gaussian properties of the transformed states. This means that Gaussian unitaries transform Gaussian states into Gaussian states.

The unitary transformations can further be discriminated in two categories: the *passive* and the *active* unitary transformations. Passive transformations preserve the mean number of photons of the state $\langle \hat{n} \rangle_\rho$ after the transformation while the active transformations do change the mean number of photons of the state. Hence, unitary transformations can be characterized as Gaussian or non-Gaussian transformations and as passive or active transformations. We will see that the family of Gaussian unitary transformations is divided into the passive Gaussian unitary transformations (containing the phase shift transformation and the beam splitter transformation) and the active Gaussian unitary transformations (containing the squeezing operation).

In the Heisenberg picture, the Gaussian unitary transformations on the bosonic annihilation and creation operators correspond to Bogoliubov transformations :

$$\hat{a} \to U^\dagger \hat{a} U = A\hat{a} + B\hat{a}^\dagger + \alpha, \tag{2.38}$$

where α is a complex number and A and B are $n \times n$ matrices that need to satisfy $AB^T = BA^T$ and $AA^T = BB^T + \mathbb{1}$ in order to preserve the bosonic commutation relations after the transformation.

Now, when we consider the continuous variable description of quantum states in terms of the quadrature operators, Gaussian unitary transformations write:

$$\hat{r} \to S\hat{r} + d. \tag{2.39}$$

where $\hat{r}$ is the vector $(\hat{x}_1, \hat{p}_1, \hat{x}_2, \hat{p}_2, ...)$ and S is a symplectic matrix. In order to preserve the commutation relation after the transformation, the matrix S has to be *symplectic* which means that it has to satisfy:

$$S\Omega S^T = \Omega, \tag{2.40}$$

where Ω is the symplectic matrix (2.4).

The symplectic Gaussian operations will be explicitly described in section 2.5.

2.3 Gaussian states

An important class of quantum states in continuous variable quantum optics are the *Gaussian states*. A state can be called Gaussian if its Wigner function (2.22) is a Gaussian distribution. Hence, a Gaussian state is completely characterized by its moments of order 1 and 2, namely its *mean value vector* $\langle \mathbf{r} \rangle$ (also named *displacement vector*) and its *covariance matrix* γ that we introduce in this section. Therefore, the Wigner function of a Gaussian state can always be written as:

$$W_G(\mathbf{x}, \mathbf{p}) = \frac{1}{(2\pi)^n \sqrt{\det \gamma}} e^{-\frac{1}{2}(\mathbf{r}-\langle \mathbf{r} \rangle)^T \gamma^{-1} (\mathbf{r}-\langle \mathbf{r} \rangle)}. \tag{2.41}$$

where $\mathbf{x} = \{x_1, x_2, ..., x_n\}$ and $\mathbf{p} = \{p_1, p_2, ..., p_n\}$ are respectively the x- and p-vectors and the mean value vector is defined as:

$$\langle \mathbf{r} \rangle = \mathrm{Tr}(\mathbf{r}\rho), \tag{2.42}$$

where $\mathbf{r} = \{\hat{x}_1, \hat{p}_1, \hat{x}_2, \hat{p}_2, ..., \hat{x}_n, \hat{p}_n\}$ is the $2n-$dimensional quadratures vector.

In the particular case of a 1-mode state, the covariance matrix writes:

$$\gamma = \begin{pmatrix} \sigma_x^2 & \sigma_{xp} \\ \sigma_{px} & \sigma_p^2 \end{pmatrix}, \tag{2.43}$$

where the diagonal entries are the variance of the quadrature variables (sometimes written $\sigma_x^2 = \Delta x^2$ and $\sigma_p^2 = \Delta p^2$) and the off-diagonal elements are the covariance of the quadrature variables. More generally, the covariance matrix elements can be written in terms of the quadrature vectors as:

$$\gamma_{ij} = \frac{1}{2}\langle \{\hat{r}_i, \hat{r}_j\} \rangle - \langle \hat{r}_i \rangle \langle \hat{r}_j \rangle. \tag{2.44}$$

Since the Wigner function for Gaussian states (2.41) is completely determined by the mean value vector and the covariance matrix, we will only give, in the following examples of Gaussian states, their mean value vector and covariance matrix.

It must be noted that all covariance matrix γ do not represent physical quantum systems. Indeed, they must, at least, satisfy the well known Heisenberg uncertainty relation:

$$\sigma_x^2 \sigma_p^2 \geq \frac{1}{4}. \tag{2.45}$$

However, the issue with the Heisenberg uncertainty relation is that it is not invariant under rotation in phase space. To overcome this problem, Schrödinger and Robertson proposed a more general uncertainty relation, usually called the *Schrödinger-*

Robertson uncertainty relation, which writes:

$$\det(\gamma) \geq \frac{1}{4}, \tag{2.46}$$

when applied to quadrature operators. This relation inherits from the nice properties of the determinant and is hence obviously invariant under all symplectic transformation since the determinant of symplectic matrices is equal to 1. Therefore, all pure Gaussian states (as the coherent and squeezed states introduced below) saturate the Schrödinger-Robertson relation (2.46) which was not necessarily the case for the Heisenberg uncertainty relation.

In the two-mode case, it is always possible by applying symplectic transformations S to transform the covariance matrix into its *standard forms* [21]. There exists two different standard forms.

The first type of standard form, noted *standard form I*, is the following:

$$\gamma = \begin{pmatrix} a & 0 & c & 0 \\ 0 & a & 0 & d \\ c & 0 & b & 0 \\ 0 & d & 0 & b \end{pmatrix}, \tag{2.47}$$

where the elements a, b needs to satisfy $a, b \geq 1/2$ in order for the covariance matrix γ to satisfy the Heisenberg uncertainty relation. Moreover, as the covariance matrix is positive semi-definite, this imposes that $c^2,\ d^2 \leq ab$. Finally, the last physicality condition is that the symplectic values of the covariance matrix γ needs to satisfy : $\nu_\pm \geq 1/2$ [4]

The second type of standard form, noted *standard form II*, is the following:

$$\gamma^{II} = \begin{pmatrix} n_1 & 0 & c_1 & 0 \\ 0 & n_2 & 0 & c_2 \\ c_1 & 0 & m_1 & 0 \\ 0 & c_2 & 0 & m_2 \end{pmatrix}, \tag{2.48}$$

where the n_i, m_i and c_i satisfy the following equalities:

$$\begin{aligned} \frac{n_1 - 1}{m_1 - 1} &= \frac{n_2 - 1}{m_2 - 1}, \\ |c_1| - |c_2| &= \sqrt{(n_1 - 1)(m_1 - 1)} - \sqrt{(n_2 - 1)(m_2 - 1)}. \end{aligned} \tag{2.49}$$

Another decomposition of the covariance matrix is given by the Williamson's theorem. This theorem states that there exists a symplectic transformation S that trans-

[4] The symplectic values of the covariance matrix can be found by searching the eigenvalues of $i\Omega\gamma$ where Ω is the symplectic matrix (2.4).

forms the covariance matrix in a diagonal form as:

$$\gamma = S\gamma^{\oplus}S^T, \tag{2.50}$$

where:

$$\gamma^{\oplus} = \oplus_{k=1}^{n} \nu_k \mathbb{1}_{2\times 2}, \tag{2.51}$$

and the diagonal elements appear in pairs of the so-called *symplectic values* ν_k. In the case of Gaussian states, the Williamson's theorem can be applied to the covariance matrix such that any Gaussian state can be constructed through Gaussian unitaries from a collection of thermal product states where $\nu_k = 1/(\bar{n}+1)$ where $\bar{n}$ is the mean number of thermal photons [5].

2.3.1 Coherent states

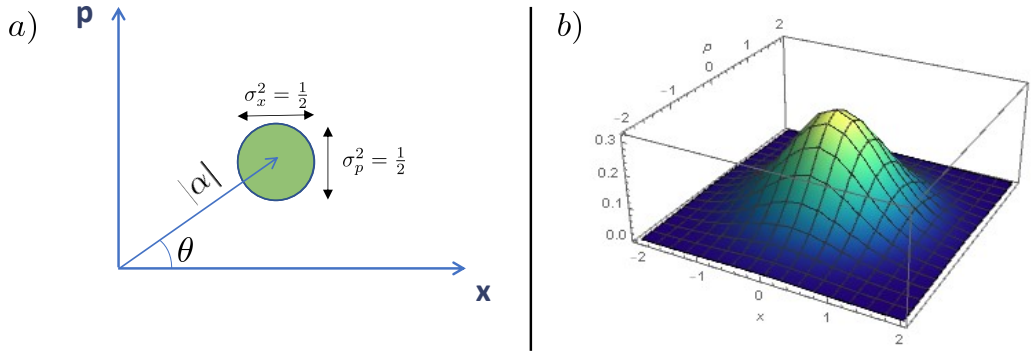

Figure 2.1: *a)* Phase space representation of a coherent state $|\alpha\rangle$. The norm $|\alpha|$ and the phase θ is represented and the green area correspond to the variance $\Delta x_\theta^2 = 1/2$. *b)* Three-dimensional phase space representation of a centered coherent state, i.e. the vacuum state.

Coherent states are the states produced by a laser. The laser technology is very-well mastered and coherent states are hence easy to produce in a laboratory. While described in quantum optics by the means of non-commuting observables, they are usually considered as *classical* states since their Glauber-Sudarshan P-function is a Dirac delta. Coherent states show no quantum advantage for some quantum tasks such as quantum parameter estimation interferometry [22] or quantum computation [23]. However, they can be used for quantum key distribution protocols [24, 25] in quantum cryptography.

Mathematically, they are the eigenstates of the annihilation operator :

$$\hat{a}|\alpha\rangle = \alpha|\alpha\rangle, \tag{2.52}$$

where the eigenvalue α is a complex number and his polar decomposition is $\alpha =$

[5] see (2.80) for the definition of $\bar{n}$

$|\alpha|e^{i\theta}$ (see Fig. 2.1).

As we will see, they can be generated by the means of the *Weyl displacement operator* defined as :

$$\hat{D}(\alpha) = e^{\alpha\hat{a}^\dagger - \alpha^*\hat{a}}. \tag{2.53}$$

The Weyl displacement operator is an unitary operator and its inverse can be found simply by taking the opposite sign of the variable α as :

$$\hat{D}^\dagger(\alpha) = \hat{D}^{-1}(\alpha) = \hat{D}(-\alpha). \tag{2.54}$$

The application of the displacement operator on the creation and annihilation operators is given by the following transformation :

$$\hat{D}^\dagger(\alpha)\hat{a}\hat{D}(\alpha) = \hat{a} + \alpha \quad \text{and} \quad \hat{D}^\dagger(\alpha)\hat{a}\hat{D}^\dagger(\alpha) = \hat{a}^\dagger + \alpha^*. \tag{2.55}$$

From the equations (2.52) and (2.55) , we can now see that coherent states can be produced by applying the displacement operator on the vacuum state $|0\rangle$. The decomposition of the coherent state in the Fock basis $\{|n\rangle\}$ is :

$$|\alpha\rangle = \hat{D}(\alpha)|0\rangle = e^{-\frac{|\alpha|}{2}} \sum_{n=0}^{\infty} \frac{\alpha^n}{\sqrt{n!}}|n\rangle. \tag{2.56}$$

The coherent states are not orthogonal since :

$$\langle\beta|\alpha\rangle = e^{\frac{|\beta-\alpha|^2}{2}}. \tag{2.57}$$

However they form an over-complete basis of the Hilbert space, meaning that :

$$\frac{1}{\pi}\int d^2\alpha|\alpha\rangle\langle\alpha| = 1. \tag{2.58}$$

The photon number statistics can be calculated from equation (2.56) and follow a Poisson distribution :

$$P(n) = |\langle n|\alpha\rangle|^2 = e^{-|\alpha|^2}\frac{|\alpha|^{2n}}{n!}. \tag{2.59}$$

Moreover, a property of Poisson distributed statistics is that its variance $\sigma_n^2 = \langle\Delta(\hat{n})^2\rangle = \langle\hat{n^2}\rangle - \langle\hat{n}\rangle^2$ is equal to its mean value $\langle\hat{n}\rangle$. This is indeed the case for coherent states since :

$$\sigma_n^2 = \langle\hat{n}\rangle = |\alpha|. \tag{2.60}$$

The Poissonian character of the number distribution of the coherent states is also confirmed by evaluating the so-called *Mandel Q parameter* defined as :

$$Q = \frac{\langle\Delta(\hat{n})^2\rangle - \langle\hat{n}\rangle}{\langle\hat{n}\rangle}. \tag{2.61}$$

The Mandel Q parameter was introduced by Leonard Mandel in 1979 [26] and evaluates how much an occupation number distribution is distant from a Poisson distribution. The value of the Mandel Q parameter for a Poisson distribution is $Q = 0$. Obviously, the Mandel Q parameter for coherent states is : $Q_{|\alpha\rangle} = 0$. A negative value for the Mandel Q parameter is a signature of nonclassicality and the minimal value is : $Q_{min} = -1$ and is realised for Fock states.

Finally, the effect of the displacement operator on the quadrature operators is :

$$\hat{D}^\dagger(\alpha)\hat{x}\hat{D}(\alpha) = \hat{x} + \sqrt{2}\Re(\alpha) \quad \text{and} \quad \hat{D}^\dagger(\alpha)\hat{p}\hat{D}^\dagger(\alpha) = \hat{p}^\dagger + \sqrt{2}\Im(\alpha), \tag{2.62}$$

where $\Re(\alpha)$ and $\Im(\alpha)$ stand for the real and imaginary part of the complex number α. From equation (2.62), we can evaluate the first and second order moment of the coherent states. These moments are summarized in the displacement vector $\mathbf{r}$ and the covariance matrix γ :

$$\mathbf{r} = \begin{pmatrix} \sqrt{2}\Re(\alpha) \\ \sqrt{2}\Im(\alpha) \end{pmatrix} \quad \text{and} \quad \gamma = \frac{1}{2}\mathbb{1}. \tag{2.63}$$

Hence, we see that the action of the displacement operator is to displace the vacuum states in phase space. Therefore, the coherent state and the vacuum state share the same covariance matrix $\gamma_{|\alpha\rangle} = \gamma_{vac}$. Finally, coherent states are states that saturate the Heisenberg uncertainty relation 2.45 with equal variances $\sigma_x^2 = \sigma_y^2 = 1/2$ in agreement with equation (2.63).

2.3.2 Squeezed states

The Gaussian operator for squeezing is:

$$S(\xi) = e^{\frac{\xi\hat{a}^{\dagger 2} - \xi^*\hat{a}^2}{2}}, \tag{2.64}$$

with $\xi = re^{i\phi}$, where r is a real number called the *squeezing factor* and ϕ is the *squeezing angle* and takes values in the set $[0, \pi]$. The squeezing operator is an unitary operator and its inverse can be found by taking the opposite sign of the variable ξ:

$$S^\dagger(\xi) = S^{-1}(\xi) = S(-\xi). \tag{2.65}$$

The application of the squeezing operator on the creation and annihilation operators is given by the following transformations:

$$\begin{aligned} \hat{S}^\dagger(\xi)\hat{a}\hat{S}(\xi) &= \cosh(r)\hat{a} - e^{i\phi}\sinh(r)\hat{a}^\dagger \\ \hat{S}^\dagger(\xi)\hat{a}\hat{S}^\dagger(\xi) &= \cosh(r)\hat{a}^\dagger - e^{-i\phi}\sinh(r)\hat{a}. \end{aligned} \tag{2.66}$$

In order to create a vacuum squeezed state, one has to apply the squeezing operator

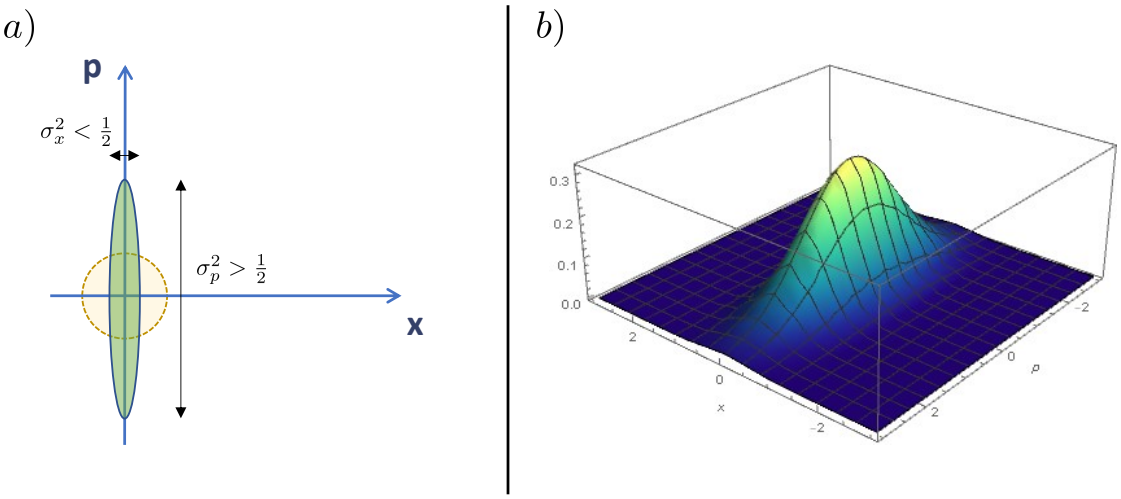

Figure 2.2: *a)* Phase space representation of a squeezed state $|\xi\rangle$ (in green). The state is squeezed in the x-quadrature. Indeed, the variance in the x-quadrature is $\Delta x^2 = e^{-2r}/2$ while the variance in the p-quadrature is $\Delta p^2 = e^{2r}/2$. The yellow dashed disc is the phase space representation of the vacuum state. Note that the area of the yellow and green ellipses is equal. *b)* Three-dimensional phase space representation of a squeezed state.

to the vacuum state as follows (see Fig. 2.2):

$$|\xi\rangle = S(\xi)|0\rangle. \tag{2.67}$$

As the Hamiltonian of the squeezing operator in equation (2.64) is quadratic in the creation and annihilation operators, the decomposition of a squeezed vacuum state in the Fock basis involve only the even Fock states :

$$|\xi\rangle = \frac{1}{\sqrt{\cosh(r)}} \sum_{n=0}^{\infty} \frac{\sqrt{(2n)!}}{2^n n!} e^{in\phi} (\tanh(r))^n |2n\rangle. \tag{2.68}$$

In general, a squeezed state might be displaced in phase space. This state is then described by the following state :

$$|\alpha, \xi\rangle = D(\alpha)S(\xi)|0\rangle. \tag{2.69}$$

Note that squeezing and displacement operator do not commute $D(\alpha)S(\xi) \neq S(\xi)D(\alpha)$. However, the following relation holds:

$$D(\alpha)S(\xi) = S(\xi)D(\cosh(r)\alpha + e^{i\phi}\sinh(r)\alpha^*). \tag{2.70}$$

Hence, one can first act with a well calibrated displacement operator and then apply a squeezing operation to the displaced state in order to generate the displaced squeezed state $|\alpha, \xi\rangle$ given by equation (2.69).

Let us focus on the effect of squeezing on the quadrature operators. For the purpose of clarity, we will fix the squeezing angle to $\phi = 0$ such that $\xi = r$. Then, we can write the following transformation of the quadrature operators under the application of the squeezing operator:

$$\hat{S}^\dagger(\xi)\hat{x}\hat{S}(\xi) = e^{-r}\hat{x} \quad \text{and} \quad \hat{S}^\dagger(\xi)\hat{p}\hat{S}^\dagger(\xi) = e^{r}\hat{p}. \tag{2.71}$$

By squeezing a vacuum state $|0\rangle$, it can be seen from equation (2.71) that the first moments $\langle\hat{x}\rangle$ and $\langle\hat{p}\rangle$ are unchanged and remain equal to 0. In order to displace a squeezed vacuum state, obtained by applying the squeezing operator $\hat{S}(\xi)$ to the vacuum state, in phase space, one has to further apply a displacement operator to it.

Nevertheless, from the equations (2.71), we can calculate the second order moment of a squeezed state (displaced or not). These moments are summarized in the following covariance matrix γ:

$$\gamma = \frac{1}{2}\begin{pmatrix} e^{-2r} & 0 \\ 0 & e^{2r} \end{pmatrix}. \tag{2.72}$$

This means that by applying a squeezing operator of squeezing parameter $\xi = r$ (with $r > 0$), the state is squeezed in the x-quadrature and is anti squeezed in the p-parameter.

Finally, we give some moments of the creation and annihilation operators up to order 4:

$$\begin{aligned} \langle\hat{a}^\dagger\hat{a}\rangle_S &= \sinh^2(r), \\ \langle\hat{a}^{\dagger 2}\rangle_S = \langle\hat{a}^2\rangle_S &= -\sinh(r)\cosh(r), \\ \langle\hat{a}^{\dagger 2}\hat{a}^2\rangle_S &= \sinh^2(r)(\cosh^2(r) + 2\sinh^2(r)), \\ \langle\hat{a}^{\dagger 3}\hat{a}\rangle_S = \langle\hat{a}^\dagger\hat{a}^3\rangle_S &= -3\sinh^3(r)\cosh(r), \\ \langle\hat{a}^{\dagger 4}\rangle_S = \langle\hat{a}^4\rangle_S &= 3\sinh^2(r)\cosh^2(r). \end{aligned} \tag{2.73}$$

These results are used in section 8.1 to calculate the different determinants of principal submatrices taken from matrix of moments (Eq. 7.23) for squeezed states.

2.3.3 Two-mode squeezed vacuum state

The *two-mode squeezing operator* (TMSO) is a two-mode Gaussian unitary that writes:

$$U_{TMS} = e^{\frac{r}{2}\left(\hat{a}_1\hat{a}_2 - \hat{a}_1^\dagger\hat{a}_2^\dagger\right)}, \tag{2.74}$$

where r is the squeezing parameter. Indeed, by sending two orthogonal squeezed states on a balanced beam splitter (see section 2.5.2), one generates a *two-mode squeezed vacuum* (TMSV):

$$|TMSV\rangle = U_{BS}^{50:50}|\xi, -\xi\rangle. \tag{2.75}$$

Equivalently, the TMSV can be generated by applying the TMSO on the vacuum state:

$$|TMSV\rangle = U_{TMS}|0\rangle. \tag{2.76}$$

The physical implementation of the TMSO will be given in section 2.5.4.

The TMSV is a two-mode entangled Gaussian state and its decomposition in the Fock basis is the following:

$$|TMSV\rangle = \frac{1}{\cosh(r)} \sum_{n=0}^{\infty} (\tanh(r))^n |n,n\rangle. \tag{2.77}$$

Hence, the TMSV state has perfect photon number correlation. An alternative notation that can be encountered in the literature is:

$$|TMSV\rangle = \sqrt{1-\lambda} \sum_{n=0}^{\infty} \lambda^n |n,n\rangle, \tag{2.78}$$

where $\lambda = \tanh(r)$.

The covariance matrix of the TMSV state is given by:

$$\gamma = \begin{pmatrix} \cosh(2r) & 0 & \sinh(2r) & 0 \\ 0 & \cosh(2r) & 0 & -\sinh(2r) \\ \sinh(2r) & 0 & \cosh(2r) & 0 \\ 0 & -\sinh(2r) & 0 & \cosh(2r) \end{pmatrix}. \tag{2.79}$$

The standard TMSV state has correlation between the $\hat{x}$-quadratures of both modes and anti-correlations between the $\hat{p}$-quadratures. In the (unphysical) limit of infinite squeezing, $r \to \infty$, we tend to the EPR state were the correlations and anti-correlation are perfect. Finally, it is worth to mention that the EPR state is the common eigenstate of the operators $\hat{x}_1 - \hat{x}_2$ and $\hat{p}_1 + \hat{p}_2$.

2.3.4 Thermal states

The thermal state is a one-mode mixed Gaussian state. Its decomposition in the Fock basis is:

$$\rho_{th} = \sum_{n=0}^{\infty} \frac{\overline{n}^n}{(\overline{n}+1)^{n+1}} |n\rangle\langle n|, \tag{2.80}$$

where $\overline{n} = \langle \hat{n} \rangle_{th}$ is the mean number of photons of a thermal state also known as the *number of thermal photons*.

Interestingly, thermal states can be obtained by tracing out one mode of the TMSV

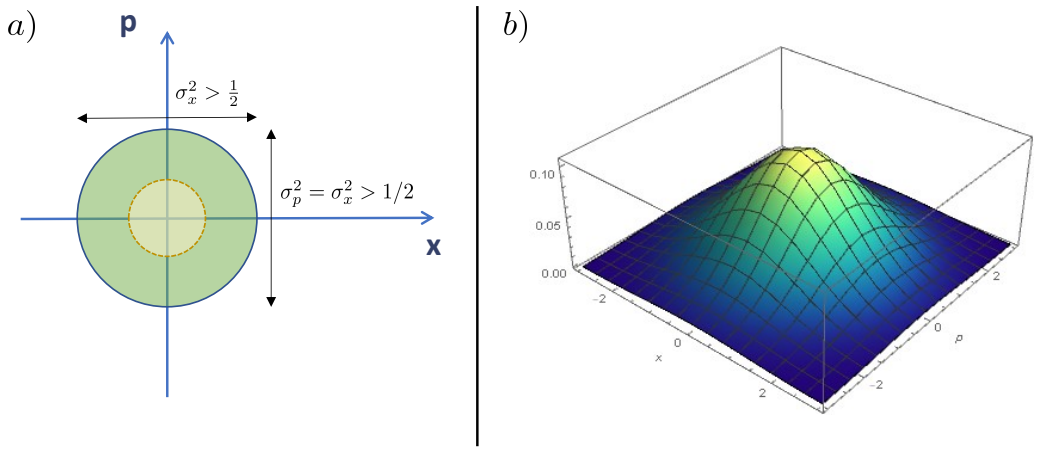

Figure 2.3: *a)* Phase space representation of a thermal state $|\overline{n}\rangle$ (in green).The variance in the x-quadrature is equal to the variance in the p-quadrature $\Delta x^2 = \Delta p^2 = \overline{n} + 1/2$. The yellow dashed disc is the phase space representation of the vacuum state and its variances are $\Delta x^2 = \Delta p^2 = 1/2$. *b)* Three-dimensional representation of a centered thermal state.

state (2.77), one finds:

$$\rho_{th} = \mathrm{Tr}_2(|TMSV\rangle\langle TMSV|) = \frac{1}{(\cosh(r))^2}\sum_{n=0}^{\infty}(\tanh(r))^2|n\rangle\langle n|, \tag{2.81}$$

which actually corresponds to a thermal state as it can be seen by taking $\overline{n} = \sinh^2(r)$ in the definition (2.80).

The covariance matrix of a thermal state is:

$$\gamma = \begin{pmatrix} \overline{n} + \frac{1}{2} & 0 \\ 0 & \overline{n} + \frac{1}{2} \end{pmatrix}. \tag{2.82}$$

Hence, thermal states have a larger variance that the coherent states (see Fig. 2.3 for the phase space representation of a centered thermal state) and do not saturate the Heisenberg uncertainty relation. However, the variance is the same in both x- and p-quadratures.

The importance of thermal states comes from the fact that the symplectic diagonal form of a covariance matrix can be interpreted as the covariance matrix of a tensor product of thermal states. Indeed, the diagonal elements of the symplectic diagonal form of a covariance matrix, i.e. its symplectic values ν_i, can be expressed through the mean number of photons of the thermal state : $\nu_i = \overline{n} + 1/2$.

2.4 Non-Gaussian states

2.4.1 Fock states

The Fock states have already been introduced in section 2.1 and used in the previous section. However, as they are an important example of non-Gaussian states, we describe here some more properties of these states that have not been introduced yet.

Fock states are important non-Gaussian pure states. They are the eigenstate of the number operator $\hat{n} = \hat{a}^\dagger \hat{a}$. Indeed,

$$\hat{n}|n\rangle = n|n\rangle. \tag{2.83}$$

Note that the number operator is an observable. Hence, Fock states are the eigenstates of an observable. For $n = 0$, the associated Fock state $|0\rangle$ is the vacuum state.

They form an orthonormal basis of states since :

$$\langle n|m\rangle = \delta_{n,m}. \tag{2.84}$$

Hence, they are commonly used as a basis for the decomposition of states.

Fock state of n photons can be obtained by applying the *creation operator* $\hat{a}^\dagger$ on the vacuum state:

$$|n\rangle = \frac{(\hat{a}^\dagger)^n}{\sqrt{n!}}|0\rangle. \tag{2.85}$$

Since Fock states are non Gaussian states, we give their Wigner function:

$$W_n(x,p) = \frac{(-1)^n}{\pi} e^{-(x^2+p^2)} L_n(2(x^2+p^2), \tag{2.86}$$

where $L_n(x)$ is the n-th Laguerre polynomial.

2.4.2 Cat states

Another interesting family of non-Gaussian states are the even and odd optical cat states, written $|c_+\rangle$ and $|c_-\rangle$ respectively . They are defined as superposition of coherent states with opposite phases as follows :

$$|c_+^\beta\rangle = \frac{1}{\sqrt{N_+}}(|\beta\rangle + |-\beta\rangle), \tag{2.87}$$

$$|c_-^\beta\rangle = \frac{1}{\sqrt{N_-}}(|\beta\rangle - |-\beta\rangle), \tag{2.88}$$

where N_+ and N_- are normalization constants equal to $N_\pm = \sqrt{2\left(1 \pm e^{-2|\beta|^2}\right)}$. Remarkably, odd cat states are orthogonal to even cat states : $\langle c_\pm^\alpha | c_\mp^\beta \rangle = 0$. Moreover, applying the annihilation operator to an odd cat states gives a state proportional to an even cat states and vice-versa. Indeed :

$$\hat{a}|c_\pm^\beta\rangle = \frac{1}{\sqrt{N_\pm}}(\beta|\beta\rangle + (-\beta)|-\beta\rangle) = \beta\sqrt{\frac{N_\mp}{N_\pm}}|c_\mp^\beta\rangle. \tag{2.89}$$

We give here some of the non-zero moments up to $k+l=4$:

$$\begin{aligned}
\langle \hat{a}^\dagger \hat{a} \rangle_{c_\pm} &= \frac{N_\mp}{N_\pm}|\beta|^2, \\
\langle \hat{a}^2 \rangle_{c_\pm} = \langle \hat{a}^{\dagger 2} \rangle_{c_\pm}^* &= \beta^2, \\
\langle \hat{a}^{\dagger 2} \hat{a}^2 \rangle_{c_\pm} &= |\beta|^4, \\
\langle \hat{a}^\dagger \hat{a}^3 \rangle_{c_\pm} = \langle \hat{a}^{\dagger 3} \hat{a} \rangle_{c_\pm}^* &= \frac{N_\mp}{N_\pm}\beta^2|\beta|^2, \\
\langle \hat{a}^4 \rangle_{c_\pm} = \langle \hat{a}^{\dagger 4} \rangle_{c_\pm}^* &= \beta^4.
\end{aligned} \tag{2.90}$$

These results are used in section 8.1 to calculate the different determinants of principal submatrices taken from matrix of moments (Eq. 7.23) for even and odd cat states.

2.5 Passive and active Gaussian unitaries in interferometry

2.5.1 Phase-shift operator

The *phase shift* operator corresponds a rotation of angle ϕ in phase space. It is a passive Gaussian unitary as it preserves the number of photons and the Gaussian character of the state. It is described by the free evolution unitary of an harmonic oscillator:

$$R(\phi) = e^{-i\phi\hat{a}^\dagger\hat{a}} = e^{-i\phi\hat{n}}. \tag{2.91}$$

The associated Bogoliubov transformation consists in the multiplication of the annihilation operator by a phase of angle ϕ:

$$\hat{a} \to e^{-i\phi}\hat{a}. \tag{2.92}$$

Hence, the effect of a phase shift operation on the quadratures writes:

$$\begin{aligned}
\hat{x} &\to \cos(\phi)\hat{x} + \sin(\phi)\hat{p}, \\
\hat{p} &\to -\sin(\phi)\hat{x} + \cos(\phi)\hat{p},
\end{aligned} \tag{2.93}$$

and the associated symplectic matrix for the phase shift writes:

$$R(\phi) = \begin{pmatrix} \cos(\phi) & \sin(\phi) \\ -\sin(\phi) & \cos(\phi) \end{pmatrix}, \tag{2.94}$$

which correspond to a rotation matrix. Indeed, The effect of a phase shift on the Wigner function is:

$$W(x,p) \to W(\cos(\phi)\ x + \sin(\phi)\ p, -\sin(\phi)\ x + \cos(\phi)\ p), \tag{2.95}$$

and the phase shift appears to act as a rotation of angle ϕ in phase space.

2.5.2 Beam splitter

The beam splitter is a semi-transparent mirror that has two input modes and two output modes. It is very important in quantum optics since it can generate entanglement between two modes. It is also used to model losses in a mode by taking the vacuum state as the input of the ancillary mode. Then, it model a pure-loss channel where the transmissivity is proportional to the beam splitter transmittance τ. The unitary operation of the beam splitter is written:

$$B(\tau) = e^{\theta(\hat{a}^\dagger \hat{b} - \hat{a}\hat{b}^\dagger)}, \tag{2.96}$$

where $\tau = \cos^2(\theta)$ is the transmittance of the beam splitter. Indeed, from the conservation of the number of photons, the transmittance τ and the reflectance $r = \sin^2(\theta)$ need to satisfy:

$$\tau + r = \cos^2(\theta) + \sin^2(\theta) = 1. \tag{2.97}$$

Therefore, we can identify $r = 1 - \tau$. Hence, the beam splitter can be expressed in terms of the transmittance only.

The transformation of the operators, when considered in the Heisenberg picture, through the beam splitter writes:

$$\begin{pmatrix} \hat{a} \\ \hat{b} \end{pmatrix} \to \begin{pmatrix} \sqrt{\tau} & \sqrt{1-\tau} \\ -\sqrt{1-\tau} & \sqrt{\tau} \end{pmatrix} \begin{pmatrix} \hat{a} \\ \hat{b} \end{pmatrix}. \tag{2.98}$$

Other definition does exist in the literature. They are typically equivalent to this one up to a phase shift. In terms of the quadratures operators $\hat{r} = (\hat{x}, \hat{p})^T$, the beam splitter transformation writes:

$$\begin{pmatrix} \hat{r}_1 \\ \hat{r}_2 \end{pmatrix} \to \begin{pmatrix} \sqrt{\tau}\mathbb{1} & \sqrt{1-\tau}\mathbb{1} \\ -\sqrt{1-\tau}\mathbb{1} & \sqrt{\tau}\mathbb{1} \end{pmatrix} \begin{pmatrix} \hat{r}_1 \\ \hat{r}_2 \end{pmatrix}. \tag{2.99}$$

These expressions will be widely used in the calculations present in this thesis.

The beam splitter and the phase shift are the only tools necessary to implement passive interferometry where the total number of photons of the input and the output states is conserved.

2.5.3 One-mode squeezer

The *single mode squeezer* is the simplest example of an active unitary transformation. Indeed, it consists of a non-linear medium that is pumped with an intense laser. The corresponding Hamiltonian writes:

$$H = \frac{1}{2}(\xi^* \hat{a}^2 - \xi \hat{a}^{\dagger 2}), \tag{2.100}$$

where $\xi = re^{i\phi}$ is the complex squeezing parameter and can be decomposed as the multiplication of the real squeezing factor r and the real squeezing angle ϕ. The Hamiltonian is composed of the terms $\hat{a}^2$ and $\hat{a}^{\dagger 2}$ which generate the pairs of photons. Hence, in the case of the squeezed vacuum, the decomposition in the Fock state basis (2.68) involves only the even Fock states elements. The action of the single mode squeezing operation on the annihilation and creation operators in the Heisenberg picture is:

$$\begin{pmatrix} \hat{a} \\ \hat{a}^\dagger \end{pmatrix} \rightarrow \begin{pmatrix} \cosh(r) & -e^{i\phi}\sinh(r) \\ -e^{-i\phi}\sinh(r) & \cosh(r) \end{pmatrix} \begin{pmatrix} \hat{a} \\ \hat{a}^\dagger \end{pmatrix}. \tag{2.101}$$

In the specific case of $\phi = 0$, the effect of the squeezing operator on the quadrature operators is the following:

$$\begin{pmatrix} \hat{x} \\ \hat{p} \end{pmatrix} \rightarrow \begin{pmatrix} e^{-r} & 0 \\ 0 & e^{r} \end{pmatrix} \begin{pmatrix} \hat{x} \\ \hat{p} \end{pmatrix}, \tag{2.102}$$

which has the effect of squeezing the state along the x-axis and anti-squeezing it along the p-axis as expected. This effect is better seen in terms of the covariance matrix in (2.72). In order to achieve an arbitrary squeezing operation $S(\xi)$, one can first apply a phase shift $P(-\phi)$, then a squeezing operation along the x-axis $S(r)$ and then a final phase shift $P(\phi)$. This justifies the use for the variable notation ϕ for both the phase shift and the squeezing operations.

2.5.4 Two-mode squeezer

The two-mode squeezer is the last Gaussian unitary we will cover in this introduction. The Hamiltonian of the two-mode squeezing operator (2.74) is Gaussian.

The action of the TMSO on the quadratures writes:

$$\begin{pmatrix} \hat{x}_1 \\ \hat{p}_1 \\ \hat{x}_2 \\ \hat{p}_2 \end{pmatrix} \rightarrow \begin{pmatrix} \cosh(r) & 0 & \sinh(r) & 0 \\ 0 & \cosh(r) & 0 & -\sinh(r) \\ \sinh(r) & 0 & \cosh(r) & 0 \\ 0 & -\sinh(r) & 0 & \cosh(r) \end{pmatrix} \begin{pmatrix} \hat{x}_1 \\ \hat{p}_1 \\ \hat{x}_2 \\ \hat{p}_2 \end{pmatrix} \tag{2.103}$$

Hence the TMSO shows correlation between the x-quadratures and anti-correlations between the p-quadratures of the two-modes. This can be seen by noticing that the superposition of the quadratures $\hat{X} = \hat{x}_1 - \hat{x}_2$ and $\hat{P} = \hat{p}_1 + \hat{p}_2$[6] are squeezed and $\hat{x}_1 + \hat{x}_2$ and $\hat{p}_1 - \hat{p}_2$ are anti-squeezed. Therefore, by applying the TMSO in the limit of infinite squeezing ($r \rightarrow \infty$) to vacuum states, the correlation in the x-quadratures of the two modes are perfectly correlated ($\hat{x}_1 = \hat{x}_2$) and the p-quadratures of the two modes are perfectly anti-correlated ($\hat{p}_1 = -\hat{p}_2$). Hence, in that limit, we recover the famous EPR entangled state that was introduced by Einstein, Podolsky and Rosen in 1932 [13]. Therefore, the nomenclature *EPR state* is sometimes used to refer to the two-mode squeezed state, even for a finite value of the squeezing factor r.

The TMSO can be decomposed by first applying a balanced beam splitter followed by two single mode squeezing of opposite squeezing parameter on each mode and finally by applying a second balanced beam splitter.

2.6 Discrete and Continuous variable measurements

2.6.1 Discrete variable measurements

The main discrete variable that is used in measurement is the number of quanta of the electromagnetic fields, namely the *number of photons*. Therefore, this type of measurements are called *photo-detectors*.

Photon number resolving detection

A perfect measurement of the number of photons detected in a photo-detector is represented in theory by perfect projective operators $\hat{P}_n$ that project the measured states into the subspace of the associated Fock state, where:

$$\hat{P}_n = |n\rangle\langle n|. \tag{2.104}$$

[6] Note that the operators $\hat{X}$ and $\hat{P}$ commute.

Hence the photon statistic of the state ρ is derived as:

$$p_n = \mathrm{Tr}(\rho \hat{P}_n), \tag{2.105}$$

which becomes $p_n = \langle\psi|(|n\rangle\langle n|)|\psi\rangle = |\langle\psi|n\rangle|$, in the case of a pure state $\rho_\psi = |\psi\rangle\langle\psi|$. These perfect projectors on Fock states are called *photon number resolving* detector (PNR).

However, ideal photon number resolving detectors are not practically achievable. The current experimental record can resolve up to 24 photons [27]. The limitations comes form the inefficiencies of the detector and the dark counts. Hence, real photo-counting techniques involve a finite number of POVM elements instead of projective measurements that span the entire Hilbert space (as for (2.104)).

On-Off detection

One of the simplest detector one can imagine is the one that detects the presence or absence of light. This is the purpose of the *ON-OFF detectors*. The POVM elements representing the action of the ON-OFF detectors are:

$$\begin{aligned} \hat{\Pi}_{off} &= |0\rangle\langle 0|, \\ \hat{\Pi}_{on} &= \mathbf{1} - |0\rangle\langle 0|. \end{aligned} \tag{2.106}$$

These correspond to the detection of *some* light $\hat{\Pi}_{on}$ or no light $\hat{\Pi}_{off}$. This ON-OFF detection is realised by the *avalanche photo-detectors* (APD).

Real APD detectors are affected by some inefficiency η, which takes into account the photon losses. This is modeled by adding a beam splitter of transmittance η equal to the inefficiency of the detector followed by an ideal ON-OFF detector. In the case of no losses, $\eta = 1$. The real APD POVM elements are:

$$\begin{aligned} \hat{\Pi}_{off} &= \sum_m (1-\eta)^m |m\rangle\langle m|, \\ \hat{\Pi}_{on} &= \mathbf{1} - \hat{\Pi}_{off}, \end{aligned} \tag{2.107}$$

where the $\hat{\Pi}_{off}$ takes into account the fact that the detector clicks "off" while there was some photon present in the state initially but were lost.

As an example, let us consider the case of the Fock state $\rho_n = |n\rangle\langle n|$. In this case, the outcomes of the real ON-OFF detectors are:

$$\begin{aligned} p_{off} &= \mathrm{Tr}\left(\hat{\Pi}_{off}|n\rangle\langle n|\right) = \langle n|\hat{\Pi}_{off}|n\rangle = (1-\eta)^n, \\ p_{on} &= \mathrm{Tr}\left(\hat{\Pi}_{on}|n\rangle\langle n|\right) = \langle n|\hat{\Pi}_{on}|n\rangle = 1-(1-\eta)^n, \end{aligned} \tag{2.108}$$

Hence, in the case of a very efficient detector, i.e. $\eta = 1-\epsilon$, we have that the proba-

bility that "off" clicks is $p_{off} = \epsilon^n$ and that "on" clicks is $p_{on} = 1 - \epsilon^n$.

Another interesting example is to consider a coherent state $|\alpha\rangle$ with a very small amplitude $|\alpha| \ll 1$. In this case, the probability of having "on" as an outcome is:

$$p_{on} = 1 - p_{off} = 1 - \sum_m p_m(\alpha)(1-\eta)^n, \tag{2.109}$$

where $p_m(\alpha) = |\langle\alpha|n\rangle|$. In the case we truncate the Hilbert space and take only into account the vacuum and first Fock state, we have that $p_0(\alpha) + p_1(\alpha) \approx 1$ and hence:

$$p_{on} \approx p_1(\alpha). \tag{2.110}$$

Therefore, ON-OFF detectors can evaluate the single photon component of a coherent state with very small amplitude.

2.6.2 Continuous variable measurements

The *continuous variable measurements* techniques are measurement whose spectrum of outcomes is continuous. As it is showed in the next section, it involves naturally the quadratures operators $\hat{x}$ and $\hat{p}$ since they have continuous spectra. Hence, since the quadrature operators are associated with the notion of fields, the continuous variable measurement techniques in quantum optics need an interferometric measurement. We will describe in the following sections two common interferometric measurements : the homodyne and heterodyne (also called double-homodyne) detection.

Homodyne detection

The homodyne detection allows to measure one of the quadratures of the electromagnetic field. It works as follows. First, the target mode $\hat{a}_t$ is combined with an intense local oscillator α_{LO} into a balanced beam splitter. After this, photodetectors measure the intensity of the fields in each output mode and are subtracted afterwards. The difference between the field intensities being proportional to the number of photons in each mode, we can access to information about a quadrature of the target state.

More specifically, the Bogolioubov transformation associated to the balanced beam splitter transformation are:

$$\begin{aligned} \hat{a}_1 &= \frac{1}{\sqrt{2}}(\hat{a}_t + \hat{a}_{LO}), \\ \hat{a}_2 &= \frac{1}{\sqrt{2}}(\hat{a}_t - \hat{a}_{LO}). \end{aligned} \tag{2.111}$$

Hence, the difference of photon number from each output mode writes in terms of

the input modes:

$$\Delta\hat{n} = \hat{n}_1 - \hat{n}_2 = \hat{a}_t^\dagger \hat{a}_{LO} + \hat{a}_{LO}^\dagger \hat{a}_t. \tag{2.112}$$

The local oscillator can be understood as a coherent state $|\alpha_{LO}\rangle$with high amplitude $|\alpha_{LO}| \gg 1$. Therefore, by using (2.112) in the case of a pure target state $|\psi_t\rangle$, we have:

$$\begin{aligned} \langle\alpha_{LO}|\langle\psi_t|\, \Delta\hat{n}\, |\alpha_{LO}\rangle|\psi_t\rangle &= \langle\alpha_{LO}|\langle\psi_t|\, (\hat{a}_t^\dagger \hat{a}_{LO} + \hat{a}_{LO}^\dagger\, \hat{a}_t)|\alpha_{LO}\rangle|\psi_t\rangle, \\ &= |\alpha_{LO}|\langle\psi_t|\, e^{i\phi_{LO}}\hat{a}_t^\dagger + e^{-i\phi_{LO}}\hat{a}_t\, |\psi_t\rangle, \\ &= \sqrt{2}\, |\alpha_{LO}|\, \langle\hat{x}_t(\phi_{LO})\rangle_{\phi_t}. \end{aligned} \tag{2.113}$$

The measurement of any quadrature is possible through homodyne detection by tuning the phase of the local oscillator ($\phi_{LO} = 0$ correspond to the measurement of the $\hat{x}$ quadrature and $\phi_{LO} = \pi/2$ correspond to the $\hat{p}$ quadrature). The factor $\sqrt{2}\,|\alpha_{LO}|$ can be easily removed since the local oscillator is bright and can be considered classical. Indeed, the noise contribution from the local oscillator field can be neglected as the variance of the difference of the photon number is:

$$\Delta(\hat{n}_1 - \hat{n}_2)^2 = 2\,|\alpha_{LO}|^2\, \Delta\hat{x}_t^2(\phi_{LO}). \tag{2.114}$$

The homodyne detection allows one to measure any quadrature of the target states and hence to fully characterize the state via the reconstruction of the Wigner function $W(x, p)$ of the state.

Heterodyne detection

Heterodyne detection, or double-homodyne detection, is a continuous variable measurement that is described by a Gaussian POVM:

$$H(\alpha) = \frac{1}{\pi}|\alpha\rangle\langle\alpha|, \tag{2.115}$$

consisting in a projection onto coherent states. In practice, it consist of the target state being combined with a vacuum ancillary mode into a balanced beam splitter [28]. After this, each of the output modes are measured through homodyne detection of each of the quadratures respectively. This enables to access both quadrature of the states at the expense of an extra vacuum noise $\Delta x_0 = \Delta p_0 = 1/2$ coming from the ancillary input mode.

The probability density at the output of a heterodyne detection of some state ρ is:

$$\mathrm{Tr}(H(\alpha)\rho) = \frac{1}{\pi}\langle\alpha|\rho|\alpha\rangle = Q(\alpha), \tag{2.116}$$

where $Q(\alpha)$ is the Husimi Q-function (2.31). Hence, the Husimi Q-function is usually used to represented the results of heterodyne detection. This is coherent with the

observation that the Husimi Q-function is non negative.

Part II | Continuous-variable parameter estimation

3 Introduction to quantum parameter estimation

3.1 Introduction

In the framework of quantum parameter estimation, the goal is to estimate some unknown parameter of interest, usually noted θ taking values in $[-\epsilon, \epsilon]$, on which depends a state $\rho(\theta)$. We assume the state $\rho(\theta)$ depends on the parameter θ through some unitary operator:

$$\rho(\theta) = e^{-i\theta\hat{G}}\rho_0 e^{i\theta\hat{G}}, \tag{3.1}$$

where $\hat{G}$ is called the *generator* of the parameter and $\rho_0 = \rho(0)$. Let us now discuss how we can estimate the value of θ from $\rho(\theta)$.

In order to accomplish this task, we allow ourself to make some measurements on the state $\rho(\theta)$ from which we will have to infer an estimator $\tilde{\theta}$ of the parameter. The brute force technique is to allow us to make full tomography of the state and then infer the value of θ by inverting the dependence of $\rho(\theta)$ on the parameter. However, this is expensive in terms of time and the parameter might be time dependent. In order to overcome this caveat, we can think about a more direct strategy by building up an observable $\hat{O}_\theta$ which is optimized on estimating the parameter θ. In this situation, by measuring the observable $\hat{O}_\theta$ we get some function of θ:

$$\langle \hat{O}_\theta \rangle_{\rho(\theta)} = \mathrm{Tr}(\rho(\theta)\hat{O}_\theta) = f(\theta), \tag{3.2}$$

from which we can infer the value of θ by taking the inverse of f:

$$\theta = f^{-1}\left(\langle \hat{O}_\theta \rangle_{\rho(\theta)}\right). \tag{3.3}$$

The observable $\hat{O}_\theta$ is called an *unbiased estimator* of θ if:

$$\langle \hat{O}_\theta \rangle_{\rho(\theta)} = \mathrm{Tr}(\hat{O}_\theta\, \rho(\theta)) = \theta, \tag{3.4}$$

for all possible values of θ. Demanding that $\hat{O}_\theta$ is an unbiased estimator is a strong

requirement on $\hat{O}_\theta$. A weaker requirement, is that $\hat{O}_\theta$ is asked to be a *locally unbiased estimator* which is the case if:

$$\frac{\partial}{\partial\theta}\mathrm{Tr}\left(\hat{O}_\theta\,\rho(\theta)\right)|_{\theta=0} = 1. \tag{3.5}$$

Obviously, any unbiased estimator is also a locally unbiased estimator. Indeed, by Taylor development, a locally unbiased estimator can be written as:

$$\langle\hat{O}_\theta\rangle_{\rho(\theta)} \approx \theta + O(\theta^2). \tag{3.6}$$

A useful figure of merit to assess how good an unbiased estimator $\hat{O}_\theta$ does estimate the parameter θ is given by the variance:

$$\Delta^2_\theta\hat{O}_\theta = \mathrm{Tr}\left(\hat{O}^2_\theta\,\rho(\theta)\right) - \mathrm{Tr}\left(\hat{O}_\theta\,\rho(\theta)\right)^2. \tag{3.7}$$

Indeed, the variance is one of the most used measure of spread of a statistical distribution. Hence, an estimator $\hat{O}_\theta$ that has a low variance $\Delta^2_\theta\hat{O}_\theta$ is expected to converge quicker towards the values of the parameter θ. Hence, a natural question that arises is : what is the minimal value of the variance of a given estimator $\Delta^2_\theta\hat{O}_\theta$? The answer to this question is given by the so-called *quantum Cramér–Rao bound* (QCRB) which is the subject of the following sections.

3.2 Cramér–Rao bound and Fisher information

3.2.1 Classical Cramér–Rao bound and Fisher information

Let us take a step back and review the notions of Cramér–Rao bound and Fisher information in the context of classical parameter estimation theory, where the locally unbiased estimator[1] of the parameter θ is a function $\tilde{\theta} = \tilde{\theta}(x_1, x_2, ...)$ of the outputs of a set of measurement outcomes x_i.

In this classical case, the Cramér–Rao bound (or CR bound) provides a lower bound on the variance $\Delta^2\tilde{\theta}$ of any unbiased estimator $\tilde{\theta}$ of the parameter θ:

$$\Delta^2\tilde{\theta} \geq \frac{1}{NF_C(\theta)}, \tag{3.8}$$

where N is the number of measurement outcomes and $F_C(\theta)$ is the *classical Fisher*

[1] the locally unbiased estimator in classical parameter estimation is defined similarly as in (3.5): it needs to satisfy $\partial_\theta\tilde{\theta}|_{\theta=0} = 1$ where ∂_θ is the partial derivative with respect to θ. Similarly, a classical unbiased estimator needs to satisfy $\langle\tilde{\theta}\rangle = \theta$.

information defined as:

$$F_C(\theta) = \int dx p(x|\theta) \left(\frac{\partial}{\partial \theta} \ln(p(x|\theta)) \right)^2 = \int dx \frac{1}{p(x|\theta)} \left(\frac{\partial}{\partial \theta} p(x|\theta) \right)^2, \tag{3.9}$$

where $p(x|\theta)$ is the conditional probability of obtaining the outcome x given that the parameter takes the value θ and $\frac{\partial}{\partial \theta} \ln(p(x|\theta))$ is called the *score function*.

For identical and independently distributed samples, the Cramér–Rao bound (3.8) is asymptotically saturated by the maximum-likelihood estimator [2] for $N \to \infty$.

3.2.2 Quantum Cramér–Rao bound and Fisher information

The transition from the classical definition (3.9) to the quantum version of the Fisher information is made through the Born rule :

$$p(x|\theta) = \mathrm{Tr}(\Pi_x \rho(\theta)), \tag{3.10}$$

where Π_x are the elements of a positive operator-valued measure (POVM).

For a state $\rho(\theta)$, the *quantum Fisher information* (QFI) is defined through the *symmetric logarithmic derivative* (SLD) L_θ, which is the selfadjoint operator satisfying the following Lyapunov equation [18]:

$$\frac{\partial \rho}{\partial \theta} = \frac{L_\theta \rho + \rho L_\theta}{2}. \tag{3.11}$$

This enables us to express the classical Fisher information in terms of POVM elements and SLD as:

$$\begin{aligned} F_C(\theta) &= \int dx \frac{1}{p(x|\theta)} \left(\frac{\partial}{\partial \theta} p(x|\theta) \right)^2, \\ &= \int dx \frac{(\mathrm{Tr}(\Pi_x \partial_\theta \rho(\theta)))^2}{\mathrm{Tr}(\Pi_x \rho(\theta))}, \\ &= \int dx \frac{\Re\,(\mathrm{Tr}(\Pi_x L_\theta \rho(\theta)))^2}{\mathrm{Tr}(\Pi_x \rho(\theta))}, \end{aligned} \tag{3.12}$$

[2] the maximum-likelihood estimator is an estimator built from finding the maximum of the likelihood function $\mathbf{L}(x|\theta)$, i.e. from the condition $\partial_\theta \mathbf{L}(x|\theta) = 0$.

where the last equality comes from

$$\begin{aligned}
\mathrm{Tr}(\Pi_x \partial_\theta \rho(\theta)) &= \frac{1}{2}\mathrm{Tr}(\Pi_x L_\theta \rho + \rho L_\theta), \\
&= \frac{1}{2}\mathrm{Tr}(\Pi_x L_\theta \rho + (L_\theta \rho)^\dagger), \\
&= \frac{1}{2}\left(\mathrm{Tr}(\Pi_x L_\theta \rho) + \mathrm{Tr}(\Pi_x (L_\theta \rho)^\dagger)\right), \\
&= \frac{1}{2}\left(\mathrm{Tr}(\Pi_x L_\theta \rho) + \mathrm{Tr}(\Pi_x L_\theta \rho)^*\right), \\
&= \Re(\mathrm{Tr}(\Pi_x L_\theta \rho(\theta)).
\end{aligned} \tag{3.13}$$

The definition (3.12) is not yet the quantum version of the Fisher information. Indeed, it still depends on the POVM $\{\Pi_x\}$ that is used to measure the state $\rho(\theta)$. In order to find the ultimate quantum Cramér–Rao bound, we need to maximize the Fisher information (3.12) over all possible POVM's [29]:

$$\begin{aligned}
F_C(\theta) &= \int dx \, \frac{\Re\left(\mathrm{Tr}(\Pi_x L_\theta \rho(\theta))\right)^2}{\mathrm{Tr}(\Pi_x \rho(\theta))}, \\
&\leq \int dx \, \left|\frac{\mathrm{Tr}(\Pi_x L_\theta \rho(\theta))}{\mathrm{Tr}(\Pi_x \rho(\theta))}\right|^2, \\
&= \int dx \, \left|\mathrm{Tr}\left(\frac{\sqrt{\rho(\theta)}\sqrt{\Pi_x}}{\sqrt{\mathrm{Tr}(\Pi_x \rho(\theta))}}\sqrt{\Pi_x} L_\theta \sqrt{\rho(\theta)}\right)\right|^2, \\
&\leq \int dx \, \mathrm{Tr}(\Pi_x L_\theta \rho(\theta) L_\theta), \\
&= \mathrm{Tr}(L_\theta \rho(\theta) L_\theta), \\
&= \mathrm{Tr}(\rho(\theta) L_\theta^2),
\end{aligned} \tag{3.14}$$

where the second inequality results from the Schwartz inequality $\mathrm{Tr}(A^\dagger B) \leq \mathrm{Tr}(A^\dagger A)\mathrm{Tr}(B^\dagger B)$ with $A^\dagger = \sqrt{\rho(\theta)}\sqrt{\Pi_x}/\sqrt{\mathrm{Tr}(\Pi_x \rho(\theta))}$ and $B = \sqrt{\Pi_x} L_\theta \sqrt{\rho(\theta)}$.

We can now define the *quantum Fisher information* (QFI) as:

$$F_Q(\theta) = \mathrm{Tr}(\rho(\theta) L_\theta^2). \tag{3.15}$$

As expected, the QFI only depends on the state $\rho(\theta)$ and the associated SLD L_θ and is independent of the quantum measurement POVM $\{\Pi_x\}$. Let us remember the following inequality between the classical and quantum Fisher information:

$$F_C(\theta) \leq F_Q(\theta), \tag{3.16}$$

and that the classical Cramér–Rao bound (3.8) can always be saturated, asymptotically in the number of repetition of the experiment.

Hence, the *quantum Cramér–Rao bound* reads:

$$\Delta^2\tilde{\theta} \geq \frac{1}{NF_C(\theta)} \geq \frac{1}{NF_Q(\theta)}, \tag{3.17}$$

and gives a lower bound for any estimator of the parameter θ of the state ρ_θ. Hence, it is also a lower bound for the estimator $\hat{O}_\theta$:

$$\Delta^2\hat{O}_\theta \geq \frac{1}{NF_Q(\theta)}, \tag{3.18}$$

where $\Delta^2\hat{O}_\theta$ is defined in (3.7). The saturation of the QCRB is possible by choosing the POVM to be the eigenvectors of the SLD L_θ [29].

3.3 Quantum Cramér–Rao bound for multiple parameters

In quantum metrology, the parameters encoded in some quantum carrier are usually taken to be phases $\Theta = (\theta_1, \theta_2, ..., \theta_n)$. The optimization goal is to lower the variance of the estimators as much as possible. However, the lowest possible variance on each (unbiased) estimator $\tilde{\theta}_i$ is limited by the *Quantum Cramér–Rao Bound* (QCRB) [29, 30], namely

$$\Delta^2\tilde{\theta}_i \geq \frac{(F^{-1}(\Theta))_{ii}}{N}, \tag{3.19}$$

where $F(\Theta)$ is the so-called quantum Fisher information matrix (QFIM) and N is the number of repetitions of the scheme. If a measurement scheme saturates the QCRB, it is called *optimal* since no other scheme can do better. Note that since the right hand side in (3.19) involves the inverse of the QFIM, it is needed to for the QFIM to be invertible.

Similarly to the definition of QFI for single parameter (3.15), for a state ρ, the QFIM is defined through the symmetric logarithmic derivatives (SLDs) L_{θ_i} for $i = 1, 2, ..., n$, which is the selfadjoint operator satisfying the following Lyapunov equation [18]:

$$\frac{\partial\rho}{\partial\theta_i} = \frac{L_{\theta_i}\rho + \rho L_{\theta_i}}{2}. \tag{3.20}$$

The matrix elements of the QFIM are then defined in terms of the SLDs as $F_{ij}(\Theta) = \Re\left[\mathrm{Tr}\left(\rho L_{\theta_i} L_{\theta_j}\right)\right]$, where symbol $\Re$ denotes the real part of the expression since the QFIM is real.

In the case of a pure state $\rho = |\psi\rangle\langle\psi|$, simple expressions can be found for both the SLDs and the QFIM in [31]. The SLD for a pure state is written as

$$L_{\theta_i} = |\psi\rangle\langle\partial_i\psi| + |\partial_i\psi\rangle\langle\psi|, \tag{3.21}$$

and the matrix elements of the QFIM are given by

$$F_{ij}(\Theta) = 4\,\Re\left[\langle\partial_i\psi|\partial_j\psi\rangle - \langle\partial_i\psi|\psi\rangle\langle\psi|\partial_j\psi\rangle\right], \tag{3.22}$$

where ∂_i denotes partial derivative with respect to the ith parameter θ_i in both Equations (3.21) and (3.22). We remark that the QFIM depends on the states but is not depending on the measurement being performed since it gives a bound on the best measurement.

3.4 Attainability of the quantum Cramér–Rao bound

In general, when dealing with multiple parameters Θ, it is not always possible to saturate the multiple parameter Cramér–Rao bound (3.19). The origin of this effect comes from the fact that, for unitary encoded parameters, the generators $\hat{G}_i$ of the different parameters θ_i do not necessarily commute. Hence, a strong necessary condition for the QCRB (3.19) to be saturated, called the *strong commutation relation*, is that the parameters generators commute:

$$\left[\hat{G}_i, \hat{G}_j\right] = 0. \tag{3.23}$$

However, even in the case where all generators of the different parameters do not commute, it is possible to saturate the inequality (3.19). For example, in the case when all the SLD's L_{θ_i} do commute, the attainability of the QCRB is assured. Nevertheless, it is possible that the SLD's do not commute. This last scenario is less conclusive and needs further development (see [32]).

For pure states $\rho_\psi = |\psi\rangle\langle\psi|$, a necessary and sufficient condition for the attainability of the QCRB does exist and was introduced by Matsumoto [33]. This condition, which was referred to as the *weak commutation condition* in [32] is expressed as

$$\mathrm{Tr}(\rho_\psi(\theta)[L_{\theta_i}, L_{\theta_j}]) = 0, \tag{3.24}$$

which is the expectation value of the commutator between the SLDs operator on the state $\rho_\psi(\theta)$ that is asked to vanish. This weak commutation relation can also be expressed more explicitly for pure state $\rho_\psi = |\psi\rangle\langle\psi|$ by replacing the SLDs in (3.24) by their expression (3.21) :

$$\Im(|\partial_{\theta_i}\psi\rangle\langle\partial_{\theta_j}\psi|) = 0, \quad \forall i, j = 1, ..., n. \tag{3.25}$$

The weak commutation condition is a necessary and sufficient condition for the existence of some pair of SLDs of which commutes and which common eigenbasis is an optimal measurement for estimating the parameters θ_i and θ_j. Hence, it is possible to saturate the QCRB (3.19) for both parameters simultaneously.

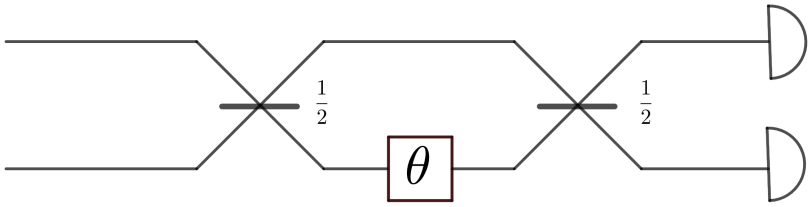

Figure 3.1: Mach-Zehnder interferometer implementation. We first apply a balanced beam-splitter (transmittance $\tau = 1/2$), after a phase shift of an unknown phase θ to be estimated is applied in one of the arms of the interferometer. Finally a second balanced beam-splitter is applied and both modes are measured.

3.5 Optical implementations and performances

3.5.1 Mach-Zehnder interferometer

The Mach-Zehnder interferometer is a standard interferometric setup studied in the context of quantum parameter estimation theory. It is composed of two balanced beam splitter and photodetectors, ideally photon number resolving detectors, at the output to measure the intensities of the output modes. The path of the interferometer are usually assumed to have the same length. In one of the path of the interferometer lies a phase shifter whose phase shift ϕ is usually unknown and is the parameter to be estimated.

Hence, the output mode field operators write in terms of the input mode field operators as:

$$\begin{pmatrix} \hat{b}_1 \\ \hat{b}_2 \end{pmatrix} = \frac{1}{\sqrt{2}} \begin{pmatrix} 1 & 1 \\ 1 & -1 \end{pmatrix} \begin{pmatrix} 1 & 0 \\ 0 & e^{-i\phi} \end{pmatrix} \frac{1}{\sqrt{2}} \begin{pmatrix} 1 & 1 \\ 1 & -1 \end{pmatrix} \begin{pmatrix} \hat{a}_1 \\ \hat{a}_2 \end{pmatrix}, \tag{3.26}$$

$$= \frac{1}{2} \begin{pmatrix} 1+e^{-i\phi} & 1-e^{-i\phi} \\ 1+e^{-i\phi} & 1+e^{-i\phi} \end{pmatrix} \begin{pmatrix} \hat{a}_1 \\ \hat{a}_2 \end{pmatrix}, \tag{3.27}$$

such that if $\phi = 0$, we have that $\hat{b}_1 = \hat{a}_1$ and $\hat{b}_2 = \hat{a}_2$.

In particular, if the second input mode is in the vacuum state, then one would observe the following statistics from the output photodetectors:

$$\begin{aligned} \langle \hat{b}_1^\dagger \hat{b}_1 \rangle &= \cos^2\left(\frac{\phi}{2}\right) \langle \hat{a}_1^\dagger \hat{a}_1 \rangle, \\ \langle \hat{b}_2^\dagger \hat{b}_2 \rangle &= \sin^2\left(\frac{\phi}{2}\right) \langle \hat{a}_1^\dagger \hat{a}_1 \rangle. \end{aligned} \tag{3.28}$$

From this interference pattern, the value of ϕ can be inferred.

3.5.2 Standard quantum limit

Estimating the precision with which one can estimate a parameter ϕ is central in quantum parameter estimation. More precisely, the question of how does the precision scale with the number of particles or photons used during the experiment. The *classical* limit, i.e. achievable with *classical* light such as coherent states, is called the *standard quantum limit* and scales as the square root of the number of particles:

$$\Delta\phi \sim \frac{1}{\sqrt{N}}, \tag{3.29}$$

where N is the number of photons used in the interferometer. This limit is not fundamental as it can be beaten by quantum resource states such as squeezed states or entangled states.

3.5.3 Heisenberg limit

The fundamental limit on the precision one can estimate a parameter ϕ with N particles is the *Heisenberg limit*. It shows a quadratic enhancement toward the standard quantum limit as:

$$\Delta\phi \sim \frac{1}{N}. \tag{3.30}$$

The Heisenberg limit can be, in theory, achievable by means of entanglement (NOON states for example [34, 35]) but is in general not achievable in experiment due to decoherence effects [36].

4 | Optimal estimation of parameters encoded in coherent states quadratures

The content of this chapter is mainly based on the article "Optimal Estimation of Parameters Encoded in Quantum Coherent State Quadratures" that I have published with Evgueni Karpov and Nicolas Cerf as co-authors [1].

4.1 Introduction

Quantum estimation theory as introduced by Helstrom [18] in the 1960s sets fundamental bounds on the extraction of classical parameters encoded in quantum systems. Since then, a large body of work has been devoted to the estimation of parameters, especially phases encoded in quantum optical states (see, e.g., [37, 38, 39, 40, 41] for recent works on multiparameter phase estimation and [42, 43, 44, 45, 46, 47] for the problem of estimation of parameters induced by non-commuting generators). We recommend to the interested reader the review by Demkowicz-Dobrzański *et al.* [48]. In most of these studies, it is usually assumed that we have no control on the value of the parameters being estimated. In this chapter, we consider a communication protocol between Alice and Bob where Alice can *choose* the values of the parameters she wants to send and *how* she encodes these parameters in a collection of coherent states she has at her disposal.

More precisely, we consider the problem of encoding and estimating classical parameters in canonically conjugate quantum variables, such as the quadrature components of coherent states of light. We derive the quantum Cramèr–Rao bounds (QCRB) for an arbitrary linear encoding of two classical parameters into the quadratures of two coherent states. Furthermore, we present an encoding and estimation protocol that achieves the QCRB for the simultaneous estimation of the two parameters. Finally, we generalize our protocol to encode a set of n classical parameters into the tensor product of n coherent states so that one can always simultaneously

estimate all parameters optimally, using a measurement technique involving linear optics components followed by homodyne measurements.

A corollary of this work is the proof of optimality of the scheme based on phase-conjugate coherent states proposed by Cerf and Iblisdir [4] in 2001, which was left as an open problem in [49].

This chapter is organized as follows. In Section 4.2, we introduce the parameter communication problem that we address and explicitly write the encoding of two classical parameters in the quadratures of two coherent states. In Section 4.3, we review the quantum Cramér–Rao bound, which provides a lower bound on the variance of any (unbiased) estimator of the classical parameters encoded into the quantum states. This bound, which is valid for any measurement, relies on the quantum Fisher information. We thus calculate the quantum Fisher information with respect to the parameters encoded into the coherent states in the considered schemes, and write conditions on the attainability of the corresponding quantum Cramér–Rao bound. In Section 4.4, we show that the variances obtained in the Cerf–Iblisdir scheme based on phase-conjugate coherent states [4] saturate the quantum Cramér–Rao bound, hence proving the optimality of the scheme. More generally, we characterize a family of encoding schemes of two variables into a pair of coherent states which all saturate the quantum Cramér–Rao bound. Within this family, the Cerf–Iblisdir scheme provides the highest precision enhancement achieved by a joint measurement in comparison with local measurements. In Section 4.5, we further generalize the scheme to n variables encoded into n states, while we conclude in Section 4.6.

4.2 Two-mode coherent-state parameter communication scheme with linear encoding

Usually, a parameter estimation problem can be divided into three stages: the first stage consists in preparing a probe state, which, in the second stage, acquires some unknown parameters (often phases) by interacting with the probed media. The probe state is then measured in the third stage and the parameters are inferred from the measurement outcomes. The goal is of course to estimate the unknown parameters as precisely as possible, that is, to minimize the variance of each parameter estimator.

In this Chapter, we adopt a variant of this procedure, more suitable for parameter communication purposes. We consider the first two stages of the above scheme to be performed by the sender, Alice, who prepares the states and encodes some parameters into them. The third stage is then performed by the receiver, Bob, who is allowed to use linear optics and homodyne measurements. Moreover, we authorize Alice and Bob to exchange prior messages on the measurement settings with the restriction that no relevant information about the unknown parameters can be inferred

from these messages.

Specifically, we consider the following parameter communication scheme. To send Bob a complex number $z = (a + ib)/\sqrt{2}$ through an optical channel, Alice generates two coherent states $|\alpha_1\rangle \otimes |\alpha_2\rangle$ at her choice, encoding the real numbers a and b. Coherent states can be regarded as resulting from the action of the displacement operator on the vacuum state $|0\rangle$, namely

$$|\alpha\rangle = \exp(ip\hat{x} - ix\hat{p})|0\rangle, \tag{4.1}$$

where x and p are the displacement parameters and $\hat{x}$ and $\hat{p}$ are the quadrature operators. In this way, the state $|\alpha_1\rangle \otimes |\alpha_2\rangle$ is characterized by the quadrature vector $\mathbf{r} = (x_1, p_1, x_2, p_2)$. The commutation relations between the quadrature operators are $\left[\hat{x}_i, \hat{p}_j\right] = i\delta_{ij}$ in natural units ($\hbar = 1$) for $i, j = 1, 2$. A natural condition, which we impose on these coherent states, is some total energy constraint on the input state:

$$x_1^2 + p_1^2 + x_2^2 + p_2^2 = 2(a^2 + b^2). \tag{4.2}$$

This constraint means that average energy per mode is equal to some "signal energy" $a^2 + b^2$. Bob, on his side, has only passive linear optics (beam splitters and phase shifters) and homodyne detectors in order to build a measurement apparatus for estimating parameters a and b. The goal for Bob is to estimate optimally both a and b knowing that they are encoded linearly in the quadratures of the coherent states $|\alpha_1\rangle \otimes |\alpha_2\rangle$.

The most general linear encoding of the real parameters a and b in the quadratures of a two-mode coherent state system is

$$\begin{aligned} x_1 &= \epsilon_{x1}a + \eta_{x1}b, \\ p_1 &= \epsilon_{p1}a + \eta_{p1}b, \\ x_2 &= \epsilon_{x2}a + \eta_{x2}b, \\ p_2 &= \epsilon_{p2}a + \eta_{p2}b. \end{aligned} \tag{4.3}$$

Thus, Alice has to choose eight real constants $(\epsilon_{k,l}, \eta_{k,l})$, where $k = x, p$ and $l = 1, 2$, in a way that allows Bob to optimally retrieve the encoded parameters a and b. In the next section, optimality is defined as the attainability of the quantum Cramér–Rao bound on the variance of both estimators of classical parameters a and b. As we will show, attaining this bound imposes several constraints on the eight constants.

4.3 Parameter estimation

4.3.1 Optimal lower bound

Here, the parameters a, b are encoded into the x and p quadratures of the input product coherent state $|\psi\rangle = |\alpha_1\rangle \otimes |\alpha_2\rangle$, which justifies the use of homodyne detection in the optimal measurement scheme in Section 4.4. To find the quantum Cramér–Rao bound on the variances $\Delta^2\tilde{a}$ and $\Delta^2\tilde{b}$ of the estimators of a and b, we use the additivity of the QFIM. It implies that the QFIM for the product state $|\psi\rangle = |\alpha_1\rangle \otimes |\alpha_2\rangle$ is the sum of the QFIM of the individual states $|\alpha_1\rangle$ and $|\alpha_2\rangle$, namely

$$F_Q^{(\alpha_1\alpha_2)} = F_Q^{(\alpha_1)} + F_Q^{(\alpha_2)}. \tag{4.4}$$

Thus, we simply need to express the individual QFIM for each of the two coherent states. First, we calculate the derivatives with respect to a and b of the individual coherent states

$$\begin{aligned} \partial_a|\alpha_j\rangle &= i\left(\epsilon_{pj}\hat{x}_j - \epsilon_{xj}\hat{p}_j + 2\epsilon_{xj}\epsilon_{pj} + \frac{3\epsilon_{xj}\eta_{pj} + \epsilon_{pj}\eta_{xj}}{2}b\right)|\alpha_j\rangle, \\ \partial_b|\alpha_j\rangle &= i\left(\eta_{pj}\hat{x}_j - \eta_{xj}\hat{p}_j + 2\eta_{xj}\eta_{pj} + \frac{3\eta_{xj}\epsilon_{pj} + \eta_{pj}\epsilon_{xj}}{2}b\right)|\alpha_j\rangle, \end{aligned} \tag{4.5}$$

where $j = 1, 2$ indicates the mode number. By using (4.5) and the definition in (3.22) with $\theta_i = a, b$, we obtain the QFIM for each mode

$$F_Q^{(\alpha_j)} = 2\begin{pmatrix} \epsilon_{xj}^2 + \epsilon_{pj}^2 & \epsilon_{pj}\eta_{pj} + \epsilon_{xj}\eta_{xj} \\ \epsilon_{pj}\eta_{pj} + \epsilon_{xj}\eta_{xj} & \eta_{xj}^2 + \eta_{pj}^2 \end{pmatrix}. \tag{4.6}$$

It is worth noting that the single-mode QFIM in (4.6) is not in general an invertible matrix, which originates from the non-commutativity of the quadrature operators $\hat{x}$ and $\hat{p}$ and is a manifestation of the Heisenberg uncertainty principle. It means that it is in general not possible to extract the two parameters optimally from a single mode, that is, one cannot reach the variance $\left(F(\alpha_j)_{ii}\right)^{-1}/N$ simultaneously for both parameter estimators.

As a consequence of this non-invertibility, one cannot use the QFIM in (4.6) to calculate the QCRB on the estimator of a and b. However, the QFIM becomes invertible when applied to two coherent states $|\alpha_1\rangle \otimes |\alpha_2\rangle$, namely

$$F_Q^{(\alpha_1\alpha_2)} = 2\begin{pmatrix} A & C \\ C & B \end{pmatrix}. \tag{4.7}$$

where

$$\begin{aligned} A &= \epsilon_{x1}^2 + \epsilon_{p1}^2 + \epsilon_{x2}^2 + \epsilon_{p2}^2, \\ B &= \eta_{x1}^2 + \eta_{p1}^2 + \eta_{x2}^2 + \eta_{p2}^2, \\ C &= \epsilon_{p1}\eta_{p1} + \epsilon_{x1}\eta_{x1} + \epsilon_{p2}\eta_{p2} + \epsilon_{x2}\eta_{x2}. \end{aligned} \tag{4.8}$$

Its eigenvalues are given by

$$\lambda_{\pm} = \frac{A + B \pm \sqrt{(A+B)^2 + 4(C^2 - AB)}}{2}. \tag{4.9}$$

We want to estimate both classical parameters a and b with the same precision since they are equally important in order to estimate the complex number $z = (a + ib)/\sqrt{2}$. This *equal precision condition* imposes that both eigenvalues of (4.7) should be equal $\lambda_+ = \lambda_-$ [1], which implies the condition

$$(A - B)^2 = -4C^2. \tag{4.10}$$

According to (3.22), A, B and C should be real numbers, hence the only solution of (4.10) is expressed by two conditions

$$A = B, \qquad C = 0. \tag{4.11}$$

Furthermore, we can rewrite the energy constraint of (4.2) in terms of the QFIM parameters (4.8) as

$$(A - 2)(a^2 + b^2) = 0. \tag{4.12}$$

This equation should be satisfied for all real a and b, since they can be chosen arbitrarily by Alice, so that we only have the condition $A = 2$. Hence, by using the energy constraint in (4.12) together with the equal precision condition in (4.11), we obtain a simple expression for the QFIM associated with estimating the parameters a and b from the state $|\alpha_1\rangle \otimes |\alpha_2\rangle$, namely

$$F_Q^{(\alpha_1\alpha_2)} = \begin{pmatrix} 4 & 0 \\ 0 & 4 \end{pmatrix}. \tag{4.13}$$

This imposes three conditions on the eight encoding constants $(\epsilon_{k,l}, \eta_{k,l})$.

From the QFIM in(4.13), one can deduce the QCRB on the variance of the estimators $\tilde{a}$ and $\tilde{b}$ of the classical parameters a and b for a pair of input coherent states

$$\Delta^2\tilde{a} \geq 1/4, \qquad \Delta^2\tilde{b} \geq 1/4. \tag{4.14}$$

[1] In this case, the QFIM matrix (4.7) will be proportional to the identity matrix and both both parameters $\tilde{a}$ and $\tilde{b}$ can be estimated with the same precision.

Before we find an encoding and estimation strategy such that Bob can optimally estimate both a and b (see Section 4.4), let us discuss the attainability of the QCRB.

4.3.2 Proof of the attainability of the Quantum Cramér–Rao Bound

The commutation condition (3.24) translates into a condition on our encoding constants $(\epsilon_{i,j}, \eta_{i,j})$, as we show below.

The SLDs for a two-mode coherent state $\rho_{12} = |\alpha_1\rangle\langle\alpha_1| \otimes |\alpha_2\rangle\langle\alpha_2|$ in which the classical parameters a and b are encoded with the linear encoding strategy in (4.3) are given by

$$\begin{aligned} L_a = \; & i[\epsilon_{p1}\,(\hat{x}_1\rho_{12} - \rho_{12}\hat{x}_1) \;+\; \epsilon_{p2}\,(\hat{x}_2\rho_{12} - \rho_{12}\hat{x}_2) \\ & -\epsilon_{x1}\,(\hat{p}_1\rho_{12} - \rho_{12}\hat{p}_1) \;-\; \epsilon_{x2}\,(\hat{p}_2\rho_{12} - \rho_{12}\hat{p}_2)], \\ L_b = \; & i[\eta_{p1}\,(\hat{x}_1\rho_{12} - \rho_{12}\hat{x}_1) \;+\; \eta_{p2}\,(\hat{x}_2\rho_{12} - \rho_{12}\hat{x}_2) \\ & -\eta_{x1}\,(\hat{p}_1\rho_{12} - \rho_{12}\hat{p}_1) \;-\; \eta_{x2}\,(\hat{p}_2\rho_{12} - \rho_{12}\hat{p}_2)], \end{aligned} \tag{4.15}$$

where we have plugged Equation (4.5) into the formulas of the SLDs for pure states in (3.21) where $\theta_i = a, b$. Inserting Equation (4.15) into (3.24), we observe that the only surviving terms are those involving the commutator $[\hat{x}_i, \hat{p}_i]$, which leads to

$$\begin{aligned} \mathrm{Tr}(\rho_{12}[L_a, L_b]) \;&=\; i\langle\alpha_1|(\epsilon_{p1}\eta_{x1} - \epsilon_{x1}\eta_{p1})[\hat{x}_1, \hat{p}_1]|\alpha_1\rangle + i\langle\alpha_2|(\epsilon_{p2}\eta_{x2} - \epsilon_{x2}\eta_{p2})[\hat{x}_2, \hat{p}_2]|\alpha_2\rangle, \\ &=\; -\epsilon_{p1}\eta_{x1} + \epsilon_{x1}\eta_{p1} - \epsilon_{p2}\eta_{x2} + \epsilon_{x2}\eta_{p2}. \end{aligned} \tag{4.16}$$

As a result, we obtain the *attainability condition* on the encoding constants

$$\epsilon_{p1}\eta_{x1} - \epsilon_{x1}\eta_{p1} + \epsilon_{p2}\eta_{x2} - \epsilon_{x2}\eta_{p2} = 0. \tag{4.17}$$

Together with the energy constraint in (4.2) and equal precision conditions in Equation (4.11), the attainability condition in (4.17) gives rise to a system of four equations that an optimal encoding strategy must satisfy, namely

$$\begin{aligned} &\epsilon_{x1}^2 + \epsilon_{p1}^2 + \epsilon_{x2}^2 + \epsilon_{p2}^2 = 2, \\ &\eta_{x1}^2 + \eta_{p1}^2 + \eta_{x2}^2 + \eta_{p2}^2 = 2, \\ &\epsilon_{p1}\eta_{p1} + \epsilon_{x1}\eta_{x1} + \epsilon_{p2}\eta_{p2} + \epsilon_{x2}\eta_{x2} = 0, \\ &\epsilon_{p1}\eta_{x1} - \epsilon_{x1}\eta_{p1} + \epsilon_{p2}\eta_{x2} - \epsilon_{x2}\eta_{p2} = 0. \end{aligned} \tag{4.18}$$

As we only have four constraints for eight real constants $(\epsilon_{i,j}, \eta_{i,j})$, there is no unique solution to this system. The most general linear encoding corresponds to the one that can be optimally decoded by using the most general two-mode passive Gaussian unitaries composed of three local phases and one beam splitter. Therefore, the most

general two-mode encoding can be written in the following way:

$$\begin{aligned}
\epsilon_{x1} &= \sqrt{2T}\cos(\theta), & \eta_{x1} &= \sqrt{2(1-T)}\left(\sin(\theta)\sin(\psi) - \cos(\theta)\cos(\psi)\right), \\
\epsilon_{p1} &= \sqrt{2T}\sin(\theta), & \eta_{p1} &= -\sqrt{2(1-T)}\left(\sin(\theta)\cos(\psi) + \cos(\theta)\sin(\psi)\right), \\
\epsilon_{x2} &= \sqrt{2(1-T)}\cos(\phi), & \eta_{x2} &= \sqrt{2T}\left(\cos(\phi)\cos(\psi) - \sin(\phi)\sin(\psi)\right), \\
\epsilon_{p2} &= \sqrt{2(1-T)}\sin(\phi), & \eta_{p2} &= \sqrt{2T}\left(\cos(\phi)\sin(\psi) + \cos(\phi)\sin(\psi)\right).
\end{aligned} \tag{4.19}$$

On the decoding side (see Figure 4.1), Bob should first apply two local phase rotations of angles θ and ϕ, followed by a beam splitter of transmittance T , then a local rotation on the second mode of angle ψ and finally measure the x-quadrature on both modes. This general solution satisfies all four constraints given by (4.18). In the next Section, we discuss two families of encoding strategies, one naive guess that is shown to be not optimal, and a one-parameter family of optimal encodings, for which we describe the estimation strategy saturating the QCRB. This last family encompasses the Cerf–Iblisdir scheme [4].

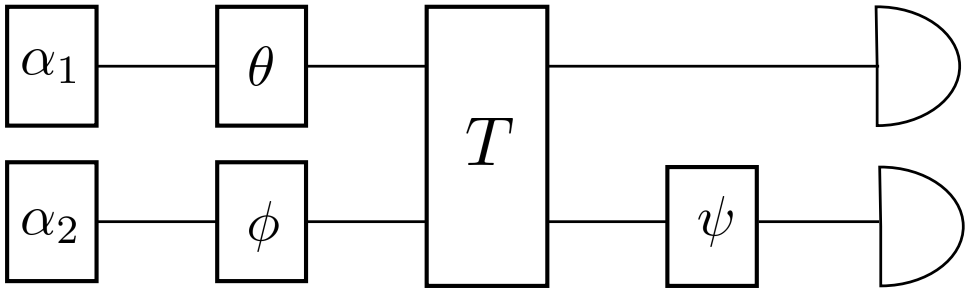

Figure 4.1: Optimal joint estimation scheme for two modes using a beam splitter of transmittance T and two homodyne detectors. The phases are all set to zero in (4.23).

4.4 Two-mode encoding and estimation schemes

4.4.1 Twin-states encoding

First, consider a "naive" protocol, where Alice encodes her classical real parameters a and b into two identical coherent states (such that $\alpha_1 = \alpha_2$, see Fig. 4.2). This imposes the following constraints on the parameters of linear encoding:

$$\begin{aligned}
\epsilon_{x1} &= \epsilon_{x2}, \quad \epsilon_{p1} = \epsilon_{p2}, \\
\eta_{x1} &= \eta_{x2}, \quad \eta_{p1} = \eta_{p2},
\end{aligned} \tag{4.20}$$

where at least ϵ_{x1} or ϵ_{p1} and η_{x1} or η_{p2} are not equal to zero. Let us show that this protocol cannot be optimal since it does not satisfy the two last conditions in (4.18). In fact, by plugging Equation (4.20) into Equations (4.18), we have

$$\begin{aligned}
\epsilon_{p1}\eta_{p1} + \epsilon_{x1}\eta_{x1} &= 0, \\
\epsilon_{p1}\eta_{x1} - \epsilon_{x1}\eta_{p1} &= 0.
\end{aligned} \tag{4.21}$$

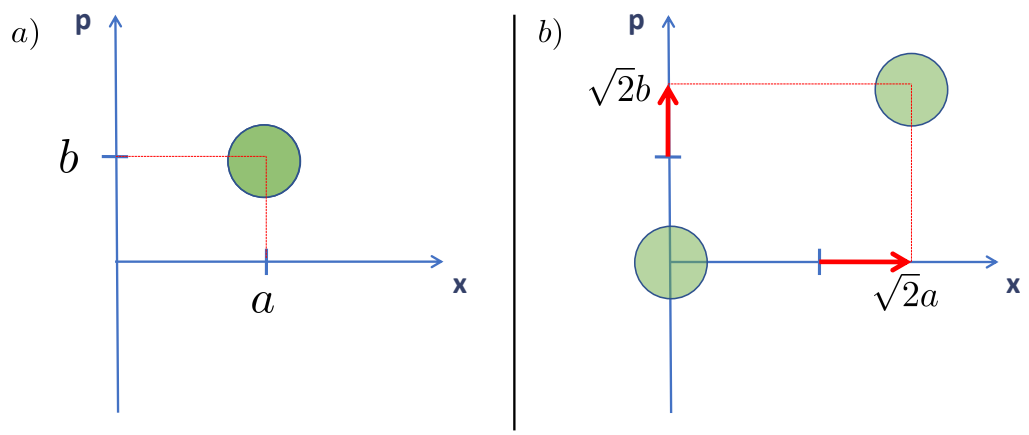

Figure 4.2: Phase space representation of the identical encoding where $x_1 = x_2 = a$ and $p_1 = p_2 = b$. a) is the identical encoding representation in phase in Alice's lab. b) is the representation in phase space of the system after Bob has applied a balanced beam splitter. All the information about the parameters a and b is concentrated in one of the modes.

Note that the left-hand side of the second equation of (4.21), which also corresponds to the attainability condition for a single-mode coherent state, is equal to the square root of the determinant of the single-mode QFIM (4.6); hence, the inversibility of the single-mode QFIM in (4.6) and the attainability condition for a single-mode coherent state are incompatible conditions. Without loss of generality, we consider ϵ_{x1} and η_{p1} to be non-zero, so that we have

$$\epsilon_{p1} = -\tfrac{\epsilon_{x1}\eta_{x1}}{\eta_{p1}}, \qquad -\eta_{x1}^2 = \eta_{p1}^2, \tag{4.22}$$

where the second equation shows a contradiction since η_{p1} is non-zero and all encoding constants $(\epsilon_{i,j}, \eta_{i,j})$ are real numbers. Hence, there exists no protocol which uses identical encoding and saturates the QCRB for both parameters a and b simultaneously.

4.4.2 Conjugate-states encoding

As we show now, an optimal encoding and estimation scheme attaining the QCRB can be obtained by selecting two appropriate input coherent states $|\alpha_1\rangle$ and $|\alpha_2\rangle$ and realizing a joint measurement, processing them through a beam splitter of transmittance T followed by two homodyne measurements, as shown in Figure 4.1.

To realize this optimal measurement, we choose a particular solution of (4.18) of the form

$$\begin{aligned} \epsilon_{x1} &= \sqrt{2T}, & \epsilon_{p1} &= 0, \\ \epsilon_{x2} &= \sqrt{2(1-T)}, & \epsilon_{p2} &= 0, \\ \eta_{x1} &= 0, & \eta_{p1} &= \sqrt{2(1-T)}, \\ \eta_{x2} &= 0, & \eta_{p2} &= -\sqrt{2T}, \end{aligned} \tag{4.23}$$

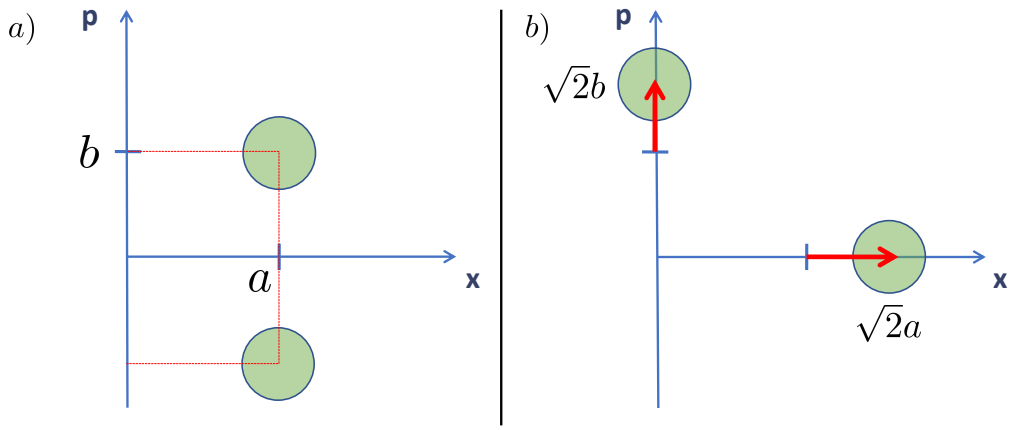

Figure 4.3: Phase space representation of the phase conjugated encoding where $x_1 = x_2 = a$ and $p_1 = -p_2 = b$ and $T = 1/2$. a) is the phase conjugated encoding representation in phase in/ Alice's lab. b) is the representation in phase space of the system after Bob has applied a balanced beam splitter. All the information about the parameter a is encoded in the coherent state aligned on the x-quadrature and the parameter b is fully encoded in the coherent state aligned on the p-quadrature .

which corresponds to the following encoding of the classical parameters a and b into the quadratures of the two input coherent states

$$\begin{aligned} x_1^{in} &= \sqrt{2T}\, a, & p_1^{in} &= \sqrt{2(1-T)}\, b, \\ x_2^{in} &= \sqrt{2(1-T)}\, a, & p_2^{in} &= -\sqrt{2T}\, b, \end{aligned} \tag{4.24}$$

that is, Alice sends the state $|\psi\rangle = |\alpha_1\rangle \otimes |\alpha_2\rangle = \left|\sqrt{T}\, a + i\sqrt{1-T}\, b\right\rangle \otimes \left|\sqrt{1-T}\, a - i\sqrt{T}\, b\right\rangle$. At the output of Bob's beam splitter, the quadratures are

$$\begin{aligned} x_1^{out} &= \sqrt{2}\, a, & p_1^{out} &= 0, \\ x_2^{out} &= 0, & p_2^{out} &= \sqrt{2}\, b, \end{aligned} \tag{4.25}$$

regardless of the value of the transmittance T (see Fig. 4.3 the case of $T = 1/2$ is showed. This case, correspond to the initial phase conjugated encoding as initially proposed in [4]). It is then easy to see that the homodyne detection of the two output modes (measuring $\hat{x}$ on mode 1 and $\hat{p}$ on mode 2) provides estimates of the parameters a and b with variances $\Delta^2\tilde{a} = \Delta^2\tilde{b} = 1/4$ saturating the QCRB in (4.14). The optimal encoding and decoding protocol is thus physically implementable with linear optics.

4.4.3 Phase conjugation and noise

Let us now emphasize on the impossibility to transform two identical copies of a coherent state into a pair of phase conjugate coherent state without adding noise. This shows that the identical encoding strategy is not unitarily equivalent to the phase-

conjugated strategy. The following argument follows the steps developped in [4].

The action of the phase conjugation operator $\hat{C}$ on a single mode annihilation operator $\hat{a}$ is the following :

$$\hat{C}\hat{a}\hat{C}^{\dagger} = \frac{\hat{C}\hat{x}\hat{C}^{\dagger} + i\hat{C}\hat{p}\hat{C}^{\dagger}}{\sqrt{2}} = \frac{\hat{x} - i\hat{p}}{\sqrt{2}} = \hat{a}^{\dagger}, \tag{4.26}$$

as the conjugation operation invert the sign of the p-quadrature operator but does not change the x-quadrature operator. Hence, the phase conjugation operation does not conserve the bosonic commutation relation between the annihilation and creation operators. Indeed, let us write the phase conjugated operator $\hat{b} = \hat{C}\hat{a}\hat{C}^{\dagger} = \hat{a}^{\dagger}$. Then, we have that:

$$\begin{aligned} \left[\hat{b}, \hat{b}^{\dagger}\right] &= \left[\hat{a}^{\dagger}, \hat{a}\right], \\ &= -\left[\hat{a}, \hat{a}^{\dagger}\right], \\ &= -1, \end{aligned} \tag{4.27}$$

and not $+1$ as it is the case for Bogoliubov transformations.

In order to find a lower bound on the noise that is needed to achieve an imperfect phase conjugation operations, we consider the case of an EPR state:

$$|EPR\rangle = \frac{1}{2\pi}\int dp\, |p, -p\rangle = \int dx\, |x, x\rangle, \tag{4.28}$$

for which the relative "position" between the two modes $\hat{X} = \hat{x}_1 - \hat{x}_2$ and the sum of the "impulsion" $\hat{P} = \hat{p}_1 + \hat{p}_2$ does commute:

$$\left[\hat{X}, \hat{P}\right] = 0. \tag{4.29}$$

Let us know define the operators $\hat{X}' = (\mathbf{1} \otimes \hat{C})\hat{X}(\mathbf{1} \otimes \hat{C}^{\dagger})$ and $\hat{P}' = (\mathbf{1} \otimes \hat{C})\hat{P}(\mathbf{1} \otimes \hat{C}^{\dagger})$ which are the new operators after the application of the phase conjugation operator on the second mode. Hence, in terms of the position and momentum operators (or equivalently quadratures operators), these operators writes :

$$\begin{aligned} \hat{X}' &\equiv \hat{x}_1' - \hat{x}_2' = \hat{x}_1 - \hat{x}_2, \\ \hat{P}' &\equiv \hat{p}_1' + \hat{p}_2' = \hat{p}_1 - \hat{p}_2. \end{aligned} \tag{4.30}$$

Hence, the operators $\hat{X}'$ and $\hat{P}'$ do not commute as:

$$\left[\hat{X}', \hat{P}'\right] = 2i. \tag{4.31}$$

Therefore, the operators $\hat{X}'$ and $\hat{P}'$ have to satisfy the following Heisenberg uncer-

tainty relation:

$$\Delta\hat{X}'\Delta\hat{P}' \geq \frac{1}{2}|\langle[\hat{X}', \hat{P}']\rangle| = \frac{|2i|}{2} = 1. \tag{4.32}$$

This relation set the minimal noise that a phase conjugation process would introduce. Let us now suppose that the mode 2 suffers, after the phase conjugation operation of some phase insensitive and unbiased noise, such that:

$$\begin{aligned} \hat{x}_2' &= \hat{x}_2 + n_x, \\ \hat{p}_2' &= \hat{p}2 + n_p, \end{aligned} \tag{4.33}$$

where $\langle n_x \rangle = \langle n_p \rangle = 0$ and $\langle n_x^2 \rangle = \langle n_p^2 \rangle = \sigma^2$ in order to satisfy the unbiased and phase insensitive hypothesis. Therefore, the variance of the resulting operators $\hat{X}' = \hat{X} - n_x$ and $\hat{P}' = \hat{P} - n_p$ is:

$$\Delta\hat{X}'^2 = \Delta\hat{P}'^2 = \sigma^2. \tag{4.34}$$

Hence, in order to satisfy the Heisenberg uncertainty relation (4.32), we find that the variance of the noise added after the phase conjugation operation is bounded by below:

$$\sigma^2 \geq 1, \tag{4.35}$$

by an amount equal to the double of the variance of a quadrature of the vacuum state: $\Delta x_0^2 = 1/2$.

In order to construct a transformation realising this imperfect phase conjugation transformation, Cerf and Iblisdir [4] consider a two-mode system where $\hat{a}_2$ is the input mode and $\hat{a}_3$ is the ancilla mode that is coupled by some unitary transformation with output modes $\hat{b}_i$ where $i = 2, 3$. The transformation can generally be written in the form:

$$\hat{b}_i = \sum_j M_{ij}\hat{a}_j + L_{ij}\hat{a}_j^\dagger, \tag{4.36}$$

where $i, j = 2, 3$ and $\hat{b}_2$ is the phase conjugator output and $\hat{b}_3$ is the ancilla that will be traced out. Now, conditions are imposed on the eight complex coefficient M_{ij} and L_{ij}:

- Phase invariance : M_{2j} and L_{2j} can always be real and positive by applying some phase transformations;
- Phase conjugator definition : $\langle\hat{b}_2\rangle = \langle\hat{a}_2^\dagger\rangle$;
- Input ancillary mode is the vacuum state by default : $\langle\hat{a}_3\rangle = \langle\hat{a}_3^2\rangle = 0$;
- The phase conjugator is phase-insensitive, which means that the input and output states have phase insensitive noise : $\langle\hat{a}_2^2\rangle = \langle\hat{a}_2\rangle^2$ and $\langle\hat{b}_2^2\rangle = \langle\hat{b}_2\rangle^2$;
- Commutation rules are conserved by the transformation (4.36) : $\left[\hat{b}_i, \hat{b}_j^\dagger\right] = \delta_{ij}$.

All these conditions impose constraints on the parameters M_{ij} and L_{ij} such that the approximate phase conjugation transformation writes:

$$\begin{aligned} \hat{b}_2 &= \hat{a}_2^\dagger + \sqrt{2}\hat{a}_3, \\ \hat{b}_3 &= \sqrt{2}\hat{a}_2 + \hat{a}_3^\dagger. \end{aligned} \tag{4.37}$$

Let us check that this phase conjugation operation is optimal, in the sense that the noise added by the phase conjugator saturates the inequality (4.35). Indeed, by considering that the input mode to be in a coherent state, we find that the output mode variances are:

$$\left(\Delta\hat{x}^2\right)_{b_2} = \left(\Delta\hat{p}^2\right)_{b_2} = \Delta\hat{x}_0^2 + 2\Delta\hat{x}_0^2 = 3/2, \tag{4.38}$$

which saturate the condition (4.35) since the added noise by the phase conjugator is indeed twice the vacuum noise $\Delta\hat{x}_0^2 = 1/2$.

This process adds the same amount of noise as the standard process of applying an heterodyne measurement on the input mode and then preparing the phase conjugated state by taking the opposite value for the p-quadrature from the heterodyne measurement output. Indeed, heterodyne measurement also adds a noise term equal to twice the vacuum noise as the measured input mode in mixed with the vacuum on a balanced beam-splitter.

4.4.4 Performance of the global strategy over the local strategies

To shed light on the feature that makes the protocol described in section 4.4.2 interesting, let us compare it with individual measurements of the quadratures of the two modes (eliminating the beam splitter) for the whole range of values of $T \in [0, 1]$. Individual homodyne measurements of two coherent states encoded according to Equation (4.24) achieve smaller relative errors when measuring x_1^{in} and p_2^{in} for $T \geq 1/2$, or x_2^{in} and p_1^{in} for $T \leq 1/2$. Thus, when comparing with the joint measurement protocol (including the beam splitter), we need to consider the individual measurements of x_1^{in} and p_2^{in} for $T \geq 1/2$ and x_2^{in} and p_1^{in} for $T \leq 1/2$.

Interestingly, we note that, for $T = 1/2$, the encoding $\mathbf{r}_{1/2}^{in} = (a, b, a, -b)$ given by (4.24) reduces to a scheme based on phase-conjugate coherent states introduced by Cerf and Iblisdir in 2001 [4]. In their paper, Cerf and Iblisdir noted that this particular encoding ($\alpha_2 = \alpha_1^*$) provides an enhancement of the measurement precision by reducing the error variances of the quadratures by a factor 2 compared to individual measurements. Nevertheless, no proof of optimality of the Cerf–Iblisdir scheme had been found in a further work investigating the superiority of joint measurements over local strategies for the estimation of product coherent states [49]. As we show below, this particular optimal scheme is the one which shows the best improvement when comparing it with individual measurements (see Figure 4.4).

A natural question is indeed to compare this improvement with the one exhibited by the other optimal protocols in this family (with other values of the beam splitter transmittance T). Observing first the limiting trivial cases $T = 1$ and $T = 0$, we see that the corresponding encodings $\mathbf{r}_1^{in} = (\sqrt{2}a, 0, 0, -\sqrt{2}b)$ and $\mathbf{r}_0^{in} = (0, \sqrt{2}a, \sqrt{2}b, 0)$ are already in optimal configurations, so that the variances of the estimators obtained by individual homodyne measurement of the input quadratures already saturate QCRB. Thus, for $T = 1$ or $T = 0$, a joint measurement cannot provide any enhancement of the measurement precision. For other values of T, we have a continuous evolution of the precision enhancement with respect to individual measurements ranging between 2 (maximum enhancement) and 1 (no enhancement at all). To see this, let us compare the error variances of the estimators of the encoded parameters a and b obtained by the optimal joint or optimal individual measurement. The variances of the joint measurement saturate the QCRB by construction, namely $\Delta\tilde{a}^2_{\mathrm{QCRB}} = \Delta\tilde{b}^2_{\mathrm{QCRB}} = 1/4$. As already mentioned, the optimal individual measurement consists in measuring $\hat{x}_1$ and $\hat{p}_2$ for $T \geq 1/2$, or $\hat{x}_2$ and $\hat{p}_1$ for $T \leq 1/2$, so we may deduce from Equation (4.24) the corresponding variances of the estimators

$$\Delta\tilde{a}^2_{ind}(T) = \frac{\Delta\hat{x}_i^2}{1+|1-2T|} = \frac{1}{2+|2-4T|}, \tag{4.39}$$

$$\Delta\tilde{b}^2_{ind}(T) = \frac{\Delta\hat{p}_{3-i}^2}{1+|1-2T|} = \frac{1}{2+|2-4T|}, \tag{4.40}$$

$$i = \begin{cases} 1, & (T > 1/2), \\ 2, & (T < 1/2), \end{cases} \tag{4.41}$$

where we have made the dependence on T explicit. Due to this dependence, the enhancement in the measurement precision can be expressed in terms of the ratio between the error variance on the estimators obtained by individual and joint measurements as a function of T:

$$\frac{\Delta\tilde{a}^2_{ind}(T)}{\Delta\tilde{a}^2_{\mathrm{QCRB}}} = \frac{\Delta\tilde{b}^2_{ind}(T)}{\Delta\tilde{b}^2_{\mathrm{QCRB}}} = \frac{2}{1+|1-2T|}. \tag{4.42}$$

As shown in Figure 4.4, the precision enhancement attains its maximum value 2 at $T = 1/2$ and its minimum value 1 at $T = 0$ or 1.

Given a and b, the beam splitter transmittance T defines a family of points (x_i, p_i) in phase space–hence, a family of pairs of coherent states–which allow an optimal encoding as defined by Equation (4.24). From this equation, it is easy to deduce that these points belong to an elliptic curve determined by the classical parameters a and b

$$\frac{x_i^2}{a^2} + \frac{p_i^2}{b^2} = 2, \quad i = 1, 2. \tag{4.43}$$

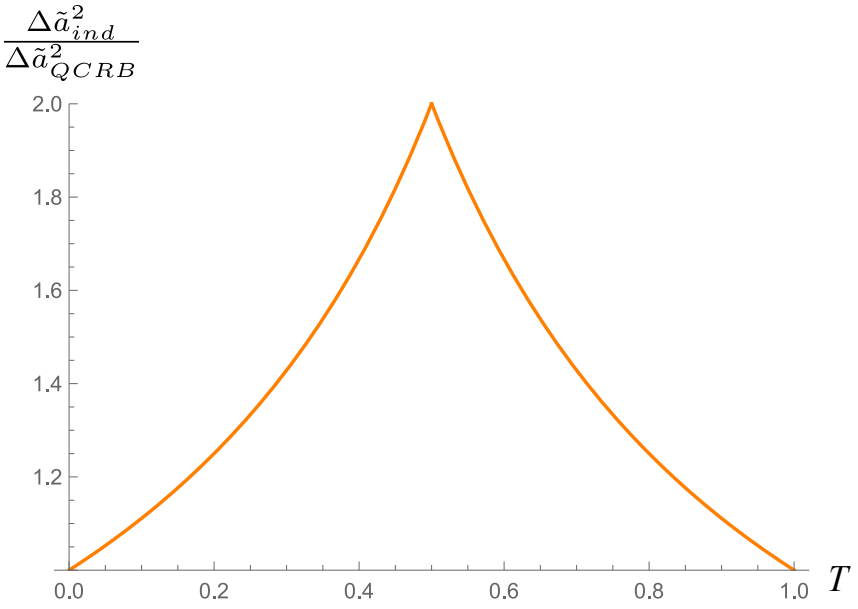

Figure 4.4: Enhancement of the measurement precision of the joint (compared to individual) measurement as a function of the beam splitter transmittance T. This is calculated as the reduction of the error variance for the joint measurement attaining the QCRB with respect to the error variance of the optimal individual measurements.

Therefore, the general encoding protocol implies the generation of two coherent states determined by the parameters a and b to be transmitted (as shown in Figure 4.5) and a measurement setting T, which has to be specified before the measurement. We note that, by allowing local phase rotations of the input states and by suitably choosing phase angles θ and ϕ, one can use any pair of coherent states for encoding two classical parameters a and b (satisfying the energy constraint), which can be further optimally extracted by joint measurement including a beam splitter with a suitable transmittance T followed by homodyne measurements on two output modes. The corresponding protocol is described in section 4.4.5.

4.4.5 Explicit optimal protocol for two modes

Here, we present a protocol which allows Alice, given two optical modes in arbitrary chosen coherent states $|\alpha_1\rangle|\alpha_2\rangle$, to provide Bob with measurement settings $\{T, \theta, \phi\}$ she has chosen in order to encode the real parameters a and b such that he can optimally extracts by homodyne measurement these two real parameters a and b. The only conditions Alice has to satisfy are an energy condition (4.2), an attainability condition (4.17) in order for Bob to be able to optimally estimate the parameters and an equal precision condition (4.10) which assures that both parameters can be estimate with the same variance.

1. Alice chooses real a, b, and $0 \leq T \leq 1$ by imposing that energies of the "optimal input states" given by Equation (4.24) are equal to the energies of the given

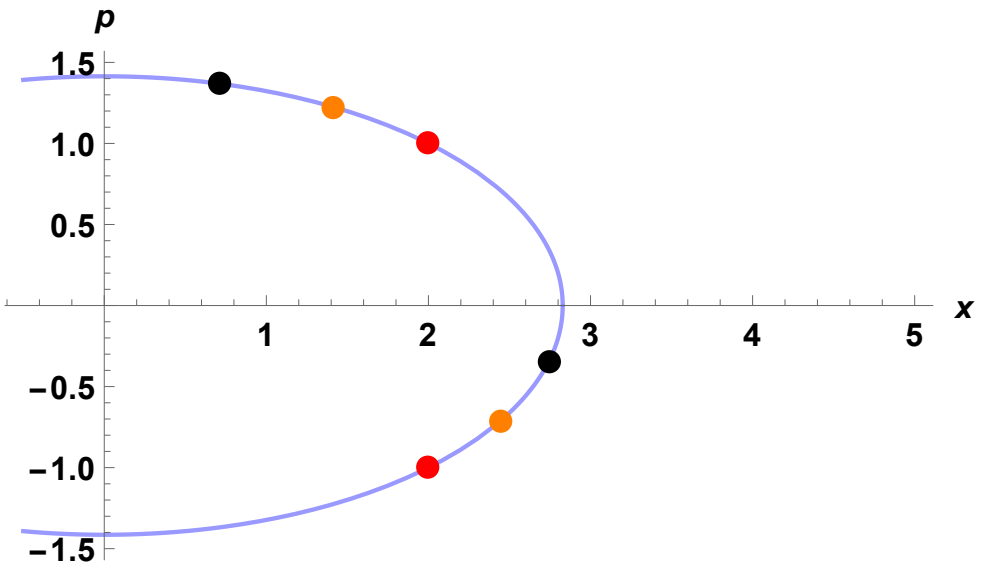

Figure 4.5: Family of optimal encoding schemes. For a given value of the parameters a and b (here, $a = 2$ and $b = 1$), each optimal encoding consists of preparing two coherent states (see two black points, two yellow points, two red points, etc.) according to (4.24).

coherent states in corresponding modes. This leads to the following equations:

$$\begin{cases} x_1^2 + p_1^2 = 2Ta^2 + 2(1-T)b^2, \\ x_2^2 + p_2^2 = 2(1-T)a^2 + 2Tb^2. \end{cases} \tag{4.44}$$

The two equations contain three unknown variables, a, b, and T. Although a and b are related by the energy conservation in (4.2), it is linearly dependent on the two equations above. Indeed, the above system is obviously equivalent to

$$\begin{cases} x_1^2 + p_1^2 + x_2^2 + p_2^2 = 2(a^2 + b^2), \\ x_1^2 + p_1^2 - x_2^2 - p_2^2 = 2(2T-1)(a^2 - b^2). \end{cases} \tag{4.45}$$

where the first equation is, in fact, the energy constraint (4.2). Let us know consider two cases.

In the first case, we consider that the energies of the given coherent states 1 and 2 are equal, then $T = 1/2$ satisfies the second equation and we are free to choose any a and b on the circle determined by the first equation. Another valid option is to choose $a^2 = b^2 = (x_1^2 + p_1^2 + x_2^2 + p_2^2)/4$ and take an arbitrary T.

In the second case, we consider that the energies of the given coherent states are not equal. Hence, we can replace the second equation by

$$\frac{x_1^2 + p_1^2 - x_2^2 - p_2^2}{a^2 - b^2} = 2(2T-1), \tag{4.46}$$

so that T becomes a function of the ratio between the differences of the number

of photon in the input and output modes. Equation (4.46) further limits the choice of x and p because $|2T-1| \leq 1$, meaning that

$$2|a^2 - b^2| \geq |x_1^2 + p_1^2 - x_2^2 - p_2^2|. \tag{4.47}$$

Once x and p are chosen, T becomes

$$T = \frac{1}{2}\left(\frac{x_1^2 + p_1^2 - x_2^2 - p_2^2}{2(a^2 - b^2)} + 1\right). \tag{4.48}$$

2. In both cases considered above, Equation (4.24) determines the parameters of two input states, which would provide the desired optimal measurement,

$$\begin{aligned} x_1^{(\mathrm{opt})} &= x\sqrt{\frac{x_1^2 + p_1^2 - x_2^2 - p_2^2}{2(a^2 - b^2)} + 1}, \\ p_1^{(\mathrm{opt})} &= p\sqrt{\frac{x_1^2 + p_1^2 - x_2^2 - p_2^2}{2(a^2 - b^2)} - 1}, \\ x_2^{(\mathrm{opt})} &= x\sqrt{\frac{x_1^2 + p_1^2 - x_2^2 - p_2^2}{2(a^2 - b^2)} - 1}, \\ p_2^{(\mathrm{opt})} &= -p\sqrt{\frac{x_1^2 + p_1^2 - x_2^2 - p_2^2}{2(a^2 - b^2)} + 1}. \end{aligned} \tag{4.49}$$

By our construction, the energies of the optimal input states are equal to the energies of the given states in corresponding input modes. Then, the given and optimal input states are related by simple rotation in phase space by angles θ and ϕ, which can be easily found from the vector algebra

$$\cos\theta_i = \frac{x_i^{(\mathrm{opt})} x_i + p_i^{(\mathrm{opt})} p_i}{x_i^2 + p_i^2}. \tag{4.50}$$

where $\theta_1 = \theta$ and $\theta_2 = \phi$.

3. After performing the calculations described above, Alice provides to Bob with the measurement settings $\{T, \theta, \phi\}$ and the given coherent states. Note that the measurement settings $\{T, \theta, \phi\}$ do not carry any information about the parameters a and b.

4. Upon receiving the measurement settings, Bob applies local rotations to the input modes followed by the beam splitter transformation and homodyne measurements in the output modes, thus realizing an optimal extraction of encoded x and p variable.

Finally, let us make an interesting observation coming from Equation (4.46). Recall that, following Equation (4.42), the precision gain monotonously increases when $|1 - 2T|$ tends to zero. Hence, when choosing a, b, and T, we are interested in attaining

the minimal possible value of the right hand side of Equation (4.46) compatible with all the constraints. This can be done by maximizing the denominator on the left hand side of this equation because the numerator there is constant. Due to the energy constraint in (4.2), the maximum is achieved when

$$\begin{aligned} a^2 &= \frac{1}{2}(x_1^2 + p_1^2 + x_2^2 + p_2^2), \\ b^2 &= 0. \end{aligned} \tag{4.51}$$

With these values for x and p the first equation of (4.44) gives us

$$T = \frac{x_1^2 + p_1^2}{x_1^2 + p_1^2 + x_2^2 + p_2^2}, \tag{4.52}$$

which equalizes the transmittance to the proportion of the number of photons in state 1 with respect to the total photon number in both given states. Here, an unfortunate aspect comes to play. Although this choice provides the better enhancement of the precision of the optimal joint measurement with respect to the individual measurement, it provides an additional constraint that removes any choice of the real parameters that Alice can transmit. Indeed, according to Equation (4.51), a becomes equal to the mean value of the total number of input photons and b becomes zero. Now, if Bob knows that Alice used this "optimal" encoding, then he does not need to know the measurement settings because a becomes directly accessible by the measurement of the intensity of the given states and b does not carry any information being always zero. Therefore, to exploit the protocol in applications using modulation of transmitted parameters, one cannot always choose the transmission coefficient, which provides the maximal enhancement of precision.

4.5 Arbitrary number of modes

Let us now extend the scheme presented in Section 4.4 to an arbitrary number n of input coherent states and same number of real classical parameters to be encoded. First, observe that one can always split a $2n$-mode input system of coherent states into n two-mode subsystems and use, for each subsystem, the optimal measurement scheme described in Section 4.4. Since the quantum Fisher information is additive, the optimal measurement scheme for $2n$ modes is realized by the optimal two-mode measurement scheme individually applied to each pair of modes. However, for $2n+1$-mode systems, the application of the optimal scheme to n pairs cannot realize the overall optimal strategy since neither heterodyne nor homodyne measurement applied to the last single mode is optimal. However, as we show in Section 4.5.1, it is possible to develop an optimal (joint) strategy for a three-mode input coherent state. Then, for any larger odd number of modes, the optimal scheme applied to

the first $n-1$ pairs supplemented with this three-mode strategy provides an optimal measurement for all $2n+1$ modes.

4.5.1 Three-mode encoding and estimation scheme

In the three-mode case, a natural guess for the optimal estimation is to concatenate two times the scheme proposed in Section 4.4 in a way that the second output mode of the first scheme will serve as an input for the second scheme (see Figure 4.6). Notice that, being an output of the first "optimal" scheme, the state in the second mode after the first beam splitter always has some fixed phase determined by the first scheme (see Equation (4.25)). Then, to bring the state into the form of an optimal input for the second scheme, a local rotation by some angle ϕ may be required, as depicted in Figure 4.6. The full transformation of the quadrature operators of the input modes into those of the output modes is written as $\hat{\mathbf{r}}' = B(T_2)U(\phi)B(T_1)\hat{\mathbf{r}}$, where $U(\phi)$ is a rotation in phase space by angle ϕ and the two beam splitter transformations are characterized by transmissivities T_1 and T_2.

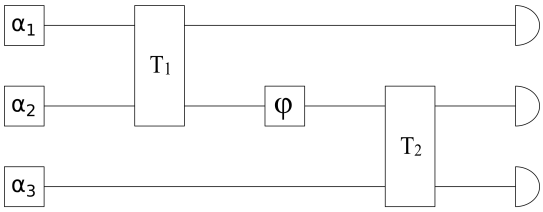

Figure 4.6: Optimal joint estimation scheme for three modes using two beam splitters of transmittance T_1 and T_2 and a phase shifter of angle ϕ.

Denoting as a, b, and c the three real parameters that are encoded into the three coherent states, we choose the final output state to be in a similar form as (4.25), namely $\mathbf{r}^{out} = (\sqrt{2}a, 0, \sqrt{2}b, 0, 0, \sqrt{2}c)$, which allows us to recover these parameters by homodyne measurement of the output quadratures with the same error variances as in the optimal two-mode scheme, hence saturating the QCRB. Using the relation between the mean value of the input and output quadratures, which is given by the same transformation $\mathbf{r}' = B(T_2)U(\phi)B(T_1)\mathbf{r}$, we obtain the parameters of the optimal input states for the three-mode scheme

$$\begin{aligned}
x_1^{(\mathrm{opt})} &= \sqrt{2T_1}\, a, \\
p_1^{(\mathrm{opt})} &= \sqrt{2(1-T_1)}\, d(T_2, b, c), \\
x_2^{(\mathrm{opt})} &= \sqrt{2(1-T_1)}\, a, \\
p_2^{(\mathrm{opt})} &= -\sqrt{2T_1}\, d(T_2, b, c), \\
x_3^{(\mathrm{opt})} &= \sqrt{2(1-T_2)}\, b, \\
p_3^{(\mathrm{opt})} &= -\sqrt{2T_2}\, c,
\end{aligned} \tag{4.53}$$

where

$$d(T_2, b, c) = \left(T_2 b^2 + (1 - T_2)c^2\right)^{1/2}, \tag{4.54}$$

and

$$\tan(\phi) = \frac{b}{c}\left(\frac{T_2}{1 - T_2}\right)^{1/2}. \tag{4.55}$$

This encoding and estimation setting enables the optimal retrieval of the three unknown parameters a, b, and c with variances saturating the QCRB $\Delta^2\tilde{a} = \Delta^2\tilde{b} = \Delta^2\tilde{c} = 1/4$. Moreover, the encoding strategy in (4.53) satisfies the three-mode extension of (4.2), which is the energy condition: $x_1^2 + p_1^2 + x_2^2 + p_2^2 + x_3^2 + p_3^2 = 2(a^2 + b^2 + c^2)$.

For a n-mode encoding strategy, the energy condition is

$$\sum_{i=1}^{n}(x_i^2 + p_i^2) = 2\sum_{i=1}^{n} a_i^2, \tag{4.56}$$

where the a_i's are the n real parameters to be encoded and estimated. The energy constraint on all the n modes given by (4.56) can always be divided in a system of $\lfloor \frac{n}{2} \rfloor$ equations corresponding to the two- and three-mode energy constraints. Hence, a combination of two- and three-mode optimal schemes allows one to encode and retrieve optimally an arbitrary number n of classical parameters encoded in n coherent states. Note that optimal combinations are not necessarily unique. For example, for six modes, three pairwise optimal measurements work as well as two three-mode optimal measurements.

4.5.2 n-mode extension

Finally, we can also generalize the constraints derived for two-mode systems to the problem of estimating optimally n parameters encoded in n coherent states. The derivation of these constraints follows the same reasoning as for the two-mode constraints explained in (4.18). To keep the expressions concise, we use the following notation for the linear encoding constants:

$$\mathcal{E}_i^{(j)} = \frac{\epsilon_{xi}^{(j)} + i\,\epsilon_{pi}^{(j)}}{\sqrt{2}}, \tag{4.57}$$

where i denotes the mode number and j is the parameter number. For example, for two modes, $\mathcal{E}_i^{(1)} = \epsilon_{xi} + i\,\epsilon_{pi}$ and $\mathcal{E}_i^{(2)} = \eta_{xi} + i\,\eta_{pi}$, for $i = 1, 2$. (4.3) then generalizes as

$$\alpha_i = \frac{x_i + i\,p_i}{\sqrt{2}} = \sum_{j}^{n} \mathcal{E}_i^{(j)} a_j, \quad i = 1, ..., n, \tag{4.58}$$

where, again, $(a_1, a_2, ..., a_n)$ denotes the vector of real parameters. Based on (4.15), we generalize the expression for the SLD as

$$L^{(j)} = i\,\Im\left(\sum_i^n \mathcal{E}_i^{(j)}\left[\hat{a}_i^\dagger, \hat{\rho}\right]\right), \tag{4.59}$$

where $\Im$ denotes the imaginary part. Using this notation, the Fisher information matrix elements can be written in a compact form as

$$F_{jk}^{(n)} = 4\,\Re\left[\sum_i^n \mathcal{E}_i^{(j)*}\mathcal{E}_i^{(k)}\right], \tag{4.60}$$

which generalizes (4.6). Following the same reasoning as for the derivation of the two-mode constraints, we can establish the n-mode constraints:

$$\begin{aligned}
\sum_i^n |\mathcal{E}_i^{(j)}| &= 1 \quad \forall j, \\
\Re\left(\sum_i^n \mathcal{E}_i^{(j)*}\mathcal{E}_i^{(k)}\right) &= 0 \quad \forall j,k \; s.t. \; j \neq k, \\
\Im\left(\sum_i^n \mathcal{E}_i^{(j)*}\mathcal{E}_i^{(k)}\right) &= 0 \quad \forall j,k \; s.t. \; j \neq k,
\end{aligned} \tag{4.61}$$

corresponding to the energy, equal precision and attainability conditions. This system of equations forms a set of n^2 constraints imposed on the set of $2n^2$ encoding constants. Moreover, the equal precision and attainability conditions together impose that the matrix $\mathcal{E}_i^{(j)}$ composed of all linear encoding constants is a unitary matrix. Any optimal n-mode scheme can be constructed as follows: Alice encodes the n parameters a_i in the x-quadrature of the ith coherent states. She applies a passive Gaussian unitary on her system and sends the output to Bob. Bob applies the inverse of the passive Gaussian unitary used by Alice and, finally, he uses homodyne detection on the x-quadratures to optimally estimate the n parameters a_i.

4.6 Conclusions

We have proved the optimality of the parameter encoding/estimation scheme based on phase-conjugate coherent states proposed by Cerf and Iblisdir [4] by showing that it saturates the quantum Cramér–Rao bound. This can be viewed as a consequence of the fact that using phase-conjugate coherent states cancels the off-diagonal terms of the QFIM matrix (4.6) and allows to simultaneously satisfy the attainability condition in Equation (4.17). We have also demonstrated that this scheme is a special case of a larger family of optimal two-mode schemes in which the decoding only requires linear optics (a single beam splitter) followed by homodyne measurement. Then, by exploiting the additivity of the quantum Fisher Information matrix for the product

of states, we have further generalized this optimal encoding/estimation scheme to an arbitrary number n of modes. The resulting scheme combines optimal two-mode and three-mode schemes in order to encompass even and odd n's.

An interesting question left for future study concerns the optimality of the considered schemes for other usual quantum states of light, e.g., squeezed states. Furthermore, it may be interesting to explore whether these parameter communication schemes may be used in order to achieve some cryptographic tasks, such as public key distribution or secret sharing (where, for example, the set of parameters to be estimated might be considered as the secret key [2]).

[2]One may consider a scenario where Alice challenges Eve to reproduce the system of phase conjugated states Alice has prepared. In this scenario, it is assumed that Eve only has access to individual attacks on one of the two mode of the system prepared by Alice and sent to Bob.

Part III | Continuous-variable separability criteria

5 Introduction to separability criteria

5.1 Separability and entanglement for bipartite states

The quantum states of a shared physical system between two parties, namely Alice and Bob or A and B, are described by a density matrix ρ_{AB} living in the Hilbert space $\mathcal{H} = \mathcal{H}_{\mathcal{A}} \otimes \mathcal{H}_{\mathcal{B}}$. These states are called *bipartite states* since they are shared between two parties. The bipartite states are divided in two classes : separable and entangled states. As pointed by Einstein, Podolsky and Rosen in their famous paper [13], entangled states are specific to the quantum description of the world. The importance of entangled states towards separable states comes from the fact that they serve as resources for certain quantum tasks such as quantum teleportation [50, 51] or quantum cryptography [52].

The more straightforward example of a separable state is the product state. Its mathematical description is given in the following definition.

Definition 1 (**Product state**). *A bipartite state ρ_{AB} is said to be a **product state** if it can be written as*

$$\rho_{AB} = \rho^A \otimes \rho^B. \tag{5.1}$$

We can understand that product states are *separable* in the sense that if one party, let say Alice, applies a local unitary operation on her part ρ_A of a product state ρ_{AB}, it does not affect the reduced state in Bob's laboratory ρ_B. If Bob applies a measure on the reduced state in his laboratory, the outcome will be independent of the operation applied by Alice. Hence, all states that are convex combinations of product states will also have this "separability" property. The general definition for a separable state is the following :

Definition 2 (**Separable state**). *A bipartite state ρ_{AB} is said to be **separable** or **unentangled** if it can be written as*

$$\rho_{AB} = \sum_i p_i \rho_i^A \otimes \rho_i^B, \tag{5.2}$$

where $p_i \geq 0$ and $\sum_i p_i = 1$. If no such convex linear combination of product states exists for a given state ρ_{AB}, then the state is called ***entangled****.*

In the following, we will use the notation σ_{AB} for separable states.

Separable states can be seen as states prepared in a *local* or *classical* way. More formally, this means that the bipartite states generated from the most general procedure, employing only local operations and classical communication (LOCC) on a product state is a separable state. Another way to state this is to say that no entangled state can be generated from a separable state by the only means of LOCC operations.

5.2 Detection of entangled states

In order to detect entangled states (i.e. non-separable states), there are different tools that one can use. Indeed, one can write down a mathematical criterion, called *separability criterion*, that gives necessary and/or sufficient conditions for separability. Note that these criteria do not necessarily need to be associated with quantum observables. Calculating such entanglement criteria usually assume to have access to the density matrix of the state under consideration. In order to use these criteria in practice, one then needs to do the expensive full tomography of the state and after that apply the operations to the density matrix in order to calculate the criteria. Hence, there is space for other, less demanding methods that avoid the need for full tomography. One interesting tool available is the so-called *entanglement witness* that is defined as follows :

Definition 3 (Entanglement witness). *An* ***entanglement witness*** *is an operator W that needs to satisfy the following conditions :*

1. *W is hermitian;*
2. *W has positive expectation values with respect to all separable states :* $\mathrm{Tr}(W\sigma_{AB}) \geq 0$*;*
3. *W has negative expectation value for, at least, one entangled state :* $\mathrm{Tr}(W\rho_{AB}) < 0$ *where ρ_{AB} is entangled.*

Hence, entanglement witnesses are associated with measurable observables W_i which are very useful since they are experimentally accessible. Moreover, entanglement witnesses have a geometric meaning. Indeed, for each witness W_i, the equality $\mathrm{Tr}\,(W_i\rho_{AB}) = 0$ defines an hyperplane in the set of states (see Fig. 5.1). From this geometric approach, it is possible to proof the following theorem (see [53]) :

Theorem 1 (Completeness of witnesses). *For each entangled state ρ_{AB} there exists an entanglement witness detecting it.*

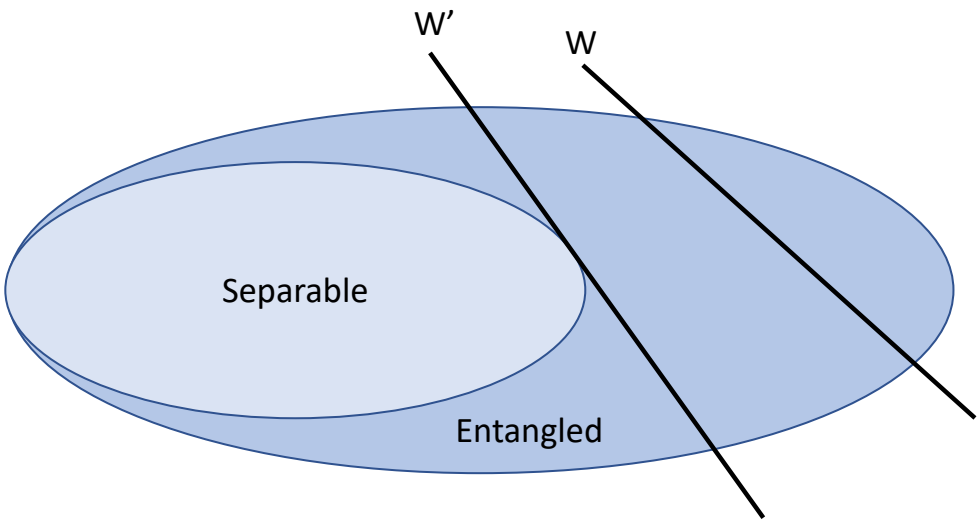

Figure 5.1: The convex sets of separable and entangled states are represented. The black lines, labelled W and W', shows possible entanglement witnesses hyperplanes defined by $\mathrm{Tr}(W\rho) = 0$ and $\mathrm{Tr}(W'\rho) = 0$. The entanglement witness W' is finer than W since W' detects all states detected by W and some more entangled states.

Hence, the whole set of entanglement witnesses define a necessary and sufficient condition of separability of states even if a single entanglement witness fail to detect all entangled states.

Finally, it is also possible to quantify *how much entanglement does a state possess*. **Entanglement measures** $E(\rho)$ (or **entanglement monotones**) do quantify the amount of entanglement of a state. In order to build a proper entanglement measure, it should satisfy, at least, the following conditions :

1. If ρ is separable, then $E(\rho) = 0$.
2. $E(\rho^{LOCC}) \leq E(\rho)$ which means that since entanglement cannot be created by LOCC operations, the entanglement witness should never increase under LOCC.

Entanglement measures are central to the description of resource theory for entanglement (see [54] for a review on quantum resource theories).

5.3 Discrete-variable separability criteria

5.3.1 Separability of pure states

Despite the compact definition of a separable state (Def. 2), deciding whether a state is separable or entangled is, in general, a non-trivial task (see [55]). However, in the case of pure states, there exists an easy criterion to check the separability of the state.

Indeed, a pure state is separable if and only if $\rho_{AB} = \rho_A \otimes \rho_B$ where $\rho_{A,B}$ are the reduced density matrix defined as $\rho_A = \mathrm{Tr}_B(\rho_{AB})$ and $\rho_B = \mathrm{Tr}_A(\rho_{AB})$. Moreover, it is well-known that any pure bipartite state can be decomposed on an orthonormal basis, $|i_A\rangle$ and $|i_B\rangle$ for subsystem A and B respectively. This is known as the *Schmidt decomposition* of a pure state and is defined as follows :

Definition 4 (Schmidt-decomposition). *Any pure bipartite state $|\psi_{AB}\rangle \in \mathcal{H}^{\mathcal{A}} \otimes \mathcal{H}^{\mathcal{B}}$ can be decomposed on an orthonormal basis $|i_A\rangle \in \mathcal{H}^{\mathcal{A}}$ and $|i_B\rangle \in \mathcal{H}^{\mathcal{B}}$ as*

$$|\psi_{AB}\rangle = \sum_{i=1}^{r_s} s_i |i_A\rangle|i_B\rangle, \tag{5.3}$$

where r_s is the Schmidt-rank and the non-zero s_i's are the Schmidt coefficients which satisfy $s_i \geq 0$ and $\sum_{i=1}^{r_s} s_i^2 = 1$.

Hence, a pure state is separable if and only if it has a Schmidt-rank of 1 exactly. Interestingly, the Schmidt rank of a pure state cannot be increased by LOCC transformations [56].

One can see that the reduced state $\rho_A = |\psi_A\rangle\langle\psi_A|$ can be written $|\rho_A\rangle = \sum_i^{r_s} s_i^2 |i_A\rangle\langle i_A|$. Hence, for $r_s = 2$ or more, the state ρ_A is mixed. This is a signature of the entanglement of $\rho_{AB} = |\psi_{AB}\rangle\langle\psi_{AB}|$. From there, one can find a measure of entanglement by considering the *von Neumann entropy* [57] of the reduced state ρ_A. The von Neumann entropy of a quantum system, described by the state ρ, is defined as

$$S(\rho) = -\mathrm{Tr}(\rho \log \rho), \tag{5.4}$$

where the log is considered in base 2. The definition of the von Neumann entropy can be re-expressed by considering the eigenvalues e_x of the quantum state ρ as

$$S(\rho) = -\sum_x e_x \log e_x. \tag{5.5}$$

A remarkable property of the von Neumann entropy is that it is equal to zero for pure states. Hence, from the Schmidt decomposition of ρ_A, we see that the von Neumann entropy is

$$S(\rho_A) = -\mathrm{Tr}(s_i^2 \log(s_i^2)). \tag{5.6}$$

Hence, it will be equal to zero only if the Schmidt-rank of ρ_{AB} is exactly one. Therefore, $S(\rho_A) > 0$ is a clear signature and measure of entanglement of ρ_{AB}.

For mixed states on the other hand, the story is longer and more complex. The next section is dedicated to a review of some of the known criteria.

5.3.2 Separability of mixed states

The PPT criterion

When considering mixed states, the most used criterion for separability is certainely the so-called *PPT* criterion (for Positive Partial Tranpose) introduced by Peres and Horodecki [58, 53]. This criterion involve the map of partial transpose $T_{A,B}$ on one of the parties A or B respectively, in the case the partial transpose in applied on B, we will use the following notation : $(\mathbf{1} \otimes T_B)\rho_{AB} = (\rho_{AB})^{T_B}$. The PPT criterion is a necessary condition for the separability of a state ρ_{AB}. It is stated as :

Theorem 2 (PPT criterion). *Let ρ_{AB} be a bipartite separable state. Then ρ_{AB} is PPT, which means that $(\rho_{AB})^{T_B} \geq 0$.*

The proof is very short and is based on the definition of separability. Indeed, since any separable state can be written as Eq. (2), we have $\sigma_{AB} = (\rho_{AB})^{T_B} = \sum_i p_i \rho_i^A \otimes (\rho_i^B)^T$ and since ρ_i^B are valid density matrices, so are the $(\rho_i^B)^T = (\rho_i^B)^*$ and hence, none of the eigenvalues of σ_{AB} are negative. Separable states ρ_{AB} are "*positive under partial transpose*".

The PPT criterion is a strong [1] and easy to calculate separability criterion. Indeed, if one has access to the density matrix of a bipartite states, one can apply the partial transposition operator to it and calculate the spectrum of the partially transposed matrix. If one of the eigenvalues is negative, then he can conclude that the state is entangled. If not, the criterion is not conclusive. However, the PPT criterion becomes necessary and sufficient in the low dimensional systems 2×2 and 2×3 [55]. This means that the PPT criterion completely characterizes the entanglement in a two-qubit-system and is therefore a very useful tool to investigate entanglement of bipartite qubit systems. In higher dimensional systems there might exist *bound entangled states* which are entangled states from which entanglement can not be distilled. Since all entangled states that are PPT [59] are bound entangled states, it implies that other separability criteria than PPT are needed to detect these bound entangled states as non-separable [60].

The entropic and reduction criteria

The entropic criterion was introduced in [53, 61]. It is stated in terms of the von Neumann conditional entropy:

$$S(A|B) \equiv -\mathrm{Tr}\left[\rho_{AB} \log_2 \rho_{A|B}\right] = S(AB) - S(B), \tag{5.7}$$

[1] The PPT criterion is a necessary and sufficient separability criterion for systems composed of 2 qubits or 2-mode Gaussian states.

where $\rho_{A|B} = 2^{-\sigma_{AB}}$ with $\sigma_{AB} = \mathbb{1}_A \times \log_2(\rho_B) - \log_2(\rho_{AB})$[2], $S(AB) = -\mathrm{Tr}\left[\rho_{AB} \log_2 \rho_{AB}\right]$ is the joint von Neumann entropy and $S(B) = -\mathrm{Tr}_B\left[\rho_B \log_2 \rho_B\right]$ is the von Neumann entropy of system B. The von Neumann conditional entropy $S(A|B)$ is always positive for separable states but can be negative for some entangled states [61].

The reduction criterion is a separability criterion based on a positive (but not completely positive) map Λ^R described in [62, 63]. The map acts on one system σ as

$$\Lambda^R(\sigma) = \mathbb{1}\,\mathrm{Tr}(\sigma) - \sigma. \tag{5.8}$$

Hence, separable states ρ_{AB} have to satisfy the following equality:

$$(\mathbb{1}_A \times \Lambda^R)(\rho_{AB}) = (\mathbb{1}_A \times (\mathbb{1}_B\,\mathrm{Tr}_B - \mathbb{1}_B))\,(\rho_{AB}) = \rho_A \times \mathbb{1}_B - \rho_{AB}, \tag{5.9}$$

where $\rho_A = \mathrm{Tr}_B(\rho_{AB})$ is the reduction of the state ρ_{AB}. Finally, the reduction criterion writes:

$$(\rho_A \times \mathbb{1}_B) - \rho_{AB} \geq 0. \tag{5.10}$$

This criterion is in general weaker that the PPT criterion. However, all states violating the reduction criterion can be distilled [62].

The majorization criterion

In 2001, Nielsen and Kempe published a famous article named "*Separable states are more disordered globally than locally*" [64]. Indeed, the notion of disorder of a quantum state is often given in terms of the von Neumann entropy. As we saw in section 5.3.1, the von Neumann entropy can be used to build an entropic separability criterion stating that if a state ρ_{AB} is separable, then the von Neumann entropy of the global state $S(\rho_{AB})$ is greater than the von Neumann entropy of his marginals $S(\rho_A)$ and $S(\rho_B)$. However, Nielsen and Kempe use a more sophisticated notion of disorder, *majorization*, in order to give a stronger separability criterion. Indeed, by considering the majorization relation between the eigenvalues λ of a bipartite state ρ_{AB} and his marginals ρ_A and ρ_B, they derive the following necessary condition for separability :

Theorem 3 (Majorization criterion for separability [64]). *If ρ_{AB} is separable, then $\lambda(\rho_{AB}) \prec \lambda(\rho_A)$ and $\lambda(\rho_{AB}) \prec \lambda(\rho_B)$.*

The majorization criterion is strictly stronger than the entropic criterion based on the von Neumann entropy since the von Neumann entropy is a Schur-concave function and is hence implied by the majorization criterion (see [65] for a reference on the theory of majorization).

[2]Note that $\rho_{A|B}$ is not a density operator as its eigenvalues can have values greater than 1. This is the origin of the violation of the entropic criterion for separability.

5.4 Continuous-variable separability criteria

Some of the separability criteria introduced in section 5.3 have a counterpart in continuous variables. For Gaussian states, we know that the displacement operation does not affect the entanglement of states since it is an invertible operation. Hence, most of the the continuous variable criteria for Gaussian states are based on the covariance matrix of the state. We review some of them in this section.

5.4.1 Duan and Simon criterion

The Duan *et al.* [21] and Simon [66] criteria is of major importance since, as showed by Simon in [66], it is the PPT criterion adapted to the continuous-variables framework. Indeed, the partial transpose operation can be easily interpreted in terms of the Wigner function (2.22) in phase space. For a bipartite quantum state, the Wigner function writes $W(x_1, x_2, p_1, p_2)$ and by applying the partial transpose operation on the second party, the Wigner function is transformed to $W(x_1, x_2, p_1, -p_2)$.

$$\rho \to (\mathbf{1} \otimes T_B)(\rho) \Leftrightarrow W(x_1, x_2, p_1, p_2) \to W(x_1, x_2, p_1, -p_2). \tag{5.11}$$

Hence, the action of the partial transpose T_B on the density matrix is equivalent to change the sign of the momentum of the second subsystems: $\xi \to \Lambda\xi$ where $\xi = (x_1, p_1, x_2, p_2)$ and $\Lambda = diag(1, 1, 1, -1)$. This can be interpreted as a local time reversal operation on the second subsystem. Another geometrical interpretation given by Simon [66] is to see the partial transpose as a mirror reflection in phase space.

Simon's argument starts from the uncertainty principle expressed for the covariance matrix V:

$$\gamma + \frac{i}{2}\Omega \geq 0, \tag{5.12}$$

where Ω is the symplectic 4×4 antisymmetric bloc matrix (2.4). The action of the partial transpose on the covariance matrix writes:

$$\gamma \to \tilde{\gamma} = \Lambda\gamma\Lambda. \tag{5.13}$$

Similarly to the argument of Peres-Horodecki reminded in section 5.3.2, if a state ρ is separable, then by taking its partial transpose, it should remain a bona fide density matrix, hence it should satisfy the uncertainty principle Eq. (5.12), leading to the necessary condition for separability:

$$\tilde{\gamma} + \frac{i}{2}\Omega \geq 0. \tag{5.14}$$

A more explicit version of the Simon separability criterion Eq. (5.14) can be written

when the covariance matrix γ is considered in its standard form γ_0 (2.47):

$$4(ab - c_1^2)(ab - c_2^2) \geq (a^2 + b^2) + 2|c_1 c_2| - \frac{1}{4}. \tag{5.15}$$

When considering the particular case of Gaussian states, the Duan and Simon criterion appears to be a necessary and sufficient criterion of separability.

As an example, we consider the case of two-mode squeezed vacuum (TMSV) states with added Gaussian noise on one of the two modes. For this type of states, the covariance matrix writes:

$$\gamma_{TMSV}^{noise} = \begin{pmatrix} \frac{\cosh(2r)}{2} + V & 0 & \frac{\sinh(2r)}{2} & 0 \\ 0 & \frac{\cosh(2r)}{2} + V & 0 & -\frac{\sinh(2r)}{2} \\ \frac{\sinh(2r)}{2} & 0 & \frac{\cosh(2r)}{2} & 0 \\ 0 & -\frac{\sinh(2r)}{2} & 0 & \frac{\cosh(2r)}{2} \end{pmatrix}. \tag{5.16}$$

Hence, applying the criterion derived by Simon on the covariance matrix Eq. (5.16) , Eq. (5.14) reads:

$$4\left(\frac{\cosh(2r)^2}{4} + \frac{V\cosh(2r)}{2} - \frac{\sinh(2r)^2}{4}\right)^2 \geq \left(\frac{\cosh(2r)}{2} + V\right)^2 + \left(\frac{\cosh(2r)}{2}\right)^2 + \frac{\sinh(2r)^2}{2} - \frac{1}{4}, \tag{5.17}$$

which can be further simplified to:

$$\sinh(2r)^2(V^2 - 1) \geq 0, \tag{5.18}$$

by using the well-known relation of hyperbolic functions : $\cosh(x)^2 - \sinh(x)^2 = 1$ and $\sinh(x)^2 + \cosh(x)^2 = 2\cosh(x) - 1$. From Eq. (5.18), it is now clear that the TMSV states with added Gaussian noise is entangled when $V < 1$ and becomes separable for $V \geq 1$. This example will be used in the section 6.5.1.

On the other hand, Duan *et al.* [21] introduced simultaneously an inseparability criterion for CV systems. The criterion is based on a bound of the total variance of a pair of Einstein-Podolski-Rosen (EPR) type operators of form:

$$\begin{aligned} \hat{u} &= |a|\hat{x}_1 + \frac{1}{a}\hat{x}_2, \\ \hat{v} &= |a|\hat{p}_1 - \frac{1}{a}\hat{p}_2, \end{aligned} \tag{5.19}$$

where $a \in \mathbb{R}^0$. By evaluating the EPR-like operators of Eq. (5.19) on separable states, Duan *et al.* proved the following theorem :

Theorem 4 (Duan *et al.* sufficient criterion for separability). *For any separable state ρ, the total variance of a pair of EPR-like operators defined by Eq.(5.19) with commutators $[\hat{x}_n, \hat{p}_m] = i\delta_{nm}$ $(n, m = 1, 2)$ satisfies the inequality*

$$\langle (\Delta\hat{u})^2 \rangle_\rho + \langle (\Delta\hat{v})^2 \rangle_\rho \geq a^2 + \frac{1}{a^2}. \tag{5.20}$$

Remarkably, the theorem 4 by Duan *et al.* and the Simon necessary criterion for separability Eq. (5.14) are equivalent. Hence, the Duan *et al.* criterion also becomes necessary and sufficient for Gaussian states ρ_G.

Indeed, when the covariance matrix is written in its standard form (II) (2.48):

$$\gamma^{II} = \begin{pmatrix} n_1 & 0 & c_1 & 0 \\ 0 & n_2 & 0 & c_2 \\ c_1 & 0 & m_1 & 0 \\ 0 & c_2 & 0 & m_2 \end{pmatrix}, \tag{5.21}$$

where the n_i, m_i and c_i satisfy the following equalities:

$$\begin{aligned} \frac{n_1 - 1}{m_1 - 1} &= \frac{n_2 - 1}{m_2 - 1}, \\ |c_1| - |c_2| &= \sqrt{(n_1 - 1)(m_1 - 1)} - \sqrt{(n_2 - 1)(m_2 - 1)}, \end{aligned} \tag{5.22}$$

then the Duan *et al.* theorem for Gaussian states writes:

Theorem 5 (Duan *et al.* necessary and sufficient criterion for Gaussian states). *A Gaussian state ρ_G is separable if and only if, when expressed in its standard form II, the following inequality is satisfied:*

$$a_0^2 \frac{n_1 + n_2}{2} + \frac{m_1 + m_2}{2a_0^2} - |c_1| - |c_2| \geq a_0^2 + \frac{1}{a_0^2}, \tag{5.23}$$

where $a_0^2 = \sqrt{\frac{m_1 - 1}{n_1 - 1}} = \sqrt{\frac{m_2 - 1}{n_2 - 1}}$.

The equation (5.23) is derived by applying the Duan *et al.* theorem with the operators:

$$\begin{aligned} \hat{u} &= a_0 \hat{x}_1 + \frac{c_1}{|c_1|} \frac{1}{a_0} \hat{x}_2, \\ \hat{v} &= a_0 \hat{p}_1 - \frac{c_2}{|c_2|} \frac{1}{a_0} \hat{p}_2. \end{aligned} \tag{5.24}$$

Finally, the Duan and Simon criterion is a necessary and sufficient criterion for the separability of bipartite $1 \times n$ [67] and $n \times m$ bisymmetric [68] Gaussian states. Indeed, it can be further generalized for $N + M$ Gaussian systems [69].

5.4.2 Continuous-variable realignment criterion

Some entangled states are PPT. Hence, they cannot be detected by the PPT criterion. This is the case in higher dimensional systems where the PPT criterion is only a necessary criterion for separability. Another criterion is available and more efficient for detecting these entangled PPT states, namely the bound entangled states : the realignment criterion. An equivalent criterion to the realignment criterion for CV exists. It has been developped by Zhang *et al.* in [70]. Given the importance of the realignment map and criterion in the present thesis, these notions are developed in details in the dedicated section 5.5.

5.5 Realignment criterion and realignment map

The content of this section is mainly based on the article "Realignment separability criterion assisted with filtration for detecting continuous-variable entanglement" that I have published with Anaelle Hertz, Ali Asadian and Nicolas Cerf as co-authors [2].

5.5.1 Operator Schmidt decomposition

It is well known that any bipartite pure state $|\psi\rangle_{AB}$ can be decomposed according to the Schmidt decomposition Eq. (5.3). An analogous Schmidt decomposition can also be defined for mixed states [71]. Let ρ be a mixed quantum state of a bipartite system AB, then it can be written in its operator Schmidt decomposition as

$$\rho = \sum_{i=1}^{r} \lambda_i \, A_i \otimes B_i, \tag{5.25}$$

with the Schmidt coefficients λ_i being some non-negative real numbers, the Schmidt rank r satisfying $1 \leq r \leq \min\{\dim A, \dim B\}$, and with $\{A_i\}$ and $\{B_i\}$ forming orthonormal bases[3] of the operator spaces for subsystems A and B with respect to the Hilbert-Schmidt inner product, i.e., $\mathrm{Tr}(A_i^\dagger A_j) = \mathrm{Tr}(B_i^\dagger B_j) = \delta_{ij}$. The Schmidt coefficients λ_i are unique for a bipartite state ρ and reveal some of its characteristic features. For example, the purity of ρ can be expressed as $\mathrm{Tr}\,\rho^2 = \sum_{i=1}^{r} \lambda_i^2$. Hence, the λ_i should satisfy the following inequality to describe a valid quantum state : $\sum_{i=1}^{r} \lambda_i^2 < 1$.

[3] If the operator is Hermitian (such as ρ), then the operators A_i and B_i can be chosen Hermitian too. But the Schmidt decomposition is not unique and there exist other possible Schmidt decompositions of an Hermitian operator with non-Hermitian operators A_i and B_i.

5.5.2 Computable cross norm criterion

Similarly as for pure states, the operator Schmidt decomposition can be employed as an entanglement criterion for mixed bipartite states; this is called the computable cross norm criterion and is defined as follows.

Theorem 6 (Computable cross norm criterion [60]). *Let ρ be a state with the operator Schmidt decomposition $\rho = \sum_{i=1}^{r} \lambda_i A_i \otimes B_i$. If ρ is separable, then $\sum_{i=1}^{r} \lambda_i \leq 1$. Conversely, if $\sum_{i=1}^{r} \lambda_i > 1$, then ρ is entangled.*

Proof. We give here the proof of Theorem 6. Let us construct an entanglement witness $\mathcal{W}$, that is, an observable with a positive expectation value on all separable states. Let us define $\mathcal{W} = \mathbb{1} - \sum_i^r A_i \otimes B_i$ and let us check that $\mathrm{Tr}(\rho_{sep}\mathcal{W}) \geq 0$ where $\rho_{sep} = (|a\rangle \otimes |b\rangle)(\langle a| \otimes \langle b|)$ is a separable (product) state. First we remark that

$$\begin{aligned} \mathrm{Tr}(\rho_{sep}\mathcal{W}) &= (\langle a| \otimes \langle b|)\mathcal{W}(|a\rangle \otimes |b\rangle), \\ &= 1 - \sum_i^r \langle a|A_i|a\rangle\langle b|B_i|b\rangle, \\ &\geq 1 - \sqrt{\sum_i^r |\langle a|A_i|a\rangle|^2}\sqrt{\sum_i^r |\langle b|B_i|b\rangle|^2}, \end{aligned} \tag{5.26}$$

where we used the Cauchy-Schwarz inequality in the last step. Now, since the $\{A_i\}$ form a basis, we can write $|a\rangle\langle a| = \sum_j \alpha_j A_j$ where $\alpha_j = \langle a|A_j|a\rangle$, and similarly for $|b\rangle\langle b|$. This allows us to write

$$\begin{aligned} 1 &= \| \, |a\rangle\langle a| \, \|^2 = \mathrm{Tr}(|a\rangle\langle a|(|a\rangle\langle a|)^\dagger) = \mathrm{Tr}(\sum_{ij} \alpha_i A_i \alpha_j^* A_j^\dagger), \\ &= \sum_{ij} \alpha_i \alpha_j^* \mathrm{Tr}(A_i A_j^\dagger) = \sum_i |\alpha_i|^2 = \sum_i |\langle a|A_i|a\rangle|^2, \end{aligned} \tag{5.27}$$

and similarly $\sum_i |\langle b|B_i|b\rangle|^2 = 1$ so that $\mathrm{Tr}(\rho_{sep}\mathcal{W}) \geq 0$. Thus, $\mathcal{W}$ is indeed an entanglement witness as any separable state is expressed as a convex mixture of states of the form ρ_{sep}. Let us now check under which condition entanglement is detected. In other words, what is the condition to have $\mathrm{Tr}(\rho\mathcal{W}) < 0$? Consider a state ρ written in its operator Schmidt decomposition. Then,

$$\begin{aligned} \mathrm{Tr}(\rho\mathcal{W}) &= 1 - \mathrm{Tr}\left(\sum_{ij}^r \lambda_i A_i A_j \otimes B_i B_j\right), \\ &= 1 - \sum_{ij}^r \lambda_i \mathrm{Tr}(A_i A_j)\mathrm{Tr}(B_i B_j), \\ &= 1 - \sum_i^r \lambda_i. \end{aligned} \tag{5.28}$$

Remember that in the operator Schmidt decomposition, the operators A_i and B_i are not unique and can be chosen hermitian in the decomposition of the hermitian den-

sity matrix ρ. Entanglement is thus detected when $\sum_i^r \lambda_i > 1$ which completes the proof. □

For example, one could consider the operator-Schmidt decomposition of the Bell state $|\Psi^+\rangle\langle\Psi^+| = 1/2(|00\rangle\langle 00| + |00\rangle\langle 11| + |11\rangle\langle 00| + |11\rangle\langle 11|)$. The operator-Schmidt decomposition writes :

$$|\Psi^+\rangle\langle\Psi^+| = \sum_{i=1}^{4} \frac{1}{4} A_i \otimes B_i, \tag{5.29}$$

where $A_i = B_i$ for all $i = 1, 2, 3, 4$ and $A_1 = |0\rangle\langle 0|$, $A_2 = |0\rangle\langle 1|$, $A_3 = |1\rangle\langle 0|$ and $A_4 = |1\rangle\langle 1|$. The rank of the Bell state is maximal $r = 4$ Hence, by applying the computable cross norm criterion, one finds that :

$$\sum_{i=1}^{4} \lambda_i = \frac{1}{2} + \frac{1}{2} + \frac{1}{2} + \frac{1}{2} = 2, \tag{5.30}$$

which shows that the computable cross norm detects the entanglement of the Bell state $|\Psi^+\rangle\langle\Psi^+|$.

5.5.3 The realignment map

There exists an alternative formulation of the computable cross norm criterion which, as we will see, turns out to be more convenient when considering continuous-variable states. This reformulation is done by defining a linear map R called *realignment map*, whose action on the tensor product of matrices $A = \sum_{ij} a_{ij}|i\rangle\langle j|$ and $B = \sum_{kl} b_{kl}|k\rangle\langle l|$ is

$$R\big(A \otimes B\big) = \sum_{ijkl} a_{ij} b_{kl} |i\rangle|j\rangle\langle k|\langle l|. \tag{5.31}$$

Since, any bipartite state ρ can be decomposed into $A \otimes B$ products according to Eq. (5.25), one can easily express its realignment $R(\rho)$ based on definition (5.31). Thus, the realignment map simply interchanges the bra-vector $\langle j|$ of the first subsystem with the ket-vector $|k\rangle$ of the second subsystem. Note that the map R is basis-dependent, namely, it depends on the basis in which the matrix elements a_{ij} and b_{kl} are expressed. When we will study the application of the realignment R to continuous-variable states in Secs. 5.5.5 and more generally in 6, we will always assume that $|i\rangle$, $|j\rangle$, $|k\rangle$, and $|l\rangle$ are Fock states, so that Eq. (5.31) must be understood in the Fock basis.

Using the state-operator correspondence implied by the Choi-Jamiolkowski isomorphism [72, 73], we can identify matrices with vectors living in the tensor-product ket space, namely $|A\rangle\!\rangle = \sum_{ij} a_{ij}|i\rangle|j\rangle$ and $|B\rangle\!\rangle = \sum_{kl} b_{kl}|k\rangle|l\rangle$. Their corresponding dual vectors are noted $\langle\!\langle A| = \sum_{ij} a_{ij}^* \langle i|\langle j|$ and $\langle\!\langle B| = \sum_{kl} b_{kl}^* \langle k|\langle l|$, living in the tensor-product

bra space. Hence, the above map can be reexpressed as

$$R\big(\, A \otimes B \,\big) = |A\rangle\langle B^*|, \tag{5.32}$$

where complex conjugation is also applied in the preferred basis. Using the fact that $(A \otimes \mathbb{1})|\Omega\rangle = \sum_{ij} a_{ij}(|i\rangle\langle j| \otimes \mathbb{1}) \sum_k |k\rangle|k\rangle = \sum_{ij} a_{ij}|i\rangle|j\rangle$, we can write the following useful equations:

$$\begin{aligned} |A\rangle &= \sum_{ij} a_{ij}|i\rangle|j\rangle = (A \otimes \mathbb{1})|\Omega\rangle, \\ \text{and} & \\ \langle B^*| &= \sum_{ij} b_{ij}\langle i|\langle j| = \langle\Omega|(B^T \otimes \mathbb{1}), \end{aligned} \tag{5.33}$$

where $|\Omega\rangle = \sum_i |i\rangle|i\rangle$ is the (unnormalized[4]) maximally entangled state and $\mathbb{1} = \sum_i |i\rangle\langle i|$ is the identity matrix, one can also rewrite the realignment map as

$$\begin{aligned} R(A \otimes B) &= (A \otimes \mathbb{1})|\Omega\rangle\langle\Omega|(B^T \otimes \mathbb{1}), \\ &= (A \otimes \mathbb{1})|\Omega\rangle\langle\Omega|(\mathbb{1} \otimes B). \end{aligned} \tag{5.34}$$

which will happen to be useful when considering the optical realization of the separability criterion.

It is obvious that $R(R(\rho)) = \rho$, so that definition (5.32) can also be restated as

$$R\big(\, |A\rangle\langle B| \,\big) = A \otimes B^*. \tag{5.35}$$

Note the special cases

$$\begin{aligned} R(\mathbb{1} \otimes \mathbb{1}) &= |\Omega\rangle\langle\Omega|, \\ R(|\Omega\rangle\langle\Omega|) &= \mathbb{1} \otimes \mathbb{1}, \end{aligned} \tag{5.36}$$

which are trivial consequences of $|\mathbb{1}\rangle = |\Omega\rangle$ and $\hat{\Omega} = \mathbb{1}$.

It will also be useful in the following to define the *dual realignment map* $R^\dagger$, which is such that $\mathrm{Tr}(\rho_1\, R(\rho_2)) = \mathrm{Tr}(R^\dagger(\rho_1)\, \rho_2)$. Definitions (5.32) and (5.34) translate into

$$\begin{aligned} R^\dagger(A \otimes B) &= |B^T\rangle\langle A^\dagger|, \\ &= (B^T \otimes \mathbb{1})|\Omega\rangle\langle\Omega|(A \otimes \mathbb{1}), \\ &= (\mathbb{1} \otimes B)|\Omega\rangle\langle\Omega|(A \otimes \mathbb{1}). \end{aligned} \tag{5.37}$$

[4]This definition of $|\Omega\rangle$ remains useful even for continuous-variable (infinite-dimensional) systems, where it can be interpreted as a (unnormalized) two-mode squeezed vacuum state with infinite squeezing. The definition of R given by Eq. (5.34) remains thus valid with $|\Omega\rangle = \sum_{i=0}^{\infty} |ii\rangle$, where $|i\rangle$ stands for Fock states.

Finally, it is worth adding that, by inspection, definition (5.31) of the realignment map can be decomposed as

$$R(A \otimes B) = \Big((A \otimes B^T) F \Big)^{T_2}, \tag{5.38}$$

where $(\cdot)^{T_2}$ denotes a partial transposition on the second subsystem (B), and $F = \sum_{i,j} |ij\rangle\langle ji| = |\Omega\rangle\langle\Omega|^{T_2}$ is the exchange operator [74]. From this, we obtain the following.

Remark 1. *For any state ρ, the realignment map can be defined as*

$$R(\rho) = \Big(\rho^{T_2} F \Big)^{T_2} = (\rho F)^{T_2} F. \tag{5.39}$$

In other words, the map R boils down to the concatenation of partial transposition on subsystem B, then applying the exchange operator F to the right, followed by partial transposition on subsystem B again. Conversely, the roles of F and $(\cdot)^{T_2}$ can be exchanged.

Of course, the dual realignment map $R^\dagger$ can also be defined similarly as in Eq. (5.39), namely

$$R^\dagger(\rho) = \Big(F \rho^{T_2} \Big)^{T_2} = F \, (F\rho)^{T_2} \, . \tag{5.40}$$

The difference with the (primal) realignment map R is that the exchange operator F is applied to the left. To be complete, let us mention that maps R and $R^\dagger$ can also be defined using partial transposition on the first subsystem denoted as $(\cdot)^{T_1}$, namely,

$$\begin{aligned} R(\rho) &= (F\rho^{T_1})^{T_1} = F(F\rho)^{T_1}, \\ R^\dagger(\rho) &= \Big(\rho^{T_1} F \Big)^{T_1} = (\rho F)^{T_1} \, F. \end{aligned} \tag{5.41}$$

These alternative definitions of the realignment map will help us (in Section 5.5.4) to explicitly derive the connection between the realignment criterion and PPT criterion for the so-called symmetric states.

5.5.4 Realignment criterion

Coming back to the question of separability, let us now state the following theorem.

Theorem 7 (Realignment criterion [75]). *If the bipartite state ρ is separable, then $\| R(\rho) \|_{tr} \leq 1$. Conversely, if $\| R(\rho) \|_{tr} > 1$, then ρ is entangled.*

Proof. From Eq. (5.32), the realignment of a product state is given by

$$R(\rho_A \otimes \rho_B) = |\rho_A\rangle\langle\rho_B^*|, \tag{5.42}$$

and therefore,

$$\begin{aligned} \| R(\rho_A \otimes \rho_B) \|_{tr} &= \mathrm{Tr}\sqrt{|\rho_A\rangle\langle\rho_B^*|\rho_B^*\rangle\langle\rho_A|}, \\ &= \sqrt{\mathrm{Tr}(\rho_B^2)}\mathrm{Tr}\sqrt{|\rho_A\rangle\langle\rho_A|}, \\ &= \sqrt{\mathrm{Tr}(\rho_B^2)}\sqrt{\langle\rho_A|\rho_A\rangle}, \\ &= \sqrt{\mathrm{Tr}(\rho_B^2)}\sqrt{\mathrm{Tr}(\rho_A^2)} \\ &= \sqrt{\mu_A\mu_B} \\ &\leq 1, \end{aligned} \tag{5.43}$$

where $\| \mathcal{O} \|_{tr} = \mathrm{Tr}(\sqrt{\mathcal{O}\mathcal{O}^\dagger})$ denotes the trace norm[5] of an operator $\mathcal{O}$, we used the Hilbert-Schmidt inner product, $\langle A|B\rangle = \mathrm{Tr}(A^\dagger B)$ and $\mu = \mathrm{Tr}(\rho^2)$ is the purity of the state ρ which is lower or equal to 1. The convexity of the trace norm implies that $\| R(\rho) \|_{tr} \leq 1$, for any separable state $\rho = \sum_i p_i \rho_i^A \otimes \rho_i^B$, with $p_i \geq 0$ and $\sum_i p_i = 1$. □

Theorem 7 is called the realignment criterion as the detection of entanglement exploits the map R. But it is interesting to note that $\| R(\rho) \|_{tr}$ coincides with the sum of the Schmidt coefficients of ρ, so the realignment criterion is actually equivalent to Theorem 1 [76]. Indeed, let ρ be a state with the operator Schmidt decomposition $\rho = \sum_i^r \lambda_i A_i \otimes B_i$. Then, according to Eq. (5.32),

$$R(\rho) = \sum_i \lambda_i R(A_i \otimes B_i) = \sum_i \lambda_i |A_i\rangle\langle B_i^*|, \tag{5.44}$$

and

$$\begin{aligned} \| R(\rho) \|_{tr} &= \mathrm{Tr}\left[\sqrt{\sum_{i,j}\lambda_i\lambda_j|A_i\rangle\langle B_i^*|B_j^*\rangle\langle A_j|}\right], \\ &= \mathrm{Tr}\left[\sqrt{\sum_i \lambda_i^2|A_i\rangle\langle A_i|}\right], \\ &= \mathrm{Tr}\left[\sum_i |\lambda_i||A_i\rangle\langle A_i|\right] = \sum_i \lambda_i, \end{aligned} \tag{5.45}$$

since $\langle A_i|A_j\rangle = \langle B_i|B_j\rangle = \delta_{ij}$. Theorem 7 is thus equivalent to Theorem 6.

As a trivial example of Theorem 7, let us consider two d-dimensional systems (with $d \geq 2$). The maximally mixed state $\rho = \mathbb{1} \otimes \mathbb{1}/d^2$ is mapped to $R(\rho) = |\Omega\rangle\langle\Omega|/d^2$, see Eq. (5.36), so its trace norm is $\| R(\rho) \|_{tr} = 1/d < 1$ as expected since ρ is separable. Conversely, according to Eq. (5.36), the maximally entangled state $\rho = |\Omega\rangle\langle\Omega|/d$ is mapped to $R(\rho) = \mathbb{1} \otimes \mathbb{1}/d$, so that $\| R(\rho) \|_{tr} = d > 1$ and the entanglement of ρ

[5] The trace norm of $\mathcal{O}$ is equivalent to the sum of the singular values of $\mathcal{O}$, which are given by the square roots of the eigenvalues of $\mathcal{O}\mathcal{O}^\dagger$. For an Hermitian operator, the trace norm is simply equal to the sum of the absolute values of the eigenvalues.

is well detected in this case.

Theorem 8. *For any bipartite state ρ, the value of the trace norm of the realignment of the state $R(\rho)$ is bounded by*

$$\frac{1}{d} \leq \| \ R(\rho) \ \|_{tr} \leq d. \tag{5.46}$$

Proof. Let us prove that the values $1/d$ and d of the bounds in theorem 8 are extremal and correspond to the trace norm of the maximally mixed and maximally entangled states. For this, we use the Lagrange multipliers technique. The constraint is the purity of the state : $P = \sum_i^d \lambda_i^2$. From Eq. (5.45), the problem can be understood as finding the point on a sphere of radius P that has the maximal length of coefficient λ_i in an Euclidean space. Indeed, the Lagrangian of this problem writes :

$$L(\lambda_i, \mu) = \sum_i^r \lambda_i + \mu(\sum_i^r \lambda_i^2 - P). \tag{5.47}$$

Hence, the partial derivatives of the Lagrangian are :

$$\begin{aligned} \frac{\partial L}{\partial \lambda_i} &= 1 + 2\mu\lambda_i = 0, \\ \frac{\partial L}{\partial \mu} &= \sum_i^r \lambda_i^2 - P = 0. \end{aligned} \tag{5.48}$$

Hence, we find that

$$\begin{aligned} \lambda_i &= \frac{-1}{2\mu}, \\ P &= \sum_i^r \lambda_i^2. \end{aligned} \tag{5.49}$$

By solving this system one finds that :

$$\begin{aligned} \lambda_i &= \frac{-1}{2\mu}, \\ \mu &= \pm\frac{1}{2}\sqrt{\frac{r}{P}}, \end{aligned} \tag{5.50}$$

and finally by taking only the negative value of μ (since the λ_i's must be positive),

$$\lambda_i = \sqrt{\frac{P}{r}}. \tag{5.51}$$

Finally, the extremal values for the realignment criterion are the extreme values of :

$$\sum_i^r \lambda_i = r\sqrt{\frac{P}{r}} = \sqrt{rP}. \tag{5.52}$$

On one hand, for maximally mixed states (i.e. $P = 1/d^2$ and $r = 1$ which are the

minimal values for P and r), we have :

$$\sum_i^1 \lambda_i = \sum_i^1 \frac{1}{d} = \frac{1}{d}. \tag{5.53}$$

On the other hand, for maximally entangled states (i.e. $P = 1$ and $r = d^2$, which are the maximal values for P and r), we have :

$$\sum_i^{d^2} \lambda_i = \sqrt{d^2} = d. \tag{5.54}$$

Hence, we have showed that $\| \ R(\rho) \ \|_{tr}$ has to satisfy the following inequalities :

$$\frac{1}{d} \leq \| \ R(\rho) \ \|_{tr} \leq d, \tag{5.55}$$

which is saturated for maximally mixed and maximally entangled states. □

Remark 2. *The alternative definition given in remark 1 of R allows us to express the trace norm as*

$$\| \ R(\rho) \ \|_{tr} = \| \ (\rho F)^{T_2} F \ \|_{tr} = \| \ (\rho F)^{T_2} \ \|_{tr}, \tag{5.56}$$

where the last equality comes from the fact that, for any operator A, we have

$$\begin{aligned} \| \ AF \ \|_{tr} &= \mathrm{Tr}\sqrt{AF(AF)^\dagger} = \mathrm{Tr}\sqrt{AFF^\dagger A^\dagger}, \\ &= \mathrm{Tr}\sqrt{AA^\dagger} = \| \ A \ \|_{tr}, \end{aligned} \tag{5.57}$$

since $FF^\dagger = FF = \mathbb{1}$.

From Eq. (5.56), it becomes obvious that for the special case of states ρ_s belonging to the symmetric subspace, i.e., states satisfying $F\rho_s = \rho_s F = \rho_s$, the realignment criterion coincides with the PPT criterion [77]. Indeed, $\| \ R(\rho_s) \ \|_{tr} = \| \ \rho_s^{T_2} \ \|_{tr}$, and $\| \ \rho_s^{T_2} \ \|_{tr} = \sum_i |\lambda_i'| > 1$ implies that at least one eigenvalue λ_i' of the partial-transposed state $\rho_s^{T_2}$ is negative, since $\mathrm{Tr}(\rho_s) = \mathrm{Tr}(\rho_s^{T_2}) = \sum_i \lambda_i' = 1$ (which is the PPT criterion). Beyond the case of states in the symmetric subspace, however, the realignment and PPT criteria are generally incomparable criteria (see Fig. 6.1).

5.5.5 Realignement criterion for Gaussian states

In [70], the authors introduced the notions of Continuous-Variable Local Orthogonal Observables (CVLOO) and use them to derive an entanglement witness (EW) which, under optimal choice of CVLOO, is equivalent to the realignment criterion.

The CVLOO are an infinite family of observables $G(\lambda)$ that are defined for each mode

and must satisfy the orthogonal relations:

$$\mathrm{Tr}\left(G(\lambda)G(\lambda')\right) = \delta(\lambda - \lambda'), \tag{5.58}$$

and the complete-set condition:

$$\rho = \int \langle G(\lambda)\rangle_\rho G(\lambda) d^2\lambda, \tag{5.59}$$

where λ and λ' are complex number indices.

By applying an optimal witness to a two-mode Gaussian state where the covariance matrix is written under its normal form I, they obtain the following separability criterion for Gaussian states:

$$\mathrm{Tr}(\rho W_{\mu_1\mu_2}) = 1 - \frac{1}{4\sqrt{(\sqrt{ab} - |c_1|)(\sqrt{ab} - |c_2|)}} \geq 0. \tag{5.60}$$

This equation will be compared to the weak realignment criterion derived for two-mode Gaussian states in chapter 6.

6 | Realignment separability criterion for detecting CV entanglement

The content of this chapter is mainly based on the article "Realignment separability criterion assisted with filtration for detecting continuous-variable entanglement" that I have published with Anaelle Hertz, Ali Asadian and Nicolas Cerf as co-authors [2].

6.1 Introduction

When it comes to mixed states, determining whether a state is entangled or not is provably a hard decision problem [55, 78]. Still, it has long been and it remains an active research topic because entanglement is a key resource for quantum information processing. Both for discrete- and continuous-variable systems, various separability criteria — conditions that must be satisfied by any separable state — have been derived. Probably the best known criterion is the Peres–Horodecki criterion [58, 53], also called the positive partial transpose (PPT) criterion. Introduced for discrete-variable systems, it states that if a quantum state is separable, then its partial transpose must remain physical (i.e., positive semidefinite). This PPT condition is, in general, only a necessary condition for separability. It becomes sufficient only for systems of dimensions 2×2 and 2×3 [53]. The PPT criterion was generalized to continuous variables (i.e., infinite-dimensional systems) by Duan *et al.* [79] and Simon [80]. Interestingly, it is necessary and sufficient for all $1 \times n$ Gaussian states [67] and $n \times m$ bisymmetric Gaussian states [81]. In all other cases, when a state is entangled but its partial transpose remains positive semidefinite, we call it a bound entangled state [82, 55]. These are entangled states from which no pure entangled state can be distilled through local (quantum) operations and classical communications (LOCC) [82].

Many other separability criteria have been developed over years (see, e.g., [83, 84, 85, 86, 87], and consult [55] for an older, but still relevant, review). Among them,

we focus in the present Chapter on the realignment criterion [75, 60]. This criterion is unrelated to the PPT criterion and thereby enables the detection of some bound entangled states in both discrete-variable [75] and continuous-variable cases [70]. Unfortunately, the realignment criterion happens to be generally hard to compute, especially for continuous-variable systems. To our knowledge, it has only been computed for Gaussian states by Zhang *et al.* [70] and yet, the difficulty increases with the number of modes.

In this work, we introduce a weaker form of the realignment criterion which is much simpler to compute and comes with a physical implementation in terms of linear optics and homodyne detection, hence it is especially suited to detect continuous-variable entanglement. It is, in general, less sensitive to entanglement than the original realignment criterion and cannot detect bound-entangled states, but it happens to be equivalent to the original realignment criterion for the class of Schmidt-symmetric states. Furthermore, we show that by supplementing this criterion with a filtration method, it is possible to greatly improve it and sometimes even surpass the original realignment criterion while keeping the simplicity of computation.

In Sec. 5.5, we have reviewed the definition of the realignment criterion, focusing especially on the realignment map R. We have linked different formulations of this criterion and its main properties have been covered. In Sec. 6.2 , we now introduce the *weak realignment criterion*, based on the trace of the realigned state $R(\rho)$ and show that for a class of states that we call *Schmidt-symmetric*, both the weak and original strong realignment criteria (as stated in Theorem 7) are equivalent while the former is much easier to compute than the latter. In Sect. 6.3, we apply the weak realignment criterion to continuous-variable states and give special attention to Gaussian states. In particular, we will provide some explicit calculations in the case of $n \times n$ mode Gaussian states, in which case it boils down to computing a simple quantity that only depends on the covariance matrix of the state. The idea is to compare to the work of Zhang *et al.* [70], which relied on the original formulation of the criterion. As expected, however, the easiness of computation comes with the price of a lower entanglement detection sensitivity than the one of the original realignment criterion for Gaussian states as calculated in [70]. We notice that several entangled states remain undetected by the weak realignment criterion and, unfortunately, the latter cannot detect bound entanglement. As a solution, we introduce in Sec. 6.4 a filtration procedure that enables a better entanglement detection by bringing the state closer to a Schmidt-symmetric state, hence increasing the sensitivity of the entanglement witness. Indeed, we may "symmetrize" the state by locally applying a noiseless amplifier or attenuator (it does not affect the separability of the state, so we may apply the weak realignment criterion on the filtered state). In Sec. 6.5, we provide some specific examples for 1×1 and 2×2 Gaussian states. In some cases, the filtration procedure supplementing the weak realignment criterion enables a better entanglement detection than the original realignment criterion. Finally, we give

some conclusions in Sec. 6.6.

6.2 Weak realignment criterion

Let us introduce the weak realignment criterion, which is in general not as strong as the original realignment criterion but has the advantage of being easily computable and physically implementable using standard optical components. The weak realignment criterion applies to all states but our main focus will be its application to continuous-variable states as detailed in Sec. 6.3.

6.2.1 Weak realignment criterion formulation

It is well known result in algebra that the trace norm of an operator is greater than or equal to its trace (and we have equality if and only if the operator is positive semidefinite). Using Eq. (5.39), we have that for any state

$$\begin{aligned} \| R(\rho) \|_{tr} &\geq \mathrm{Tr}\, R(\rho), \\ &= \mathrm{Tr}\left(\rho^{T_2} F\right), \\ &= \mathrm{Tr}\left(\rho\, F^{T_2}\right), \\ &= \mathrm{Tr}\left(\rho\, |\Omega\rangle\langle\Omega|\right) = \langle\Omega|\rho|\Omega\rangle, \end{aligned} \tag{6.1}$$

where $F = \sum_{i,j} |ij\rangle\langle ji| = |\Omega\rangle\langle\Omega|^{T_2}$ is the exchange operator [74] and we have used the invariance of the trace under partial transposition $(\cdot)^{T_2}$ (line 2), the identity $\mathrm{Tr}(A\, B^{T_2}) = \mathrm{Tr}(A^{T_2} B)$ for any bipartite operators A and B (line 3), and the definition of F (line 4). Note that this result can also be obtained by noticing that

$$\mathrm{Tr}(R(\rho)\, \mathbb{1} \otimes \mathbb{1}) = \mathrm{Tr}(\rho\, R^{\dagger}(\mathbb{1} \otimes \mathbb{1})) = \mathrm{Tr}(\rho\, |\Omega\rangle\langle\Omega|). \tag{6.2}$$

We can thus state the following theorem:

Theorem 9 (Weak realignment criterion). *For any bipartite state ρ, the trace norm of the realigned state can be lower bounded as*

$$\| R(\rho) \|_{tr} \geq \mathrm{Tr}\, R(\rho) = \langle\Omega|\rho|\Omega\rangle. \tag{6.3}$$

Hence, if ρ is separable, then $\langle\Omega|\rho|\Omega\rangle \leq 1$. Conversely, if $\langle\Omega|\rho|\Omega\rangle > 1$, then ρ is entangled.

In other words, the weak realignment criterion (6.3) amounts to computing the fi-

delity of state ρ with respect to $|\Omega\rangle$ [1]. Indeed, since $\sqrt{|\Omega\rangle\langle\Omega|} = |\Omega\rangle\langle\Omega|/\sqrt{d}$ [2] where d is the dimension of the Hilbert space, the fidelity between ρ and $|\Omega\rangle$ writes $F(|\Omega\rangle,\rho) = \left(1/\sqrt{d}\mathrm{Tr}\left(\sqrt{|\Omega\rangle\langle\Omega|\rho|\Omega\rangle\langle\Omega|}\right)\right)^2 = 1/d\left(\sqrt{\langle\Omega|\rho|\Omega\rangle}\sqrt{\mathrm{Tr}(|\Omega\rangle\langle\Omega|)}\right)^2 = \langle\Omega|\rho|\Omega\rangle$. It is immediate that its entanglement detection capability can only be lower than that of the original realignment criterion, Theorem 7 (see Fig. 6.1). Furthermore, if we deal with bound-entangled states, the weak realignment criterion cannot detect entanglement. Indeed, we can link the weak realignment criterion with the PPT criterion by expressing

$$\| R(\rho)^{T_2} \|_{tr} = \| \rho^{T_2} F \|_{tr} = \| \rho^{T_2} \|_{tr}, \tag{6.4}$$

where we have used Eqs. (5.39) and (5.57), combined with the inequality

$$\| R(\rho)^{T_2} \|_{tr} \geq \mathrm{Tr}\left(R(\rho)^{T_2}\right) = \mathrm{Tr}\, R(\rho), \tag{6.5}$$

Thus,

$$\| \rho^{T_2} \|_{tr} \geq \mathrm{Tr}\, R(\rho), \tag{6.6}$$

and we deduce that the weak realignment criterion is weaker than the PPT criterion (see 6.1). If a state is bound entangled, we have $\| \rho^{T_2} \|_{tr} = 1$ which then implies that $\mathrm{Tr}\, R(\rho) \leq 1$, so its entanglement cannot be detected with the weak realignment criterion.

It is instructive to apply the weak realignment criterion on each component of the operator Schmidt decomposition of ρ. Using Eq. (5.34), we have

$$\mathrm{Tr}\, R(A \otimes B) = \langle\Omega|A \otimes B|\Omega\rangle = \mathrm{Tr}(AB^T), \tag{6.7}$$

which implies that if $\rho = \sum_i \lambda_i\, A_i \otimes B_i$, then

$$\mathrm{Tr}\, R(\rho) = \sum_i \lambda_i\, \mathrm{Tr}(A_i B_i^T) = \sum_i \lambda_i\, \langle B_i^*|A_i\rangle. \tag{6.8}$$

Remembering that $\| R(\rho) \|_{tr} = \sum_i \lambda_i$, it appears that we must have $B_i = A_i^*$ in order to reach a situation where $\mathrm{Tr}\, R(\rho) = \| R(\rho) \|_{tr}$. This is analyzed in the following section.

6.2.2 Schmidt-symmetric states

In this section, we show that for *Schmidt-symmetric* states, the weak and original forms of the realignment criterion become equivalent (while the weak form is much

[1] The fidelity between two states ρ and σ is a measure of the *distance* between these states (while not being a proper metric) and writes $F(\rho,\sigma) = \left(\mathrm{Tr}\left(\sqrt{\sqrt{\rho}\sigma\sqrt{\rho}}\right)\right)^2$. In the case of $\rho = |\psi\rangle\langle\psi|$ being a pure state, the fidelity is given by the well-known formula $F(\rho,\sigma) = \langle\psi|\sigma|\psi\rangle$

[2] remember that $\mathrm{Tr}(|\Omega\rangle\langle\Omega|) = \langle\Omega|\Omega\rangle = d$

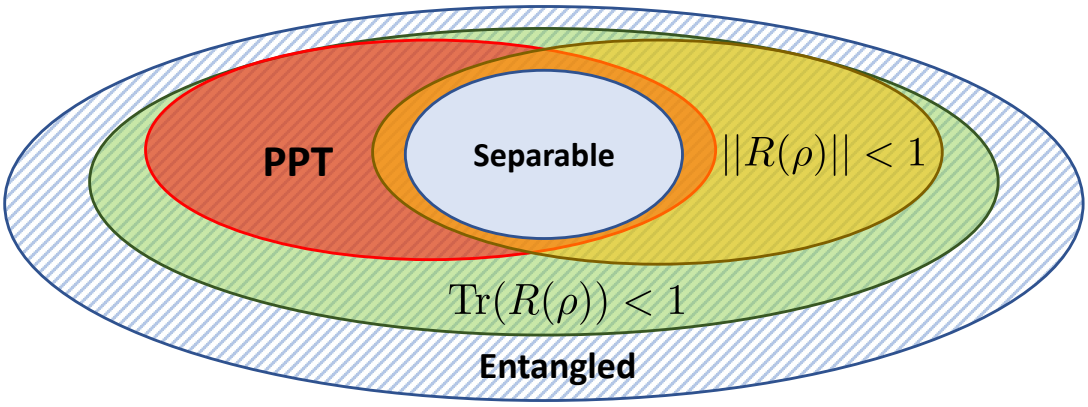

Figure 6.1: This schematic view on the convex ensemble of states. The separable states are a subset depicted in light blue. The hatched area consists of the non separable states. The red area is the ensemble of states that are PPT and the yellow area is the ensemble of states that are not detected as non separable by the realignment criterion (Theorem 7). The green area show the states that are not detected as non separable by the weak realignment criterion (Theroem 9). Hence, we see that the PPT and realignment criterion are not comparable. However, the weak realignement criterion is weaker than both PPT and realignement criterion as it detects less entangled states.

simpler to compute). Let us define Schmidt-symmetric states ρ_{sch} as the states that admit an operator Schmidt decomposition with $B_i = A_i^*, \forall i$, namely,

$$\rho_{sch} = \sum_i \lambda_i \, A_i \otimes A_i^*. \tag{6.9}$$

These states satisfy $F\rho_{sch}\,F = \rho_{sch}^*$ since applying F on both sides is equivalent to exchanging the two subsystems and since the Schmidt coefficients are real. Note that the converse is not true as there exist states ρ that satisfy $F\rho F = \rho^*$ but are not Schmidt-symmetric, for example the state $\rho = \sum_i \lambda_i \, A_i \otimes (-A_i^*)$. For any state ρ that satisfies $F\rho F = \rho^*$, it is easy to see that $R(\rho)$ is Hermitian since [3]

$$\begin{aligned} R(\rho)^\dagger &= ((\rho F)^{T_2} F)^\dagger, \\ &= F(\rho^* F)^{T_1}, \\ &= F(F\rho)^{T_1} = R(\rho), \end{aligned} \tag{6.10}$$

where we have used Eqs. (5.39) and (5.41). Thus, $R(\rho_{sch})$ is necessarily an Hermitian operator.

Actually, using the definition (5.32) of the realignment map R, it appears that $R(\rho_{sch}) = \sum_i \lambda_i |A_i\rangle\langle A_i|$ is positive semidefinite, so that $\| R(\rho_{sch}) \|_{tr} = \mathrm{Tr}\, R(\rho_{sch})$. Conversely, if the latter equality is satisfied for a state ρ, it means that $R(\rho)$ is positive semidefinite so it can be written as $R(\rho) = \sum_i \lambda_i |A_i\rangle\langle A_i|$, which is nothing else but the realignment of a Schmidt-symmetric state. We have thus proven the following theorem:

[3] Be aware that $R(\rho)^\dagger$ is the conjugate transpose of $R(\rho)$ and it is distinct from the dual map $R^\dagger(\rho)$.

Theorem 10 (Schmidt-symmetric states). *A bipartite state ρ is Schmidt-symmetric (i.e., it admits the operator Schmidt decomposition $\rho = \sum_i \lambda_i A_i \otimes A_i^*$) if and only if*

$$\| R(\rho) \|_{tr} = \mathrm{Tr}\, R(\rho). \tag{6.11}$$

This entails the coincidence between the weak form of the realignment criterion derived in Theorem 9 and the original realignment criterion of Theorem 7 in the special case of Schmidt-symmetric states (see Fig. 6.1).

Incidentally, we note that the necessary condition $F\rho F = \rho^*$ for a state to be Schmidt-symmetric resembles the necessary and sufficient condition $F\rho F = \rho$ for a state to be symmetric under the exchange of the two systems. For this reason, when building a filtration procedure in order to bring the initial state closer to a Schmidt-symmetric state (see Sec. 6.4), we will "symmetrize" the state. More precisely, we will exploit the fact that the condition $F\rho F = \rho^*$ implies that $\mathrm{Tr}_1 \rho = \mathrm{Tr}_2 \rho^*$. In other words, Schmidt-symmetric states are such that the reduced states of both subsystems are complex conjugate of each other, namely $\rho_{sch,2} = \rho^*_{sch,1}$, which is also a simple consequence of

$$\begin{aligned} \rho_{sch,1} &= \mathrm{Tr}_2(\rho_{sch}) = \sum_i \lambda_i A_i \,\mathrm{Tr} A_i^*, \\ \rho_{sch,2} &= \mathrm{Tr}_1(\rho_{sch}) = \sum_i \lambda_i A_i^* \,\mathrm{Tr} A_i. \end{aligned} \tag{6.12}$$

Hence, they have the same eigenspectrum since their eigenvalues are real, and in particular the same purity (but the converse is not true),

$$\mathrm{Tr}(\rho^2_{sch,1}) = \mathrm{Tr}(\rho^2_{sch,2}). \tag{6.13}$$

The filtration procedure that we apply in Sec. 6.4 follows Eq. (6.13) in the sense that we will "symmetrize" the initial state so that the two subsystems reach the same purity.

6.3 Weak realignment criterion for continuous-variable states

6.3.1 Examples of realigned states

It is instructive first to check the action of the realignment map R on some of the well-known states of quantum optics in order to set up some benchmarks in our intuition about the application of the realignment map on CV:

- Fock states[4]:

[4] Remember that the Fock basis $\{|n\rangle\}$ is used as the preferred basis with respect to which the realignment map R is defined.

$R(|n_1\rangle\langle n_2| \otimes |n_3\rangle\langle n_4|) = |n_1\rangle\langle n_3| \otimes |n_2\rangle\langle n_4|$. Fock states are a natural discrete basis in which one can describe quantum states.

- Position states: $R(|x_1\rangle\langle x_2| \otimes |x_3\rangle\langle x_4|) = |x_1\rangle\langle x_3| \otimes |x_2\rangle\langle x_4|$. Position states are a natural continuous basis in which one can describe quantum states. This can be proven using Eq. (5.34) and expressing $|\Omega\rangle = \sum_n |n,n\rangle$ in the position basis, namely $|\Omega\rangle = \int dx\, |x,x\rangle$.

- Momentum states: $R(|p_1\rangle\langle p_2| \otimes |p_3\rangle\langle p_4|) = |p_1\rangle\langle -p_3| \otimes |-p_2\rangle\langle p_4|$. This can be proven using Eq. (5.34) and expressing $|\Omega\rangle = \sum_n |n,n\rangle$ in the momentum basis: $|\Omega\rangle = \int dp\, |p,-p\rangle$.

- Coherent states:
  $R(|\alpha\rangle\langle\beta| \otimes |\gamma\rangle\langle\delta|) = |\alpha\rangle\langle\gamma^*| \otimes |\beta^*\rangle\langle\delta|$. In particular, $R(|\alpha\rangle\langle\alpha| \otimes |\alpha^*\rangle\langle\alpha^*|) = |\alpha\rangle\langle\alpha| \otimes |\alpha^*\rangle\langle\alpha^*|$, so that a pair of phase-conjugate coherent states is invariant under R.

- Two-mode squeezed vacuum state:
  Defining $|TMSV\rangle = (1-t^2)^{1/2} \sum_i t^i\, |i\rangle|i\rangle$ with $0 \leq t < 1$ characterizing the squeezing, we obtain $R(|TMSV\rangle\langle TMSV|) = \frac{1+t}{1-t}\, \rho_{th} \otimes \rho_{th}$ where $\rho_{th} = (1-t) \sum_i t^i |i\rangle\langle i|$ is a thermal state. Entanglement is detected in this case since $\| R(|TMSV\rangle\langle TMSV|) \|_{tr} = \frac{1+t}{1-t} > 1$ as soon as $t > 0$.

- Tensor product of thermal states:
  $R(\rho_{th} \otimes \rho_{th}) = \frac{1-t}{1+t}\, |TMSV\rangle\langle TMSV|$ so that we have $\| R(\rho_{th} \otimes \rho_{th}) \|_{tr} = \frac{1-t}{1+t} \leq 1$, as expected for a separable state.

6.3.2 Expression of $\mathrm{Tr}(R)$ for arbitrary states

In this section, we show how the weak form of the realignment criterion provides us with an implementable entanglement witness. According to Eq. (6.3), in order to access $\mathrm{Tr}\, R(\rho)$ we need to project state ρ onto $|\Omega\rangle$, which can be thought of as an unnormalized infinitely entangled two-mode vacuum squeezed state. Indeed, the state $|\Omega\rangle$ can be reexpressed as $\sqrt{\pi}\, U_{BS}^\dagger |0\rangle_{x_1} |0\rangle_{p_2}$ where U_{BS} is the unitary of a 50:50 beam splitter. By definition, it is expressed in the Fock basis as $|\Omega\rangle = \sum_n |n\rangle|n\rangle$. Thus, if $|x\rangle$ and $|y\rangle$ are position states, we have

$$\begin{aligned} \langle x|\langle y|\Omega\rangle &= \sum_n \langle x|n\rangle\langle y|n\rangle, \\ &= \sum_n \langle x|n\rangle\langle n|y\rangle, \\ &= \langle x|y\rangle = \delta(x-y), \end{aligned} \tag{6.14}$$

so that $|\Omega\rangle$ can be written in the position basis as

$$|\Omega\rangle = \int dx\, dy\, \delta(x-y) |x\rangle|y\rangle = \int dx\, |x\rangle|x\rangle. \tag{6.15}$$

Since the action of the 50:50 beam splitter unitary U_{BS} on the position eigenstates is defined as

$$U_{BS}|x\rangle|y\rangle = \left|\frac{x-y}{\sqrt{2}}\right\rangle \left|\frac{x+y}{\sqrt{2}}\right\rangle, \tag{6.16}$$

we have,

$$\begin{aligned}
\langle x|\langle y|U_{BS}^{\dagger}|0\rangle_{x_1}|0\rangle_{p_2} &= \left\langle \frac{x-y}{\sqrt{2}}\right| \left\langle \frac{x+y}{\sqrt{2}}\right| |0\rangle_{x_1}|0\rangle_{p_2}, \\
&= \left\langle \frac{x-y}{\sqrt{2}}\middle| x=0\right\rangle \left\langle \frac{x+y}{\sqrt{2}}\middle| p=0\right\rangle, \\
&= \delta\left(\frac{x-y}{\sqrt{2}}\right)\frac{1}{\sqrt{2\pi}}, \\
&= \frac{\delta(x-y)}{\sqrt{\pi}},
\end{aligned} \tag{6.17}$$

where we have used the fact that $\langle x|y\rangle = \delta(x-y)$ and $\langle x|p\rangle = \frac{1}{\sqrt{2\pi}}e^{ipx}$. Comparing with Eq. (6.14), this completes the proof that $|\Omega\rangle$ can be reexpressed as

$$|\Omega\rangle = \sqrt{\pi}\, U_{BS}^{\dagger}|0\rangle_{x_1}|0\rangle_{p_2}, \tag{6.18}$$

that is, it can formally be obtained by applying (the reverse of) a 50:50 beam splitter Gaussian unitary U_{BS} on an input state of the product form $|0\rangle_{x_1}|0\rangle_{p_1}$, where $U_{BS}|z\rangle_{x_1}|z'\rangle_{x_2} = \left|(z-z')/\sqrt{2}\right\rangle_{x_1}\left|(z+z')/\sqrt{2}\right\rangle_{x_2}$ in the position eigenbasis and $|0\rangle_{x_1}$ (resp. $|0\rangle_{p_2}$) is the position (momentum) eigenstate with zero eigenvalue. Therefore,

$$\mathrm{Tr}\, R(\rho) = \pi\, \langle 0|_{x_1}\langle 0|_{p_2}\, U_{BS}\, \rho\, U_{BS}^{\dagger}\, |0\rangle_{x_1}|0\rangle_{p_2}. \tag{6.19}$$

Hence, implementing the weak realignment criterion amounts to expressing the probability density of projecting the state $\rho' = U_{BS}\,\rho\,U_{BS}^{\dagger}$ onto $|0\rangle_{x_1}|0\rangle_{p_2}$ where ρ' is the state obtained at the output of a 50:50 beam splitter (see Fig. 6.2 for the two-mode case). This yields an experimental way of constructing an entanglement witness using standard optical components since entanglement is detected simply by applying a Gaussian measurement on the state [88, 89].

Furthermore, this entanglement witness can be generalized to $n \times n$ modes with quadrature components $\mathbf{x}_A = (x_1, \cdots, x_n)$, $\mathbf{p}_B = (p_{n+1}, \cdots, p_{2n})$. We have

$$|\Omega_{n\times n}\rangle = \pi^{n/2}\, U_{BS}^{\dagger}\, |0\rangle_{\mathbf{x}_A}|0\rangle_{\mathbf{p}_B}, \tag{6.20}$$

with the short-hand notation $|0\rangle_{\mathbf{x}_A} \equiv |0, \cdots, 0\rangle_{\mathbf{x}_A}$ and $|0\rangle_{\mathbf{p}_B} \equiv |0, \cdots, 0\rangle_{\mathbf{p}_B}$, hence

$$\mathrm{Tr}\, R(\rho) = \pi^{n}\, \langle 0|_{\mathbf{x}_A}\langle 0|_{\mathbf{p}_B}\, \rho'\, |0\rangle_{\mathbf{x}_A}|0\rangle_{\mathbf{p}_B}. \tag{6.21}$$

To be more precise, it means that if the n first modes belong to Alice and the n last modes belong to Bob, we apply n 50:50 beam splitters between Alice's ith mode and Bob's ith mode, for $i = 1, ..., n$.

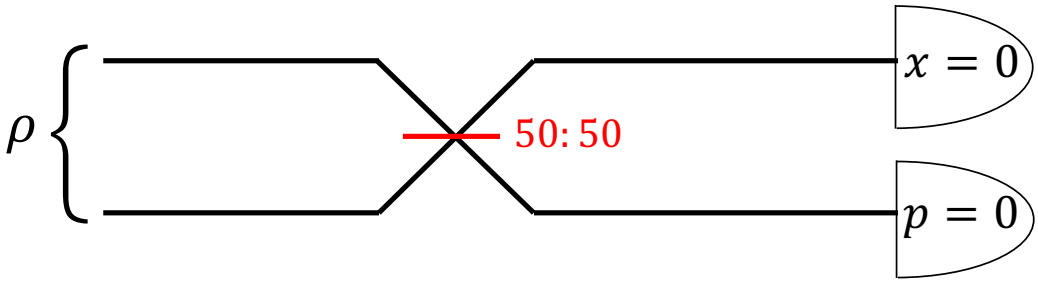

Figure 6.2: Weak realignment criterion for a two-mode state ρ. The trace of the realigned state $R(\rho)$ is obtained by computing the probability of measuring $x_1 = p_2 = 0$ on the output state after processing ρ through a $50:50$ beam splitter, see Eq. (6.19).

6.3.3 Expression of $\mathrm{Tr}(R)$ for Gaussian states

If the initial state ρ is a $n \times n$ Gaussian state, the state $\rho' = U_{BS}\,\rho\,U_{BS}^\dagger$ will be Gaussian too (since the beam splitter is a Gaussian unitary). Its Wigner function is thus given by

$$W_{\rho'}(\mathbf{r}) = \frac{1}{(2\pi)^{2n}\sqrt{\det\gamma'}} e^{-\frac{1}{2}\mathbf{r}(\gamma')^{-1}\mathbf{r}^T}, \tag{6.22}$$

where $\mathbf{r} = (x_1, p_1, x_2, p_2, \cdots, x_{2n}, p_{2n})$ and γ' is the covariance matrix of ρ' obtained as

$$\gamma' = \mathcal{S}\gamma\mathcal{S}^T \qquad \text{with} \qquad \mathcal{S} = \frac{1}{\sqrt{2}}\begin{pmatrix} \mathbb{1}_{2n} & -\mathbb{1}_{2n} \\ \mathbb{1}_{2n} & \mathbb{1}_{2n} \end{pmatrix}, \tag{6.23}$$

being the symplectic matrix representing the beam splitting transformation and γ being the covariance matrix of ρ. The probability of projecting ρ' onto $|0\rangle_{\mathbf{x}_A}|0\rangle_{\mathbf{p}_B}$ as of Eq. (6.21) is thus easy to compute. Indeed, the probability distribution of measuring $\mathbf{x}_A$ on the n modes of the first system and $\mathbf{p}_B$ on the n modes of the second system is given by[5]

$$P(\mathbf{x}_A, \mathbf{p}_B) = \frac{1}{(2\pi)^n\sqrt{\det\gamma_w}} e^{-\frac{1}{2}(\mathbf{x}_A,\mathbf{p}_B)\gamma_w^{-1}(\mathbf{x}_A,\mathbf{p}_B)^T}, \tag{6.24}$$

where γ_w ("w" is for witness) is the restricted covariance matrix obtained by removing the lines and columns of the unmeasured quadratures of γ' (see Fig. 6.3 for examples with $n = 1$ and 2). Thus $\langle\Omega|\rho|\Omega\rangle = \pi^n P(\mathbf{0}, \mathbf{0}) = \frac{1}{2^n\sqrt{\det\gamma_w}}$.

We show how to directly compute $P(0,0)$ for a two-mode state. We have to compute

[5] The probability distribution is Gaussian since we are dealing with Gaussian states.

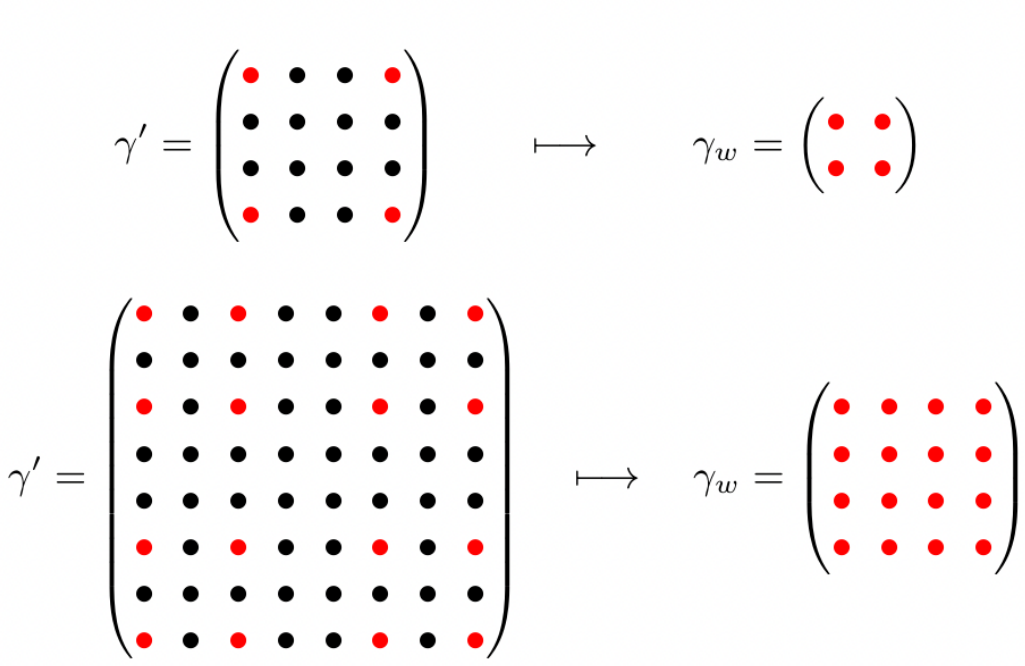

Figure 6.3: Construction of the restricted covariance matrix γ_w from the covariance matrix γ', when $n = 1$ and $n = 2$. The red bullets correspond to the entries of γ' that are copied in γ_w while the black bullets are the entries that are dropped.

the following integral where we set $x_1 = p_2 = 0$:

$$\begin{aligned}
&\langle x=0|\langle p=0|\rho'|x=0\rangle|p=0\rangle, \\
&\quad = \int dx_2 dp_1 W_{\rho'}(0,p_1,x_2,0), \\
&\quad = \frac{1}{(2\pi)^2\sqrt{\det\gamma'}} \int dx_2 dp_1\, e^{-\frac{1}{2}\begin{pmatrix}0 & p_1 & x_2 & 0\end{pmatrix}(\gamma')^{-1}\begin{pmatrix}0\\ p_1\\ x_2\\ 0\end{pmatrix}}, \\
&\quad = \frac{1}{(2\pi)^2\sqrt{\det\gamma'}} \int dx_2 dp_1\, e^{-\frac{1}{2}\begin{pmatrix}x_2 & p_1\end{pmatrix}\Gamma\begin{pmatrix}x_2\\ p_1\end{pmatrix}}, \\
&\quad = \frac{1}{(2\pi)^2\sqrt{\det\gamma'}} \frac{2\pi}{\sqrt{\det\Gamma}}, \\
&\quad = \frac{1}{2\pi\sqrt{\det\gamma'}}\sqrt{\frac{\det\gamma'}{\det\gamma_w}} = \frac{1}{2\pi\sqrt{\det\gamma_w}},
\end{aligned} \tag{6.25}$$

where Γ is a 2×2 matrix with elements given by $\Gamma_{1,1} = (\gamma')^{-1}_{3,3}$, $\Gamma_{2,2} = (\gamma')^{-1}_{2,2}$ and $\Gamma_{1,2} = \Gamma_{2,1} = (\gamma')^{-1}_{2,3}$.

We are now ready to state the following theorem:

Theorem 11 (Weak realignment criterion for Gaussian states). *For any $n \times n$ Gaus-*

sian state ρ^G, the trace norm of the realigned state can be lower bounded as

$$\| R(\rho^G) \|_{tr} \geq \mathrm{Tr}\, R(\rho^G) = \frac{1}{2^n \sqrt{\det \gamma_w}}. \tag{6.26}$$

Hence, if ρ is separable, then $\frac{1}{2^n \sqrt{\det \gamma_w}} \leq 1$. Conversely,

$$\text{if } \frac{1}{2^n \sqrt{\det \gamma_w}} > 1, \text{ then } \rho^G \text{ is entangled.} \tag{6.27}$$

Incidentally, we note that condition (6.27) is equivalent to $\det \gamma_w < 1/4^n$ and can thus be viewed as checking the nonphysicality of γ_w via the violation of the Schrödinger-Robertson uncertainty relation [6]. This is in some sense similar to the PPT criterion, which is based on checking the nonphysicality of the partially transposed state.

Consider the special case of a two-mode Gaussian state ($n = 2$). Its covariance matrix can always be transformed into the normal form [79]

$$\gamma^G = \begin{pmatrix} a & 0 & c & 0 \\ 0 & a & 0 & d \\ c & 0 & b & 0 \\ 0 & d & 0 & b \end{pmatrix}, \tag{6.28}$$

by applying local Gaussian unitary operations[7], which are combinations of squeezing transformations and rotations and hence do not influence the separability of the state. Applying Theorem 11, we get

$$\mathrm{Tr}\, R(\rho^G) = \frac{1}{\sqrt{(a+b-2c)(a+b+2d)}}, \tag{6.29}$$

and the weak realignment criterion reads

$$\frac{1}{\sqrt{(a+b-2c)(a+b+2d)}} > 1 \Rightarrow \rho^G \text{ is entangled.}$$

In comparison, it was shown in [70] that for a covariance matrix in the normal form, Eq. (6.28), the trace norm of the realigned state is given by

$$\| R(\rho^G) \|_{tr} = \frac{1}{2\sqrt{\left(\sqrt{ab} - |c|\right)\left(\sqrt{ab} - |d|\right)}}. \tag{6.30}$$

Comparing Eqs. (6.29) and (6.30) illustrates the fact that the weak realignment criterion is generally weaker than the original form of the realignment criterion (there

[6] The Schrödinger-Robertson uncertainty relation is a generalisation of the Heisenberg uncertainty relation and write in terms of the covariance matrix γ as $\det(\gamma) \geq 1/4$.

[7] The covariance matrix of the TMSV state, Eq. (2.79) is an example of the normal form.

exist states such that $\| R(\rho^G) \|_{tr} > 1$ while $\mathrm{Tr}\, R(\rho^G) \leq 1$).

As already mentioned, both criteria become equivalent if the state is in a Schmidt-symmetric form. In this case, for a general $n \times n$ Gaussian state ρ^G described by the covariance matrix

$$\gamma^G = \begin{pmatrix} A & C \\ C^T & B \end{pmatrix}, \tag{6.31}$$

it implies that both reduced covariance matrices must be identical, namely, $A = B$. Indeed, ρ^G being Schmidt-symmetric implies that $F\rho^G F = (\rho^G)^*$. Exchanging Alice and Bob's systems yields a Gaussian state $F\rho^G F$ of covariance matrix $\begin{pmatrix} B & C^T \\ C & A \end{pmatrix}$, while $(\rho^G)^* = (\rho^G)^T$ is a Gaussian state that admits the covariance matrix $\begin{pmatrix} A & C^T \\ C & B \end{pmatrix}$. Identifying these two covariance matrices, we conclude that any Schmidt-symmetric Gaussian state must have a covariance matrix of the form

$$\gamma^G_{sch} = \begin{pmatrix} A & C \\ C^T & A \end{pmatrix}. \tag{6.32}$$

In particular, both reduced covariance matrices have the same determinant, i.e., $\det A = \det B$, which is expected since we know from Eq. (6.13) that the two reduced states have the same purity, $\mathrm{Tr}((\rho^G_1)^2) = \frac{1}{2^n\sqrt{\det A}}$ and $\mathrm{Tr}((\rho^G_2)^2) = \frac{1}{2^n\sqrt{\det B}}$. In Sec. 6.4.2, we apply a filtration procedure that brings the Gaussian state closer to a Schmidt-symmetric Gaussian state, which will have the effect of bringing the covariance matrix (6.31) closer to the form (6.32). More precisely, we will consider a filtration that equalizes the determinants of the reduced covariance matrices (hence, the two subsystems reach the same purity). We say that a covariance matrix of the form (6.31) has been *symmetrized* when $\det A = \det B$.

Note that the covariance matrix in form (6.32) is a necessary but not sufficient condition for a Gaussian state to be Schmidt-symmetric. A necessary and sufficient condition must imply additional constraints on matrix C. Let us show this for a two-mode Gaussian state with covariance matrix in the normal form

$$\gamma = \begin{pmatrix} a & 0 & c & 0 \\ 0 & a & 0 & d \\ c & 0 & a & 0 \\ 0 & d & 0 & a \end{pmatrix}, \tag{6.33}$$

which is a special case of Eq. (6.32). Using Eq. (6.29), we obtain

$$\mathrm{Tr}(R(\rho)) = \frac{1}{2\sqrt{(a-c)(a+d)}}, \tag{6.34}$$

while Eq. (6.30) implies that

$$\| R(\rho) \|_{tr} = \frac{1}{2\sqrt{(a-|c|)(a-|d|)}}. \tag{6.35}$$

Both formulas are thus equivalent only if $c \geq 0$ and $d \leq 0$, which gives the additional constraint on C. Thus, the necessary and sufficient condition for a two-mode state with covariance matrix in normal form (6.28) to be Schmidt-symmetric is that $a = b$, $c \geq 0$, and $d \leq 0$.

This last point can be illustrated by considering $|\Omega\rangle = \sum_n |n\rangle|n\rangle = \int dx\, |x, x\rangle = \int dp\, |p, -p\rangle$, which can be viewed (up to normalization) as the limit of a two-mode squeezed vacuum state with infinite squeezing. It has $c > 0$ and $d < 0$ since the x's are correlated and p's are anticorrelated. It admits an operator Schmidt decomposition $|\Omega\rangle\langle\Omega| = \sum_{n,m} |n\rangle\langle m| \otimes |n\rangle\langle m|$ with all Schmidt coefficients being equal to one and the associated operators $A_{n,m} = B_{n,m} = |n\rangle\langle m|$; hence it is Schmidt-symmetric since it satisfies $B_{n,m} = A^*_{n,m}$. Now, let us apply a phase shift of π on one of the modes, yielding $|\Omega'\rangle = \sum_n (-1)^n |n\rangle|n\rangle = \int dx\, |x, -x\rangle = \int dp\, |p, p\rangle$. Here, we have $c < 0$ and $d > 0$ since the x's are anticorrelated and p's are correlated, so it should not be Schmidt-symmetric. Accordingly, it can be checked that $|\Omega'\rangle\langle\Omega'|$ does not admit an operator Schmidt decomposition with $B_{n,m} = A^*_{n,m}$. We may decompose it as $|\Omega'\rangle\langle\Omega'| = \sum_{n,m} A_{n,m} \otimes B_{n,m}$ where all Schmidt coefficients are again equal to one and, for example, $A_{n,m} = B_{n,m} = i^{n+m} |n\rangle\langle m|$ or $A_{n,m} = (-1)^{n+m} B_{n,m} = |n\rangle\langle m|$, but in all cases $B_{n,m} \neq A^*_{n,m}$. This is an example of an (unormalized) state verifying $F\rho F = \rho^*$ but that is not Schmidt-symmetric. Since $|\Omega\rangle$ and $|\Omega'\rangle$ share the same Schmidt coefficients, the trace norm of their realignments coincide and are equal to the trace of the realignment of $|\Omega\rangle$ only (in contrast, the trace of the realignment of $|\Omega'\rangle$ vanishes).

The link between $|\Omega\rangle$ and $|\Omega'\rangle$ suggests that a suitable local phase shift operation performed on one of the modes of a state can be useful to make the state closer to being Schmidt-symmetric, and hence to enhance the detection capability of the weak realignment criterion (an example of this feature is shown in Sec. 6.5.3). Applying a local phase shift operation is, however, not always sufficient to make the state exactly Schmidt-symmetric, as can be seen by considering a covariance matrix of the form (6.28), where we impose that $c \geq 0$ and $d \leq 0$. Indeed, as soon as $a \neq b$, one can verify that $\mathrm{Tr}(R(\rho)) < \| R(\rho) \|_{tr}$ as a consequence of the well-known inequality between arithmetic and geometric means, $\sqrt{ab} \leq (a+b)/2$, which is saturated if and only if $a = b$.

6.4 Improvement of the weak realignment criterion

6.4.1 The filtration procedure

According to Theorem 11, the trace norm of the realigned state $\| R(\rho) \|_{tr}$ is greater than (or equal to) $\mathrm{Tr}\, R(\rho)$, which for $n \times n$ Gaussian states is a quantity that solely depends on the determinant of the restricted covariance matrix γ_w. For this reason, while it is easier to compute (especially in higher dimension), the weak realignment criterion has generally a lower entanglement detection performance than the realignment criterion (as applied in [70]). This suggests the possibility of improving the criterion by transforming the state via a suitable (invertible) operation prior to applying the criterion.

Since the trace norm and trace of the realigned state are equivalent for a Schmidt-symmetric state, the natural idea is to find a procedure that ideally transforms the initial state into a Schmidt-symmetric state without of course creating or destroying entanglement. We focus here on $n \times n$ Gaussian states and exploit the fact that any Schmidt-symmetric Gaussian state admits a covariance matrix of the form (6.32), in particular its reduced determinants are equal. Even if this is not a sufficient condition for a state to be Schmidt-symmetric, we choose to symmetrize the initial state by equalizing the reduced determinants of its covariance matrix in order to reach a state that is closer to (ideally equal to) a Schmidt-symmetric state. We then apply Theorem 11 on the resulting symmetrized state in order to get an enhanced entanglement detection performance.

Since first-order moments are irrelevant as far as entanglement detection is concerned, we can restrict to states with $\mathbf{d} = 0$ with no loss of generality. To symmetrize the state, we will exploit a filtering operation in the Fock basis as follows. Suppose that the first subsystem has a smaller noise variance or more precisely that $\det A < \det B$ in Eq. (6.31), meaning that the purity of the first subsystem is larger than that of the second subsystem (the opposite case is treated below). We process each mode of the first subsystem through a (trace-decreasing) noiseless amplification map [90, 91, 92], that is

$$\rho_{AB} \to \tilde{\rho}_{AB} = c\, (t^{\hat{n}/2} \otimes \mathbb{1}) \rho_{AB} (t^{\hat{n}/2} \otimes \mathbb{1}), \tag{6.36}$$

where c is a constant, $\hat{n}$ is the total photon number in the modes of the first subsystem, and $t > 1$ is the transmittance or gain ($\sqrt{t}$ is the corresponding amplitude gain). It can be checked that this map effects an increase of the noise variance of the first subsystem (it increases $\det A$). Note that if the input state ρ_{AB} is Gaussian, then the output state $\tilde{\rho}_{AB}$ remains Gaussian [93]. Crucially, this map does not change the separability of the state (the amount of entanglement might change, but no entanglement can be created from scratch or fully destroyed). Therefore, $\tilde{\rho}_{AB}$ should be closer

to a Schmidt-symmetric state and is a good candidate for applying Theorem 11.

To find the covariance matrix of the output state $\tilde{\rho}_{AB}$, we follow the evolution of the Husimi function defined as

$$Q(\boldsymbol{\alpha}) = \frac{1}{\pi^n}\langle \boldsymbol{\alpha}|\rho|\boldsymbol{\alpha}\rangle, \tag{6.37}$$

where $|\boldsymbol{\alpha}\rangle$ is a vector of coherent states. For an $n \times n$ Gaussian state ρ_{AB}, the Husimi function is given by

$$Q(\boldsymbol{\alpha}, \boldsymbol{\beta}) = \frac{1}{\pi^{2n}\sqrt{\det(\gamma + \frac{\mathbb{1}}{2})}} e^{-\frac{1}{2}\boldsymbol{r}^T \Gamma \boldsymbol{r}}, \tag{6.38}$$

where α is associated to the first system and β to the second, $\Gamma = (\gamma + \mathbb{1}/2)^{-1}$, and

$$\begin{aligned}\boldsymbol{r} = \sqrt{2}\Big(&\Re(\alpha_1), \Im(\alpha_1), \cdots, \Re(\alpha_n), \Im(\alpha_n), \\ &\Re(\beta_1), \Im(\beta_1), \cdots, \Re(\beta_n), \Im(\beta_n)\Big)^T,\end{aligned} \tag{6.39}$$

with $\Re(\cdot)$ and $\Im(\cdot)$ representing the real and imaginary parts. The noiseless amplification map enhances the amplitude of a coherent state as $|\alpha\rangle \to e^{(t-1)|\alpha|^2/2}|\sqrt{t}\,\alpha\rangle$. Therefore, the Husimi function of the output state $\tilde{\rho}_{AB}$ is equal to (see [94] for more details)

$$\begin{aligned}\tilde{Q}(\boldsymbol{\alpha}, \boldsymbol{\beta}) &\propto \frac{1}{\pi^{2n}}\langle \boldsymbol{\alpha}, \boldsymbol{\beta}|(t^{\hat{n}/2} \otimes \mathbb{1})\rho_{AB}(t^{\hat{n}/2} \otimes \mathbb{1})|\boldsymbol{\alpha}, \boldsymbol{\beta}\rangle, \\ &= e^{(t-1)(|\alpha_1|^2 + \cdots + |\alpha_n|^2)} Q(\sqrt{t}\,\boldsymbol{\alpha}, \boldsymbol{\beta}).\end{aligned} \tag{6.40}$$

Since the output state $\tilde{\rho}_{AB}$ is a Gaussian state, its Husimi function is still of the form (6.38) with an output covariance matrix $\tilde{\gamma}$ (and corresponding $\tilde{\Gamma}$). Comparing the exponent of both expressions, we find that

$$\begin{aligned}\tilde{\Gamma} &= M\Gamma M - (M^2 - \mathbb{1}) \\ \tilde{\gamma} &= \left[M\left(\gamma + \frac{\mathbb{1}}{2}\right)^{-1} M - (M^2 - \mathbb{1})\right]^{-1} - \frac{\mathbb{1}}{2}\end{aligned} \tag{6.41}$$

where

$$M = \begin{pmatrix} \sqrt{t}\,\mathbb{1}_{2n\times 2n} & 0 \\ 0 & \mathbb{1}_{2n\times 2n} \end{pmatrix}. \tag{6.42}$$

The last point before applying the weak realignment criterion on $\tilde{\rho}_{AB}$ is to find a suitable value for the transmittance t (note that t must be greater than 1). A simple ansatz is to choose t so that the filtered state $\tilde{\rho}_{AB}$ is a symmetrized Gaussian state, that is, the noise variance of both subsystems are equal ($\det A = \det B$).

Now, if the first subsystem has a larger noise variance (namely $\det A > \det B$), we can simply exchange the roles of A and B and apply the noiseless amplification map on the modes of the second subsystem. Alternatively, we may consider another filtering operation in the Fock basis by processing each mode of the first subsystem through

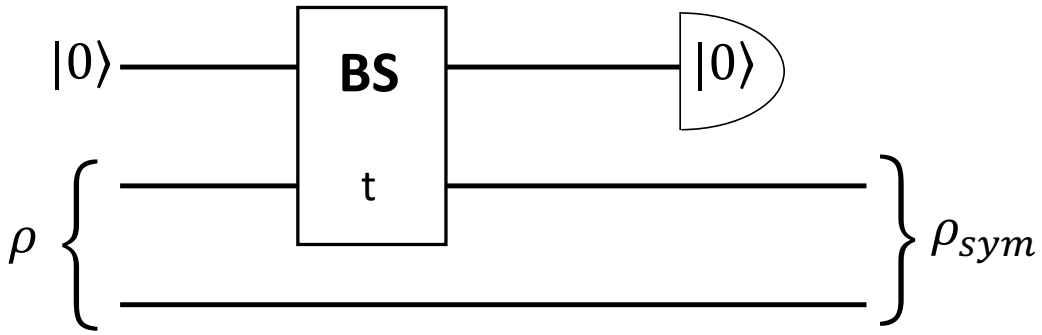

Figure 6.4: Circuit implementing the filtration on a two-mode Gaussian state ρ : a noiseless attenuation map is applied on the first mode of ρ (BS represents a beam splitter of transmittance t). The resulting state ρ_{sym} is symmetrized if the value of t is well chosen.

a (trace-decreasing) noiseless attenuation map [95, 93]. Formally, it is defined exactly as the noiseless amplification map in Eq. (6.36) but with a transmittance $t < 1$, so it leads to very similar calculations. Physically, the noiseless attenuation map has the advantage to admit an exact physical implementation (unlike the noiseless amplification map), which provides us with another method to compute the output covariance matrix $\tilde{\gamma}$ (and corresponding $\tilde{\Gamma}$). Indeed, processing the state of a mode through a noiseless attenuation map is equivalent to processing it through a beam splitter of transmittance t (with vacuum on an ancillary mode) and then postselecting the output conditionally on the vacuum on the ancillary mode (see Fig. 6.4). We give the details of this alternative calculation for the two-mode case in 6.5.1.

We note that the enhancement of the weak realignment criterion obtained via prior filtration can be viewed as the consequence of using $\mathrm{Tr}R(\rho) = \mathrm{Tr}(\rho\,|\Omega\rangle\langle\Omega|)$ but with a better witness operator than $|\Omega\rangle\langle\Omega|$. Let us define the filtration map as $\rho \to \Lambda_F(\rho)$. For example, consider the noiseless attenuation map $\Lambda_F(\rho) \propto (t^{\hat{n}/2} \otimes \mathbb{1})\rho(t^{\hat{n}/2} \otimes \mathbb{1})$ applied on a 1×1 state (with $t < 1$). The trace of the realigned state after filtration can be expressed as

$$\begin{aligned} \mathrm{Tr}(R(\Lambda_F(\rho))) &= \mathrm{Tr}(\Lambda_F(\rho)\,|\Omega\rangle\langle\Omega|), \\ &= \mathrm{Tr}(\rho\,\Lambda_F^\dagger(|\Omega\rangle\langle\Omega|)), \end{aligned} \tag{6.43}$$

where $\Lambda_F^\dagger$ stands for the dual filtration map. In this example, we note that $\Lambda_F^\dagger = \Lambda_F$ and $\Lambda_F(|\Omega\rangle\langle\Omega|))$ is proportional to the projector onto a two-mode squeezed vacuum state. In other words, the enhancement in this example is obtained by computing the fidelity of ρ with respect to $\sum_n t^{n/2}|n\rangle|n\rangle$ instead of $|\Omega\rangle = \sum_n |n\rangle|n\rangle$.

6.4.2 Physical interpretation of the symmetrization procedure for a Gaussian state

We present here an alternative way of computing the covariance matrix of the output state of a noiseless attenuation channel. To do so, we use the fact that the attenuation channel can be represented by a beam splitter followed by a postselection on the vacuum (see Fig. 6.4).

To filter the state, we process the modes of the subsystem with the higher variance (that is the higher value of the determinant of the reduced covariance matrix A or B) through a noiseless attenuation channel and then postselect the output conditionally to measuring the vacuum on the ancillary modes. Since it is a Gaussian channel, the output remains Gaussian. Processing the state through this channel will have for effect to lower the variance of the mode that traveled through the channel. The output state is the symmetrized Gaussian state ρ^{sym}. We chose the attenuator factor (that is the transmittance t of the beam splitter) so that the variance of both modes of ρ^{sym} are equal that is $\det A = \det B$. In terms of covariance matrix, the procedure is as follows.

Let us have a $n \times n$ Gaussian state ρ with covariance matrix (6.31) and let us assume $\det A \geq \det B$ with no loss of generality. We then add n vacuum state to the system. The new covariance matrix thus reads

$$\gamma_{|0\rangle^{\oplus n}+\rho} = \begin{pmatrix} \frac{1}{2}\mathbb{1}_{2n} & 0 \\ 0 & \gamma \end{pmatrix}. \tag{6.44}$$

We now apply the transformation $\mathcal{S} \oplus \mathbb{1}$ where $\mathcal{S}$ is the beam splitter transformation

$$\mathcal{S} \oplus \mathbb{1} = \begin{pmatrix} \sqrt{t}\mathbb{1}_{2n} & -\sqrt{1-t}\mathbb{1}_{2n} & 0 \\ \sqrt{1-t}\mathbb{1}_{2n} & \sqrt{t}\mathbb{1}_{2n} & 0 \\ 0 & 0 & \mathbb{1}_{2n} \end{pmatrix}. \tag{6.45}$$

to the covariance matrix $\gamma_{|0\rangle^{\oplus n}+\rho}$:

$$\gamma_{\mathcal{S}\oplus\mathbb{1}} = \mathcal{S} \oplus \mathbb{1}\, \gamma_{|0\rangle^{\oplus n}+\rho}\, \mathcal{S}^{\dagger} \oplus \mathbb{1} = \begin{pmatrix} \mathcal{A} & \mathcal{C}^T \\ \mathcal{C} & \mathcal{B} \end{pmatrix}. \tag{6.46}$$

Finally, we reduce the covariance matrix conditionally to measuring the vacuum on the ancillary modes, that is [96, 97]

$$\gamma^{sym} = \mathcal{B} - \mathcal{C}\left(\mathcal{A} + \frac{1}{2}\mathbb{1}\right)^{-1}\mathcal{C}^T = \begin{pmatrix} \mathcal{A}' & \mathcal{C}'^T \\ \mathcal{C}' & \mathcal{B}' \end{pmatrix}. \tag{6.47}$$

At this stage we obtained a new covariance matrix which depends on t. If the filtration procedure is such that we want to symmetrize the covariance matrix, we need

to make sure that the determinant of the covariance matrices of both subsystems are equal ($\det \mathcal{A}' = \det \mathcal{B}'$).

6.4.3 Explicit calculation for a two-mode case

Let us do the explicit calculations to obtain the symmetrized covariance matrix of a two-mode Gaussian state initially expressed in its normal form [79],

$$\gamma_\rho = \begin{pmatrix} a & 0 & c & 0 \\ 0 & a & 0 & d \\ c & 0 & b & 0 \\ 0 & d & 0 & b \end{pmatrix}. \tag{6.48}$$

Any covariance matrix of a two-mode state can be transformed into this form by applying local linear unitary operations which are combinations of squeezing transformations and rotations. These operations do not influence the separability of the state, and are thus always allowed when studying entanglement. Note that we assume $a \geq b$ with no loss of generality. We first add the vacuum state to the system. The new covariance matrix reads

$$\gamma_{|0\rangle+\rho} = \begin{pmatrix} 1/2 & 0 & 0 & 0 & 0 & 0 \\ 0 & 1/2 & 0 & 0 & 0 & 0 \\ 0 & 0 & a & 0 & c & 0 \\ 0 & 0 & 0 & a & 0 & d \\ 0 & 0 & c & 0 & b & 0 \\ 0 & 0 & 0 & d & 0 & b \end{pmatrix}. \tag{6.49}$$

We then apply the transformation $\mathcal{S} \oplus \mathbb{1}$ to the covariance matrix $\gamma_{|0\rangle+\rho}$ to obtain

$$\gamma_{\mathcal{S}\oplus\mathbb{1}} = \mathcal{S} \oplus \mathbb{1}\, \gamma_{|0\rangle+\rho}\, \mathcal{S}^\dagger \oplus \mathbb{1} = \begin{pmatrix} \mathcal{A} & \mathcal{C}^T \\ \mathcal{C} & \mathcal{B} \end{pmatrix}, \tag{6.50}$$

with

$$\begin{aligned} \mathcal{A} &= \begin{pmatrix} -ta + a + \frac{t}{2} & 0 \\ 0 & -ta + a + \frac{t}{2} \end{pmatrix}, \\ \mathcal{B} &= \begin{pmatrix} \left(a - \frac{1}{2}\right) t + \frac{1}{2} & 0 & c\sqrt{t} & 0 \\ 0 & \left(a - \frac{1}{2}\right) t + \frac{1}{2} & 0 & d\sqrt{t} \\ c\sqrt{t} & 0 & b & 0 \\ 0 & d\sqrt{t} & 0 & b \end{pmatrix}, \\ \mathcal{C} &= \begin{pmatrix} \frac{1}{2}(1-2a)\sqrt{-(t-1)t} & 0 \\ 0 & \frac{1}{2}(1-2a)\sqrt{-(t-1)t} \\ -c\sqrt{1-t} & 0 \\ 0 & -d\sqrt{1-t} \end{pmatrix}. \end{aligned} \tag{6.51}$$

Finally, we reduce the covariance matrix conditionally to measuring the vacuum on the first mode, that is

$$\gamma^{sym} = \mathcal{B} - \mathcal{C}\left(\mathcal{A} + \frac{1}{2}\mathbb{1}\right)^{-1}\mathcal{C}^T$$
$$= \begin{pmatrix} \frac{t-2a(t+1)-1}{4a(t-1)-2(t+1)} & 0 & \frac{2c\sqrt{t}}{-2a(t-1)+t+1} & 0 \\ 0 & \frac{t-2a(t+1)-1}{4a(t-1)-2(t+1)} & 0 & \frac{2d\sqrt{t}}{-2a(t-1)+t+1} \\ \frac{2c\sqrt{t}}{-2a(t-1)+t+1} & 0 & \frac{2(t-1)c^2}{-2a(t-1)+t+1}+b & 0 \\ 0 & \frac{2d\sqrt{t}}{-2a(t-1)+t+1} & 0 & \frac{2(t-1)d^2}{-2a(t-1)+t+1}+b \end{pmatrix}. \tag{6.52}$$

The covariance matrix will be symmetrized providing that the determinant of the covariance matrices of both subsystems are equal ($\det A = \det B$), meaning

$$\left(\frac{t-2a(t+1)-1}{4a(t-1)-2(t+1)}\right)^2 = \left(\frac{2(t-1)c^2}{-2a(t-1)+t+1}+b\right) \times \left(\frac{2(t-1)d^2}{-2a(t-1)+t+1}+b\right). \tag{6.53}$$

Solving this equation for t gives the transmittance of the beam splitter necessary to obtain a Gaussian state with a symmetric covariance matrix.

In the next section, we apply this filtration procedure on several examples of Gaussian states in order to show how the weak realignment criterion assisted with filtration can indeed improve entanglement detection.

6.5 Applications

6.5.1 Two-mode squeezed vacuum state with Gaussian additive noise

We first illustrate how the filtration procedure enables a better entanglement detection on two-mode entangled Gaussian states. In particular, we show that for specific examples, computing the trace of the realigned state (after filtration) is equivalent to computing its trace norm. Let us consider a two-mode squeezed vacuum state whose first mode is processed through a Gaussian additive-noise channel as shown in Fig. 6.5. We denote V the variance of this added noise. It is known that the entanglement of the two-mode squeezed state decreases when we increase the noise variance, until $V = 1$ at which point it becomes separable (if $V \geq 1$, the channel is entanglement

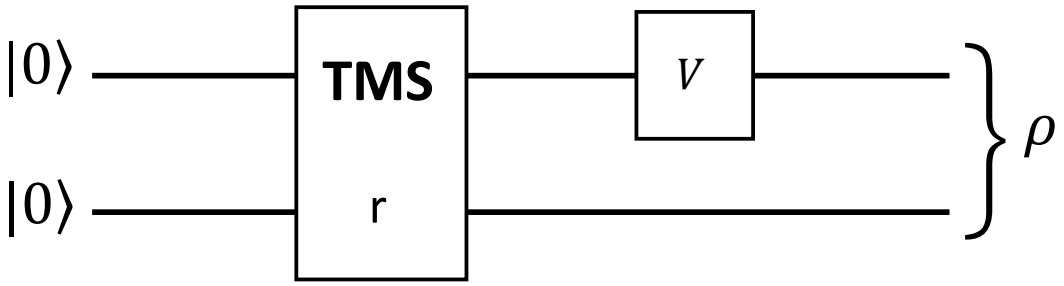

Figure 6.5: Example of a Gaussian state created from a two-mode vacuum state processed through a two-mode squeezer (with squeezing parameter $r > 0$) and a Gaussian additive-noise channel acting on the first mode (with noise variance V).

breaking [98]). Our Gaussian state has a covariance matrix

$$\gamma = \begin{pmatrix} V + \frac{\cosh 2r}{2} & 0 & \frac{\sinh 2r}{2} & 0 \\ 0 & V + \frac{\cosh 2r}{2} & 0 & -\frac{\sinh 2r}{2} \\ \frac{\sinh 2r}{2} & 0 & \frac{\cosh 2r}{2} & 0 \\ 0 & -\frac{\sinh 2r}{2} & 0 & \frac{\cosh 2r}{2} \end{pmatrix}, \tag{6.54}$$

where $r > 0$ is the squeezing parameter. By applying Eq. (6.26) where

$$\gamma_w = \begin{pmatrix} \frac{1}{2}\left(V + e^{-2r}\right) & 0 \\ 0 & \frac{1}{2}\left(V + e^{-2r}\right) \end{pmatrix}, \tag{6.55}$$

we find $\mathrm{Tr}\, R(\rho) = 1/(V + e^{-2r})$. According to Theorem 11, entanglement is thus detected if $V < 1 - e^{-2r}$. Clearly, for a finite squeezing parameter r, there exist entangled states with $1 - e^{-2r} < V < 1$ which are not detected. As a result, the weak realignment criterion does not always detect entanglement in this example (it becomes perfect at the limit of infinite squeezing, $r \to \infty$).

In comparison, it was shown in [70] that for a matrix in the normal form Eq. (6.28) the trace norm of the realignment is given by Eq. (6.30). In our example, we obtain

$$\| R(\rho) \|_{tr} = \frac{1}{\sqrt{(\cosh 2r + 2V)\cosh 2r} - \sinh 2r}, \tag{6.56}$$

so that entanglement is detected if $V < \tanh 2r$. Here again, the realignment criterion leaves some entangled states undetected (but it is more sensitive than the weak realignment criterion since $1 - e^{-2r} < \tanh 2r, \forall r > 0$).

Let us now symmetrize the state with the filtration procedure introduced in Sec.

6.4, that is, we process the first mode (which has a larger noise variance) through a noiseless attenuation map. By inspection, we find that the optimal transmittance is $t = \tanh^2 r$ and the resulting symmetrized Gaussian state ρ^{sym} admits the covariance matrix[8]

$$\gamma^{sym} = \frac{1}{8(V+\cosh 2r)} \begin{pmatrix} (4V\cosh 2r + \cosh 4r + 3)\,\mathbb{1} & (8\sinh^2 r\cosh^2 r)\,\sigma_z \\ (8\sinh^2 r\cosh^2 r)\,\sigma_z & (4V\cosh 2r + \cosh 4r + 3)\,\mathbb{1} \end{pmatrix} \tag{6.57}$$

(6.58)

where $\sigma_z = \left(\begin{smallmatrix} 1 & 0 \\ 0 & -1 \end{smallmatrix}\right)$. We now apply Eq. (6.26) to ρ^{sym}, where

$$\gamma_w^{sym} = \frac{1}{2} \begin{pmatrix} \frac{V\cosh 2r+1}{V+\cosh 2r} & 0 \\ 0 & \frac{V\cosh 2r+1}{V+\cosh 2r} \end{pmatrix}, \tag{6.59}$$

which gives

$$\mathrm{Tr}\, R(\rho^{sym}) = \frac{V+\cosh 2r}{1+V\cosh 2r}. \tag{6.60}$$

Thus, entanglement is detected if $\mathrm{Tr}R(\rho^{sym}) > 1$ which is equivalent to $V < 1$, for all r. Hence, all entangled states of the form (6.54) are now detected. Note that $\mathrm{Tr}\, R(\rho^{sym}) = \| R(\rho^{sym}) \|_{tr}$ here according to Theorem 4. Indeed, the covariance matrix (6.57) is in the form (6.33) with $c > 0$ and $d < 0$, so we have reached a Schmidt-symmetric state.

As a consequence, we have confirmed that the entanglement detection for Gaussian states is improved if one symmetrizes the state before applying the weak realignment criterion. In particular, in this specific example, the weak realignment criterion is as strong as the original realignment criterion with symmetrization since $\mathrm{Tr}\, R(\rho^{sym}) = \| R(\rho^{sym}) \|_{tr}$ and even stronger than the realignment criterion without symmetrization based on $\| R(\rho) \|_{tr}$. Moreover, applying the symmetrization procedure and computing the trace of the realigned state (via the determinant of the restricted covariance matrix) are much easier than computing the trace norm of the realigned state (as developed in [70]). In Fig. 6.6 (upper panel), we illustrate the fact that the trace and trace norm of the realigned state can be increased by the filtration procedure (the value without filtration is found when $t = 1$). We notice that, although the optimal value of the transmittance $t = \tanh^2(r)$ allows for the detection of entanglement, there are actually many other values of t that allow for such a detection too. Moreover, it seems that the symmetrized state $t = \tanh^2(r)$ is not necessarily the best way of filtering the state of this example as it does not give the highest possible value of the trace of $R(\rho)$.

As a second example, let us start with the same two-mode squeezed vacuum state

[8]Note that even if $V = 0$ (i.e. the state already has a symmetric covariance matrix) we may still process one of its modes through the noiseless attenuation map. It simply yields another (symmetric) two-mode squeezed vacuum state with lower entanglement.

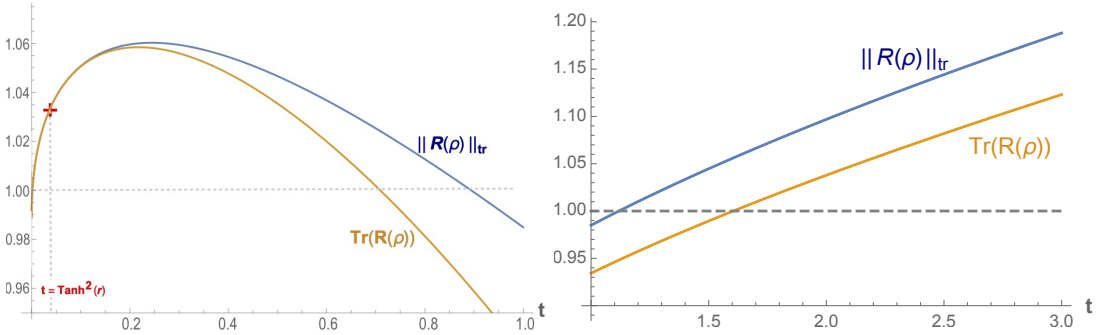

(a) Noise added on the first mode – attenuation map (b) Noise added on the second mode – amplification map

Figure 6.6: Comparison of the trace $\mathrm{Tr}\, R(\rho)$ and trace norm $\| R(\rho) \|_{tr}$ of the realigned state for a two-mode squeezed vacuum state processed through a Gaussian additive-noise channel (we choose $r = 0.2$ and $V = 0.4$).
(a) The noise is added on the first mode and filtering consists in processing this mode via a noiseless attenuation map. The red cross shows the point at $t = \tanh^2(r)$ where the covariance matrix has been symmetrized and $\mathrm{Tr}\, R(\rho) = \| R(\rho) \|_{tr}$.
(b) The noise is added on the second mode and filtering works by processing the first mode via a noiseless amplification map. The values of the trace and the trace norm coincide when $t = \frac{1}{\tanh^2 r} \approx 25.7$.

but add noise on the second mode instead of the first. The covariance matrix reads

$$\gamma = \begin{pmatrix} \frac{\cosh 2r}{2} & 0 & \frac{\sinh 2r}{2} & 0 \\ 0 & \frac{\cosh 2r}{2} & 0 & -\frac{\sinh 2r}{2} \\ \frac{\sinh 2r}{2} & 0 & V + \frac{\cosh 2r}{2} & 0 \\ 0 & -\frac{\sinh 2r}{2} & 0 & V + \frac{\cosh 2r}{2} \end{pmatrix}. \tag{6.61}$$

As before $\mathrm{Tr}\, R(\rho) = 1/(V + e^{-2r})$ so the weak realignment criterion alone does not detect all entangled states. To improve on this, we could of course apply the noiseless attenuation map on the second mode, which would give the exact same results. Alternatively, we may explore another filtration procedure, which consists in applying the noiseless amplification map on the first mode. As can be seen in Fig. 6.6 (lower panel), the values of the trace and trace norm increase with t, and if t is chosen big enough, we detect entanglement. In order to symmetrize the covariance matrix, we would need a noiseless amplifier of transmittance $t = \frac{1}{\tanh^2 r}$, which is a limiting case that would yield a two-mode squeezed vacuum state with infinite squeezing. For this optimal value of t, we have $\mathrm{Tr}\, R(\rho_{sym}) = \frac{1}{V}$ and thus entanglement is always detected when $V < 1$. Hence, here again, the weak realignment criterion assisted with filtration allows us to detect all entangled states.

6.5.2 Random two-mode Gaussian states

Let us consider two other examples of random two-mode Gaussian states with their covariance matrices written in the normal form (6.28). The random values of the a, b coefficients where taken randomly in the interval $[0.5, 1.5]$ and the c and d coefficients where taken randomly in the interval $[-\sqrt{ab}, \sqrt{ab}]$. Then, we checked that the symplectic values $\nu_\pm$ of the covariance matrix where larger than $1/2$ and that they where not PPT. Finally, we selected the two following matrices such that their c and d coefficient have opposite signs:

$$\gamma_1 = \begin{pmatrix} 1.46 & 0 & 0.83 & 0 \\ 0 & 1.46 & 0 & -0.23 \\ 0.83 & 0 & 0.80 & 0 \\ 0 & -0.23 & 0 & 0.80 \end{pmatrix},$$
$$\gamma_2 = \begin{pmatrix} 1.29 & 0 & -0.76 & 0 \\ 0 & 1.29 & 0 & 0.44 \\ -0.76 & 0 & 0.83 & 0 \\ 0 & 0.44 & 0 & 0.83 \end{pmatrix}. \tag{6.62}$$

These states are not PPT so they are entangled. These examples are interesting because in both cases $\| R(\rho) \|_{tr} > 1$ but $\mathrm{Tr}\, R(\rho) < 1$, so entanglement is detected by the realignment criterion but not by its weak formulation. We thus need to apply the filtration procedure in order to enhance the detection with the weak realignment criterion. In Fig. 6.7, we show the evolution of $\mathrm{Tr}\, R(\rho)$ as a function of the transmittance t of the noiseless attenuation map applied on the first mode ($t = 1$ corresponds to the initial value when no filtration is applied). The red cross indicates the exact point when the covariance matrix has been symmetrized. In the first example (see Fig. 6.7a), the filtration procedure works well and many values of t allow us to detect entanglement. In particular, the entanglement is detected at the optimal value of t (note that the trace and trace norm do not exactly coincide there, which witnesses the fact that the symmetrized state is not exactly a Schmidt-symmetric state). In the second example (see Fig. 6.7b), however, filtration alone is not sufficient and entanglement is never detected by the weak realignment criterion. Even if filtration is performed by applying a noiseless amplifier map on the second mode, we observe the same results. Nevertheless, entanglement can still be detected if we apply a local rotation (a π phase shift on one of the two modes which has the effect to flip the sign of the c and d elements in the normal form of the covariance matrix) prior to the filtration procedure, which makes the covariance matrix look similar to the first example. This is shown by the dashed green curve on Fig. 6.7b. Furthermore, by applying an appropriate local squeezing on the second mode of the state after the noiseless attenuator on the first mode, we may always reach a Schmidt-symmetric state (provided c and d have opposite signs in the covariance matrix (6.28) of the initial state, otherwise the state is anyway separable). This indicates that applying

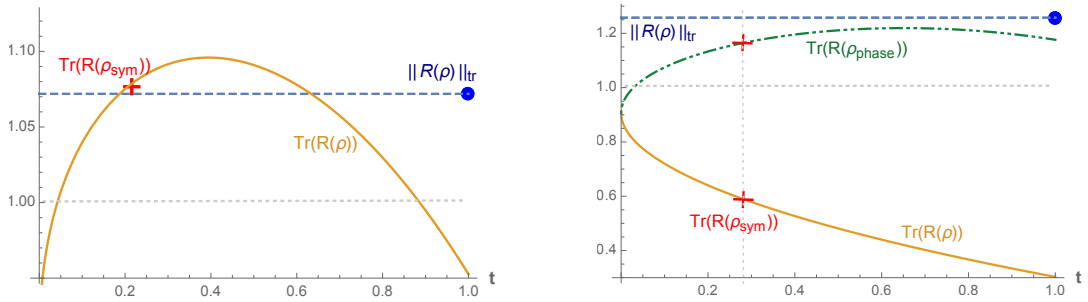

(a) Covariance matrix γ_1 (b) Covariance matrix γ_2

Figure 6.7: Evolution of the trace Tr $R(\rho)$ of the realigned state as a function of t for two-mode Gaussian states with covariance matrices (a) γ_1 and (b) γ_2 after filtering (noiseless attenuation on the first mode). Both examples are entangled states. The blue dashed line represents $\| R(\rho) \|_{tr}$ before the filtration and the red cross shows the value of Tr $R(\rho_{sym})$ when the covariance matrix has been symmetrized. The green dashed curve shows the evolution of the trace Tr $R(\rho_{phase})$, where ρ_{phase} is the state obtained by applying a π phase shift prior to the filtration.

a suitable local phase shift followed by a suitable noiseless attenuator (or amplifier) and finally a suitable local squeezer yields a filtration procedure that always allows the detection of entanglement for a two-mode Gaussian state.

Note that we cannot easily plot the evolution of $\| R(\rho) \|_{tr}$ as a function of t in Fig. 6.7 (in contrast with Fig. 6.6) since the covariance matrix after filtration is not anymore in the form (6.28). The blue dashed line represents its initial value before the filtration is applied.

6.5.3 Examples of 2×2 NPT Gaussian states

Let us now move on to examples of 2×2 Gaussian states (in which case the PPT criterion is not necessary and sufficient anymore). We extend the example of Sec. 6.5.1 by considering that Alice and Bob share two instances of a two-mode squeezed vacuum state with added noise. The covariance matrix is thus given by

$$\gamma_{EPR} = \begin{pmatrix} \left(V+\frac{\cosh 2r}{2}\right)\mathbb{1} & 0 & \frac{\sinh 2r}{2}\sigma_z & 0 \\ 0 & \left(V+\frac{\cosh 2r}{2}\right)\mathbb{1} & 0 & \frac{\sinh 2r}{2}\sigma_z \\ \frac{\sinh 2r}{2}\sigma_z & 0 & \frac{\cosh 2r}{2}\mathbb{1} & 0 \\ 0 & \frac{\sinh 2r}{2}\sigma_z & 0 & \frac{\cosh 2r}{2}\mathbb{1} \end{pmatrix}. \tag{6.63}$$

This state is always detected by the PPT separability criterion. We can also add some rotations on Bob's modes in order to get another state whose covariance matrix is

given by $\gamma'_{EPR} = R(\theta,t)\,\gamma_{EPR}\,R^T(\theta,t)$ with

$$
\begin{aligned}
R(\theta,t) &= \begin{pmatrix} \mathbb{1}_{4\times4} & 0 & 0 & 0 \\ 0 & \cos\theta & \sin\theta & 0 \\ 0 & -\sin\theta & \cos\theta & 0 \\ 0 & 0 & 0 & \mathbb{1}_{2\times2} \end{pmatrix} \\
&\times \begin{pmatrix} \mathbb{1}_{4\times4} & 0 & 0 & 0 & 0 \\ 0 & \sqrt{t} & 0 & -\sqrt{1-t} & 0 \\ 0 & 0 & \sqrt{t} & 0 & -\sqrt{1-t} \\ 0 & \sqrt{1-t} & 0 & \sqrt{t} & 0 \\ 0 & 0 & \sqrt{1-t} & 0 & \sqrt{t} \end{pmatrix}.
\end{aligned}
\tag{6.64}
$$

This rotated state is always entangled and detected by the PPT criterion. The entanglement detection effected by the weak realignment criterion is, however, depending on the values of θ and t as follows.

- If $\theta = 0$ and $t = 1$ we have $\gamma'_{EPR} = \gamma_{EPR}$ and the calculations are exactly the same as in Sec. 6.5.1 (but everything is squared because we now have two states). It means in particular that $\mathrm{Tr}\,R(\rho_{EPR}) = \frac{1}{(e^{-2r}+V)^2}$ is not always greater than 1, but if we applied a suitable filtration with $t = \tanh^2(r)$, entanglement becomes always detected.

- If $\theta = \pi$ and regardless of the value of t, we have $\mathrm{Tr}\,R(\rho'_{EPR}) = \frac{1}{1+V^2+2V\cosh 2r}$ which is always smaller than 1. Entanglement is thus never detected. Note that in this particular case, the filtration does not improve the value of $\mathrm{Tr}\,R(\rho')$ even if we try to add a rotation before the filtration. The key point is that this state does not have EPR-like correlations.

- If $\theta = 0$ and regardless of the value of t, we have $\mathrm{Tr}\,R(\rho'_{EPR}) = \frac{1}{(\cosh 2r - \sqrt{t}\sinh 2r + V)^2}$. In some cases, entanglement is detected without any filtration. In some other cases, entanglement is not straightforwardly detected, but the filtration helps in the detection. For example, if $r = 1$, $V = 0.8$, and $t = 0.9$, then $\mathrm{Tr}\,R(\rho'_{EPR}) \approx 0.8 < 1$ and entanglement is not detected as such. However, if we apply the filtration procedure, we see in Fig. 6.8 (upper panel) that there are many values of t that enable entanglement detection.

6.6 Conclusions

We have introduced a weak formulation of the realignment criterion based on the trace of the realigned state $R(\rho)$, which has the advantage of being much easier to compute than the original formulation of the realignment criterion, especially in higher dimensions. It has a simple physical implementation as computing $\mathrm{Tr}\,R(\rho)$

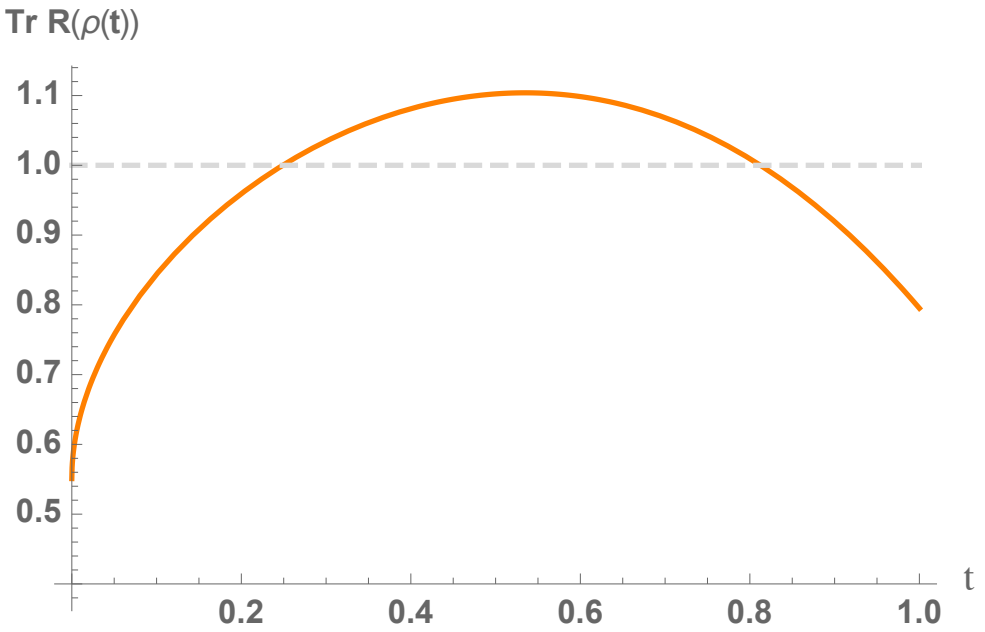

Figure 6.8: Evolution of the trace Tr $R(\rho'_{EPR})$ of the realigned state after filtration as a function of t for $r = 1, V = 0.8, t = 0.9$ and $\theta = 0$.The entanglement is detected in the interval of t values such that the trace exceeds 1.

is equivalent to measuring the $|\Omega\rangle$ component of state ρ via linear optics and homodyne measurements. Moreover, for states in the Schmidt-symmetric form, both realignment criteria — the weak and the original formulations — are equivalent. We focused especially on Gaussian states and showed that applying a suitable filtration procedure prior to applying the weak realignment criterion often allows for a better entanglement detection. In particular, we have explored a filtration based on noiseless amplification or attenuation, which is an invertible operation that transforms the state into a symmetrized form such that the entanglement detection is enhanced (this procedure may even surpass the original realignment criterion while it is simpler but needs some knowledge about the reduced covariance matrices A and B in (6.31) in order to symmetrize the state). We have provided examples of the application of this procedure for various 1×1 and 2×2 Gaussian states. These examples illustrate the power of the method (it can be made to detect all entangled 1×1 Gaussian states), even though we have found cases where it leaves the entanglement of 2×2 states undetected.

A question that we leave open in this work is whether the weak realignment criterion assisted with suitable prior filtration can be stronger than the PPT criterion to the degree that it can detect bound entangled states. The weak realignment criterion is weaker than both the original realignment and PPT criteria, which are two incomparable criteria (except for states in the symmetric subspace, where they coincide). Hence, as such, it cannot detect bound entanglement. We have not been able to find instances where adding filtration allowed us to detect bound entangled states, although it should in principle be possible to bring the state close enough to a Schmidt

symmetric state so that bound entanglement is detected. Note, however, that this can only be the case if the original realignment criterion detects the entanglement of the state, that is, if the Schmidt-symmetric state that is approached via filtration is not within the symmetric subspace (otherwise, the weak realignment criterion tends to the realignment criterion which itself coincides with the PPT criterion, so no bound entanglement can be detected). This puts severe constraints on where to seek the detection of bound entanglement using the weak realignment criterion assisted with filtration.

As a future work, it would also be interesting to explore other possible filtration procedures in order to further improve the entanglement detection in higher dimensions. Alternatively, another interesting goal would be to find a physically implementable protocol for the original realignment criterion and not its weak form (that is, for evaluating the trace norm of $R(\rho)$ instead of its trace with optical components).

Part IV | Nonclassicality criteria

7 Introduction to nonclassicality criteria

7.1 The notion of nonclassicality

7.1.1 The Glauber-Sudarshan P-function

Any density matrix $\hat{\rho}$ representing the quantum state of a single oscillator (bosonic) mode can be represented in a diagonal form in the coherent state basis $|\alpha\rangle$, namely:

$$\hat{\rho} = \int P(\alpha)|\alpha\rangle\langle\alpha| d^2\alpha, \tag{7.1}$$

where the $P(\alpha)$ function is the so-called *Glauber-Sudarshan P function*. Note that $P(\alpha)$ completely defines state $\hat{\rho}$ and is normalized since $\mathrm{Tr}(\hat{\rho}) = 1$.

The expectation value of any normally-ordered operator function $: \hat{g}(\hat{a}, \hat{a}^\dagger) :$ of the annihilation and creation operators can be expressed using the P-function as follows:

$$\langle : \hat{g}(\hat{a}, \hat{a}^\dagger) : \rangle = \int d^2\alpha P(\alpha) g(\alpha, \alpha^*). \tag{7.2}$$

In this expression, the colon stands for normal ordering, which means that all creation operators must be placed on the left of annihilation operators. Hence, if the P-function $P(\alpha)$ admits negative values, then Eq. (7.2) can become negative for some well chosen function $g(\hat{a}, \hat{a}^\dagger)$, witnessing the nonclassicality of state $\hat{\rho}$. This suggests a close connection between the expectation values of normally-ordered functions and the nonclassical character of the P-function.

7.1.2 Classical and nonclassical states

A quantum state is said to be *classical* if its associated P-function behaves as a probability distribution $P(\alpha) = P_{cl}(\alpha)$, hence it is non-negative. Any convex mixture of coherent states $|\alpha\rangle$ is thus classical by definition. Conversely, a quantum state $\hat{\rho}$ is

considered to be *nonclassical* if it cannot be written as a *statistical* mixture of coherent states, i.e. if the P-function does not show the properties of a classical probability density : $P(\alpha) \neq P_{cl}(\alpha)$. Simple examples of nonclassical states include Fock states or squeezed states, whose P-functions are not regular (their expressions involve derivatives of Dirac δ-functions).

Hence, nonclassical states are defined as states that cannot be described as a classical mixture of coherent states, meaning that their density matrix cannot be described as a convex mixture of coherent states:

$$\hat{\rho}_{NC} \neq \int P_{cl}(\alpha)|\alpha\rangle\langle\alpha|d^2\alpha, \tag{7.3}$$

where the label "NC" means "nonclassical" and "cl" means "classical". Note that a classical distribution is understood as statistical distribution including the delta function distribution as a limiting case (but not its derivatives).

This definition of nonclassicality reminds the definition of entanglement as both of them are defined as the negation of the fact that a state belongs to some set of well-defined states (classical or separable). Therefore and since the P-function of nonclassical states is not directly accessible, we use witnesses in order to certify to nonclassical character of a state. Hence, there exist a variety of nonclassicality criteria and parameters. We will review some of them in the following sections.

7.1.3 Nonclassicality and entanglement

Entanglement is certainly the most common nonclassical feature of quantum physics. In this section, we will review the result of Kim *et al.* [99] that shows a connection between the notion of nonclassicality of a state following the definition (7.3) and its entanglement.

When sending two bosonic states on a beam splitter, it is well known that the output state might be entangled. One of the most known example of this effect is the so-called *Hong-Ou-Mandel effect* where two single-photon Fock states $|1,1\rangle$ experience a transformation through a balanced beam splitter. The output state is the NOON state with $N = 2$ writes $1/\sqrt{2}(|2,0\rangle - |0,2\rangle)$ and it is an entangled state.

Another well known example entangled state in quantum optics is the two-mode squeezed vacuum (TMSV) descibed in section 2.3.3. Indeed, by sending two squeezed states that have the same non-zero squeezing parameter but are squeezing in orthogonal direction in phase space on a beam-splitter, the state at the output of the beam splitter is a TMSV (see Eq. (2.77)) which is an archetype of entangled state in CV.

Kim *et al.* [99] studied under which conditions on the input states of a beam splitter the output states are entangled. They found that a necessary condition for the out-

put state of a beam splitter to be entangled is that the input states are nonclassical. Furthermore, they conjectured that only a single input state had to be nonclassical in order to have a necessary condition for the output state to be entangled.

7.2 Nonclassicality criteria

7.2.1 The Mandel Q-parameter

The Mandel Q-parameter was introduced by Leonard Mandel in 1979 [26]. This parameter is closely connected to the Poisson distribution. Indeed, Mandel remarked that the photon number distribution of a coherent state is Poissonian. Hence, any photon number distribution that is narrower than the Poisson distribution must be nonclassical. Hence, the Mandel Q-parameter:

$$Q = \frac{\langle \Delta(\hat{n})^2 \rangle - \langle \hat{n} \rangle}{\langle \hat{n} \rangle}, \tag{7.4}$$

indicates if a photon number distribution of some state is:

1. subpoissonian : $-1 \leq Q < 0$;
2. Poissonian : $Q = 0$;
3. superpoissonian : $0 < Q$.

The Q-parameter only depends on the number of photons statistics and does not carry any information about the phase of the state.

Let us now remember the proof given by Mandel [26] on why the negativity of the Q-parameter imply the nonclassicality of the state. First, since we are interested in the negativity of the Q-parameter and since the denominator of Q is always positive, we are only interested in the numerator of Q (7.4):

$$f = \langle \Delta(\hat{n})^2 \rangle - \langle \hat{n} \rangle = \langle (\hat{a}^\dagger \hat{a})^2 \rangle - \langle \hat{a}^\dagger \hat{a} \rangle^2 - \langle \hat{a}^\dagger \hat{a} \rangle. \tag{7.5}$$

Now, we can re-express each of these mean values in terms of the P-function since:

$$\langle \hat{a}^{\dagger n} \hat{a}^m \rangle = \int P(\alpha) \alpha^{*n} \alpha^m \, d^2\alpha = \langle \alpha^{*n} \alpha^m \rangle_P. \tag{7.6}$$

Hence, the numerator function of the Q-parameter writes in terms of the mean values

of the P-function as :

$$\begin{aligned} f &= \langle(\hat{a}^\dagger\hat{a})^2\rangle - \langle\hat{a}^\dagger\hat{a}\rangle^2 - \langle\hat{a}^\dagger\hat{a}\rangle, \\ &= \langle\hat{a}^{\dagger 2}\hat{a}^2\rangle - \langle\hat{a}^\dagger\hat{a}\rangle^2, \\ &= \langle(\alpha^{*2}\alpha^2 - \langle\alpha^*\alpha\rangle_P^2)\rangle_P, \end{aligned} \tag{7.7}$$

which is always positive if $P(\alpha)$ is a classical probability distribution since it corresponds to the variance of $\alpha^*\alpha$.

The extremal value $Q_{|n\rangle} = -1$ is attained by the Fock state $|n\rangle$ since it is a perfectly defined photon number state with exactly n photons and has a null variance $\Delta n = 0$. The coherent state admits a $Q_{|\alpha\rangle} = 0$ since its photon number statistics follows a Poisson distribution. For thermal state, the Q-parameter is always positive and is equal to $Q_T = \langle\hat{n}\rangle$. Finally, for squeezed states the Q-parameter is equal to $Q_S = 1 + 2\langle\hat{a}^\dagger\hat{a}\rangle = 1 + 2\sinh^2(r)$, where r is the squeezing parameter. Hence, both thermal and squeezed states are not detected as nonclassical by the Q-parameter. However, as we will see in 7.2.2, squeezed states actually are nonclassical states.

7.2.2 The squeezing parameter

In order to construct the squeezing parameter criterion for nonclassicality, let us introduce a general form of the quadrature operator $\hat{x}_\theta$:

$$\hat{x}_\theta = \frac{\hat{a}e^{i\theta} + \hat{a}^\dagger e^{-i\theta}}{\sqrt{2}}. \tag{7.8}$$

For $\theta = 0$, we fall back on the definition of the x-quadrature and $\theta = \pi/2$ correspond to the p-quadrature. The general quadratures satisfy the commutation relation:

$$\left[\hat{x}_\theta, \hat{x}_{\theta+\frac{\pi}{2}}\right] = i. \tag{7.9}$$

Based on (7.8), the squeezing parameter for nonclassicality writes:

$$S_\theta = \langle : \hat{x}_\theta^2 : \rangle - \langle\hat{x}_\theta\rangle^2, \tag{7.10}$$

where $: \cdot :$ means that one should consider the operator in their normal form $: \hat{a}\hat{a}^\dagger := \hat{a}^\dagger\hat{a}$ [1]. Hence, we can write the expression of $: \hat{x}_\theta^2 :$ in terms of annihilation and creation operators :

$$: \hat{x}_\theta^2 := \frac{\hat{a}^2 e^{-2i\theta} + \hat{a}^{\dagger 2} e^{2i\theta} + 2\hat{a}^\dagger\hat{a}}{2}. \tag{7.11}$$

The squeezing parameter criterion is the following. If the squeezing parameter is negative $S_\theta < 0$, then the state is nonclassical.

[1] Note that : $\hat{x}_\theta := \hat{x}_\theta$

In order to prove this condition, we use the averages over the P-function representation such that:

$$\begin{aligned} \langle \hat{x}_\theta \rangle &= \int P(\alpha) \left(\frac{\alpha e^{i\theta} + \alpha^* e^{-i\theta}}{\sqrt{2}} \right) d^2\alpha, \\ \langle : (\hat{x}_\theta)^2 : \rangle &= \int P(\alpha) \left(\frac{\alpha e^{i\theta} + \alpha^* e^{-i\theta}}{\sqrt{2}} \right)^2 d^2\alpha. \end{aligned} \tag{7.12}$$

Hence, the squeezing parameter S_θ writes :

$$\begin{aligned} S_\theta &= \int P(\alpha) \left(\frac{\alpha e^{i\theta} + \alpha^* e^{-i\theta}}{\sqrt{2}} \right)^2 d^2\alpha - \left(\int P(\alpha) \left(\frac{\alpha e^{i\theta} + \alpha^* e^{-i\theta}}{\sqrt{2}} \right) d^2\alpha \right)^2, \\ &= \langle \left(\frac{\alpha e^{i\theta} + \alpha^* e^{-i\theta}}{\sqrt{2}} \right)^2 \rangle_P - \langle \left(\frac{\alpha e^{i\theta} + \alpha^* e^{-i\theta}}{\sqrt{2}} \right) \rangle_P^2, \end{aligned} \tag{7.13}$$

which is always positive if the P-function is classical.

From the form of the squeezing parameter S_θ in (7.10), we can see the link between the S_θ parameter and the variance of the general quadrature since:

$$S_\theta = \Delta^2 \hat{x}_\theta - \frac{1}{2}. \tag{7.14}$$

This shows that if $\Delta^2 \hat{x}_\theta < 1/2$, the state is nonclassical. This also shows that the S_θ parameter admits the value $-1/2$ as a lower bound. Hence, we can easily evaluate the value of the squeezing parameter for states that are commonly encountered in quantum optics:

1. Fock states $|n\rangle$: $S_\theta = n$;
2. Thermal states $\rho(\overline{n})$: $S_\theta = \overline{n}$;
3. Coherent state $|\alpha\rangle$: $S_\theta = 0$;
4. Squeezed vacuum state $|r\rangle$: $S_{\frac{\pi}{2}} = \frac{1}{2}(e^{-2r} - 1)$.

In this case, only the squeezed states are detected as being nonclassical states. Both Fock states and thermal states always show positive values for the squeezing parameter S_θ. The coherent state plays a pivot role as his value is just at the limit of being detected as nonclassical.

We are now equipped with two sufficient conditions for nonclassicality of quantum states. As we will see, there exist many more conditions of nonclassicality. Hence, if a state has positive values for both the Mandel Q-parameter and the squeezing parameter S_θ, one can not conclude that the state is classical.

An interesting case to study is the case where we add some mixedness to a squeezed state and see how robust is the squeezing criterion against the degradation of a pure

squeezed state. This is the subject of the following section.

7.2.3 Degradation of the squeezing criterion for mixed states

In the previous section, we only studied the nonclassicality of pure states and of the most simple Gaussian states, the thermal states. In this section, we review some results about the nonclassicality of the squeezed thermal states:

$$\rho_{S,T} = S(\xi)\rho_T S^\dagger(\xi), \tag{7.15}$$

where ρ_T is the thermal state and $S(\xi)$ is the single mode squeezing operator. The study of the nonclassicality of this squeezed thermal state is interesting since the squeezing will lower the variance in one direction while the variance increases with the number of thermal photons. On one side, the squeezing will reduce the variance of the state in the squeezing direction such that it will lower the value of the squeezing criterion S_θ in the squeezing direction and eventually be detected as nonclassical. On the other side, as the number of thermal photons grows, it will increase the value of the variance of any general quadrature. Hence, these two effects will lead to a non trivial bound for detecting nonclassicality.

Let us evaluate the squeezing parameter for a centered [2] squeezed thermal state $\rho_{S,T}$ as defined in (7.15). By using the expression of the squeezing parameter (7.10) together with the expression of the first and second order moments of the general quadrature (7.8) and (7.11) in terms of the annihilation and creation operators, on can write the squeezing parameter S_θ as:

$$\begin{aligned} S_\theta(\rho_{S,T}) &= \frac{1}{2}\left[\mathrm{Tr}\left(\rho_{S,T}\hat{a}^2\right)e^{-2i\theta} + \mathrm{Tr}\left(\rho_{S,T}\hat{a}^{\dagger 2}\right)e^{2i\theta} + 2\mathrm{Tr}\left(\rho_{S,T}\hat{a}^\dagger\hat{a}\right)\right], \\ &= \frac{1}{2}\left[\mathrm{Tr}\left(\rho_T\hat{a}_S^2\right)e^{-2i\theta} + \mathrm{Tr}\left(\rho_T\hat{a}_S^{\dagger 2}\right)e^{2i\theta} + 2\mathrm{Tr}\left(\rho_T\hat{a}_S^\dagger\hat{a}_S\right)\right], \end{aligned} \tag{7.16}$$

where, by using the cyclic property of the trace, $\hat{a}_S = S(\xi)\hat{a}S^\dagger(\xi)$. From the Bogoliubov transformation (2.66) of the annihilation and creation operators under the squeezing operation, we are able to calculate the different terms:

$$\begin{aligned} \mathrm{Tr}\left(\rho_T\hat{a}_S^2\right) = \mathrm{Tr}\left(\rho_T\hat{a}_S^{\dagger 2}\right)^* &= \frac{1}{2}(1+2\overline{n})\sinh(2r)\,e^{i\theta}, \\ \mathrm{Tr}\left(\rho_T\hat{a}_S^\dagger\hat{a}_S\right) &= \frac{1}{2}(1+2\overline{n})\cosh(2r) - \frac{1}{2}, \end{aligned} \tag{7.17}$$

where θ is the squeezing angle.

Finally, by replacing (7.17) into the expression (7.16) for the squeezing parameter S_θ,

[2] this implies that $\mathrm{Tr}(\rho_{S,T}\hat{a})$ and $\mathrm{Tr}(\rho_{S,T}\hat{a}^\dagger)$ are both equal to zero.

we find the following condition (in the case of $\theta = \phi = 0$):

$$S_{\theta}^{S,T} = \frac{1}{2}\left[(1+2\overline{n})e^{-2r} - 1\right] = \Delta^2\hat{x} - \frac{1}{2}, \tag{7.18}$$

where $\Delta^2\hat{x} = \langle\hat{x}^2\rangle_{\rho_{S,T}} - \langle\hat{x}\rangle^2_{\rho_{S,T}} = 1/2(1+2\overline{n})e^{-2r}$ is the minimal quadrature variance of the squeezed thermal state. This condition was derived in [100]. Moreover, the condition (7.18) is a necessary and sufficient condition for the nonclassicality of Gaussian states [101, 102]

7.2.4 Necessary and sufficient criteria for nonclassicality

As observed in Ref. [20], any operator of the form $:\hat{f}^\dagger\hat{f}:$ is an Hermitian operator that yields a sufficient condition of nonclassicality.

From (7.2), the expectation value of $:\hat{f}^\dagger\hat{f}:$ can be written in terms of the P-function as

$$\langle :\hat{f}^\dagger\hat{f}: \rangle = \int d^2\alpha\, P(\alpha)\, |f(\alpha)|^2, \tag{7.19}$$

which is always positive for any $f(\alpha)$ provided $P(\alpha)$ is a classical probability distribution $P_{cl}(\alpha)$. Hence, a witness of nonclassicality of the considered state $\hat{\rho}$ is the existence of negative expectation values for some well chosen operator function $\hat{f}$, that is

$$\exists\, \hat{f} \qquad \text{s.t.} \qquad \langle :\hat{f}^\dagger\hat{f}: \rangle < 0. \tag{7.20}$$

Furthermore, as shown in Ref. [20], these nonclassicality criteria can be reformulated in terms of an infinite countable set of inequalities, which involve the principal minors of an infinite-dimensional matrix of moments. The infinite set of inequalities completely characterizes the nonclassicality of the quantum state under study. As shown in [103], these criteria can be constructed for three different sets of operators $(\hat{a}, \hat{a}^\dagger)$, $(\hat{x}_\phi, \hat{p}_\phi)$ and $(\hat{x}_\phi, \hat{n})$, but we only consider the set $(\hat{a}, \hat{a}^\dagger)$ in the next Chapter. In this case, one exploits the fact that any operator $\hat{f}$ can be expressed as a (normally-ordered) Taylor series

$$\hat{f} = f(\hat{a}, \hat{a}^\dagger) = \sum_{k=0}^{\infty}\sum_{l=0}^{\infty} c_{kl}\, \hat{a}^{\dagger k}\hat{a}^l. \tag{7.21}$$

Hence, a necessary criterion for classicality can be reformulated as

$$\langle :\hat{f}^\dagger\hat{f}: \rangle = \sum_{k,m=0}^{\infty}\sum_{l,n=0}^{\infty} c^*_{mn}c_{kl}\, \langle \hat{a}^{\dagger(k+n)}\, \hat{a}^{l+m} \rangle \geq 0, \tag{7.22}$$

for any coefficients c_{ij}'s. By using Silvester's criterion, this can be reexpressed as the

positivity of the determinant of the matrix of moments D_N, defined as

$$\begin{pmatrix} 1 & \langle\hat{a}\rangle & \langle\hat{a}^\dagger\rangle & \langle\hat{a}^2\rangle & \langle\hat{a}^\dagger\hat{a}\rangle & \langle\hat{a}^{\dagger 2}\rangle & \dots \\ \langle\hat{a}^\dagger\rangle & \langle\hat{a}^\dagger\hat{a}\rangle & \langle\hat{a}^{\dagger 2}\rangle & \langle\hat{a}^\dagger\hat{a}^2\rangle & \langle\hat{a}^{\dagger 2}\hat{a}\rangle & \langle\hat{a}^{\dagger 3}\rangle & \dots \\ \langle\hat{a}\rangle & \langle\hat{a}^2\rangle & \langle\hat{a}^\dagger\hat{a}\rangle & \langle\hat{a}^3\rangle & \langle\hat{a}^\dagger\hat{a}^2\rangle & \langle\hat{a}^{\dagger 2}\hat{a}\rangle & \dots \\ \langle\hat{a}^{\dagger 2}\rangle & \langle\hat{a}^{\dagger 2}\hat{a}\rangle & \langle\hat{a}^{\dagger 3}\rangle & \langle\hat{a}^{\dagger 2}\hat{a}^2\rangle & \langle\hat{a}^{\dagger 3}\hat{a}\rangle & \langle\hat{a}^{\dagger 4}\rangle & \dots \\ \langle\hat{a}^\dagger\hat{a}\rangle & \langle\hat{a}^\dagger\hat{a}^2\rangle & \langle\hat{a}^{\dagger 2}\hat{a}\rangle & \langle\hat{a}^\dagger\hat{a}^3\rangle & \langle\hat{a}^{\dagger 2}\hat{a}^2\rangle & \langle\hat{a}^{\dagger 3}\hat{a}\rangle & \dots \\ \langle\hat{a}^2\rangle & \langle\hat{a}^3\rangle & \langle\hat{a}^\dagger\hat{a}^2\rangle & \langle\hat{a}^4\rangle & \langle\hat{a}^\dagger\hat{a}^3\rangle & \langle\hat{a}^{\dagger 2}\hat{a}^2\rangle & \dots \\ \vdots & \vdots & \vdots & \vdots & \vdots & \vdots & \ddots \end{pmatrix}. \tag{7.23}$$

which contains all normally-ordered moments of $\hat{a}$ and $\hat{a}^\dagger$ up to N. The matrix of moments D_N can be defined for any dimension $N \times N$ (its block structure is shown on Fig. 8.1), and its determinant will be written $d_{1\cdots N} = \det(D_N)$ in the next Chapter, where the index of d means that all row and columns of D_N are kept in the range $1 \cdots N$. Note that the block structure of D_N will be explained in details in the next Chapter.

Remarkably, as a consequence of Bochner's theorem, the classicality criteria become necessary and sufficient when the determinants are positive for all orders [103], that is, $\hat{\rho}$ is classical if and only if

$$d_{1\dots N} \geq 0, \ \forall N. \tag{7.24}$$

The determinants $d_{1\dots N}$ are the *dominant* principal minors of matrix D_N, i.e., the determinants of the matrices constructed by taking *all* the rows and columns in the upper left corner of the matrix. Hence, the negativity of any single determinant $d_{1\dots N}$ of order N is a sufficient condition for nonclassicality.

Note that one can construct various matrices of moments having similar properties and nonclassicality detection power. In the next Chatper, we will restrict to the principal minors of the matrix of moments (7.23), which are built by selecting *some* rows and corresponding columns and then taking the determinant of the resulting matrix. For example, if rows and columns i, j, and k are selected, the associated determinant is written d_{ijk}. Interestingly, any principal minor such as d_{ijk} provides a sufficient criterion for nonclassicality: if $d_{ijk} < 0$, then the state $\hat{\rho}$ is nonclassical. Each of these criteria might have a distinct physical interpretation and hence, detect different types of nonclassical states (see [104] for a review of nonclassicality criteria). Some examples of principal minors that are not dominant are $d_{14}, d_{15}, d_{124}, d_{134}$ and d_{145}, while examples of dominant principal minors are $d_{12}, d_{123}, d_{1234}$ and d_{1235} (note that we adopt a slightly relaxed definition of dominant principal minors. Indeed, from the block structure of the matrix of moments D_N as described in section 8.2, we slightly adapt the definition of a dominant principal minor: it is associated with the upper left submatrix but the ordering of rows and columns is irrelevant within a given block. Hence, d_{1235} is understood as a dominant principal minor, justifying why this criterion is also invariant under displacement).

8 | Multicopy Nonclassicality Criteria

The content of this chapter is mainly based on the article "Multicopy observables for the detection of optically nonclassical states" that I have published with Célia Griffet and Nicolas Cerf as co-authors [3]. The article is currently submitted to a peer-reviewed journal.

8.1 Introduction

Determining whether a quantum optical state admits nonclassical properties or not is an ubiquitous question in the theory of quantum optics as well as in the development of quantum technologies. Numerous propositions for identifying quantum states displaying nonclassicality have been discussed in the literature, see e.g. [105, 106, 107, 108, 109, 110, 111] (or see [104] for a review). We focus here on the definition of *optical nonclassicality* as introduced by Glauber and Sudarshan [112, 10, 113], starting from the assertion that classical states are those that are expressible as convex mixtures of coherent states. Accordingly, when the Glauber-Sudarshan P-function of a state is incompatible with a true probability distribution (i.e., when it admits negative values in phase space or is not regular in the sense that it cannot be expressed as a function), the state is said to be optically nonclassical. Being able to identify and characterize such nonclassical optical states is essential since nonclassical features are viewed as resources for quantum information tasks [114, 115] such as quantum computation [116], distributed quantum computing [117], quantum networks [118], quantum boson sampling [119], quantum metrology [120] or quantum communication [121]. Moreover, a straightforward operational meaning of optical nonclassicality is that it is a necessary condition in order to produce entanglement with a beam splitter [99].

Various implementation methods have been proposed for identifying nonclassical states, exploiting measurements ranging from single-photon detection [122, 123] to continuous-variable measurements such as homodyne detection [103] or heterodyne detection [124]. In this Chapter, we introduce a technique that uses multiple repli-

cas (identical copies) of a quantum state in order to build a nonclassicality observable. The relevance of multicopy observables in quantum optics has already been explored in the context of uncertainty relations [125]. It relies on the observation that polynomial functions of the elements of a density operator can always be expressed by defining an observable acting on several replicas of the state, avoiding the need for quantum tomography [126]. In the present case, we consider the nonclassicality criteria resulting from the matrix of moments of the optical field introduced in [103, 20]. In the simplest cases that we analyze, the multicopy observable enables an original implementation of a nonclassicality witness through linear interferometry and photon-number detectors.

This chapter is constructed as follows. First we present some of the basic properties of the matrix of moments in Section 8.2. Then, in Section 8.3, we benchmark the performances of the nonclassicality criteria derived from the determinant of these matrices [103, 20]. We consider a variety of states that are known to be nonclassical (Fock states, squeezed states, cat states, squeezed thermal states, photon-added or photon-subtracted thermal states) in order to identify which criterion can detect them. Our results are summarized in table 8.1. This is useful to guide our search for multicopy nonclassicality observables as carried out in Section 8.4. There, we focus on the most interesting criteria as identified in Sec. 8.3 and provide a physical implementations for them. In Section 8.5 we show a recursion relation on d_N that might lead to further development in finding an implementation for some higher order criteria. Finally, in Section 8.6, we give our conclusions and further perspectives on applying this multicopy observable technique for designing implementable nonclassicality criteria.

8.2 Basic properties of the matrix of moments

Before evaluating the performance of the nonclassicality criteria derived from the matrix of moments, we inspect some of the properties of the matrix of moments such as the invariance of the criteria under rotation or displacement operations.

Structure of the matrix d_N. By inspection of the matrix of moments Eq. (7.23), we see that the element on line i and column j is composed of the corresponding operators on the first line and first column taken in normal order and in expectation value as :

$$m_{i,j} = \langle \hat{m}_{i,j} \rangle = \langle : \hat{m}_{i,1} \hat{m}_{1,j} : \rangle = \langle : \hat{m}_{1,i}^{\dagger} \hat{m}_{1,j} : \rangle, \tag{8.1}$$

where the first line element writes :

$$\hat{m}_{1,j} = \hat{a}^{\dagger l} \hat{a}^{n-l}, \tag{8.2}$$

in which two indices n and l are introduced. Each of these indices can be linked to the structure of the matrix. Indeed, the analysis of the matrix shows a block structure as represented on figure 8.1.

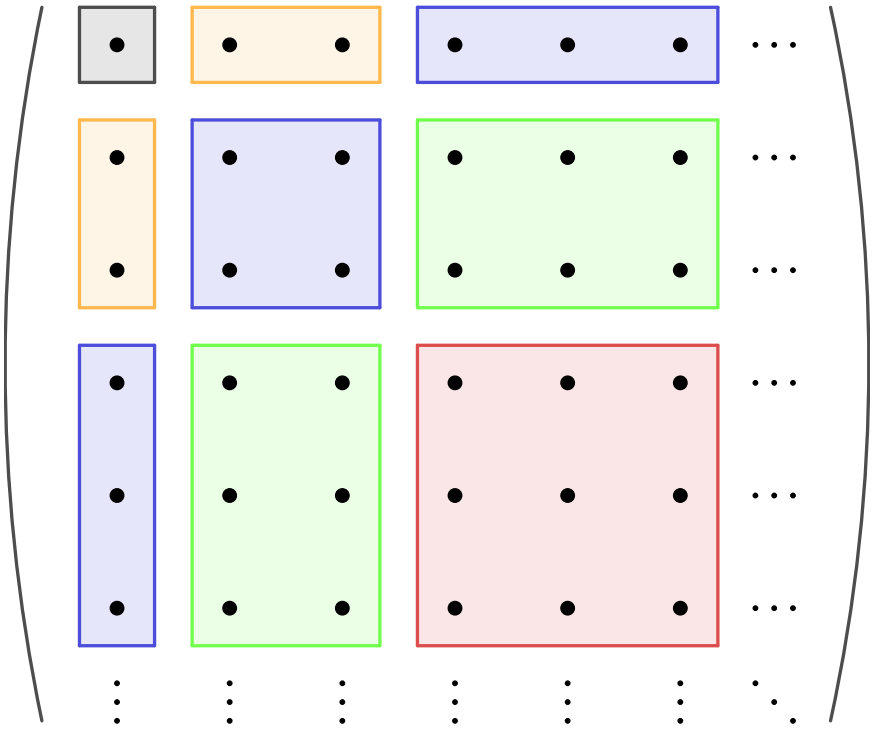

Figure 8.1: Representation of the block structure of the matrix. Blocks of the same color contains the same matrix elements.

The index n that goes from 0 to infinity corresponds to the number of the block while l that goes from 0 to n corresponds to the position of the element in the corresponding block.

Equivalently, we can formulate the elements of the first row using two indices n' and l':

$$\hat{m}_{i,1} = \hat{m}^{\dagger}_{1,i} = \hat{a}^{\dagger n'-l'}\hat{a}^{l'}, \tag{8.3}$$

These double indices for the columns can be related to the usual index corresponding to the column by:

$$j = \frac{n(n+1)}{2} + l + 1. \tag{8.4}$$

Hence, we can find the reverse equations, n and l in terms of j:

$$\frac{-3+\sqrt{1+8j}}{2} \leq n \leq \frac{-1+\sqrt{-7+8j}}{2}, \tag{8.5}$$

$$l = j - 1 - \frac{n(n+1)}{2}. \tag{8.6}$$

The value of n can also be found by using $n = \left\lceil \frac{-3+\sqrt{1+8j}}{2} \right\rceil$.

By using the equation (8.1) together with (8.2) and (8.3), we have an explicit formula for any element of the matrix d_N :

$$\begin{aligned} \hat{m}_{i,j} &= :\hat{m}_{i,1}\hat{m}_{1,j}:, \\ &= :\hat{a}^{\dagger n'-l'}\hat{a}^{l'}\hat{a}^{\dagger l}\hat{a}^{n-l}:, \\ &= \hat{a}^{\dagger n'-l'+l}\hat{a}^{n+l'-l}, \\ &= \hat{a}^{\dagger n'-(l'-l)}\hat{a}^{n+(l'-l)}, \\ &= \hat{a}^{\dagger n'-r}\hat{a}^{n+r}, \end{aligned} \tag{8.7}$$

where $r = l' - l$ and runs from $-n$ to $+n'$.

The matrix of moment D_N is Hermitian. The hermiticity of the matrix of moment, Eq. (7.23), is easily seen from Eq. (8.7) since $\langle \hat{\alpha}_{i,j} \rangle = \langle \hat{a}^{\dagger m-r}\hat{a}^{n+r} \rangle = \langle \hat{a}^{\dagger n+r}\hat{a}^{m-r} \rangle^* = \langle \hat{\alpha}_{j,i} \rangle^*$ where $\langle \hat{O} \rangle = \mathrm{Tr}(\hat{O}\hat{\rho})$ for some operator $\hat{O}$ and quantum density operator $\hat{\rho}$. Hence, its determinant as well as all its principal minors are real-valued.

All principal minors of matrix D_N are invariant under rotations in phase space. The principal minors of the matrix of moments (7.23) are built by selecting *some* rows and corresponding columns and then taking the determinant of the resulting matrix. For example, if rows and columns i, j, and k are selected, the associated determinant is written d_{ijk}.

The invariance under rotation of the principal minors is obvious. Indeed, applying a rotation transforms the operator $\hat{a}$ into $e^{i\theta}\hat{a}$ and $\hat{a}^\dagger$ into $e^{-i\theta}\hat{a}^\dagger$. Since each term in the development of the determinant of any matrix of moments always involve the same number of "$\hat{a}$" and "$\hat{a}^\dagger$", the factors $e^{i\theta}$ and $e^{-i\theta}$ cancel each other out. Hence, the observable is not affected by phase shifts and the criterion is therefore invariant under rotation. By the construction of the matrix of moment, Eq. (7.23), this rotation invariance is also true for any of its principal minors. Hence, all corresponding nonclassicality criteria are invariant under rotations in phase space. Finally, we show

this invariance property explicitly in the case of the d_{123} :

$$\begin{aligned} d^{\theta}_{123} &= \begin{vmatrix} 1 & \langle \hat{a} e^{-i\theta} \rangle & \langle \hat{a}^{\dagger} e^{i\theta} \rangle \\ \langle \hat{a}^{\dagger} e^{i\theta} \rangle & \langle \hat{a}^{\dagger} e^{i\theta} \hat{a} e^{-i\theta} \rangle & \langle \hat{a}^{\dagger 2} e^{2i\theta} \rangle \\ \langle \hat{a} e^{-i\theta} \rangle & \langle \hat{a}^{2} e^{-2i\theta} \rangle & \langle \hat{a}^{\dagger} e^{i\theta} \hat{a} e^{-i\theta} \rangle \end{vmatrix}, \\ &= \langle \hat{a}^{\dagger} \hat{a} \rangle^2 - \langle \hat{a}^{\dagger 2} \rangle \langle \hat{a}^2 \rangle - 2 \langle \hat{a}^{\dagger} \rangle \langle \hat{a} \rangle \langle \hat{a}^{\dagger} \hat{a} \rangle + \langle \hat{a}^{\dagger 2} \rangle \langle \hat{a} \rangle^2 + \langle \hat{a}^{\dagger} \rangle^2 \langle \hat{a}^2 \rangle, \\ &= d_{123}. \end{aligned} \tag{8.8}$$

This invariance property is consistent with the fact that nonclassicality is a feature that is unaffected by such rotations. This simplifies the calculations since all phase terms can be given arbitrary values and will typically be set to zero.

All dominant principal minors of matrix D_N are invariant under displacements in phase space. The *dominant* principal minors of matrix D_N are the determinants of the matrices constructed by taking *all* the rows and columns in the upper left corner of the matrix. Hence, all d_N are dominant principal minors.

The invariance by displacement of the dominant principal minors d_N of the matrix of moments of any order can be demonstrated for a simple example by using the properties of the determinant: adding to a column (or a line) a linear combination of any other columns (or lines) does not change the value of the determinant. By using this property recursively to d_{123}, we show that it is equal to d^{α}_{123} where the superscript α means that the state has been transformed by the displacement operator $\hat{D}(\alpha) = \exp\left(\alpha \hat{a}^{\dagger} - \alpha^* \hat{a}\right)$.

$$\begin{aligned} d_{123} &= \begin{vmatrix} 1 & \langle \hat{a} \rangle & \langle \hat{a}^{\dagger} \rangle \\ \langle \hat{a}^{\dagger} \rangle & \langle \hat{a}^{\dagger} \hat{a} \rangle & \langle \hat{a}^{\dagger 2} \rangle \\ \langle \hat{a} \rangle & \langle \hat{a}^{2} \rangle & \langle \hat{a}^{\dagger} \hat{a} \rangle \end{vmatrix}, \\ &= \begin{vmatrix} 1 & \langle \hat{a} \rangle + \alpha & \langle \hat{a}^{\dagger} \rangle + \alpha^* \\ \langle \hat{a}^{\dagger} \rangle & \langle \hat{a}^{\dagger} \hat{a} \rangle + \alpha \langle \hat{a}^{\dagger} \rangle & \langle \hat{a}^{\dagger 2} \rangle + \alpha^* \langle \hat{a}^{\dagger} \rangle \\ \langle \hat{a} \rangle & \langle \hat{a}^{2} \rangle + \alpha \langle \hat{a} \rangle & \langle \hat{a}^{\dagger} \hat{a} \rangle + \alpha^* \langle \hat{a} \rangle \end{vmatrix}, \\ &= \begin{vmatrix} 1 & \langle \hat{a} \rangle + \alpha & \langle \hat{a}^{\dagger} \rangle + \alpha^* \\ \langle \hat{a}^{\dagger} \rangle + \alpha^* & \langle \hat{a}^{\dagger} \hat{a} \rangle + \alpha \langle \hat{a}^{\dagger} \rangle + \alpha^* (\langle \hat{a} \rangle + \alpha) & \langle \hat{a}^{\dagger 2} \rangle + \alpha^* \langle \hat{a}^{\dagger} \rangle + \alpha^* (\langle \hat{a}^{\dagger} \rangle + \alpha^*) \\ \langle \hat{a} \rangle + \alpha & \langle \hat{a}^{2} \rangle + \alpha \langle \hat{a} \rangle + \alpha (\langle \hat{a} \rangle + \alpha) & \langle \hat{a}^{\dagger} \hat{a} \rangle + \alpha^* \langle \hat{a} \rangle + \alpha (\langle \hat{a}^{\dagger} \rangle + \alpha^*) \end{vmatrix}, \\ &= \begin{vmatrix} 1 & \langle \hat{a} + \alpha \rangle & \langle \hat{a}^{\dagger} + \alpha^* \rangle \\ \langle \hat{a}^{\dagger} + \alpha^* \rangle & \langle (\hat{a}^{\dagger} + \alpha^*)(\hat{a} + \alpha) \rangle & \langle (\hat{a}^{\dagger} + \alpha^*)^2 \rangle \\ \langle \hat{a} + \alpha \rangle & \langle (\hat{a} + \alpha)^2 \rangle & \langle (\hat{a}^{\dagger} + \alpha^*)(\hat{a} + \alpha) \rangle \end{vmatrix}, \\ &= d^{\alpha}_{123}. \end{aligned} \tag{8.9}$$

The argument can be generalized to any dominant principal minors d_N but, in general, not to the principal minors of the matrix of moments (some of the non-dominant

principal minors as d_{1235} are still invariant by displacement).

This property is consistent with the fact that nonclassicality is unaffected by such displacements. Hence, we can simplify our calculations by considering states that are centered in phase space. Note that, unfortunately, the non-dominant principal minors do not enjoy this invariance property. In Section 8.4.2, we will consider the effect of displacements in some non-dominant principal minors and see how it affects the detection capability of the corresponding criteria.

All principal minors of matrix D_N vanish for coherent states $|\alpha\rangle$ Coherent states $|\alpha\rangle$ are extremal classical quantum state. Indeed, their Glauber-Sudarshan P-function is $P(\alpha) = \delta(\alpha)$ and any classical state can be written as a classical mixture of coherent states. Hence, they will not only never be detected by any nonclassicality criteria derived from the matrix of moments but also the value of any principal minors (dominant or not) of the matrix of moment for coherent states will always be equal to 0. Indeed, the action of the creation and the annihilation operator on coherent states $|\alpha\rangle$ is:

$$\begin{cases} \hat{a}|\alpha\rangle = \alpha|\alpha\rangle, \\ \hat{a}^\dagger|\alpha\rangle = \alpha^*|\alpha\rangle. \end{cases} \tag{8.10}$$

Hence, let us write the matrix of moments $D_{123}^{|\alpha\rangle}$ as :

$$D_{123}^{|\alpha\rangle} = \begin{pmatrix} 1 & \alpha & \alpha^* \\ \alpha^* & \alpha^*\alpha & \alpha^{*2} \\ \alpha & \alpha^2 & \alpha^*\alpha \end{pmatrix}. \tag{8.11}$$

One may see that $D_{123}^{|\alpha\rangle}$ is a rank-one matrix since it can be written as the outer product of $\boldsymbol{\alpha} = (1, \alpha, \alpha^*)$ and $\boldsymbol{\alpha}^\dagger$: $D_{123}^{|\alpha\rangle} = \boldsymbol{\alpha}\boldsymbol{\alpha}^\dagger$. Hence, the determinant $d_{123}^{|\alpha\rangle}$ is equal to 0. By construction of the matrix of moments and more precisely Eq. (8.1), this argument holds for all principal minors of the matrix of moments (of order strictly greater than one) which are therefore equal to 0 for coherent states. This shows the specific role played by coherent states as extremal classical states in the sense that they saturate all inequalities in Eq. (7.24). Moreover, any statistical mixture of coherent states is classical and can only get a higher value of all principal minors. Conversely, a slight deviation from a coherent state to a nonclassical state may induce some principal minor to have a negative value.

8.3 Nonclassicality criteria based on the matrix of moments

Let us benchmark the performance of the nonclassicality criteria derived from the principal submatrices of the matrix of moments D_N (up to $N = 5$) in terms of their

ability to detect various nonclassical states. We express the corresponding principal minors for common classes of nonclassical pure states, such as Fock states, squeezed states, or cat states (note that all these states are centered in phase space). All values are listed in Table 8.1, where negative values imply the actual detection of nonclassicality (see entries with grey background). We then study the performance of the criteria when applied to Gaussian (pure or mixed) states and determine that d_{123} is a necessary and sufficient nonclassicality criterion for these states. Finally, we consider a restricted class of non-Gaussian mixed states that are nonclassical (resulting from photon addition or subtraction from a Gaussian state). Overall, our observations lead us to focus on d_{15}, d_{23}, d_{123} and d_{1235} when constructing multicopy nonclassicality observables in Section 8.4.

8.3.1 Nonclassical pure states

Fock states

Fock states $|n\rangle$ (except the vacuum state $|0\rangle$) are well-known nonclassical states, which can be detected by criteria such as d_{15}, d_{125}, d_{135}, d_{145} or d_{1235}, as can be seen in Table 8.1. In a nutshell, the Fock states are only detected when an odd number of off-diagonal entries of the type $\langle \hat{a}^{\dagger k} \hat{a}^k \rangle$ appear in the principal submatrix of the matrix of moments (7.23). This explains why Fock states are never detected in Table 8.1 for criteria that are not involving the 5th row or column since the first non-zero off-diagonal element of D_5 is $(D_5)_{1,5} = (D_5)_{5,1}$.

Squeezed states

Squeezed states are nonclassical quantum states which can be used, for instance, to enhance the sensitivity of the LIGO experiment [127, 128]. In order to check which principal minors detect them as nonclassical states, we need to evaluate the entries of the matrix of moments D_5. First, we observe that all terms of odd order vanish since squeezed states can be decomposed into even Fock states [88], that is

$$|S\rangle = \frac{1}{\sqrt{\cosh(r)}} \sum_{k=0}^{\infty} (-e^{i\psi} \tanh(r))^k \frac{\sqrt{2k!}}{2^k k!} |2k\rangle. \tag{8.12}$$

where r is the squeezing factor and ψ is the squeezing angle. The non-vanishing low-order terms are as follows (as a consequence of the rotation invariance, we may

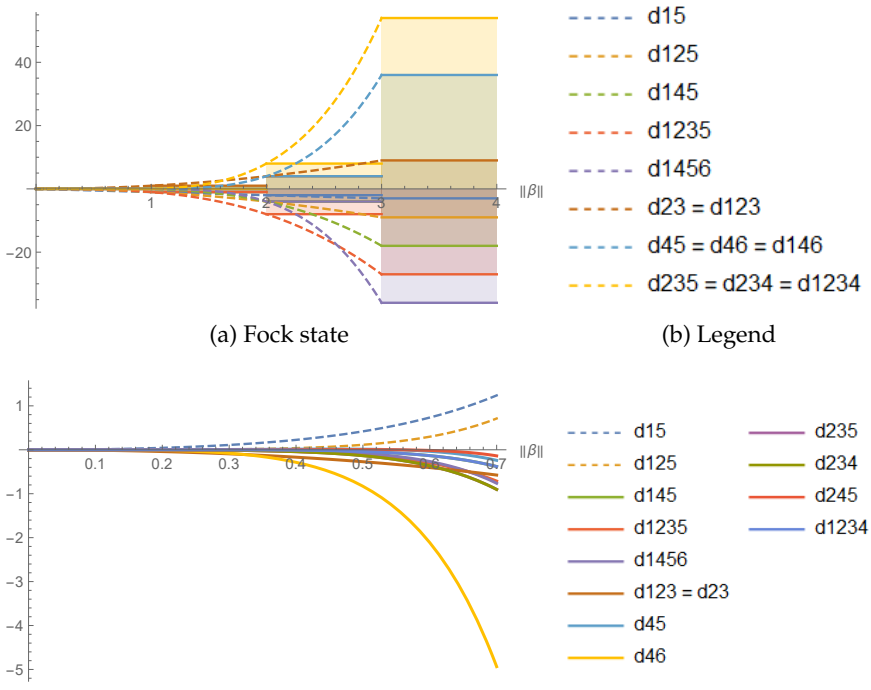

(a) Fock state (b) Legend

(c) Squeezed state (d)

Figure 8.2: The criteria are stronger when the number of photon of the Fock states or the squeezing parameter for the squeezed increase.
(a) Comparison of the criteria for detecting the nonclassicality of Fock states.
(b) The dashed lines are guides to evaluate the efficiency of the criteria to detect the nonclassicality of Fock states.
(c) Comparison of the criteria for detecting the nonclassicality of Squeezed states.
(d) The dashed lines show the value of the criteria that do not detect squeezed states as nonclassical while the plain lines show the criteria that can detect squeezed states as non classical.

assume $\phi = 0$ without loss of generality):

$$\begin{aligned}
\langle \hat{a}^\dagger \hat{a} \rangle_S &= \sinh^2(r), \\
\langle \hat{a}^{\dagger 2} \rangle_S = \langle \hat{a}^2 \rangle_S &= -\sinh(r)\cosh(r), \\
\langle \hat{a}^{\dagger 2} \hat{a}^2 \rangle_S &= \sinh^2(r)(\cosh^2(r) + 2\sinh^2(r)), \\
\langle \hat{a}^{\dagger 3} \hat{a} \rangle_S = \langle \hat{a}^\dagger \hat{a}^3 \rangle_S &= -3\sinh^3(r)\cosh(r), \\
\langle \hat{a}^{\dagger 4} \rangle_S = \langle \hat{a}^4 \rangle_S &= 3\sinh^2(r)\cosh^2(r).
\end{aligned} \tag{8.13}$$

These results allow us to easily calculate the different determinants of principal submatrices taken from matrix of moments (Eq. 7.23) for squeezed states (see table 8.1). The nonclassicality of squeezed states is detected, for example, by d_{23}, d_{123}, d_{234}, d_{235} or d_{1235}.

dimension	criterion	Fock	Squeezed	Odd cat states	Even cat states
2	$d_{12} = d_{13}$	n	$\sinh^2(r)$	$\|\beta\|^2 \frac{N_+}{N_-}$	$\|\beta\|^2 \frac{N_-}{N_+}$
2	$d_{14} = d_{16}$	$n(n-1)$	$2\sinh^4(r)$	0	0
2	d_{15}	$-n$	$\cosh(2r)\sinh^2(r)$	$\|\beta\|^4(1-\frac{N_+^2}{N_-^2})$	$\|\beta\|^4(1-\frac{N_-^2}{N_+^2})$
2	d_{23}	n^2	$-\sinh^2(r)$	$\|\beta\|^4(\frac{N_+^2}{N_-^2}-1)$	$\|\beta\|^4(\frac{N_-^2}{N_+^2}-1)$
2	$d_{24} = d_{26} = d_{34} = d_{36}$	$n^2(n-1)$	$\sinh^4(r)(\cosh^2(r)+2\sinh^2(r))$	$\|\beta\|^6 \frac{N_+}{N_-}$	$\|\beta\|^6 \frac{N_-}{N_+}$
2	$d_{25} = d_{35}$	$n^2(n-1)$	$\sinh^4(r)(\cosh^2(r)+2\sinh^2(r))$	$\|\beta\|^6 \frac{N_+}{N_-}$	$\|\beta\|^6 \frac{N_-}{N_+}$
2	$d_{45} = d_{56}$	$n^2(n-1)^2$	$\frac{1}{2}(5-3\cosh(2r))\sinh^4(r)$	$\|\beta\|^8(1-\frac{N_+^2}{N_-^2})$	$\|\beta\|^8(1-\frac{N_-^2}{N_+^2})$
2	d_{46}	$n^2(n-1)^2$	$-2(1+3\cosh(2r))\sinh^4(r)$	0	0
3	d_{123}	n^2	$-\sinh^2(r)$	$\|\beta\|^4(\frac{N_+^2}{N_-^2}-1)$	$\|\beta\|^4(\frac{N_-^2}{N_+^2}-1)$
3	$d_{124} = d_{126} = d_{134} = d_{136}$	$n^2(n-1)$	$2\sinh^6(r)$	0	0
3	$d_{125} = d_{135}$	$-n^2$	$\sinh^4(r)\cosh(2r)$	$\|\beta\|^6 \frac{N_+}{N_-}(1-\frac{N_+^2}{N_-^2})$	$\|\beta\|^6 \frac{N_-}{N_+}(1-\frac{N_-^2}{N_+^2})$
3	$d_{145} = d_{156}$	$-n^2(n-1)$	$-2\sinh^6(r)$	0	0
3	d_{146}	$n^2(n-1)^2$	$-4\cosh(2r)\sinh^4(r)$	0	0
3	$d_{234} = d_{236}$	$n^3(n-1)$	$\frac{1}{2}(1-3\cosh(2r))\sinh(r)^4$	$\|\beta\|^8(\frac{N_+^2}{N^2}-1)$	$\|\beta\|^8(\frac{N_-^2}{N^2}-1)$
3	d_{235}	$n^3(n-1)$	$-\sinh(r)^4(\cosh(r)^2+2\sinh(r)^2)$	$\|\beta\|^8(\frac{N_+^2}{N_-^2}-1)$	$\|\beta\|^8(\frac{N_-^2}{N_+^2}-1)$
3	$d_{245} = d_{256} = d_{345} = d_{356}$	$n^3(n-1)^2$	$\frac{1}{2}(5-3\cosh(2r))\sinh^6(r)$	$\|\beta\|^{10}\frac{N_+}{N_-}(1-\frac{N_+^2}{N_-^2})$	$\|\beta\|^{10}\frac{N_-}{N_+}(1-\frac{N_-^2}{N_+^2})$
3	$d_{246} = d_{346}$	$n^3(n-1)^2$	$-2(1+3\cosh(2r))\sinh^6(r)$	0	0
3	d_{456}	$n^3(n-1)^3$	$-8\sinh^6(r)$	0	0
4	d_{1234}	$n^3(n-1)$	$-2\sinh^6(r)$	0	0
4	d_{1235}	$-n^3$	$-\cosh(2r)\sinh^4(r)$	$-\|\beta\|^8(\frac{N_+^2}{N_-^2}-1)^2$	$-\|\beta\|^8(\frac{N_-^2}{N_+^2}-1)^2$
4	d_{1456}	$-n^3(n-1)^2$	$-4\sinh^6(r)$	0	0
5	d_{12345}	$-n^4(n-1)$	$2\sinh^8(r)$	0	0

Table 8.1: Summary of the minors of the matrix of moment up to N=5 evaluated for different classes of nonclassical centered states. The determinant d_{1235} corresponds to the strongest criterion since it detects Fock, squeezed and cat states as nonclassical states. Light gray cases corresponds to states detected as the determinant is negative while gray cases corresponds to states that are detected from a certain threshold values for the squeezing parameter r. It is worth to mention that the determinant $d_{24} = d_{26} = d_{34} = d_{36}$ and $d_{25} = d_{35}$ are positive for all states for which the moments of odd order is zero.

Cat-states

Another archetype of nonclassical states consist of the even and odd optical cat states, written $|c_+\rangle$ and $|c_-\rangle$ respectively . They are defined as superpositions of coherent states of opposite phases $|\beta\rangle$ and $|-\beta\rangle$, namely

$$|c_+^\beta\rangle = \frac{1}{\sqrt{N_+}}(|\beta\rangle + |-\beta\rangle), \tag{8.14}$$

$$|c_-^\beta\rangle = \frac{1}{\sqrt{N_-}}(|\beta\rangle - |-\beta\rangle), \tag{8.15}$$

where N_+ and N_- are normalization constants defined as $N_\pm = \sqrt{2\left(1 \pm e^{-2|\beta|^2}\right)}$. Remember that even cat states and odd cat states are orthogonal to each other, i.e., $\langle c_\pm^\alpha | c_\mp^\beta \rangle = 0$, while applying the annihilation operator to an odd cat state results in a state proportional to an even cat state and vice-versa:

$$\hat{a}|c_\pm^\beta\rangle = \beta\sqrt{\frac{N_\mp}{N_\pm}}|c_\mp^\beta\rangle. \tag{8.16}$$

Therefore, the only non-zero entries in the matrix of moments are those of form $\langle \hat{a}^{\dagger k}\hat{a}^l\rangle$ where $k+l$ is even. As an illustration, we show here some of these non-zero moments up to $k+l=4$:

$$\begin{aligned}
\langle \hat{a}^\dagger \hat{a}\rangle_{c_\pm} &= \frac{N_\mp}{N_\pm}|\beta|^2, \\
\langle \hat{a}^2\rangle_{c_\pm} = \langle \hat{a}^{\dagger 2}\rangle^*_{c_\pm} &= \beta^2, \\
\langle \hat{a}^{\dagger 2}\hat{a}^2\rangle_{c_\pm} &= |\beta|^4, \\
\langle \hat{a}^\dagger \hat{a}^3\rangle_{c_\pm} = \langle \hat{a}^{\dagger 3}\hat{a}\rangle^*_{c_\pm} &= \frac{N_\mp}{N_\pm}\beta^2|\beta|^2, \\
\langle \hat{a}^4\rangle_{c_\pm} = \langle \hat{a}^{\dagger 4}\rangle^*_{c_\pm} &= \beta^4.
\end{aligned} \tag{8.17}$$

This allows us to easily calculate the different determinants of principal submatrices from matrix of moments (Eq. 7.23) for even and odd cat states (see table 8.1).

Observations for pure states

From table 8.1, we can make the following observations (limited to the matrix of moments up to dimension 5):

- Increasing the dimension of the matrix of moments does not necessarily lead to a stronger criterion. For example, d_{12345} does not detect *more* states than d_{1234} while being of higher order.
- Some criteria seem to be complementary in the sense that if a state is detected

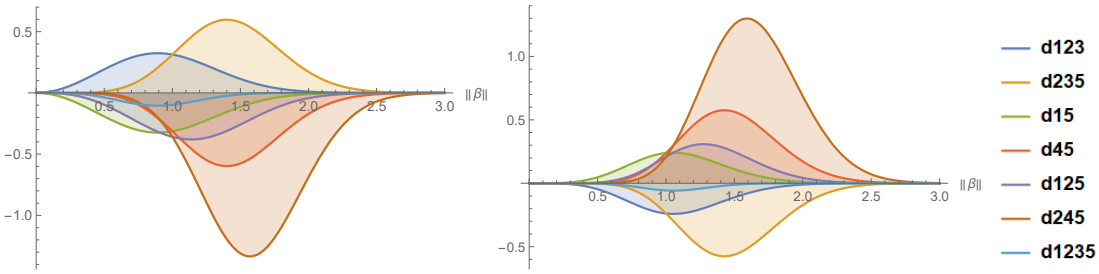

(a) Odd cat state (b) Even cat state

Figure 8.3: Comparison of the criteria detecting odd and even cat states. Interestingly, while all the displayed always detects the nonclassicality, the different criteria have a deeper detection value for different range of value of $|\beta|$. Hence, all these criteria do not show the same performance in detecting the nonclassicality of cat states. (a) The d_{245} looks to be the most robust criteria to detect odd cat state with $|\beta|$ ranging from 1 to 2,3. However, it looks more prudent to use d_{15} or d_{125} for values of $|\beta|$ around and below 1. d_{1235} detects both odd and even cat states but is the less strong criteria in terms of deep of the negative value it can take.
(b) Again, d_{235} is the most reliable nonclassicality criteria for values of $|\beta|$. However, for values of $|\beta|$ below 1, d_{123} is stronger.

by one criterion, it will not be detected by the complementary criterion and vice-versa. This is for instance the case of d_{15} (detecting Fock states but not squeezed states) and d_{23} (detecting squeezed states but not Fock states). Furthermore, it is often the case that a criterion detecting Fock states such as d_{15} also detects odd cat states (similarly, a criterion detecting squeezed states such as d_{23} also detects even cat states).

- The strongest criterion seems to be based on d_{1235} since it is the lowest order determinant that detects the nonclassicality of Fock states, squeezed, and (even and odd) cat states.

These observation motivates the structure of this Chapter and explains why we will focus on the determinants d_{15}, d_{23}, d_{123} and d_{1235} in section 8.4.

8.3.2 Nonclassical mixed states

Gaussian states

The nonclassicality of mixed states has been studied for example in Refs. [100, 129]. In the simplest case of Gaussian mixed states, the limit of nonclassicality is well known: a state is nonclassical when the smallest quadrature variance is smaller than the quadrature variance of the vacuum [100]. The relevant Gaussian mixed states are the squeezed thermal states (since a displacement does not affect nonclassicality). It

is also sufficient to consider squeezing along the x-quadrature since all the considered criteria are invariant under rotation. The covariance matrix of these states is written as

$$\gamma^G = (\overline{n} + \frac{1}{2}) \begin{pmatrix} e^{-2r} & 0 \\ 0 & e^{2r} \end{pmatrix}, \tag{8.18}$$

where $\overline{n}$ is the mean number of thermal photons and r is the squeezing parameter.

In order to calculate the principal minors of interest (d_{15}, d_{23}, d_{123} and d_{1235}) for squeezed thermal states, we take advantage of the property that, for Gaussian states, the moments of order higher than two can be expressed as a function of the first- and second-order moments only. Given that squeezed thermal states are centered states, all elements of the matrix of moments (7.23) can thus be expressed from the covariance matrix γ^G. For example, the fourth-order moment $\langle \hat{a}^{\dagger 2}\hat{a}^2 \rangle$ can be calculated from the Wigner function $W(x,p)$ of the state $\hat{\rho}$ by using the overlap formula

$$\langle \hat{A} \rangle = \mathrm{Tr}(\hat{A}\hat{\rho}) = \int dx\, dp\, W(x,p)\, \bar{A}(x,p), \tag{8.19}$$

where $\bar{A}(x,p)$ is the Weyl transform of $\hat{A}$. The latter can be obtained by exploiting the commutation relation $[\hat{a}, \hat{a}^\dagger] = 1$ in such a way as to write $\hat{A} = \hat{a}^{\dagger 2}\hat{a}^2$ in its symmetrically-ordered form, namely

$$\frac{1}{6}(\hat{a}^{\dagger 2}\hat{a}^2 + \hat{a}^\dagger\hat{a}\hat{a}^\dagger\hat{a} + \hat{a}^\dagger\hat{a}^2\hat{a}^\dagger + \hat{a}\hat{a}^\dagger\hat{a}\hat{a}^\dagger + \hat{a}\hat{a}^{\dagger 2}\hat{a} + \hat{a}^2\hat{a}^{\dagger 2}) - (\hat{a}^\dagger\hat{a} + \hat{a}\hat{a}^\dagger) + \frac{1}{2}, \tag{8.20}$$

which can then be reexpressed in terms of the $\hat{x}$ and $\hat{p}$ quadrature operators as

$$\frac{1}{12}(\hat{x}^2\hat{p}^2 + \hat{p}^2\hat{x}^2 + \hat{x}\hat{p}\hat{x}\hat{p} + \hat{x}\hat{p}^2\hat{x} + \hat{p}\hat{x}^2\hat{p} + \hat{p}\hat{x}\hat{p}\hat{x}) + \frac{1}{4}(\hat{x}^4 + \hat{p}^4) - (\hat{x}^2 + \hat{p}^2) + \frac{1}{2}. \tag{8.21}$$

The Weyl transform of this expression yields

$$\bar{A}(x,p) = \frac{1}{2}x^2p^2 + \frac{1}{4}(x^4 + p^4) - (\hat{x}^2 + \hat{p}^2) + \frac{1}{2}, \tag{8.22}$$

so that the mean value of $\hat{A}$ can be written as

$$\langle \hat{a}^{\dagger 2}\hat{a}^2 \rangle = \frac{1}{2}\langle x^2p^2 \rangle + \frac{1}{4}\left(\langle x^4 \rangle + \langle p^4 \rangle\right) - \left(\langle \hat{x}^2 \rangle + \langle \hat{p}^2 \rangle\right) + \frac{1}{2}. \tag{8.23}$$

For a Gaussian distribution, we have

$$\begin{aligned} \langle x^4 \rangle &= 3\,\Delta x^4 = 3\left(\overline{n} + \frac{1}{2}\right)^2 e^{-4r}, \\ \langle x^2p^2 \rangle &= \Delta x^2 \Delta p^2 = \left(\overline{n} + \frac{1}{2}\right)^2, \\ \langle p^4 \rangle &= 3\,\Delta p^4 = 3\left(\overline{n} + \frac{1}{2}\right)^2 e^{4r}, \end{aligned} \tag{8.24}$$

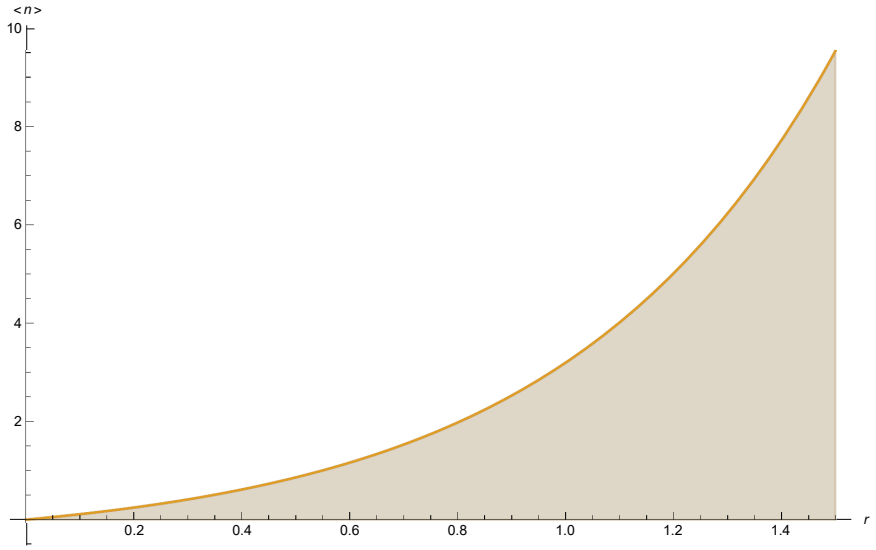

Figure 8.4: Nonclassicality limit for Gaussian states in the plane $(r, \overline{n})$. All points lying below the orange line correspond to nonclassical states, as witnessed by Eq. (8.26) or equivalently $d_{123} < 0$. Hence, pure squeezed states are nonclassical as soon as $r > 0$.

so that we obtain finally

$$\langle \hat{a}^{\dagger 2} \hat{a}^2 \rangle = \frac{1}{2} \left(\overline{n} + \frac{1}{2} \right)^2 [3\cosh(4r) + 1] - 2 \left(\overline{n} + \frac{1}{2} \right) \cosh(2r) + \frac{1}{2}. \tag{8.25}$$

By using the same method to calculate the other moments, we obtain the values of the determinants that are presented in Table 8.2.

criterion	Fock
d_{15}	$\frac{1}{4}(1 - 2(1+2\overline{n})\cosh(2r) + (1+2\overline{n})^2 \cosh(4r))$
$d_{123} = d_{23}$	$\frac{1}{2} + \overline{n} + \overline{n}^2 - \frac{1}{2}(1+2\overline{n})\cosh(2r)$
d_{1235}	$d_{15}\, d_{23}$

Table 8.2: Determinants evaluated for squeezed thermal states.

We see that d_{15} is always positive for any values of parameters $\overline{n}$ and r, so it does not yield a criterion. In contrast, d_{23} is interesting as it can be negative for some values of $\overline{n}$ and r. Of course, when the mean number of thermal photons $\overline{n} = 0$, we recover the result for squeezed states and $d_{23} = -\sinh^2(r)$ is negative for all values of the squeezing parameter $r > 0$. However, when $\overline{n}$ increases, the determinant becomes positive below some threshold value of r, as shown in Fig. 8.4. From Ref. [100], we know that a necessary and sufficient condition for a squeezed thermal state with covariance matrix γ^G to be nonclassical writes

$$(\overline{n} + \frac{1}{2})\, e^{-2r} < \frac{1}{2}. \tag{8.26}$$

It is easy to check that this precisely corresponds to the condition $d_{23} < 0$, so the crite-

rion based on the sign of d_{23} is necessary and sufficient for squeezed thermal states. Note that d_{23} is not invariant under displacements, so that this criterion looses its power when applied to an arbitrary Gaussian state (i.e., a displaced squeezed thermal state). However, the determinant d_{123} can be used instead since it is invariant under displacements and coincides with d_{23} for centered states. Thus, $d_{123} < 0$ provides a necessary and sufficient criterion for the nonclassicality detection of Gaussian states.

Note finally that for the special case of centered Gaussian states (squeezed thermal states), d_{1235} is equal to the product of d_{15} and d_{23} since all entries of odd order in the annihilation and creation operators in the matrix of moments (7.23) vanish. Since d_{15} is always positive for Gaussian states, d_{1235} has the same detection power as d_{23}. Furthermore, since it is invariant under displacements, d_{1235} actually has the same detection power as d_{123} for arbitrary Gaussian states.

Non-Gaussian states

To complete the study of mixed states, we also explore the performance of the above criteria for detecting nonclassical states in the set of non-Gaussian states. These states are essential for the development of quantum technologies such as quantum computing (for which non-Gaussian states are a necessary ressource [23, 130]) and have attracted a lot interest [131]. By adding or subtracting a photon from the Gaussian states as studied in Sec. 8.3.2, we obtain non-Gaussian states. A special case of these states is the photon subtracted squeezed states, also known as the kitten state.

Photon-added and -subtracted Gaussian states Interestingly, all the moments of the photon-added or -subtracted Gaussian states appearing in the matrix of moments (7.23) can be calculated from the moments of corresponding Gaussian states as calculated in Sec. 8.3.2. Indeed, for the photon-subtracted Gaussian states, the moments are

$$\begin{aligned}\langle \hat{a}^{\dagger k}\hat{a}^{l}\rangle &= \mathrm{Tr}(\hat{a}^{\dagger k}\hat{a}^{l}\hat{a}\rho^{G}\hat{a}^{\dagger}) = \mathrm{Tr}(\hat{a}^{\dagger(k+1)}\hat{a}^{(l+1)}\rho^{G}),\\ &= \langle \hat{a}^{\dagger(k+1)}\hat{a}^{(l+1)}\rangle_{G}\end{aligned} \tag{8.27}$$

where we have used the cyclic invariance property of the trace. For the photon-added Gaussian states, it can be shown that

$$\begin{aligned}\langle \hat{a}^{\dagger k}\hat{a}^{l}\rangle &= \mathrm{Tr}(\hat{a}^{\dagger k}\hat{a}^{l}\hat{a}^{\dagger}\rho^{G}\hat{a})\\ &= \mathrm{Tr}((\hat{a}^{\dagger(k+1)}\hat{a}^{(l+1)} + (l+k+1)\hat{a}^{\dagger k}\hat{a}^{l} + kl\hat{a}^{\dagger(k-1)}\hat{a}^{(l-1)})\rho^{G}).\\ &= \langle \hat{a}^{\dagger(k+1)}\hat{a}^{(l+1)}\rangle_{G} + (l+k+1)\ \langle \hat{a}^{\dagger k}\hat{a}^{l}\rangle_{G} + kl\ \langle \hat{a}^{\dagger(k-1)}\hat{a}^{(l-1)}\rangle_{G}.\end{aligned} \tag{8.28}$$

Hence, we can derive the values of the principal minors for photon-added and -subtracted Gaussian states directly from the matrix of moments calculated for the

corresponding Gaussian states. It is worth noticing that the criterion based on d_{15} can detect photon-subtracted Gaussian states for small values of squeezing and mean number of thermal photons, while it was useless in the case of Gaussian states (see Table 8.2).

moment	Fock	Squeezed	$\|c_-\rangle$	$\|c_+\rangle$	Gaussian
$\langle\hat{a}^\dagger\hat{a}\rangle$	n	$\sinh^2(r)$	$\|\beta\|^2\frac{N_+}{N_-}$	$\|\beta\|^2\frac{N_-}{N_+}$	$(\overline{n}+\frac{1}{2})\cosh(2r)-\frac{1}{2}$
$\langle\hat{a}^2\rangle=\langle\hat{a}^2\rangle^*$	0	$-\sinh(r)\cosh(r)$	β^2	β^2	$-(\overline{n}+\frac{1}{2})\sinh(2r)$
$\langle\hat{a}^{\dagger 2}\hat{a}^2\rangle$	$n(n-1)$	$\sinh^2(r)(\cosh^2(r)+2\sinh^2(r))$	$\|\beta\|^4$	$\|\beta\|^4$	$3(\overline{n}+\frac{1}{2})^2\frac{\cosh(4r)}{2}+\frac{(\overline{n}+\frac{1}{2})^2}{2}-2(\overline{n}+\frac{1}{2})\cosh(2r)+\frac{1}{2}$
$\langle\hat{a}^\dagger\hat{a}^3\rangle=\langle\hat{a}^{\dagger 3}\hat{a}\rangle^*$	0	$-3\sinh^3(r)\cosh(r)$	$\beta^2\|\beta\|^2\frac{N_+}{N_-}$	$\beta^2\|\beta\|^2\frac{N_-}{N_+}$	$-3(\overline{n}+\frac{1}{2})^2\frac{\sinh(4r)}{2}+3(\overline{n}+\frac{1}{2})\sinh(2r)/2$
$\langle\hat{a}^4\rangle=\langle\hat{a}^4\rangle^*$	0	$3\sinh^2(r)\cosh^2(r)$	β^4	β^4	$3(\overline{n}+\frac{1}{2})^2\frac{\cosh(4r)}{2}-3(\overline{n}+\frac{1}{2})^2/2$

Table 8.3: Summary of the non-zero moments up to order 4 evaluated for different classes of nonclassical centered states. This moments of the creation and annihilation operators appear in the criteria based on the matrix of moments of Eq. (7.23).

8.4 Implementation of the nonclassicality multicopy observables

Potential implementations of nonclassicality criteria based on the matrix of moments (7.23) have been considered in Ref. [103], but the idea was to experimentally evaluate all individual elements of the matrix before calculating its determinant. Instead, in the present work, we look for an optical implementation that makes it possible to directly access the value of the determinant by measuring the expectation value of some nonclassicality observable. Since the principal minors discussed in Sec. 8.3 (especially d_{15}, d_{23}, d_{123} and d_{1235}) are polynomial functions of the matrix elements of $\hat{\rho}$, we turn to multicopy observables following Ref. [126]. This method seems to be well adapted here since the nonclassicality criteria involve determinants (a similar technique was successfully applied for accessing determinants of other matrices of moments in quantum optics, see Ref. [125]).

After a reminder on the Schwinger representation in section 8.4.1, we start by detailing the design of 2-copy observables for accessing the determinants d_{12}, d_{14}, d_{23} and d_{15}. Then, we increase the number of copies and consider the 3-copy nonclassicality observable d_{123} and 4-copy nonclassicality observable d_{1235}. We also discuss the optical implementation of all these observables up to 3 copies.

8.4.1 Schwinger representation and linear interferometry

The Schwinger representation connects the angular momentum algebra to two bosonic modes operators as follows :

$$\hat{L}_j = \frac{1}{2}\hat{A}^\dagger\sigma_j\hat{A}, \tag{8.29}$$

where $\hat{A} = \begin{pmatrix} \hat{a}_1 \\ \hat{a}_2 \end{pmatrix}$ and σ_j are the Pauli matrices with $j = x, y, z$. The associated Casimir operator $\hat{L}_0 = \frac{1}{2}\hat{A}^\dagger \sigma_0 \hat{A}$ where $\sigma_0 = \mathbf{1}$ is the 2×2 identity matrix.

Let us derive the effect of linear interferometric operations on the $\hat{L}_j$ operators. When applying a beam-splitter operation of transmittance τ, the Schwinger operators transforms as follows:

$$\begin{aligned} &\hat{L}_0 \to \hat{L}_0, \\ &\hat{L}_x \to -(2\tau - 1)\, \hat{L}_x + 2\sqrt{\tau(1-\tau)}\, \hat{L}_z, \\ &\hat{L}_y \to -\hat{L}_y, \\ &\hat{L}_z \to (2\tau - 1)\, \hat{L}_z + 2\sqrt{\tau(1-\tau)}\, \hat{L}_x. \end{aligned} \tag{8.30}$$

When applying a phase-shift operation on the second mode of phase ϕ, the Schwinger operators transforms as follows:

$$\begin{aligned} &\hat{L}_0 \to \hat{L}_0, \\ &\hat{L}_x \to \cos(\phi)\, \hat{L}_x - \sin(\phi)\, \hat{L}_y, \\ &\hat{L}_y \to \cos(\phi)\, \hat{L}_y + \sin(\phi)\, \hat{L}_x, \\ &\hat{L}_z \to \hat{L}_z. \end{aligned} \tag{8.31}$$

These expressions are very usefull in order to find implementable schemes of the multicopy observables. Indeed, they allow us to transform the $\hat{L}_y$ into $\hat{L}_x$ via the phase shift operator and the $\hat{L}_x$ operator into $\hat{L}_z$ and vice versa via the beam-splitter transformation. In this way, we can transform the multicopy operators through linear interferometry such that they only depend on $\hat{L}_0$ and $\hat{L}_z$ operators.

8.4.2 Two-copy observables

Instructive examples: d_{12} and d_{14}

The determinant d_{12}, which is expressed as

$$d_{12} = \begin{vmatrix} 1 & \langle \hat{a} \rangle \\ \langle \hat{a}^\dagger \rangle & \langle \hat{a}^\dagger \hat{a} \rangle \end{vmatrix} = \langle \hat{a}^\dagger \hat{a} \rangle - \langle \hat{a} \rangle \langle \hat{a}^\dagger \rangle, \tag{8.32}$$

is useless for nonclassicality detection in the sense that it is positive for all (classical or nonclassical) states. Indeed, d_{12} is simply the thermal (or chaotic) photon number, i.e., the total photon number minus the coherent photon number. Since d_{12} is invariant under displacements, centering the state on the origin in phase space simply results in $d_{12} = \langle \hat{a}^\dagger \hat{a} \rangle \geq 0$.

Nevertheless, it is instructive to illustrate the multicopy observable technique with this simple example, where we need two copies of the original state $\hat{\rho}$. We consider a 2×2 operator matrix mimicking the matrix of moments D_2 except that we remove all expectation values. Then, we associate the first row of this operator matrix with the first copy (mode 1) and the second row with the second copy (mode 2). In a last step, we average over all permutations $\sigma \in S_2$ on the mode indices in order to ensure the Hermiticity of the resulting multicopy observable:

$$\begin{aligned} \hat{B}_{12} &= \frac{1}{|S_2|} \sum_{\sigma \in S_2} \begin{vmatrix} 1 & \hat{a}_{\sigma(1)}, \\ \hat{a}^{\dagger}_{\sigma(2)} & \hat{a}^{\dagger}_{\sigma(2)} \hat{a}_{\sigma(2)} \end{vmatrix} \\ &= \frac{1}{2}(\hat{a}_2^{\dagger}\hat{a}_2 + \hat{a}_1^{\dagger}\hat{a}_1 - \hat{a}_1\hat{a}_2^{\dagger} - \hat{a}_2\hat{a}_1^{\dagger}), \end{aligned} \tag{8.33}$$

where, in the r.h.s of the first equality, the first line of the matrix is associated to the first mode and the second line on the matrix is associated with the second mode. The sum over all possible permutation of the modes labels assures the hermiticity of the multicopy operator. The value of the determinant d_{12} is obtained by measuring the expectation value of this observable on two copies of the same state $\hat{\rho}$, namely $\langle\langle \hat{B}_{12} \rangle\rangle \equiv \mathrm{Tr}[(\hat{\rho} \otimes \hat{\rho})\, \hat{B}_{12}]$. Indeed, we have

$$\begin{aligned} \langle\langle \hat{B}_{12} \rangle\rangle &= \frac{1}{2}\langle\langle\, \hat{a}_2^{\dagger}\hat{a}_2 + \hat{a}_1^{\dagger}\hat{a}_1 - \hat{a}_1\hat{a}_2^{\dagger} - \hat{a}_2\hat{a}_1^{\dagger}\,\rangle\rangle, \\ &= \frac{1}{2}(\langle \hat{a}_2^{\dagger}\hat{a}_2 \rangle + \langle \hat{a}_1^{\dagger}\hat{a}_1 \rangle - \langle \hat{a}_1 \rangle\langle \hat{a}_2^{\dagger} \rangle - \langle \hat{a}_2 \rangle\langle \hat{a}_1^{\dagger} \rangle) \\ &= \langle \hat{a}^{\dagger}\hat{a} \rangle - \langle \hat{a} \rangle\langle \hat{a}^{\dagger} \rangle = d_{12}, \end{aligned} \tag{8.34}$$

where $\langle \cdot \rangle \equiv \mathrm{Tr}[\hat{\rho}\, \cdot]$.

Finally, we look for an optical implementation of observable $\hat{B}_{12}$ by means of linear optics and photon-number resolving detectors. It is not immediately obvious from Eq. (8.33), but we can exploit the Schwinger representation of angular momenta in terms of bosonic annihilation and creation operators. Here, we can express $\hat{B}_{12}$ as the difference between the Casimir operator $\hat{L}_0 = \frac{1}{2}(\hat{a}_1^{\dagger}\hat{a}_1 + \hat{a}_2^{\dagger}\hat{a}_2)$ and the angular momentum operator $\hat{L}_x = \frac{1}{2}(\hat{a}_2^{\dagger}\hat{a}_1 + \hat{a}_1^{\dagger}\hat{a}_2)$, namely

$$\hat{B}_{12} = \hat{L}_0 - \hat{L}_x. \tag{8.35}$$

Since the application of any linear optics (passive) transformation does not change the total number of photons, $\hat{L}_0$ is unaffected by such a transformation. In contrast, $\hat{L}_x$ can be turned by an appropriate linear optics transformation into L_z, which corresponds to the difference of the photon numbers between the two modes. Indeed, following Ref. [125], we apply a 50:50 beam splitter, which transforms the mode operators according to

$$\hat{a}_1 = \frac{\hat{a}_1' + \hat{a}_2'}{\sqrt{2}}, \qquad \hat{a}_2 = \frac{\hat{a}_1' - \hat{a}_2'}{\sqrt{2}}, \tag{8.36}$$

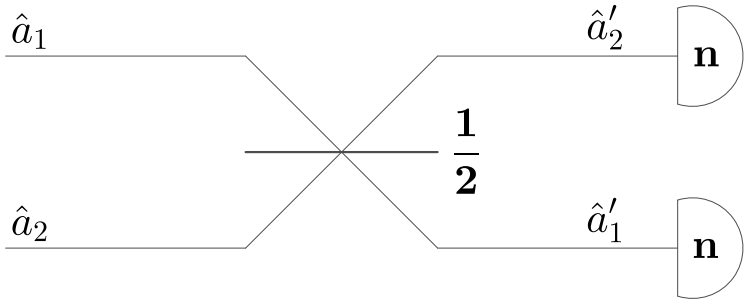

Figure 8.5: Implementation to measure the value of d_{12}. We first apply a balanced beam-splitter (transmittance $\tau = 1/2$) and then we use a photon number resolving detector on the second mode only.

so that $\hat{L}_x$ transforms into $\hat{L}'_z = \frac{1}{2}(\hat{a}_1'^{\dagger}\hat{a}'_1 - \hat{a}_2'^{\dagger}\hat{a}'_2)$, where the primes refer to mode operators after the beam splitter. Hence, the operator $\hat{B}_{12}$ is transformed into

$$\hat{B}_{12} = \hat{L}_0 - \hat{L}'_z = \frac{1}{2}(\hat{n}'_1 + \hat{n}'_2 - \hat{n}'_1 + \hat{n}'_2) = \hat{n}'_2, \tag{8.37}$$

where $\hat{n}'_1 = \hat{a}_1'^{\dagger}\hat{a}'_1$ and $\hat{n}'_2 = \hat{a}_2'^{\dagger}\hat{a}'_2$.

This implies that measuring the mean photon number in the second mode after the beam splitter transformation of Fig. 8.5 gives the value of the determinant

$$d_{12} = \langle\langle \hat{B}_{12}\rangle\rangle = \langle \hat{n}'_2\rangle. \tag{8.38}$$

Obviously, we have $d_{12} \geq 0$, so that d_{12} does not yield a useful criterion to detect nonclassical states. It is trivial to understand from Eq. (8.36) that this scheme gives access to the thermal (or chaotic) photon number since the coherent component of the two identical input states is concentrated on the first output mode $\hat{a}'_1$, while the mean field vanishes in the second output mode $\hat{a}'_2$. The latter is then only populated by the thermal photons.

Before moving to principal minors that are actually useful to detect nonclassicality, let us briefly consider the next case in Table 8.1, namely

$$d_{14} = \begin{vmatrix} 1 & \langle \hat{a}^2\rangle \\ \langle \hat{a}^{\dagger 2}\rangle & \langle \hat{a}^{\dagger 2}\hat{a}^2\rangle \end{vmatrix} = \langle \hat{a}^{\dagger 2}\hat{a}^2\rangle - \langle \hat{a}^2\rangle\langle \hat{a}^{\dagger 2}\rangle. \tag{8.39}$$

By building the corresponding two-copy observable, it is straightforward to check

that $d_{14} \geq 0$ so it is useless for nonclassicality detection. Indeed, we have

$$\begin{aligned}\hat{B}_{14} &= \frac{1}{|S_2|}\sum_{\sigma\in S_2}\begin{vmatrix} 1 & \hat{a}^2_{\sigma(1)} \\ \hat{a}^{\dagger 2}_{\sigma(2)} & \hat{a}^{\dagger 2}_{\sigma(2)}\hat{a}^2_{\sigma(2)}\end{vmatrix}, \\ &= \frac{1}{2}(\hat{a}^{\dagger 2}_1\hat{a}^2_1 + \hat{a}^{\dagger 2}_2\hat{a}^2_2 - \hat{a}^{\dagger 2}_2\hat{a}^2_1 - \hat{a}^{\dagger 2}_1\hat{a}^2_2),\end{aligned} \tag{8.40}$$

In analogy with Eq. (8.35), this two-copy observable can be reexpressed in terms of angular momentum operators, namely

$$\hat{B}_{14} = 2\,(\hat{L}^2_0 - \hat{L}^2_x). \tag{8.41}$$

As before, we may transform $\hat{L}_x$ into $\hat{L}'_z$ by using a 50:50 beam splitter as described in Eq. (8.36), which gives

$$\hat{B}_{14} = 2\,(\hat{L}^2_0 - \hat{L}'^2_z) = 2\,\hat{n}'_1\hat{n}'_2. \tag{8.42}$$

Thus, this determinant can be accessed by applying a 50:50 beam splitter on the two identical copies as in Fig. 8.5 and then measuring the mean value of the product of the photon numbers, that is

$$d_{14} = \langle\langle \hat{B}_{14}\rangle\rangle = 2\,\langle \hat{n}'_1\hat{n}'_2\rangle \geq 0. \tag{8.43}$$

In the following, we apply the same technique to determinants that enable the detection of nonclassicality. The calculations follow exactly the same path: we assign a mode to each row of the operator matrix and then symmetrize it as in Eq. (8.33) or (8.40). Finally, whenever possible, we find a linear optics transformation such that the observable can be measured by means of photon number resolving detectors. Since the difficulty of this procedure increases with the number of copies, we limit our search to matrices of moments up to dimension $N = 5$.

Detection of squeezed states: d_{23}

As shown in Table 8.1, the two most interesting principal submatrices of dimension 2×2 for detecting nonclassical states are d_{23} and d_{15}. We start with d_{23}, expressed as

$$d_{23} = \begin{vmatrix} \langle \hat{a}^\dagger\hat{a}\rangle & \langle \hat{a}^{\dagger 2}\rangle \\ \langle \hat{a}^2\rangle & \langle \hat{a}^\dagger\hat{a}\rangle \end{vmatrix} = \langle \hat{a}^\dagger\hat{a}\rangle^2 - \langle \hat{a}^2\rangle\langle \hat{a}^{\dagger 2}\rangle. \tag{8.44}$$

The criterion derived from d_{23} detects squeezed states and even cat states (it does not detect Fock states and odd cat states). Note that d_{23} is not invariant under displacements (as we shall see, this invariance can be enforced by considering d_{123} instead).

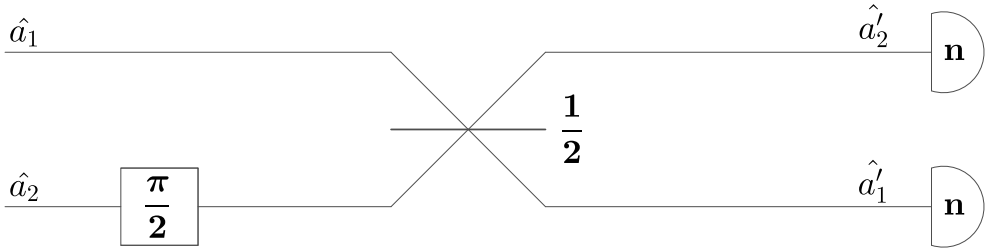

Figure 8.6: Implementation to measure the value of d_{23}. We first apply a phase of phase $\pi/2$ and then a balanced beam splitter of transmittance $\tau = 1/2$. Hence, the criteria can be evaluated by measuring the number of photons in both modes according to Eq.(8.50).

Following the procedure described in Sec. 8.4.2, we obtain the multicopy observable

$$\begin{aligned}\hat{B}_{23} &= \frac{1}{|S_2|}\sum_{\sigma\in S_2}\begin{vmatrix}\hat{a}^\dagger_{\sigma(1)}\hat{a}_{\sigma(1)} & \hat{a}^{\dagger 2}_{\sigma(1)}\\ \hat{a}^2_{\sigma(2)} & \hat{a}^\dagger_{\sigma(2)}\hat{a}_{\sigma(2)}\end{vmatrix},\\ &= \hat{a}^\dagger_1\hat{a}_1\hat{a}^\dagger_2\hat{a}_2 - \frac{1}{2}\left(\hat{a}^{\dagger 2}_1\hat{a}^2_2 + \hat{a}^{\dagger 2}_2\hat{a}^2_1\right).\end{aligned} \tag{8.45}$$

Similarly as for $\hat{B}_{12}$ or $\hat{B}_{14}$, we can express $\hat{B}_{23}$ in terms of the angular momentum operator $\hat{L}_y = \frac{i}{2}(\hat{a}^\dagger_2\hat{a}_1 - \hat{a}^\dagger_1\hat{a}_2)$ and the Casimir operator $\hat{L}_0$, namely

$$\hat{B}_{23} = 2\,\hat{L}^2_y - \hat{L}_0. \tag{8.46}$$

It must be noted that Eq. (8.46) can also be reexpressed more concisely as an operator in normally ordered form, namely

$$\hat{B}_{23} = 2\ :L^2_y: \tag{8.47}$$

where the normal ordering symbol must be understood term by term, that is, we must expand L^2_y in power series in $\hat{a}$ and $\hat{a}^\dagger$ and then normally order each term.

Using Eq. (8.46), we may design a linear interferometer in order to measure $\hat{B}_{23}$ by means of photon-number resolving detection. We consider the same interferometer as considered in Ref. [125], which is composed of a $\pi/2$ phase shifter on the second mode followed by a 50:50 beam splitter as shown in Fig. 8.6. Under the $\pi/2$ local phase shift, the second mode operator transforms according to

$$\hat{a}_2 = i\,\hat{a}'_2, \tag{8.48}$$

while the 50:50 beam splitter transformation is described in Eq. (8.36). The Casimir operator $\hat{L}_0$ is invariant under these operations, but $\hat{L}_y$ transforms into $\hat{L}_x$ following the phase shifter on the second mode and then transforms into $\hat{L}'_z$ after the 50:50 beam splitter. Hence, after applying the interferometer shown in Fig. 8.6, the non-

classicality observable takes the form

$$\begin{aligned}\hat{B}_{23} &= 2\,\hat{L}_z'^2 - \hat{L}_0 \\ &= \frac{1}{2}(\hat{n}_1' - \hat{n}_2')^2 - \frac{1}{2}(\hat{n}_1' + \hat{n}_2'),\end{aligned} \tag{8.49}$$

and its expectation value yields

$$\begin{aligned}d_{23} &= 2\langle \hat{L}_z'^2 \rangle - \langle \hat{L}_0 \rangle \\ &= \left\langle \frac{1}{2}(\hat{n}_1' - \hat{n}_2')^2 - \frac{1}{2}(\hat{n}_1' + \hat{n}_2') \right\rangle .\end{aligned} \tag{8.50}$$

As a consequence, the principal minor d_{23} can be evaluated simply by accessing the photon number statistics on the two output modes $\hat{a}_1'$ and $\hat{a}_2'$.

It is instructive to understand how the nonclassicality of a squeezed state is detected by Eq. (8.50). Two copies of a squeezed state are transformed through the interferometer of Fig. 8.6 as follows. The phase shift rotates the second squeezed states by $\pi/2$, and the 50:50 beam splitter produces (from the original and rotated squeezed states) a two-mode squeezed vacuum (TMSV) state, $\sum_{n=0}^{\infty}(\tanh r)^n/\cosh r\,|n,n\rangle$. This state exhibits a perfect photon-number correlation. Hence, the squared photon-number difference in Eq. (8.50) vanishes while the second term, which is proportional to the sum of photon numbers, comes with a negative sign. Thus, squeezed states are detected as nonclassical with $d_{23} < 0$ as soon as $r > 0$.

Note that Eq. (8.50) can also be reformulated as

$$d_{23} = \frac{1}{2}\left(Q_1'\langle \hat{n}_1' \rangle + Q_2'\langle \hat{n}_2' \rangle + \langle \hat{n}_1' \rangle^2 + \langle \hat{n}_2' \rangle^2 - 2\langle \hat{n}_1'\hat{n}_2' \rangle\right), \tag{8.51}$$

where Q_1' and Q_2' denote the Mandel Q-parameter of the state on modes $\hat{a}_1'$ and $\hat{a}_2'$, defined as

$$Q = \frac{(\Delta\hat{n})^2 - \langle n \rangle}{\langle n \rangle}, \tag{8.52}$$

which measures the "Poissonianity" of the state (it vanishes for a coherent state, associated with a Poisson distribution). If the input state is a coherent state, it is transformed under the interferometer of Fig. 8.6 into a product of two coherent states, hence $Q_1' = Q_2' = 0$. Further, $\langle \hat{n}_1' \rangle^2 = \langle \hat{n}_2' \rangle^2 = \langle \hat{n}_1'\hat{n}_2' \rangle$ since the two coherent states are independent and have equal squared amplitudes. This confirms that $d_{23} = 0$ for coherent states.

Detection of Fock states: d_{15}

The criterion based on d_{15} is complementary to the one based on d_{23} as it detects Fock states and odd cat states (it does not detect squeezed states and even cat states). It is

defined as

$$d_{15} = \begin{vmatrix} 1 & \langle \hat{a}^\dagger \hat{a} \rangle \\ \langle \hat{a}^\dagger \hat{a} \rangle & \langle \hat{a}^{\dagger 2} \hat{a}^2 \rangle \end{vmatrix} = \langle \hat{a}^{\dagger 2} \hat{a}^2 \rangle - \langle \hat{a}^\dagger \hat{a} \rangle^2. \tag{8.53}$$

and is not invariant under displacements (just as d_{23}). It can be rewritten as

$$d_{15} = \langle \hat{n}^2 \rangle - \langle \hat{n} \rangle^2 - \langle \hat{n} \rangle = (\Delta \hat{n})^2 - \langle n \rangle. \tag{8.54}$$

and can thus be reexpressed in terms of the Mandel Q-parameter of the input state as

$$d_{15} = Q \langle n \rangle, \tag{8.55}$$

so that the nonclassicality criterion based on d_{15} is simply a witness of the sub-Poissonian statistics ($Q < 0$) of the state. Obviously, we have $d_{15} = 0$ for coherent states while $d_{15} > 0$ for (classical) thermal states, as expected.

The procedure described in Sec. 8.4.2 yields the following two-copy nonclassicality observable

$$\hat{B}_{15} = \frac{1}{2}(\hat{n}_2 - \hat{n}_1)^2 - \frac{1}{2}(\hat{n}_1 + \hat{n}_2), \tag{8.56}$$

whose expectation value is written as

$$d_{15} = \left\langle \frac{1}{2}(\hat{n}_2 - \hat{n}_1)^2 - \frac{1}{2}(\hat{n}_1 + \hat{n}_2) \right\rangle. \tag{8.57}$$

Interestingly, d_{15} involves a similar observable as the one used to measure d_{23} [see Eq. (8.50)] except that we do not need a prior interferometer. This similarity will be exploited in the next section.

Interpolation between d_{23} and d_{15}

As we observe in Table 8.1, the criteria d_{23} and d_{15} taken together detect the four considered kinds of pure states. Given the similarity between Eq. (8.50) and (8.57), it is tempting to construct a common multicopy observable that interpolates between d_{23} and d_{15}. It is based on a linear optical interferometer composed of a phase shifter of phase ϕ and a beam splitter of transmittance τ (see Fig. 8.7), followed by the measurement of the observable

$$\hat{B}_{15,23} = \frac{1}{2}(\hat{n}_2' - \hat{n}_1')^2 - \frac{1}{2}(\hat{n}_1' + \hat{n}_2'), \tag{8.58}$$

where the primes refer to output modes. By applying the interferometer of Fig. 8.7 backwards on Eq. (8.58), we may reexpress it as a function of the input mode opera-

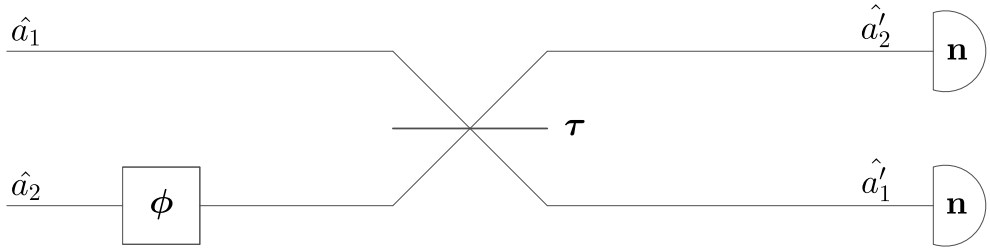

Figure 8.7: General two-mode scheme made of linear optics and photodetectors to detect nonclassicalities. By using photon number detection, we only need one phase shifter of phase ϕ and one beam splitter of transmittance τ.

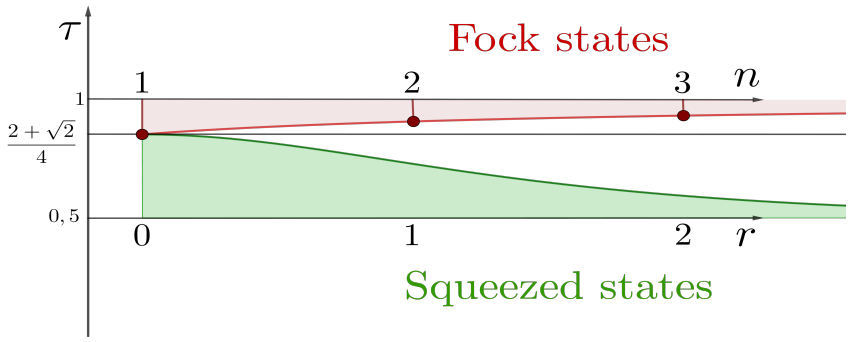

Figure 8.8: Detection limit of the transmittance as a function of the characteristic parameter of the state. The red area correspond to parameters values where Fock states are detected and the green region correspond to the region where squeezed states are detected. The phase is fixed to $\phi = \pi/2$.

tors, namely

$$\begin{aligned}\hat{B}_{15,23} =& \frac{1}{2}[(\hat{a}_2^\dagger \hat{a}_1\, e^{-i\phi} + \hat{a}_1^\dagger \hat{a}_2\, e^{i\phi})\, 2\sqrt{(1-\tau)\tau} \\ &+ (\hat{a}_1^\dagger \hat{a}_1 - \hat{a}_2^\dagger \hat{a}_2)\,(-1+2\tau)]^2.\end{aligned} \tag{8.59}$$

This observable clearly interpolates between $\hat{B}_{15}$ ($\tau = 1$) and $\hat{B}_{23}$ ($\phi = \pi/2$ and $\tau = 1/2$). Since Eq. (8.59) is the square of a Hermitian operator, $\hat{B}_{15,23}$ can be written under the form $:\hat{f}^\dagger \hat{f}:$, and is indeed a valid observable witnessing nonclassicality.

We start by setting the phase shift to $\phi = \pi/2$ as it does not play any role in $\hat{B}_{15}$ and study the detection of the different types of nonclassical states as a function of the transmittance τ (with $1/2 \leq \tau \leq 1$), see Fig. 8.8. It appears that all Fock states $|n\rangle$ with $n \geq 1$ are detected when the transmittance is above a threshold value $\tau^* = (2+\sqrt{2})/4$, while all squeezed states with $r > 0$ are detected only for values of the transmittance lower than this threshold τ^*. The value of τ^* is such that the coefficients of the two operators terms in Eq. (8.59) are equal. Moreover, it is possible to show that the odd cat states are always detected when $\tau > \tau^*$ while the

even cat states are always detected when $\tau < \tau^*$. This means that there is no value of the transmittance enabling the detection of the four classes of nonclassical states considered in Table 8.1. Unfortunately, changing the value of the phase shift ϕ does not change the situation, so we cannot find a single 2-copy observable that detects all four classes of nonclassical states.

Note that the criteria based on d_{23} and d_{15} can be viewed as complementary: if one of them detects a nonclassical state, i.e., its value is negative, then the other one is necessarily positive for that state (of course, they can be both positive as, for example, for classical states). Indeed, we have

$$d_{23} + d_{15} = d_{14} \geq 0 \tag{8.60}$$

where the inequality comes from Eq. (8.43). Hence, the witnesses d_{23} and d_{15} never detect nonclassicality simultaneously for a given state, as illustrated for a superposition of three Fock states in the next section.

Example of the complementarity of d_{15} and d_{23}

As observed in Table 8.1 and on Fig. 8.8, d_{15} and d_{23} play a complementary role (see (8.60)). Indeed, any benchmark pure states that were studied are never detected by both d_{15} and d_{23}. In order to insist on this fact, we will study a pure state that is the superposition of $|0\rangle$, $|1\rangle$ and $|2\rangle$ Fock states :

$$|\psi_{012}\rangle = \alpha|0\rangle + \beta|1\rangle + \gamma|2\rangle, \tag{8.61}$$

where $|\alpha|^2 + |\beta|^2 + |\gamma|^2 = 1$ for normalisation. We can restrict ourselve to only the norm of the coefficients, $|\alpha| = a$, $|\beta| = b$ and $|\gamma| = c$ and replace $a = \sqrt{1 - b^2 - c^2}$.

First, in the case where $c = 0$ in Eq. (8.61), meaning that we have a superposition of $|0\rangle$ and $|1\rangle$ Fock state only, the determinant d_{23} is always positive (since $\langle \hat{a}^{\dagger 2} \rangle = \langle \hat{a}^2 \rangle = 0$) while d_{15} is at least negative the state reduces to $|1\rangle$. In fact, $d_{15} \leq 0$ for all superposition of the vacuum and Fock state $|1\rangle$.

Second, in the case where $b = 0$ in Eq. (8.61), meaning that we have a superposition of $|0\rangle$ and $|2\rangle$ Fock state only, the answer is more subtle.

Effect of a displacement on d_{23} and d_{15}

In general, we expect that the nonclassical character of a quantum state will be harder to detect when the state is moved away from the origin in phase space. As we shall see, this is often (but not always) the case. We can calculate the difference between the determinant when the state is displaced by $\hat{D}(\alpha)$ with $\alpha = |\alpha|e^{i\theta_\alpha}$ and the determinant

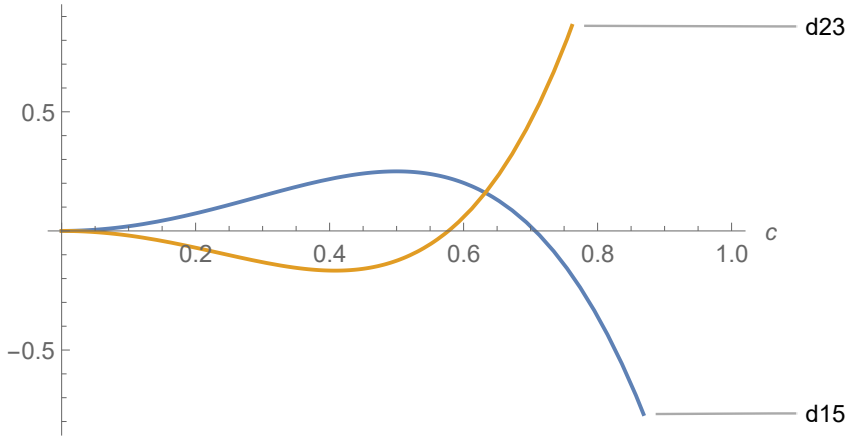

Figure 8.9: Comparison of the values of d_{15} and d_{23} for a superposition of $|0\rangle$ and $|2\rangle$ Fock states. Remarkably, the two criteria does not detects nonclassicality simultaneously. This supports the idea of complementarity of d_{15} and d_{23}.

State	$\Delta^\alpha = d_{15}^\alpha - d_{15}$
Squeezed	$\Delta^\alpha = 2\sinh(r)\|\alpha\|^2(\cosh(r)\cos(2\theta_\alpha - \psi) + \sinh(r))$
Fock	$\Delta^\alpha = 2n\|\alpha\|^2$
Even cat	$\Delta^\alpha = 2\|\alpha\|^2\|\beta\|^2(\frac{N_-}{N_+} - \cos(2\theta_\alpha - 2\theta_\beta))$
Odd cat	$\Delta^\alpha = 2\|\alpha\|^2\|\beta\|^2(\cos(2\theta_\alpha - 2\theta_\beta) + \frac{N_+}{N_-})$

Table 8.4: Effect of displacement. Difference between the determinant when the state is displaced and when it is not for the squeezed states, Fock states, even cat states and odd cat states.

when it is centered. The differences are presented in Table 8.4 for the different kinds of states.

For Fock states as well as odd cat states, the effect of a displacement on d_{15} is given by an extra positive factor Δ^α, so that displacements always deteriorate the detection. For squeezed states as well as even cat states, the result of a displacement on d_{23} is that it can either enhance ($\Delta^\alpha < 0$) or deteriorate ($\Delta^\alpha > 0$) the detection of nonclassicality. Indeed, the sign of Δ^α will depend on the difference between the angle of squeezing ψ (or the angle of the cat state θ_β) and the angle of the displacement θ_α.

8.4.3 Three-copy observables

As we have observed in Sec. 8.4.2, the two-mode criteria d_{23} and d_{15} are not invariant under displacement. This comes with the fact that some nonclassical states become undetected if they are displaced in phase space. In order to overcome this effect of displacements, we build an observable involving an extra copy, following a similar reasoning as in Ref. [125]. With three copies, we start by applying a transformation that concentrates the coherent component of the input states in the first mode, which

is traced out. Then, we apply the same scheme as for d_{23} but on the second and third modes, which leads the following observable

$$\hat{B}_{123} = \frac{1}{2}(\hat{n}'_2 - \hat{n}'_3)^2 - \frac{1}{2}(\hat{n}'_2 + \hat{n}'_3). \tag{8.62}$$

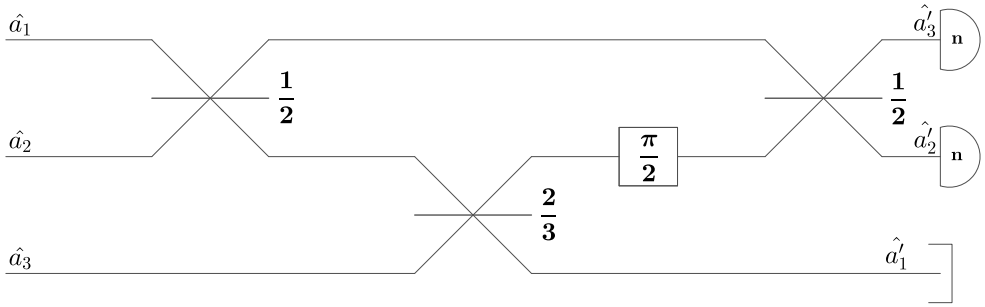

Figure 8.10: Three-mode circuit of d_{123} to detect nonclassicalities. This corresponds to the d_{23} implementation preceded by two beam splitter of transmittance $\tau_{12} = 1/2$ and $\tau_{13} = 2/3$. The role of these beam splitters is to concentrate the coherent part of the input states to the mode 1.

Up to a mode relabelling, the operator in Eq. (8.62) is thus the same as the one used for evaluating d_{23}, see Eq. (8.50). The corresponding circuit is shown in Fig. 8.10 and leads to the d_{123} criteria. Interestingly, the exact same circuit was used by in Ref. [125] in order to measure an uncertainty observable; the difference here is the measured observable at the output of the circuit.

The three-copy observable $\hat{B}_{123}$ can also be found by using the same procedure as described in Sec. 8.4.2 for two copies. Indeed, from the explicit form of d_{123}, namely

$$\begin{aligned} d_{123} &= \begin{vmatrix} 1 & \langle\hat{a}\rangle & \langle\hat{a}^\dagger\rangle \\ \langle\hat{a}^\dagger\rangle & \langle\hat{a}^\dagger\hat{a}\rangle & \langle\hat{a}^{\dagger 2}\rangle \\ \langle\hat{a}\rangle & \langle\hat{a}^2\rangle & \langle\hat{a}^\dagger\hat{a}\rangle \end{vmatrix}, \\ &= \langle\hat{a}^\dagger\hat{a}\rangle^2 - \langle\hat{a}^{\dagger 2}\rangle\langle\hat{a}^2\rangle - 2\langle\hat{a}^\dagger\rangle\langle\hat{a}\rangle\langle\hat{a}^\dagger\hat{a}\rangle \\ &\quad + \langle\hat{a}^{\dagger 2}\rangle\langle\hat{a}\rangle^2 + \langle\hat{a}^\dagger\rangle^2\langle\hat{a}^2\rangle, \end{aligned} \tag{8.63}$$

we get the three-copy observable

$$\begin{aligned}\hat{B}_{123} &= \frac{1}{|S_3|}\sum_{\sigma\in S_3}\begin{vmatrix} 1 & \hat{a}_{\sigma(1)} & \hat{a}^\dagger_{\sigma(1)} \\ \hat{a}^\dagger_{\sigma(2)} & \hat{a}^\dagger_{\sigma(2)}\hat{a}_{\sigma(2)} & \hat{a}^{\dagger 2}_{\sigma(2)} \\ \hat{a}_{\sigma(3)} & \hat{a}^2_{\sigma(3)} & \hat{a}^\dagger_{\sigma(3)}\hat{a}_{\sigma(3)} \end{vmatrix} \\ &= \frac{1}{3}\left(\hat{a}_2^\dagger\hat{a}_2\hat{a}_3^\dagger\hat{a}_3 + \hat{a}_1^\dagger\hat{a}_1\hat{a}_3^\dagger\hat{a}_3 + \hat{a}_1^\dagger\hat{a}_1\hat{a}_2^\dagger\hat{a}_2\right) \\ &- \frac{1}{6}(\hat{a}_2^{\dagger 2}\hat{a}_3^2 + \hat{a}_2^2\hat{a}_3^{\dagger 2} + \hat{a}_1^{\dagger 2}\hat{a}_3^2 + \hat{a}_1^2\hat{a}_3^{\dagger 2} + \hat{a}_1^{\dagger 2}\hat{a}_2^2 + \hat{a}_1^2\hat{a}_2^{\dagger 2}) \\ &- \frac{1}{3}(\hat{a}_1^\dagger\hat{a}_1\hat{a}_2^\dagger\hat{a}_3 + \hat{a}_1^\dagger\hat{a}_1\hat{a}_2\hat{a}_3^\dagger + \hat{a}_1\hat{a}_2^\dagger\hat{a}_2\hat{a}_3^\dagger \\ &\quad + \hat{a}_1^\dagger\hat{a}_2^\dagger\hat{a}_2\hat{a}_3 + \hat{a}_1\hat{a}_2^\dagger\hat{a}_3^\dagger\hat{a}_3 + \hat{a}_1^\dagger\hat{a}_2\hat{a}_3^\dagger\hat{a}_3) \\ &+ \frac{1}{3}\left(\hat{a}_1^{\dagger 2}\hat{a}_2\hat{a}_3 + \hat{a}_1\hat{a}_2^{\dagger 2}\hat{a}_3 + \hat{a}_1\hat{a}_2\hat{a}_3^{\dagger 2}\right) \\ &+ \frac{1}{3}\left(\hat{a}_1^2\hat{a}_2^\dagger\hat{a}_3^\dagger + \hat{a}_1^\dagger\hat{a}_2^2\hat{a}_3^\dagger + \hat{a}_1^\dagger\hat{a}_2^\dagger\hat{a}_3^2\right).\end{aligned} \tag{8.64}$$

It is straightforward to check from Eq. (8.64) that the mean value of $\hat{B}_{123}$ over three identical copies gives

$$\langle\langle \hat{B}_{123}\rangle\rangle = d_{123}. \tag{8.65}$$

Interestingly, the nonclassicality observable $\hat{B}_{123}$ can also be written in a much more compact form by using the normally ordered expression

$$\hat{B}_{123} = :\frac{2}{3}\left(\hat{L}_y^{12} + \hat{L}_y^{23} + \hat{L}_y^{31}\right)^2:, \tag{8.66}$$

where $\hat{L}_y^{kl} = \frac{i}{2}(\hat{a}_l^\dagger\hat{a}_k - \hat{a}_k^\dagger\hat{a}_l)$.

After applying the unitary presented on figure 8.10, $\hat{B}_{123}$ transforms into :

$$\hat{B}'_{123} = \frac{1}{2}(\hat{n}_2 - \hat{n}_3)^2 - \frac{1}{2}(\hat{n}_2 + \hat{n}_3). \tag{8.67}$$

Another option is to apply the DFT on the three copies input observable $\hat{B}_{123}$, this leads to the same output observable. d_{123} presents an advantage with respect to d_{23} as it is invariant by displacement.

We have introduced d_{123} as the displacement invariant version of d_{23}. However, the criteria d_{123} is also superior as it is able to detect states that are different from displaced states detected by d_{23}. The easiest example is the superposition of the two Fock states $|0\rangle$ and $|1\rangle$ given in Eq. (8.61) with $c = 0$. The values of d_{15}, d_{23} and d_{123} are plotted in Fig. 8.11. We see, that while d_{23} never detects any such superposition, d_{123} detects superpositions of the two first Fock states up to $b = 0.7$. Moreover, d_{15} detects all superposition of the vacuum with Fock state $|1\rangle$.

More general example of states detected by d_{123} but not by d_{23} can be found by look-

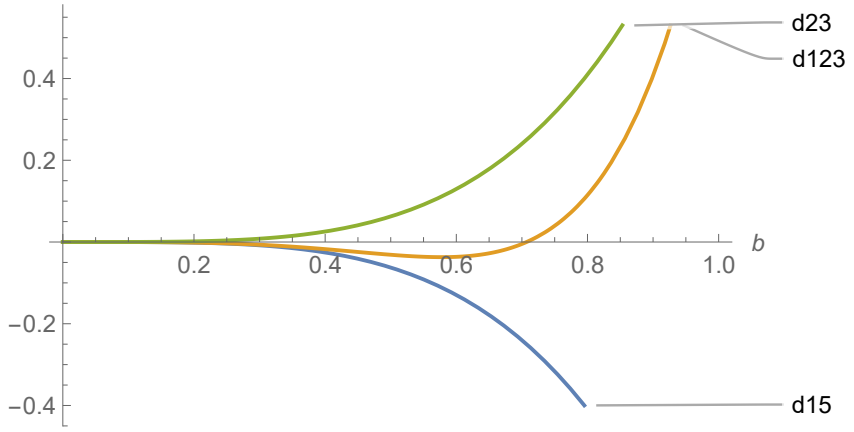

Figure 8.11: Comparison of the values of d_{123} and d_{23} for a superposition of $|0\rangle$ and $|1\rangle$ Fock states. While d_{23} never detects any such superposition, d_{123} detects superpositions of the two first Fock states up to $b = 0.7$.

ing to arbitrary superpositions of the type of Eq. (8.61).

8.4.4 Four-copy observables

The d_{1235} criteria for nonclassicality

The most promising criteria derived from a 4×4 matrix is certainly d_{1235} since it detects the nonclassicality of all squeezed, Fock and cat states (see table 8.1). Hence, we will study his structure in more details in this section.

$$d_{1235} = \begin{vmatrix} 1 & \langle \hat{a} \rangle & \langle \hat{a}^\dagger \rangle & \langle \hat{a}^\dagger \hat{a} \rangle \\ \langle \hat{a}^\dagger \rangle & \langle \hat{a}^\dagger \hat{a} \rangle & \langle \hat{a}^{\dagger 2} \rangle & \langle \hat{a}^{\dagger 2} \hat{a} \rangle \\ \langle \hat{a} \rangle & \langle \hat{a}^2 \rangle & \langle \hat{a}^\dagger \hat{a} \rangle & \langle \hat{a}^\dagger \hat{a}^2 \rangle \\ \langle \hat{a}^\dagger \hat{a} \rangle & \langle \hat{a}^\dagger \hat{a}^2 \rangle & \langle \hat{a}^{\dagger 2} \hat{a} \rangle & \langle \hat{a}^{\dagger 2} \hat{a}^2 \rangle \end{vmatrix}. \tag{8.68}$$

We start by considering the multicopy technique used for deriving physical implementation for the 2- and 3-copy nonclassicality observables. Hence, we write the multimode operator $\hat{B}_{1235}$ by assigning a different mode to each matrix lines :

$$\hat{B}_{1235} = \frac{1}{|S_4|} \sum_{\sigma \in S_4} \begin{vmatrix} 1 & \hat{a}_{\sigma(1)} & \hat{a}^\dagger_{\sigma(1)} & \hat{a}^\dagger_{\sigma(1)} \hat{a}_{\sigma(1)} \\ \hat{a}^\dagger_{\sigma(2)} & \hat{a}^\dagger_{\sigma(2)} \hat{a}_{\sigma(2)} & \hat{a}^{\dagger 2}_{\sigma(2)} & \hat{a}^{\dagger 2}_{\sigma(2)} \hat{a}_{\sigma(2)} \\ \hat{a}_{\sigma(3)} & \hat{a}^2_{\sigma(3)} & \hat{a}^\dagger_{\sigma(3)} \hat{a}_{\sigma(3)} & \hat{a}^\dagger_{\sigma(3)} \hat{a}^2_{\sigma(3)} \\ \hat{a}^\dagger_{\sigma(4)} \hat{a}_{\sigma(4)} & \hat{a}^\dagger_{\sigma(4)} \hat{a}^2_{\sigma(4)} & \hat{a}^{\dagger 2}_{\sigma(4)} \hat{a}_{\sigma(4)} & \hat{a}^{\dagger 2}_{\sigma(4)} \hat{a}^2_{\sigma(4)} \end{vmatrix}. \tag{8.69}$$

Hence, by calculating the mean value $\langle\langle \hat{B}_{1235} \rangle\rangle$, it is equal to d_{1235}. The symmetrized operator $\hat{B}_{1235}$ is Hermitian and of the form of : $\hat{f}^\dagger \hat{f}$: where $\hat{f}_{1235}$ is hermitian itself

and writes :

$$\begin{aligned}\hat{f}_{1235} = \frac{-i}{2\sqrt{6}}(&\hat{a}_1^\dagger\hat{a}_1\hat{a}_2^\dagger\hat{a}_3 - \hat{a}_1^\dagger\hat{a}_2^\dagger\hat{a}_2\hat{a}_3 - \hat{a}_1^\dagger\hat{a}_1\hat{a}_2\hat{a}_3^\dagger \\ &+ \hat{a}_1\hat{a}_2^\dagger\hat{a}_2\hat{a}_3^\dagger + \hat{a}_1^\dagger\hat{a}_2\hat{a}_3^\dagger\hat{a}_3 - \hat{a}_1\hat{a}_2^\dagger\hat{a}_3^\dagger\hat{a}_3 \\ &- \hat{a}_1^\dagger\hat{a}_1\hat{a}_2^\dagger\hat{a}_4 + \hat{a}_1^\dagger\hat{a}_2^\dagger\hat{a}_2\hat{a}_4 + \hat{a}_1^\dagger\hat{a}_1\hat{a}_3^\dagger\hat{a}_4 \\ &- \hat{a}_2^\dagger\hat{a}_2\hat{a}_3^\dagger\hat{a}_4 - \hat{a}_1^\dagger\hat{a}_3^\dagger\hat{a}_3\hat{a}_4 + \hat{a}_2^\dagger\hat{a}_3^\dagger\hat{a}_3\hat{a}_4 \\ &+ \hat{a}_1^\dagger\hat{a}_1\hat{a}_2\hat{a}_4^\dagger - \hat{a}_1\hat{a}_2^\dagger\hat{a}_2\hat{a}_4^\dagger - \hat{a}_1^\dagger\hat{a}_1\hat{a}_3\hat{a}_4^\dagger \\ &+ \hat{a}_2^\dagger\hat{a}_2\hat{a}_3\hat{a}_4^\dagger + \hat{a}_1\hat{a}_3^\dagger\hat{a}_3\hat{a}_4^\dagger - \hat{a}_2\hat{a}_3^\dagger\hat{a}_3\hat{a}_4^\dagger \\ &- \hat{a}_1^\dagger\hat{a}_2\hat{a}_4^\dagger\hat{a}_4 + \hat{a}_1\hat{a}_2^\dagger\hat{a}_4^\dagger\hat{a}_4 + \hat{a}_1^\dagger\hat{a}_3\hat{a}_4^\dagger\hat{a}_4 \\ &- \hat{a}_2^\dagger\hat{a}_3\hat{a}_4^\dagger\hat{a}_4 - \hat{a}_1\hat{a}_3^\dagger\hat{a}_4^\dagger\hat{a}_4 + \hat{a}_2\hat{a}_3^\dagger\hat{a}_4^\dagger\hat{a}_4), \\ = \frac{2}{\sqrt{6}}(&\hat{L}_z^{14}\hat{L}_y^{23} + \hat{L}_z^{13}\hat{L}_y^{42} + \hat{L}_z^{12}\hat{L}_y^{34} \\ &+ \hat{L}_z^{24}\hat{L}_y^{31} + \hat{L}_z^{23}\hat{L}_y^{14} + \hat{L}_z^{34}\hat{L}_y^{12}), \\ = \frac{1}{\sqrt{6}}&\sum_{\sigma\in P_4}\hat{L}_z^{\sigma(1)\sigma(2)}\hat{L}_y^{\sigma(3)\sigma(4)},\end{aligned} \tag{8.70}$$

where P_4 is the group of even permutations and the complete observable is $\hat{B}_{1235} =: \hat{f}_{1235}^\dagger\hat{f}_{1235} :$. However, since $\hat{f}_{1235}$ is made of products of non-commuting operators $\hat{L}_z^{ij}$ and $\hat{L}_y^{kl}$ (when at least one of the i, j is equal to one of the k, l), we are not able to find a 4-copy physical implementation in terms of linear optical interferometric elements. Indeed, applying local phase shifts and beam-splitters does not help in bringing all the $\hat{L}_z^{ij}\hat{L}_y^{kl}$ elements into $\hat{L}_z^{ij}$ or $\hat{L}_0^{kl}$.

Indeed, we applied different types of transformations based on the Discrete Fourier Transform whose elements in its matrix representation writes:

$$[DFT(n)]_{jk} = \frac{e^{i2\pi jk/n}}{\sqrt{n}}, \tag{8.71}$$

where n is the dimension of the matrix and i is the imaginary number satisfying $i^2 = -1$. By applying a tensor product of two $DFT(2)$ matrices $DFT(2) \otimes DFT(2)$, one can transform $\hat{f}_{1235}$ into:

$$\hat{f}_{1235} \to \frac{-i}{2\sqrt{6}}(\hat{a}_2^{\dagger 2}(\hat{a}_4^2 - \hat{a}_3^2) + \hat{a}_2^2(\hat{a}_3^{\dagger 2} - \hat{a}_4^{\dagger 2}) + \hat{a}_3^2\hat{a}_4^{\dagger 2} - \hat{a}_3^{\dagger 2}\hat{a}_4^2), \tag{8.72}$$

which is the shortest expression we could find and where the mode "1" does not appear in accordance with the fact that $DFT(2) \otimes DFT(2)$ does concentrate all the coherent part of the states in the first mode and that d_{1235} is invariant under displacement.

Decomposition of the d_{1235} criterion

In order to simplify the problem, we can restrict the study to certain class of states. In some case, it is possible to find a multicopy implementation of d_{1235} by factorizing it and finding implementation for the individual factors.

Determinant properties In order to factorize the determinant d_{1235}, we will be using basic properties of determinants :

1. First, if A^{-1} exists and if A and D are squared matrices, then

$$\det\begin{pmatrix} A & B \\ C & D \end{pmatrix} = \det(A)\det(D - CA^{-1}B). \tag{8.73}$$

2. If A^{-1} and D^{-1} exist, then

$$\det(D - CAB) = \det(A^{-1} - BD^{-1}C)\det(A)\det(D), \tag{8.74}$$

where $A \in \mathbf{M}_{m\times m}$, $D \in \mathbf{M}_{n\times n}$, $B \in \mathbf{M}_{m\times n}$ and $C \in \mathbf{M}_{n\times m}$

These properties will be used in the next sections. Note that a recursion relation on $d_{1\ldots N}$ is derived in section 8.5.

Determinant d_{1235} for centered states First, we consider the case of centered states. Hence, this imposes some restriction on the matrix of moment, namely that $\langle\hat{a}\rangle = \langle\hat{a}^\dagger\rangle = 0$. Hence, under this assumption d_{1235} can be written:

$$d_{1235} = \begin{vmatrix} 1 & 0 & 0 & \langle\hat{a}^\dagger\hat{a}\rangle \\ 0 & \langle\hat{a}^\dagger\hat{a}\rangle & \langle\hat{a}^{\dagger 2}\rangle & \langle\hat{a}^{\dagger 2}\hat{a}\rangle \\ 0 & \langle\hat{a}^2\rangle & \langle\hat{a}^\dagger\hat{a}\rangle & \langle\hat{a}^\dagger\hat{a}^2\rangle \\ \langle\hat{a}^\dagger\hat{a}\rangle & \langle\hat{a}^\dagger\hat{a}^2\rangle & \langle\hat{a}^{\dagger 2}\hat{a}\rangle & \langle\hat{a}^{\dagger 2}\hat{a}^2\rangle \end{vmatrix}. \tag{8.75}$$

By using the method of the cofactors to calculate the determinant, we have:

$$d_{1235} = d_{235} - \langle\hat{a}^\dagger\hat{a}\rangle^2 d_{23}. \tag{8.76}$$

In order to further factorize the determinant d_{235}, we assume the extra constraint that

D_{23} is invertible. Hence:

$$\begin{aligned} d_{1235} &= d_{23}(\langle \hat{a}^{\dagger 2}\hat{a}^2\rangle - \begin{pmatrix}\langle \hat{a}^\dagger \hat{a}^2\rangle & \langle \hat{a}^{\dagger 2}\hat{a}\rangle\end{pmatrix} D_{23}^{-1} \begin{pmatrix}\langle \hat{a}^{\dagger 2}\hat{a}\rangle \\ \langle \hat{a}^\dagger \hat{a}^2\rangle\end{pmatrix}) - \langle \hat{a}^\dagger \hat{a}\rangle^2 d_{23}, \\ &= d_{23}(d_{15} - \begin{pmatrix}\langle \hat{a}^\dagger \hat{a}^2\rangle & \langle \hat{a}^{\dagger 2}\hat{a}\rangle\end{pmatrix} D_{23}^{-1} \begin{pmatrix}\langle \hat{a}^{\dagger 2}\hat{a}\rangle \\ \langle \hat{a}^\dagger \hat{a}^2\rangle\end{pmatrix}). \end{aligned} \tag{8.77}$$

In particular, under the assumption that D_{23} is positive definite and hence $d_{23} > 0$ and that D_{15} is negative definite , then nonclassicality can be detected for sure. Moreover, we see that d_{1235} is stronger than d_{23} and d_{15} since if d_{15} is smaller than the last term in Eq.(8.77), then d_{1235} will detect the state as nonclassical.

By exchanging the role of d_{15} and d_{23}, we find another decomposition for d_{1235}:

$$\begin{aligned} d_{1235} &= d_{23} \det(D_{15} \\ &- \frac{1}{d_{23}} \begin{pmatrix} 0 & 0 \\ 0 & 2\langle \hat{a}^\dagger \hat{a}\rangle\langle \hat{a}^{\dagger 2}\hat{a}\rangle\langle \hat{a}^\dagger \hat{a}^2\rangle - \langle \hat{a}^{\dagger 2}\rangle\langle \hat{a}^\dagger \hat{a}^2\rangle^2 - \langle \hat{a}^2\rangle\langle \hat{a}^{\dagger 2}\hat{a}\rangle^2 \end{pmatrix}). \\ &= d_{23}d_{15} - 2\langle \hat{a}^\dagger \hat{a}\rangle\langle \hat{a}^{\dagger 2}\hat{a}\rangle\langle \hat{a}^\dagger \hat{a}^2\rangle + \langle \hat{a}^{\dagger 2}\rangle\langle \hat{a}^\dagger \hat{a}^2\rangle^2 + \langle \hat{a}^2\rangle\langle \hat{a}^{\dagger 2}\hat{a}\rangle^2 \end{aligned} \tag{8.78}$$

In this case again, we see that d_{1235} is stronger than d_{15} and d_{23} as it can be negative even if d_{15} and d_{23} are both positive.

Finally, in the particular cases of states for which we assume that $\langle \hat{a}^{\dagger 2}\hat{a}\rangle = \langle \hat{a}^\dagger \hat{a}^2\rangle = 0$, we have the simple formula:

$$d_{1235} = d_{15}d_{23}. \tag{8.79}$$

This equality is satisfied for Fock, squeezed and cat states. Hence, a simple concatenation of the implementation of the d_{15} and d_{23} circuits is sufficient to calculate the value of d_{1235}. In section 8.4.4, we give another equivalent writting of $d_{1...N}$ by showing that it can always be rewritten as a covariance type matrix.

d_{1235} as a covariance matrix

Interestingly, the matrix of moments in Eq. (7.23) can be expressed in a covariance-type matrix of lower order. Indeed, by identifying the first line and first column element in Eq.(7.23) as A in Eq.(8.73), we have :

$$d_N = \det(1)\det(D_{23...N} - \mathbf{c}\mathbf{c}^\dagger) = \det(D_{23...N} - \mathbf{c}\mathbf{c}^\dagger). \tag{8.80}$$

where $D_{23...N}$ is the matrix of moments with the first line and column removed and $\mathbf{c}$ is the first column of the matrix of moments d_N with the first line element removed. Hence, since $\hat{D}_{23...N;ij} =: \hat{c}_i\hat{c}_j^\dagger :$, we see that the elements of the reduced

matrix $D_{23...N} - \mathbf{c}\mathbf{c}^\dagger$ can be written as :

$$(D_{23...N} - \mathbf{c}\mathbf{c}^\dagger)_{ij} = \langle : \hat{c}_i \hat{c}_j^\dagger : \rangle - \langle \hat{c}_i \rangle \langle \hat{c}_j^\dagger \rangle, \tag{8.81}$$

which is a covariance matrix in terms of creation and annihilation operators. For example, we can rewrite d_{1235} as a 3×3 covariance matrix :

$$d_{1235} = \begin{vmatrix} \langle \hat{a}^\dagger \hat{a} \rangle - \langle \hat{a}^\dagger \rangle \langle \hat{a} \rangle & \langle \hat{a}^{\dagger 2} \rangle - \langle \hat{a}^\dagger \rangle^2 & \langle \hat{a}^{\dagger 2} \hat{a} \rangle - \langle \hat{a}^\dagger \hat{a} \rangle \langle \hat{a}^\dagger \rangle \\ \langle \hat{a}^2 \rangle - \langle \hat{a} \rangle^2 & \langle \hat{a}^\dagger \hat{a} \rangle - \langle \hat{a}^\dagger \rangle \langle \hat{a} \rangle & \langle \hat{a}^\dagger \hat{a}^2 \rangle - \langle \hat{a} \rangle \langle \hat{a}^\dagger \hat{a} \rangle \\ \langle \hat{a}^\dagger \hat{a}^2 \rangle - \langle \hat{a}^\dagger \hat{a} \rangle \langle \hat{a} \rangle & \langle \hat{a}^{\dagger 2} \hat{a} \rangle - \langle \hat{a}^\dagger \hat{a} \rangle \langle \hat{a}^\dagger \rangle & \langle \hat{a}^{\dagger 2} \hat{a}^2 \rangle - \langle \hat{a}^\dagger \hat{a} \rangle^2 \end{vmatrix}, \tag{8.82}$$

where element of the first line and first column is d_{12}. This re-writing might lead to knew interpretations of the SRV criteria.

8.5 Recursion relation on $d_{1...N}$

Let us consider the case where one has tested all principal matrix of moments criteria up to $d_{1...N}$ without any detection of nonclassicality or a result of zero. This means that $d_{1...n} > 0$ for all $n = 1, ..., N$. Hence, by the Sylvester criterion, the matrix $D_{N\times N}$ is positive definite. What could we say about $d_{1...N+1}$?

First, let us use Eq.(8.73) and the matrix determinant lemma Eq.(8.74) on $d_{1...N+1}$ where $A = D_N$, $D = d = \langle \hat{a}^{\dagger k} \hat{a}^k \rangle$ for some integer k and $B^\dagger = C$ is a column vector, noted $\mathbf{c} = C$:

$$\begin{aligned} d_{1...N+1} &= \det(D_{N\times N}) \det(d - \mathbf{c}^\dagger D_{N\times N}^{-1} \mathbf{c}), \\ &= d_{1...N}(d - \mathbf{c}^\dagger D_{N\times N}^{-1} \mathbf{c}), \end{aligned} \tag{8.83}$$

since $(d - \mathbf{c}^\dagger D_{N\times N}^{-1} \mathbf{c})$ is a scalar. Since $D_{N\times N}$ is positive definite, $D_{N\times N}^{-1}$ is also positive definite and hence $\mathbf{c}^\dagger D_{N\times N}^{-1} \mathbf{c}$ is positive. Therefore, in order to detect a new type of nonclassicality, it suffices to check if the following inequality is violated :

$$(d - \mathbf{c}^\dagger D_{N\times N}^{-1} \mathbf{c}) \geq 0, \tag{8.84}$$

which might be easier to detect in certain favorable cases than considering the whole observable of $d_{1...N+1}$.

8.6 Conclusion and Perspectives

In summary, we have analyzed the nonclassical criteria of the so-called matrix of moments up to dimension $N = 5$ and benchmarked their performances by their ability to detect some well-known and interesting nonclassical states, such as Fock states,

squeezed states and the cat states. We identified the criteria that lead to the detection of nonclassicality in the family of Gaussian states. We give the relation between the moments of photon added and substracted Gaussian states and the moments of the associated Gaussian state.

We also identified some remarkable criteria, d_{15} and d_{23} that are connected to known nonclassical features such as sub-Poissonian photon number statistics or squeezing. For these criteria, we developped the multicopy technique in order to propose multicopy nonclassicality observables that have a physical implementation in terms of linear interferometry and photodetectors. We identified that the criteria d_{123} is invariant under translation and has the same detection performances as d_{23} and proposed a 3-copy implementable nonclassicality criteria.

Finally, we identified the criteria d_{1235} to be very interesting since it can detect all the states detected by d_{15} and d_{23} but also states that cannot be detected neither by d_{15} nor d_{23}. We identified its relation with d_{15} and d_{23} and derived the multicopy observable associated. Finding an implementation in terms of linear interferometry and photon number detectors is pretty challenging and is left as an open problem.

9 | Conclusion

This thesis encompasses three distinct research areas : parameter estimation, separability criteria, and nonclassicality criteria. Each of them has led to an original contribution to the field, as developed in Chapters 4, 6 and 8, respectively. The bonding agent among these three topics is the general approach revolving around quantum phase space, so that the coherence of the thesis lies in the methodology more than in the particular subjects. In all cases, we have strived to develop protocols that have a practical implementation. Specifically, we have proposed a scheme for estimating several continuous variables encoded in multiple coherent states, a scheme for testing the weak realignment criterion, and finally a multi-copy scheme for testing a variety of nonclassicality criteria. These developments systematically exploit the advantages of the phase-space representation of quantum optics, especially the Heisenberg picture and the symplectic formalism, in order to achieve the main goals. The structure of the thesis reflects this approach as we first introduce the basic notions of quantum optics in Part I, then move to parameter estimation in Part II and separability criteria in Part III, and finally address the nonclassicality criteria in Part IV.

In Chapter 4, we provide a proof to the fifteen years old conjecture by S. Iblisdir and N. J. Cerf stating that the optimal way to encode information about two continuous variables in the quadratures of two coherent states consists in using phase-conjugate states. After an experimental verification of their prediction and a first attempt of a proof in 2008, we addressed the problem with the proper tools of quantum parameter estimation theory, namely the quantum Cramér-Rao bound and the Fisher information. We proved that the encoding strategy proposed by Iblisdir and Cerf actually saturates the Cramér-Rao bound for both parameters simultaneously. Moreover, we extended the special case of phase-conjugate states to a larger family of states for which we provide a protocol for optimal parameter estimation. Finally, we generalized this strategy to any number of continuous parameter being encoded in the same number of coherent states and proved that it is sufficient to encode pairs of parameters in pairs of coherent states (and, eventually, an ensemble of three parameters in an ensemble of three coherent states). These work might be extended by providing links with cryptographic primitives such as secret sharing.

In Chapter 6, we provide a comprehensive and pedagogical overview of the so-called realignment separability criterion by reformulating the realignment map in terms of a trace norm. We define a new separability criterion based on the trace instead of the trace norm, which we call the weak realignment criterion. It is generally weaker than the original realignment criterion but we show that the two coincide for a special class of states that we define as Schmidt-symmetric state. While the weak realignment criterion thus detects less entangled states than the original realignment criterion, we provide a physical implementation of the weak realignment map which can be tested directly, without the need to have all knowledge about the state. Moreover, we enhance the detection capability of the weak realignment map by supplementing it with a filtering operation (namely, applying a noiseless attenuator on the noisiest of the two modes of the state) that brings the state closer to a Schmidt-symmetric form. Finally, we illustrate the enhanced performance of the filtration-assisted weak realignment criterion by applying it to different families of states that are commonly encountered in quantum optics. Future directions are to study the ability of the weak realignment criterion to detect entanglement of non-Gaussian states.

In Chapter 8, we review the properties of the matrix of moments of the electromagnetic field. We benchmark the performances of the nonclassicality criteria that can be derived from the minors of this matrix up to dimension 5×5 by considering different classes of nonclassical states, such as the Fock states, the squeezed states or the cat states. We also consider the set of Gaussian (pure or mixed) states and show that only a single nonclassicality criterion is sufficient for identifying all nonclassical states in this set. We then apply the multicopy technique developed by T. Brun in order to define multicopy nonclassicality observables, following a similar line of reasoning as for the definition of uncertainty observables by A. Hertz *et al*. We then propose physically implementable schemes for evaluating the nonclassicality criteria by means of passive interferometry and photon number detectors. In particular, we find two- and three-copy implementations of nonclassicality criteria, and show how a strong nonclassicality criterion could be tested and implemented by a combination of two-copy implementations under some restriction. Finally, we propose relations that allow the detection of nonclassicality for some specific families of non-Gaussian states. Ideally, future work might provide a systematic procedure for an implementable multicopy nonclassicality detection for any relevant minors of the matrix of moments.

Bibliography

[1] M. Arnhem, E. Karpov, and N. J. Cerf, "Optimal Estimation of Parameters Encoded in Quantum Coherent State Quadratures," *Applied Sciences*, vol. 9, p. 4264, Oct. 2019.

[2] A. Hertz, M. Arnhem, A. Asadian, and N. J. Cerf, "Realignment separability criterion assisted with filtration for detecting continuous-variable entanglement," *Physical Review A*, vol. 104, p. 022427, Aug. 2021.

[3] M. Arnhem, C. Griffet, and N. J. Cerf, "Multicopy observables for the detection of optically nonclassical states," p. 17.

[4] N. J. Cerf and S. Iblisdir, "Phase conjugation of continuous quantum variables," *Physical Review A*, vol. 64, p. 032307, Aug. 2001.

[5] O. Rudolph, "Further Results on the Cross Norm Criterion for Separability," *Quantum Information Processing*, vol. 4, pp. 219–239, Aug. 2005.

[6] A. Hertz, O. Oreshkov, and N. J. Cerf, "Multi-copy uncertainty observable inducing a symplectic-invariant uncertainty relation in position and momentum phase space," *Physical Review A*, vol. 100, p. 052112, Nov. 2019.

[7] A. Einstein, "Über einen die Erzeugung und Verwandlung des Lichtes betreffenden heuristischen Gesichtspunkt," *Annalen der Physik*, vol. 322, no. 6, pp. 132–148, 1905.

[8] M. Planck, "On the Law of the Energy Distribution in the Normal Spectrum," *Annalen der Physik*, vol. 4, no. 561, 1901.

[9] Arons, A. B. , Peppard M. B., "Einstein's Proposal of the Photon Concept—a Translation of the Annalen der Physik Paper of 1905," *American Journal of Physics*, vol. 33, no. 367, 1965.

[10] R. J. Glauber, "The Quantum Theory of Optical Coherence," *Physical Review*, vol. 130, pp. 2529–2539, June 1963.

[11] J. F. Clauser and A. Shimony, "Bell's theorem. Experimental tests and implications," *Reports on Progress in Physics*, vol. 41, pp. 1881–1927, Dec. 1978.

[12] A. Aspect, P. Grangier, and G. Roger, "Experimental Realization of Einstein-Podolsky-Rosen-Bohm *Gedankenexperiment* : A New Violation of Bell's Inequalities," *Physical Review Letters*, vol. 49, pp. 91–94, July 1982.

[13] A. Einstein, B. Podolsky, and N. Rosen, "Can Quantum-Mechanical Description of Physical Reality Be Considered Complete?," *Physical Review*, vol. 47, pp. 777–780, May 1935.

[14] C. H. Bennett and G. Brassard, "Quantum cryptography: Public key distribution and coin tossing," *Theoretical Computer Science*, vol. 560, pp. 7–11, Dec. 2014.

[15] P. R. Tapster, J. G. Rarity, and P. C. M. Owens, "Violation of Bell's Inequality over 4 km of Optical Fiber," *Physical Review Letters*, vol. 73, pp. 1923–1926, Oct. 1994.

[16] P. W. Shor, "POLYNOMIAL-TIME ALGORITHMS FOR PRIME FACTORIZATION AND DISCRETE LOGARITHMS ON A QUANTUM COMPUTER," p. 27.

[17] L. K. Grover, "Quantum Mechanics Helps in Searching for a Needle in a Haystack," *Physical Review Letters*, vol. 79, pp. 325–328, July 1997.

[18] C. W. Helstrom, "Quantum detection and estimation theory," p. 22.

[19] Y.-A. Chen, Q. Zhang, T.-Y. Chen, W.-Q. Cai, S.-K. Liao, J. Zhang, K. Chen, J. Yin, J.-G. Ren, Z. Chen, S.-L. Han, Q. Yu, K. Liang, F. Zhou, X. Yuan, M.-S. Zhao, T.-Y. Wang, X. Jiang, L. Zhang, W.-Y. Liu, Y. Li, Q. Shen, Y. Cao, C.-Y. Lu, R. Shu, J.-Y. Wang, L. Li, N.-L. Liu, F. Xu, X.-B. Wang, C.-Z. Peng, and J.-W. Pan, "An integrated space-to-ground quantum communication network over 4,600 kilometres," *Nature*, vol. 589, pp. 214–219, Jan. 2021.

[20] E. Shchukin, T. Richter, and W. Vogel, "Nonclassicality criteria in terms of moments," *Physical Review A*, vol. 71, p. 011802, Jan. 2005.

[21] L.-M. Duan, G. Giedke, J. I. Cirac, and P. Zoller, "Inseparability criterion for continuous variable systems," *Physical Review Letters*, vol. 84, pp. 2722–2725, Mar. 2000. arXiv: quant-ph/9908056.

[22] C. M. Caves, "Quantum-mechanical noise in an interferometer," *Physical Review D*, vol. 23, pp. 1693–1708, Apr. 1981.

[23] A. Mari and J. Eisert, "Positive Wigner Functions Render Classical Simulation of Quantum Computation Efficient," *Physical Review Letters*, vol. 109, p. 230503, Dec. 2012.

[24] F. Grosshans and P. Grangier, "Continuous Variable Quantum Cryptography Using Coherent States," *Physical Review Letters*, vol. 88, p. 057902, Jan. 2002.

[25] C. Weedbrook, A. M. Lance, W. P. Bowen, T. Symul, T. C. Ralph, and P. K. Lam, "Quantum Cryptography Without Switching," *Physical Review Letters*, vol. 93, p. 170504, Oct. 2004.

[26] L. Mandel, "Sub-Poissonian photon statistics in resonance fluorescence," *Opt. Lett.*, vol. 4, pp. 205–207, July 1979. Publisher: OSA.

[27] F. Mattioli, Z. Zhou, A. Gaggero, R. Gaudio, R. Leoni, and A. Fiore, "Photon-counting and analog operation of a 24-pixel photon number resolving detector based on superconducting nanowires," *Optics Express*, vol. 24, p. 9067, Apr. 2016.

[28] G. Giedke and J. I. Cirac, "Characterization of Gaussian operations and distillation of Gaussian states," *Physical Review A*, vol. 66, p. 032316, Sept. 2002.

[29] S. L. Braunstein and C. M. Caves, "Statistical distance and the geometry of quantum states," *Physical Review Letters*, vol. 72, pp. 3439–3443, May 1994.

[30] S. L. Braunstein, C. M. Caves, and G. J. Milburn, "Generalized uncertainty relations: Theory, examples, and Lorentz invariance," *Annals of Physics*, vol. 247, pp. 135–173, Apr. 1996. arXiv: quant-ph/9507004.

[31] M. G. A. Paris, "QUANTUM ESTIMATION FOR QUANTUM TECHNOLOGY," *International Journal of Quantum Information*, vol. 07, pp. 125–137, Jan. 2009.

[32] S. Ragy, M. Jarzyna, and R. Demkowicz-Dobrzański, "Compatibility in multiparameter quantum metrology," *Physical Review A*, vol. 94, p. 052108, Nov. 2016.

[33] K. Matsumoto, "A new approach to the Cramér-Rao-type bound of the pure-state model," *Journal of Physics A: Mathematical and General*, vol. 35, pp. 3111–3123, Apr. 2002.

[34] H. Lee, P. Kok, and J. P. Dowling, "A Quantum Rosetta Stone for Interferometry," *Journal of Modern Optics*, vol. 49, pp. 2325–2338, Nov. 2002. arXiv: quant-ph/0202133.

[35] T. Nagata, R. Okamoto, J. L. O'Brien, K. Sasaki, and S. Takeuchi, "Beating the Standard Quantum Limit with Four Entangled Photons," *Science*, vol. 316, pp. 726–729, May 2007. arXiv: 0708.1385.

[36] R. Demkowicz-Dobrzanski, J. Kolodynski, and M. Guta, "The elusive Heisenberg limit in quantum enhanced metrology," *Nature Communications*, vol. 3, p. 1063, Jan. 2012. arXiv: 1201.3940.

[37] P. C. Humphreys, M. Barbieri, A. Datta, and I. A. Walmsley, "Quantum Enhanced Multiple Phase Estimation," *Physical Review Letters*, vol. 111, p. 070403, Aug. 2013.

[38] C. N. Gagatsos, D. Branford, and A. Datta, "Gaussian systems for quantum enhanced multiple phase estimation," *Physical Review A*, vol. 94, p. 042342, Oct. 2016. arXiv: 1605.04819.

[39] O. Pinel, J. Fade, D. Braun, P. Jian, N. Treps, and C. Fabre, "Ultimate sensitivity of precision measurements with intense Gaussian quantum light: A multimodal approach," *Physical Review A*, vol. 85, p. 010101, Jan. 2012.

[40] O. Pinel, P. Jian, C. Fabre, N. Treps, and D. Braun, "Quantum parameter estimation using general single-mode Gaussian states," *Physical Review A*, vol. 88, p. 040102, Oct. 2013. arXiv: 1307.5318.

[41] C. Sparaciari, S. Olivares, and M. G. A. Paris, "Bounds to precision for quantum interferometry with Gaussian states and operations," *Journal of the Optical Society of America B*, vol. 32, p. 1354, July 2015.

[42] M. G. Genoni, M. G. A. Paris, G. Adesso, H. Nha, P. L. Knight, and M. S. Kim, "Optimal estimation of joint parameters in phase space," *Physical Review A*, vol. 87, p. 012107, Jan. 2013. arXiv: 1206.4867.

[43] Y. Gao and H. Lee, "Bounds on quantum multiple-parameter estimation with Gaussian state," *The European Physical Journal D*, vol. 68, p. 347, Nov. 2014.

[44] T. Baumgratz and A. Datta, "Quantum Enhanced Estimation of a Multidimensional Field," *Physical Review Letters*, vol. 116, p. 030801, Jan. 2016.

[45] M. Bradshaw, S. M. Assad, and P. K. Lam, "A tight Cramér–Rao bound for joint parameter estimation with a pure two-mode squeezed probe," *Physics Letters A*, vol. 381, pp. 2598–2607, Aug. 2017.

[46] M. Bradshaw, P. K. Lam, and S. M. Assad, "Ultimate precision of joint quadrature parameter estimation with a Gaussian probe," *Physical Review A*, vol. 97, p. 012106, Jan. 2018.

[47] F. Albarelli, J. F. Friel, and A. Datta, "Evaluating the Holevo Cramér-Rao Bound for Multiparameter Quantum Metrology," *Physical Review Letters*, vol. 123, p. 200503, Nov. 2019.

[48] R. Demkowicz-Dobrzanski, M. Jarzyna, and J. Kolodynski, "Quantum limits in optical interferometry," *arXiv:1405.7703 [quant-ph]*, vol. 60, pp. 345–435, 2015. arXiv: 1405.7703.

[49] J. Niset, A. Acín, U. L. Andersen, N. J. Cerf, R. García-Patrón, M. Navascués, and M. Sabuncu, "Superiority of Entangled Measurements over All Local Strategies for the Estimation of Product Coherent States," *Physical Review Letters*, vol. 98, p. 260404, June 2007.

[50] C. H. Bennett, G. Brassard, C. Crépeau, R. Jozsa, A. Peres, and W. K. Wootters, "Teleporting an unknown quantum state via dual classical and Einstein-Podolsky-Rosen channels," *Physical Review Letters*, vol. 70, pp. 1895–1899, Mar. 1993.

[51] D. Bouwmeester, J.-W. Pan, K. Mattle, M. Eibl, H. Weinfurter, and A. Zeilinger, "Experimental quantum teleportation," vol. 390, p. 5, 1997.

[52] A. K. Ekert, "Quantum cryptography based on Bell's theorem," *Physical Review Letters*, vol. 67, pp. 661–663, Aug. 1991.

[53] M. Horodecki, P. Horodecki, and R. Horodecki, "Separability of mixed states: necessary and sufficient conditions," *Physics Letters A*, vol. 223, pp. 1–8, Nov. 1996.

[54] E. Chitambar and G. Gour, "Quantum resource theories," *Rev. Mod. Phys.*, vol. 91, p. 025001, Apr. 2019. Publisher: American Physical Society.

[55] R. Horodecki, P. Horodecki, M. Horodecki, and K. Horodecki, "Quantum entanglement," *Reviews of Modern Physics*, vol. 81, pp. 865–942, June 2009.

[56] M. A. Nielsen and I. L. Chuang, *Quantum computation and quantum information*. Cambridge: Cambridge university press, 10th anniversary edition ed., 2010.

[57] J. Von Neumann, *Mathematische Grundlagen der Quantenmechanik*. Die grundlehren der mathematischen wissenschaften in einzeldarstellungen... bd. XXXVIII, J. Springer, 1932.

[58] A. Peres, "Separability Criterion for Density Matrices," *Physical Review Letters*, vol. 77, pp. 1413–1415, Aug. 1996.

[59] M. Horodecki, P. Horodecki, and R. Horodecki, "Mixed-State Entanglement and Distillation: Is there a "Bound" Entanglement in Nature?," *Physical Review Letters*, vol. 80, pp. 5239–5242, June 1998.

[60] O. Rudolph, "Further Results on the Cross Norm Criterion for Separability," *Quantum Information Processing*, vol. 4, pp. 219–239, Aug. 2005.

[61] N. J. Cerf and C. Adami, "Negative Entropy and Information in Quantum Mechanics," *Physical Review Letters*, vol. 79, pp. 5194–5197, Dec. 1997.

[62] M. Horodecki and P. Horodecki, "Reduction criterion of separability and limits for a class of distillation protocols," *Physical Review A*, vol. 59, pp. 4206–4216, June 1999.

[63] N. J. Cerf, C. Adami, and R. M. Gingrich, "Reduction criterion for separability," *Physical Review A*, vol. 60, pp. 898–909, Aug. 1999.

[64] M. A. Nielsen and J. Kempe, "Separable States Are More Disordered Globally than Locally," *Physical Review Letters*, vol. 86, pp. 5184–5187, May 2001.

[65] A. W. Marshall, I. Olkin, and B. C. Arnold, *Inequalities: Theory of Majorization and Its Applications*. Springer Series in Statistics, New York, NY: Springer New York, 2011.

[66] R. Simon, "Peres-Horodecki Separability Criterion for Continuous Variable Systems," *Physical Review Letters*, vol. 84, pp. 2726–2729, Mar. 2000.

[67] R. F. Werner and M. M. Wolf, "Bound Entangled Gaussian States," *Physical Review Letters*, vol. 86, pp. 3658–3661, Apr. 2001.

[68] A. Serafini, G. Adesso, and F. Illuminati, "Unitarily localizable entanglement of Gaussian states," *Physical Review A*, vol. 71, p. 032349, Mar. 2005.

[69] G. Adesso and F. Illuminati, "Entanglement in continuous-variable systems: recent advances and current perspectives," *Journal of Physics A: Mathematical and Theoretical*, vol. 40, pp. 7821–7880, July 2007.

[70] C. Zhang, S. Yu, Q. Chen, and C. H. Oh, "Detecting and estimating continuous-variable entanglement by local orthogonal observables," *Physical Review Letters*, vol. 111, p. 190501, Nov. 2013. arXiv: 1307.7487.

[71] A. Peres, "Quantum theory: concepts and methods," 0000. ISBN: 9780306471209 OCLC: 1159901051.

[72] M.-D. Choi, "Completely positive linear maps on complex matrices," *Linear Algebra and its Applications*, vol. 10, pp. 285–290, June 1975.

[73] A. Jamiołkowski, "Linear transformations which preserve trace and positive semidefiniteness of operators," *Reports on Mathematical Physics*, vol. 3, pp. 275–278, Dec. 1972.

[74] D. J. I. Cirac, "1. Referent: Prof. Dr. Reinhard F. Werner," p. 111.

[75] K. Chen and L.-A. Wu, "A matrix realignment method for recognizing entanglement," *arXiv:quant-ph/0205017*, Apr. 2003. arXiv: quant-ph/0205017.

[76] C.-J. Zhang, Y.-S. Zhang, S. Zhang, and G.-C. Guo, "Entanglement detection beyond the cross-norm or realignment criterion," *Physical Review A*, vol. 77, p. 060301, June 2008. arXiv: 0709.3766.

[77] G. Tóth and O. Gühne, "Entanglement and Permutational Symmetry," *Physical Review Letters*, vol. 102, p. 170503, May 2009.

[78] O. Gühne and G. Tóth, "Entanglement detection," *Physics Reports*, vol. 474, pp. 1–75, Apr. 2009.

[79] L.-M. Duan, G. Giedke, J. I. Cirac, and P. Zoller, "Inseparability Criterion for Continuous Variable Systems," *PHYSICAL REVIEW LETTERS*, vol. 84, no. 12, p. 4, 2000.

[80] R. Simon, "Peres-Horodecki Separability Criterion for Continuous Variable Systems," *Physical Review Letters*, vol. 84, pp. 2726–2729, Mar. 2000.

[81] A. Serafini, G. Adesso, and F. Illuminati, "Unitarily localizable entanglement of Gaussian states," *Physical Review A*, vol. 71, p. 032349, Mar. 2005.

[82] M. Horodecki, P. Horodecki, and R. Horodecki, "Mixed-State Entanglement and Distillation: Is there a "Bound" Entanglement in Nature?," *Physical Review Letters*, vol. 80, pp. 5239–5242, June 1998.

[83] E. Shchukin and W. Vogel, "Inseparability Criteria for Continuous Bipartite Quantum States," *Physical Review Letters*, vol. 95, p. 230502, Nov. 2005.

[84] S. P. Walborn, B. G. Taketani, A. Salles, F. Toscano, and R. L. de Matos Filho, "Entropic Entanglement Criteria for Continuous Variables," *Physical Review Letters*, vol. 103, p. 160505, Oct. 2009.

[85] L. Lami, A. Serafini, and G. Adesso, "Gaussian entanglement revisited," *New Journal of Physics*, vol. 20, p. 023030, Feb. 2018. arXiv: 1612.05215.

[86] Y. Mardani, A. Shafiei, M. Ghadimi, and M. Abdi, "Continuous-variable entanglement distillation by cascaded photon replacement," *Physical Review A*, vol. 102, p. 012407, July 2020.

[87] T. Mihaescu, H. Kampermann, G. Gianfelici, A. Isar, and D. Bruß, "Detecting entanglement of unknown continuous variable states with random measurements," *New Journal of Physics*, vol. 22, p. 123041, Dec. 2020.

[88] C. Weedbrook, S. Pirandola, R. García-Patrón, N. J. Cerf, T. C. Ralph, J. H. Shapiro, and S. Lloyd, "Gaussian quantum information," *Reviews of Modern Physics*, vol. 84, pp. 621–669, May 2012.

[89] C. Fabre and N. Treps, "Modes and states in quantum optics," *Reviews of Modern Physics*, vol. 92, p. 035005, Sept. 2020.

[90] T. C. Ralph, A. P. Lund, and A. Lvovsky, "Nondeterministic Noiseless Linear Amplification of Quantum Systems," in *AIP Conference Proceedings*, (Calgary (Canada)), pp. 155–160, AIP, 2009.

[91] C. N. Gagatsos, E. Karpov, and N. J. Cerf, "Probabilistic phase-insensitive optical squeezer in compliance with causality," *Physical Review A*, vol. 86, p. 012324, July 2012.

[92] M. He, R. Malaney, and B. A. Burnett, "Noiseless linear amplifiers for multimode states," *Physical Review A*, vol. 103, p. 012414, Jan. 2021.

[93] C. N. Gagatsos, J. Fiurášek, A. Zavatta, M. Bellini, and N. J. Cerf, "Heralded noiseless amplification and attenuation of non-Gaussian states of light," *Physical Review A*, vol. 89, p. 062311, June 2014.

[94] J. Fiurášek and N. J. Cerf, "Gaussian postselection and virtual noiseless amplification in continuous-variable quantum key distribution," *Physical Review A*, vol. 86, p. 060302, Dec. 2012.

[95] M. Mičuda, I. Straka, M. Miková, M. Dušek, N. J. Cerf, J. Fiurášek, and M. Ježek, "Noiseless Loss Suppression in Quantum Optical Communication," *Physical Review Letters*, vol. 109, p. 180503, Nov. 2012.

[96] J. Fiurášek, "Gaussian Transformations and Distillation of Entangled Gaussian States," *Physical Review Letters*, vol. 89, p. 137904, Sept. 2002.

[97] G. Giedke and J. I. Cirac, "Characterization of Gaussian operations and distillation of Gaussian states," *Physical Review A*, vol. 66, p. 032316, Sept. 2002.

[98] A. S. Holevo, "Entanglement-breaking channels in infinite dimensions," *arXiv:0802.0235 [quant-ph]*, Feb. 2008. arXiv: 0802.0235.

[99] M. S. Kim, W. Son, V. Bužek, and P. L. Knight, "Entanglement by a beam splitter: Nonclassicality as a prerequisite for entanglement," *Physical Review A*, vol. 65, p. 032323, Feb. 2002.

[100] M. S. Kim, F. A. M. de Oliveira, and P. L. Knight, "Properties of squeezed number states and squeezed thermal states," *Physical Review A*, vol. 40, pp. 2494–2503, Sept. 1989.

[101] P. Marian, T. A. Marian, and H. Scutaru, "Quantifying Nonclassicality of One-Mode Gaussian States of the Radiation Field," *Physical Review Letters*, vol. 88, p. 153601, Mar. 2002.

[102] M. Frigerio, S. Olivares, and M. G. A. Paris, "Steering nonclassicality of Gaussian states," *Physical Review A*, vol. 103, p. 022209, Feb. 2021.

[103] E. V. Shchukin and W. Vogel, "Nonclassical Moments and their Measurement," *Physical Review A*, vol. 72, p. 043808, Oct. 2005.

[104] A. Miranowicz, M. Bartkowiak, X. Wang, Y. Liu, and F. Nori, "Testing nonclassicality in multimode fields: A unified derivation of classical inequalities," *Physical Review A*, vol. 82, p. 013824, July 2010.

[105] G. S. Agarwal and K. Tara, "Nonclassical character of states exhibiting no squeezing or sub-Poissonian statistics," *Physical Review A*, vol. 46, pp. 485–488, July 1992.

[106] N. Lütkenhaus and S. M. Barnett, "Nonclassical effects in phase space," *Physical Review A*, vol. 51, pp. 3340–3342, Apr. 1995.

[107] T. Richter and W. Vogel, "Nonclassicality of Quantum States: A Hierarchy of Observable Conditions," *Physical Review Letters*, vol. 89, p. 283601, Dec. 2002.

[108] A. Rivas and A. Luis, "Nonclassicality of states and measurements by breaking classical bounds on statistics," *Phys. Rev. A*, vol. 79, p. 042105, Apr. 2009. Publisher: American Physical Society.

[109] S. Ryl, J. Sperling, E. Agudelo, M. Mraz, S. Köhnke, B. Hage, and W. Vogel, "Unified nonclassicality criteria," *Physical Review A*, vol. 92, p. 011801, July 2015.

[110] S. De Bièvre, D. B. Horoshko, G. Patera, and M. I. Kolobov, "Measuring Nonclassicality of Bosonic Field Quantum States via Operator Ordering Sensitivity," *Physical Review Letters*, vol. 122, p. 080402, Feb. 2019.

[111] A. Hertz, N. J. Cerf, and S. De Bièvre, "Relating the entanglement and optical nonclassicality of multimode states of a bosonic quantum field," *Physical Review A*, vol. 102, p. 032413, Sept. 2020.

[112] R. J. Glauber, "Coherent and Incoherent States of the Radiation Field," *Physical Review*, vol. 131, pp. 2766–2788, Sept. 1963.

[113] E. C. G. Sudarshan, "Equivalence of Semiclassical and Quantum Mechanical Descriptions of Statistical Light Beams," *Physical Review Letters*, vol. 10, pp. 277–279, Apr. 1963.

[114] J. L. O'Brien, A. Furusawa, and J. Vučković, "Photonic quantum technologies," *Nature Photonics*, vol. 3, pp. 687–695, Dec. 2009. arXiv: 1003.3928.

[115] S. Slussarenko and G. J. Pryde, "Photonic quantum information processing: A concise review," *Applied Physics Reviews*, vol. 6, p. 041303, Dec. 2019.

[116] E. Knill and R. La, "A scheme for ef®cient quantum computation with linear optics," vol. 409, p. 7, 2001.

[117] F. Shahandeh, A. P. Lund, and T. C. Ralph, "Quantum correlations and global coherence in distributed quantum computing," *Physical Review A*, vol. 99, p. 052303, May 2019.

[118] B. Yadin, F. C. Binder, J. Thompson, V. Narasimhachar, M. Gu, and M. Kim, "Operational Resource Theory of Continuous-Variable Nonclassicality," *Physical Review X*, vol. 8, p. 041038, Dec. 2018.

[119] F. Shahandeh, A. P. Lund, and T. C. Ralph, "Quantum Correlations in Nonlocal Boson Sampling," *Physical Review Letters*, vol. 119, p. 120502, Sept. 2017.

[120] H. Kwon, K. C. Tan, T. Volkoff, and H. Jeong, "Nonclassicality as a Quantifiable Resource for Quantum Metrology," *Physical Review Letters*, vol. 122, p. 040503, Feb. 2019.

[121] T. C. Ralph and P. K. Lam, "A bright future for quantum communications," *Nature Photonics*, vol. 3, pp. 671–673, Dec. 2009.

[122] J. Sperling, M. Bohmann, W. Vogel, G. Harder, B. Brecht, V. Ansari, and C. Silberhorn, "Uncovering Quantum Correlations with Time-Multiplexed Click Detection," *Physical Review Letters*, vol. 115, p. 023601, July 2015.

[123] M. Avenhaus, K. Laiho, M. V. Chekhova, and C. Silberhorn, "Accessing Higher Order Correlations in Quantum Optical States by Time Multiplexing," *Physical Review Letters*, vol. 104, p. 063602, Feb. 2010.

[124] M. Bohmann, E. Agudelo, and J. Sperling, "Probing nonclassicality with matrices of phase-space distributions," *Quantum*, vol. 4, p. 343, Oct. 2020.

[125] A. Hertz, O. Oreshkov, and N. J. Cerf, "Multicopy uncertainty observable inducing a symplectic-invariant uncertainty relation in position and momentum phase space," *Physical Review A*, vol. 100, p. 052112, Nov. 2019.

[126] T. A. Brun, "Measuring polynomial functions of states," *Quantum Information and Computation*, vol. 4, no. 401, 2004.

[127] J. Aasi, J. Abadie, B. P. Abbott, R. Abbott, T. D. Abbott, M. R. Abernathy, C. Adams, T. Adams, P. Addesso, R. X. Adhikari, C. Affeldt, O. D. Aguiar, P. Ajith, B. Allen, E. Amador Ceron, D. Amariutei, S. B. Anderson, W. G. Anderson, K. Arai, M. C. Araya, C. Arceneaux, S. Ast, S. M. Aston, D. Atkinson, P. Aufmuth, C. Aulbert, L. Austin, B. E. Aylott, S. Babak, P. T. Baker, S. Ballmer, Y. Bao, J. C. Barayoga, D. Barker, B. Barr, L. Barsotti, M. A. Barton, I. Bartos, R. Bassiri, J. Batch, J. Bauchrowitz, B. Behnke, A. S. Bell, C. Bell, G. Bergmann, J. M. Berliner, A. Bertolini, J. Betzwieser, N. Beveridge, P. T. Beyersdorf, T. Bhadbhade, I. A. Bilenko, G. Billingsley, J. Birch, S. Biscans, E. Black, J. K. Blackburn, L. Blackburn, D. Blair, B. Bland, O. Bock, T. P. Bodiya, C. Bogan, C. Bond, R. Bork, M. Born, S. Bose, J. Bowers, P. R. Brady, V. B. Braginsky, J. E. Brau, J. Breyer, D. O. Bridges, M. Brinkmann, M. Britzger, A. F. Brooks, D. A. Brown, D. D. Brown, K. Buckland, F. Brückner, B. C. Buchler, A. Buonanno, J. Burguet-Castell, R. L. Byer, L. Cadonati, J. B. Camp, P. Campsie, K. Cannon, J. Cao, C. D. Capano, L. Carbone, S. Caride, A. D. Castiglia, S. Caudill, M. Cavaglià, C. Cepeda, T. Chalermsongsak, S. Chao, P. Charlton, X. Chen, Y. Chen, H.-S. Cho, J. H. Chow, N. Christensen, Q. Chu, S. S. Y. Chua, C. T. Y. Chung, G. Ciani, F. Clara, D. E. Clark, J. A. Clark, M. Constancio Junior, D. Cook, T. R. Corbitt, M. Cordier, N. Cornish, A. Corsi, C. A. Costa, M. W. Coughlin, S. Countryman, P. Couvares, D. M. Coward, M. Cowart, D. C. Coyne, K. Craig, J. D. E. Creighton, T. D. Creighton, A. Cumming, L. Cunningham, K. Dahl, M. Damjanic, S. L. Danilishin, K. Danzmann, B. Daudert, H. Daveloza, G. S. Davies, E. J. Daw, T. Dayanga, E. Deleeuw, T. Denker, T. Dent, V. Dergachev, R. DeRosa, R. DeSalvo, S. Dhurandhar, I. Di Palma, M. Díaz, A. Dietz, F. Donovan, K. L. Dooley, S. Doravari, S. Drasco, R. W. P. Drever, J. C. Driggers, Z. Du, J.-C. Dumas, S. Dwyer, T. Eberle, M. Edwards, A. Effler, P. Ehrens, S. S. Eikenberry, R. Engel, R. Essick, T. Etzel, K. Evans, M. Evans,

T. Evans, M. Factourovich, S. Fairhurst, Q. Fang, B. F. Farr, W. Farr, M. Favata, D. Fazi, H. Fehrmann, D. Feldbaum, L. S. Finn, R. P. Fisher, S. Foley, E. Forsi, N. Fotopoulos, M. Frede, M. A. Frei, Z. Frei, A. Freise, R. Frey, T. T. Fricke, D. Friedrich, P. Fritschel, V. V. Frolov, M.-K. Fujimoto, P. J. Fulda, M. Fyffe, J. Gair, J. Garcia, N. Gehrels, G. Gelencser, L. . Gergely, S. Ghosh, J. A. Giaime, S. Giampanis, K. D. Giardina, S. Gil-Casanova, C. Gill, J. Gleason, E. Goetz, G. González, N. Gordon, M. L. Gorodetsky, S. Gossan, S. Goßler, C. Graef, P. B. Graff, A. Grant, S. Gras, C. Gray, R. J. S. Greenhalgh, A. M. Gretarsson, C. Griffo, H. Grote, K. Grover, S. Grunewald, C. Guido, E. K. Gustafson, R. Gustafson, D. Hammer, G. Hammond, J. Hanks, C. Hanna, J. Hanson, K. Haris, J. Harms, G. M. Harry, I. W. Harry, E. D. Harstad, M. T. Hartman, K. Haughian, K. Hayama, J. Heefner, M. C. Heintze, M. A. Hendry, I. S. Heng, A. W. Heptonstall, M. Heurs, M. Hewitson, S. Hild, D. Hoak, K. A. Hodge, K. Holt, M. Holtrop, T. Hong, S. Hooper, J. Hough, E. J. Howell, V. Huang, E. A. Huerta, B. Hughey, S. H. Huttner, M. Huynh, T. Huynh-Dinh, D. R. Ingram, R. Inta, T. Isogai, A. Ivanov, B. R. Iyer, K. Izumi, M. Jacobson, E. James, H. Jang, Y. J. Jang, E. Jesse, W. W. Johnson, D. Jones, D. I. Jones, R. Jones, L. Ju, P. Kalmus, V. Kalogera, S. Kandhasamy, G. Kang, J. B. Kanner, R. Kasturi, E. Katsavounidis, W. Katzman, H. Kaufer, K. Kawabe, S. Kawamura, F. Kawazoe, D. Keitel, D. B. Kelley, W. Kells, D. G. Keppel, A. Khalaidovski, F. Y. Khalili, E. A. Khazanov, B. K. Kim, C. Kim, K. Kim, N. Kim, Y.-M. Kim, P. J. King, D. L. Kinzel, J. S. Kissel, S. Klimenko, J. Kline, K. Kokeyama, V. Kondrashov, S. Koranda, W. Z. Korth, D. Kozak, C. Kozameh, A. Kremin, V. Kringel, B. Krishnan, C. Kucharczyk, G. Kuehn, P. Kumar, R. Kumar, B. J. Kuper, R. Kurdyumov, P. Kwee, P. K. Lam, M. Landry, B. Lantz, P. D. Lasky, C. Lawrie, A. Lazzarini, A. Le Roux, P. Leaci, C.-H. Lee, H. K. Lee, H. M. Lee, J. Lee, J. R. Leong, B. Levine, V. Lhuillier, A. C. Lin, V. Litvine, Y. Liu, Z. Liu, N. A. Lockerbie, D. Lodhia, K. Loew, J. Logue, A. L. Lombardi, M. Lormand, J. Lough, M. Lubinski, H. Lück, A. P. Lundgren, J. Macarthur, E. Macdonald, B. Machenschalk, M. MacInnis, D. M. Macleod, F. Magaña-Sandoval, M. Mageswaran, K. Mailand, G. Manca, I. Mandel, V. Mandic, S. Márka, Z. Márka, A. S. Markosyan, E. Maros, I. W. Martin, R. M. Martin, D. Martinov, J. N. Marx, K. Mason, F. Matichard, L. Matone, R. A. Matzner, N. Mavalvala, G. May, G. Mazzolo, K. McAuley, R. McCarthy, D. E. McClelland, S. C. McGuire, G. McIntyre, J. McIver, G. D. Meadors, M. Mehmet, T. Meier, A. Melatos, G. Mendell, R. A. Mercer, S. Meshkov, C. Messenger, M. S. Meyer, H. Miao, J. Miller, C. M. F. Mingarelli, S. Mitra, V. P. Mitrofanov, G. Mitselmakher, R. Mittleman, B. Moe, F. Mokler, S. R. P. Mohapatra, D. Moraru, G. Moreno, T. Mori, S. R. Morriss, K. Mossavi, C. M. Mow-Lowry, C. L. Mueller, G. Mueller, S. Mukherjee, A. Mullavey, J. Munch, D. Murphy, P. G. Murray, A. Mytidis, D. Nanda Kumar, T. Nash, R. Nayak, V. Necula, G. Newton, T. Nguyen, E. Nishida, A. Nishizawa, A. Nitz, D. Nolting, M. E. Normandin, L. K. Nuttall, J. O'Dell, B. O'Reilly, R. O'Shaughnessy,

E. Ochsner, E. Oelker, G. H. Ogin, J. J. Oh, S. H. Oh, F. Ohme, P. Oppermann, C. Osthelder, C. D. Ott, D. J. Ottaway, R. S. Ottens, J. Ou, H. Overmier, B. J. Owen, C. Padilla, A. Pai, Y. Pan, C. Pankow, M. A. Papa, H. Paris, W. Parkinson, M. Pedraza, S. Penn, C. Peralta, A. Perreca, M. Phelps, M. Pickenpack, V. Pierro, I. M. Pinto, M. Pitkin, H. J. Pletsch, J. Pöld, F. Postiglione, C. Poux, V. Predoi, T. Prestegard, L. R. Price, M. Prijatelj, S. Privitera, L. G. Prokhorov, O. Puncken, V. Quetschke, E. Quintero, R. Quitzow-James, F. J. Raab, H. Radkins, P. Raffai, S. Raja, M. Rakhmanov, C. Ramet, V. Raymond, C. M. Reed, T. Reed, S. Reid, D. H. Reitze, R. Riesen, K. Riles, M. Roberts, N. A. Robertson, E. L. Robinson, S. Roddy, C. Rodriguez, L. Rodriguez, M. Rodruck, J. G. Rollins, J. H. Romie, C. Röver, S. Rowan, A. Rüdiger, K. Ryan, F. Salemi, L. Sammut, V. Sandberg, J. Sanders, S. Sankar, V. Sannibale, L. Santamaría, I. Santiago-Prieto, G. Santostasi, B. S. Sathyaprakash, P. R. Saulson, R. L. Savage, R. Schilling, R. Schnabel, R. M. S. Schofield, D. Schuette, B. Schulz, B. F. Schutz, P. Schwinberg, J. Scott, S. M. Scott, F. Seifert, D. Sellers, A. S. Sengupta, A. Sergeev, D. A. Shaddock, M. S. Shahriar, M. Shaltev, Z. Shao, B. Shapiro, P. Shawhan, D. H. Shoemaker, T. L. Sidery, X. Siemens, D. Sigg, D. Simakov, A. Singer, L. Singer, A. M. Sintes, G. R. Skelton, B. J. J. Slagmolen, J. Slutsky, J. R. Smith, M. R. Smith, R. J. E. Smith, N. D. Smith-Lefebvre, E. J. Son, B. Sorazu, T. Souradeep, M. Stefszky, E. Steinert, J. Steinlechner, S. Steinlechner, S. Steplewski, D. Stevens, A. Stochino, R. Stone, K. A. Strain, S. E. Strigin, A. S. Stroeer, A. L. Stuver, T. Z. Summerscales, S. Susmithan, P. J. Sutton, G. Szeifert, D. Talukder, D. B. Tanner, S. P. Tarabrin, R. Taylor, M. Thomas, P. Thomas, K. A. Thorne, K. S. Thorne, E. Thrane, V. Tiwari, K. V. Tokmakov, C. Tomlinson, C. V. Torres, C. I. Torrie, G. Traylor, M. Tse, D. Ugolini, C. S. Unnikrishnan, H. Vahlbruch, M. Vallisneri, M. V. van der Sluys, A. A. van Veggel, S. Vass, R. Vaulin, A. Vecchio, P. J. Veitch, J. Veitch, K. Venkateswara, S. Verma, R. Vincent-Finley, S. Vitale, T. Vo, C. Vorvick, W. D. Vousden, S. P. Vyatchanin, A. Wade, L. Wade, M. Wade, S. J. Waldman, L. Wallace, Y. Wan, M. Wang, J. Wang, X. Wang, A. Wanner, R. L. Ward, M. Was, M. Weinert, A. J. Weinstein, R. Weiss, T. Welborn, L. Wen, P. Wessels, M. West, T. Westphal, K. Wette, J. T. Whelan, S. E. Whitcomb, A. G. Wiseman, D. J. White, B. F. Whiting, K. Wiesner, C. Wilkinson, P. A. Willems, L. Williams, R. Williams, T. Williams, J. L. Willis, B. Willke, M. Wimmer, L. Winkelmann, W. Winkler, C. C. Wipf, H. Wittel, G. Woan, R. Wooley, J. Worden, J. Yablon, I. Yakushin, H. Yamamoto, C. C. Yancey, H. Yang, D. Yeaton-Massey, S. Yoshida, H. Yum, M. Zanolin, F. Zhang, L. Zhang, C. Zhao, H. Zhu, X. J. Zhu, N. Zotov, M. E. Zucker, and J. Zweizig, "Enhanced sensitivity of the LIGO gravitational wave detector by using squeezed states of light," *Nature Photonics*, vol. 7, pp. 613–619, Aug. 2013.

[128] S. S. Y. Chua, B. J. J. Slagmolen, D. A. Shaddock, and D. E. McClelland, "Quantum squeezed light in gravitational-wave detectors," *Classical and Quantum*

Gravity, vol. 31, p. 183001, Sept. 2014.

[129] A. I. Lvovsky and J. H. Shapiro, "Nonclassical character of statistical mixtures of the single-photon and vacuum optical states," *Physical Review A*, vol. 65, p. 033830, Feb. 2002.

[130] U. Chabaud, G. Ferrini, F. Grosshans, and D. Markham, "Classical simulation of Gaussian quantum circuits with non-Gaussian input states," *Physical Review Research*, vol. 3, p. 033018, July 2021.

[131] M. Walschaers, "Non-Gaussian Quantum States and Where to Find Them," *PRX Quantum*, vol. 2, p. 030204, Sept. 2021.